



**HAL**  
open science

# Control of the iron-sparing response in *Staphylococcus aureus* by a regulatory RNA

Maxime Barrault

► **To cite this version:**

Maxime Barrault. Control of the iron-sparing response in *Staphylococcus aureus* by a regulatory RNA. Bacteriology. Université Paris-Saclay, 2023. English. NNT: 2023UPASL104 . tel-04815488

**HAL Id: tel-04815488**

**<https://theses.hal.science/tel-04815488v1>**

Submitted on 3 Dec 2024

**HAL** is a multi-disciplinary open access archive for the deposit and dissemination of scientific research documents, whether they are published or not. The documents may come from teaching and research institutions in France or abroad, or from public or private research centers.

L'archive ouverte pluridisciplinaire **HAL**, est destinée au dépôt et à la diffusion de documents scientifiques de niveau recherche, publiés ou non, émanant des établissements d'enseignement et de recherche français ou étrangers, des laboratoires publics ou privés.

# Control of the iron-sparing response in *Staphylococcus aureus* by a regulatory RNA

*Adaptation à la carence en fer du staphylocoque doré par un ARN régulateur*

## Thèse de doctorat de l'Université Paris-Saclay

École doctorale n° 577, Structure et Dynamique des Systèmes Vivants (SDSV)  
Spécialité de doctorat : Microbiologie  
Graduate School : Life Sciences and Health  
Référent : Faculté des sciences d'Orsay

Thèse préparée à l'Institut de Biologie Intégrative de la Cellule (I2BC) (Université Paris-Saclay, CEA, CNRS), sous la direction de **Philippe BOULOC**, directeur de recherche.

Thèse soutenue à Paris-Saclay, le 1<sup>er</sup> décembre 2023, par

**Maxime BARRAULT**

### Composition du Jury

Membres du jury avec voix délibérative :

**Olga SOUTOURINA**

Professeure, Institut de Biologie Intégrative de la Cellule,  
Université Paris-Saclay

Présidente

**Pierre MANDIN**

Chargé de recherche, HDR, Laboratoire de Chimie  
Bactérienne,  
Aix-Marseille Université

Rapporteur & examinateur

**Peter REDDER**

Professeur, Centre de Biologie Intégrative de Toulouse,  
Université Toulouse III – Paul Sabatier

Rapporteur & examinateur

**Sarah DUBRAC**

Chargée de recherche, HDR, Institut Pasteur

Examinatrice

## Summary of the thesis

**Titre :** Adaptation à la carence en fer du staphylocoque doré par un ARN régulateur

**Mots clés :** Staphylocoque doré, ARN régulateur, fer, Citrate, aconitase, méthylthiotransférase

**Résumé :** Le Fer est un élément essentiel pour le développement de nombreux microorganismes. Dans le cadre d'une infection, un des mécanismes principaux de défense de l'hôte consiste à séquestrer certains métaux tels que le fer, afin de limiter la croissance bactérienne. Récemment, l'ARN régulateur IsrR a été découvert et caractérisé chez *S. aureus* comme étant un régulateur de la réponse à la carence en Fer. En effet, IsrR contrôle le métabolisme bactérien en limitant l'utilisation du Fer lorsque celui-ci vient à manquer. L'objectif de cette thèse est de caractériser le rôle d'IsrR dans le contrôle du métabolisme du citrate.

Ces travaux montrent que IsrR réprime l'aconitase, une enzyme clé du cycle de Krebs, ainsi que son activateur transcriptionnel CcpE, en s'appariant sur

leurs ARNs messager et en empêchant leur traduction.

En conditions de carence en Fer, l'aconitase devient une protéine se liant à l'ARN et permettant la régulation de plusieurs gènes impliqués dans le métabolisme du Fer. Ces travaux sont les premiers à caractériser cette activité RNA-binding chez *S. aureus* et ont permis de démontrer qu'en conditions de carence en fer, l'aconitase modifie le métabolisme de *S. aureus* en réprimant le cycle de Krebs et en favorisant la production d'oxaloacetate.

Enfin, ces travaux ont également permis l'élargissement de la liste des cibles d'IsrR. En effet, ils démontrent le rôle d'IsrR dans la régulation d'une enzyme possédant un noyau Fer-Soufre qui est la méthylthiotransférase MiaB.

**Title:** Control of the iron-sparing response in *Staphylococcus aureus* by a regulatory RNA

**Keywords:** *Staphylococcus aureus*, regulatory RNA, iron, citrate, aconitase, methylthiotransferase

**Abstract:** Iron is an essential element for the development of many microorganisms. In the course of infection, one of the main host defense mechanisms consists in sequestering certain metals such as iron in order to limit bacterial growth. Recently, the sRNA IsrR was discovered and characterized in *S. aureus* as a regulator of the response to iron starvation. Indeed, IsrR controls bacterial metabolism by limiting iron utilization when necessary. The aim of this thesis is to characterize the role of IsrR in the control of citrate metabolism.

This work shows that IsrR represses aconitase, a key enzyme from the TCA cycle, as well as its transcriptional activator CcpE, by pairing on their

mRNAs and preventing their translation.

Upon iron starvation, aconitase becomes an RNA-binding protein and regulates several genes involved in iron metabolism. This work is the first to characterize this RNA-binding activity in *S. aureus* and allowed us to demonstrate that upon iron starvation, aconitase modifies *S. aureus* metabolism by switching off TCA cycle and favoring production of oxaloacetate.

Finally, this work also allowed us to expand the list of IsrR targets. Indeed, we demonstrate the role of IsrR in the regulation of a Fe-S cluster containing enzyme which is methylthiotransferase MiaB.

# Table of contents

---

|  |           |
|--|-----------|
| SUMMARY OF THE THESIS.....   | 2         |
| TABLE OF CONTENTS.....   | 3         |
| A: ACKNOWLEDGMENTS .....   | 6         |
| B: LIST OF FIGURES AND TABLES.....   | 7         |
| C. INTRODUCTION .....  | 8         |
| <b>1. Iron and living organisms .....</b>  | <b>8</b>  |
| 1.1. Iron in the environment .....   | 8         |
| 1.2. Iron in biology .....   | 8         |
| 1.3. Iron homeostasis within the bacteria .....  | 13        |
| 1.4. Iron homeostasis within the host .....  | 25        |
| 1.5. Nutritional immunity.....   | 28        |
| <b>2. The role of citrate metabolism in bacteria .....</b>   | <b>29</b> |
| 2.1. Synthesis of citrate: The citrate synthase .....  | 29        |
| 2.2. Acquisition of exogenous citrate.....   | 30        |
| 2.3. Citrate as a carbon source.....   | 31        |
| 2.4. Citrate in the TCA cycle: the moonlighting role of aconitase.....   | 36        |
| <b>3. Regulatory RNAs in bacteria.....</b>   | <b>43</b> |
| 3.1. <i>Cis</i> -acting regulatory RNAs.....   | 44        |
| 3.2. <i>Trans</i> -acting regulatory RNAs .....  | 45        |
| 3.3. RNA chaperones.....   | 50        |
| 3.4. RyhB .....  | 52        |
| <b>4. <i>Staphylococcus aureus</i> .....</b>   | <b>55</b> |
| 4.1. Generalities and pathogenicity of <i>S. aureus</i> .....  | 55        |
| 4.2. Virulence factors of <i>S. aureus</i> .....   | 57        |
| 4.3. Iron acquisition systems in <i>S. aureus</i> .....  | 60        |
| 4.4. Citrate metabolism of <i>S. aureus</i> .....  | 65        |
| 4.5. IsrR .....  | 65        |
| D: OUTLINE.....  | 67        |
| E: SRNA-CONTROLLED IRON SPARING RESPONSE IN STAPHYLOCOCCI .....  | 68        |
| F: REGULATION OF STAPHYLOCOCCAL ACONITASE EXPRESSION IN IRON DEFICIENCY: CONTROL BY SRNA-DRIVEN FEEDFORWARD LOOP AND MOONLIGHTING ACTIVITY ..... | 93        |

|   |     |
|---|-----|
| TABLE S2. PLASMIDS.....   | 130 |
| TABLE S3. PRIMERS.....  | 132 |
| TABLE S4. HG003 $\Delta$ ISRR VS HG003 TRANSCRIPTOMIC ANALYSIS IN IRON STARVED GROWTH CONDITION .....   | 136 |
| TABLE S5. HG003 <i>CITB</i> <sub>RBP</sub> VS HG003 TRANSCRIPTOMIC ANALYSIS IN IRON STARVED GROWTH CONDITION .....  | 137 |
| FIGURE S1. RNA SEQUENCES USED FOR GEL RETARDATION .....   | 139 |
| FIGURE S2: GROWTH IN BHI OF HG003 AND HG003 $\Delta$ ISRR WITH <i>CITB</i> <sup>+</sup> AND <i>CITB</i> -FLAG ALLELES.....                                  | 140 |
| FIGURE S3. CHROMOSOMAL REPORTER FUSIONS FOR DETECTION OF ISRR ACTIVITY.....   | 141 |
| FIGURE S4. INTARNA PAIRING PREDICTIONS .....  | 142 |
| FIGURE S5. ENZYMATIC AND RBP ACONITASE SITES .....  | 143 |
| FIGURE S6. GROWTH IN BHI OF HG003 AND <i>CITB</i> MUTANT DERIVATIVES.....   | 144 |
| FIGURE S7. INTRACELLULAR CITRATE CONCENTRATION IN HG003 AND <i>CITB</i> MUTANT DERIVATIVES .....  | 145 |
| FIGURE S8: ISRR REGULATION OF ACONITASE AS A FEEDFORWARD LOOP.....  | 146 |
| REFERENCES .....  | 147 |
| G: <i>STAPHYLOCOCCAL</i> SRNA ISRR DOWN-REGULATES METHYLTHIOTRANSFERASE MIAB UNDER IRON-DEFICIENT CONDITIONS .....  | 148 |
| H: ADDITIONAL DISCUSSION.....   | 172 |
| I: REFERENCES.....  | 178 |
| J: RESUME SUBSTANTIEL EN FRANCAIS .....   | 201 |
| Introduction:.....  | 201 |
| Contenu de la thèse .....   | 203 |
| Régulation de l'expression de l'aconitase en conditions de carence en fer chez <i>S. aureus</i> : Contrôle par un ARN régulateur et activité moonlight..... | 205 |

|   |            |
|---|------------|
| <b>L'ARN régulateur IsrR réprime la méthylthiotransférase MiaB en conditions de carence en fer chez <i>S. aureus</i></b><br>..... | <b>208</b> |
| <b>Conclusion.....</b>  | <b>210</b> |
| <b>Schéma récapitulatif : .....</b>   | <b>211</b> |

# A: Acknowledgments

---

Je tiens tout d'abord à remercier mon directeur de thèse, Philippe, pour son soutien constant, ses remarques toujours pertinentes, les discussions scientifiques ou non que nous avons pu avoir ensemble, mais surtout pour m'avoir fait grandir et devenir le microbiologiste que je suis aujourd'hui.

Je remercie ensuite tous les membres du labo SRRB, ceux actuels (Etornam, Alan, Nello, Nara et Patricia), mais aussi les anciens (Kam Pou, Marick, Rodrigo et Elise). Je tiens à remercier tout particulièrement Rodrigo, pour m'avoir permis de travailler sur IsrR et m'avoir appris tant de choses. Merci également à Sveta et Claire pour leur aide précieuse dans la réalisation de mes dernières expériences.

Bien sûr, je remercie tous mes collègues de l'ex bâtiment 400 et de l'actuel bâtiment 23, qui sont devenus des amis, pour les bons moments que l'on a pu passer et le nombre incalculables de bières que nous avons pu boire. Alors bien sûr je n'en vais pas tous les citer mais je vais au moins citer mes comparses d'apéro : Lucie, Gabriela, Lisa, Emilie, Marion, Alexia, Adriana, Benoit, Kenza, Benjamin.

Je tiens ensuite à remercier les membres de mon comité de suivi, Olga et Sylvain, pour leur remarques toujours pertinentes et leur conseils bienveillants, mais également les membres de mon jury (Peter Redder, Pierre Mandin, Sarah Dubrac et Olga Soutourina) pour avoir accepté d'évaluer mes travaux.

Merci à tous mes amis de YourI2BC, pour m'avoir aidé dans l'organisation de tous ces événements.

Merci à Alex, pour toutes nos discussions au sujet de tout et de rien au magasin mais qui font vraiment du bien.

Merci à mes amis, en particulier Mathis et Thibaut, pour avoir égayé mes soirées autour d'une (ou plusieurs) bières, d'un match de foot, d'un épisode de Koh lanta ou d'un escape game après une dure journée au laboratoire.

Merci à mes parents, Cathy et Christophe, pour leur amour et leur soutien incommensurable durant mes années d'études qui m'ont permis d'en arriver là. Merci également à mon petit frère Paul.

Et enfin, un énorme merci à celle qui partage ma vie et sans qui je ne serai sûrement pas entrain d'écrire ce texte, Adèle. Tu es la personne qui compte le plus à mes yeux, celle qui m'a accompagné, soutenu et motivé durant ces trois ans, et qui me pousse toujours à aller de l'avant. Je t'aime.

*"J'ai commis une incroyable erreur de jeunesse, j'ai trop bien travaillé »- Michael Kyle*

## B: List of figures and tables

---

|  |     |
|--|-----|
| FIGURE 1: MOST COMMON FE-S CLUSTERS FOUND IN NATURE.   | 9   |
| FIGURE 2: FE-S CLUSTER BIOSYNTHESIS  | 10  |
| FIGURE 3: MODEL REPRESENTATION OF THE H-CLUSTER AND THE P-CLUSTER.   | 12  |
| FIGURE 4: HEME SYNTHESIS PATHWAYS IN BACTERIA  | 13  |
| FIGURE 5: FUR REGULATION   | 14  |
| FIGURE 6: EXAMPLES OF DIFFERENT FAMILIES OF SIDEROPHORES   | 17  |
| FIGURE 7: HEME ACQUISITION PATHWAYS IN GRAM-NEGATIVE (LEFT) AND GRAM-POSITIVE (RIGHT) BACTERIA.                                      | 20  |
| FIGURE 8: ORGANIZATION AND PREVALENCE OF THE FEO OPERON IN BACTERIA.   | 21  |
| FIGURE 9: OVERVIEW OF INORGANIC IRON ACQUISITION PATHWAYS IN <i>S. CEREVISIAE</i> , <i>L. MONOCYTOGENES</i> , AND <i>B. SUBTILIS</i> | 22  |
| FIGURE 10: DIFFERENT FAMILIES OF BACTERIAL IRON EFFLUX SYSTEMS   | 23  |
| FIGURE 11: UTILIZATION AND RENEWAL OF THE IRON POOL IN THE HUMAN BODY  | 26  |
| FIGURE 12: FUNCTIONING OF THE IRE-IRP RESPONSE   | 27  |
| FIGURE 13: METAL ION SPECIFICITY OF CITM AND CITH  | 31  |
| FIGURE 14: TRANSFORMATION OF CITRATE INTO OXALOACETATE BY THE CITRATE LYASE ENZYMATIC COMPLEX  | 33  |
| FIGURE 15: FORMATION OF PYRUVATE BY THE OAD ENZYMATIC COMPLEX  | 34  |
| FIGURE 16: GENETIC ORGANIZATION OF THE CITRATE FERMENTATION GENE CLUSTER ACROSS SPECIES  | 35  |
| FIGURE 17: ISOMERIZATION OF CITRATE INTO ISOCITRATE BY ACONITASE   | 37  |
| FIGURE 18: CONFORMATIONAL CHANGE OF CYTOPLASMIC ACONITASE (C-ACN) UPON IRON STARVATION   | 38  |
| FIGURE 19: REGULATION OF CITB EXPRESSION BY METABOLIC REGULATORS   | 41  |
| FIGURE 20: ROLE OF APO-ACONITASE IN THE PROTECTION OF ACNB MRNA  | 42  |
| FIGURE 21: MODE OF ACTION OF RIBOSWITCHES  | 44  |
| FIGURE 22: REGULATION OF YOYJ AND YONT MRNAS BY SR6  | 47  |
| FIGURE 23: REGULATORY FUNCTIONS OF SRNAS   | 48  |
| FIGURE 24: SECONDARY STRUCTURE OF RSAE   | 49  |
| FIGURE 25: ROLES OF HFQ IN GENE REGULATION IN BACTERIA   | 51  |
| FIGURE 26: SECONDARY STRUCTURE OF RYHB   | 52  |
| FIGURE 27: <i>S. AUREUS</i> IS THE LEADING CAUSE OF BACTERIAL INFECTIONS IN THE WORLD  | 57  |
| FIGURE 28: <i>S. AUREUS</i> RESISTANCE TO OXIDATIVE STRESS INSIDE NEUTROPHILS  | 60  |
| FIGURE 29: DIFFERENT IRON ACQUISITION SYSTEMS IN <i>S. AUREUS</i>  | 61  |
| FIGURE 30: SA AND SB BIOSYNTHESIS AND UPTAKE SYSTEMS IN <i>S. AUREUS</i>   | 63  |
| FIGURE 31: XENOSIDEROPHORES UPTAKE SYSTEMS IN <i>S. AUREUS</i>   | 64  |
| FIGURE 32: SECONDARY STRUCTURE OF ISRR   | 66  |
| FIGURE 33: LA REGULATION DU METABOLISME DE <i>S. AUREUS</i> EN CONDITIONS DE CARENCE EN FER  | 211 |
| TABLE 1: CONFIRMED BIFUNCTIONAL ACONITASES IN BACTERIA.....  | 38  |
| TABLE 2: FUNCTIONAL HOMOLOGS OF RYHB IN OTHER BACTERIA.....  | 55  |

## C. Introduction

---

### 1. Iron and living organisms

#### 1.1. Iron in the environment

Iron is the fourth most abundant element on Earth's crust, representing about 6.3% of its total mass (Frey and Reed 2012). It is a transition metal that exists under ten different oxidation states ranging from -2 to +7, but only two are relevant for biology:  $\text{Fe}^{2+}$  (ferrous) and  $\text{Fe}^{3+}$  (ferric) forms. On Earth, iron is mostly found under the  $\text{Fe}^{3+}$  form due to the presence of oxygen in the atmosphere. However,  $\text{Fe}^{3+}$  is poorly water soluble under aerobic conditions, making it difficult to use for living organisms that need oxygen for growth. On the contrary, in anaerobic, microaerobic, and acidic environments, the predominant form of iron is  $\text{Fe}^{2+}$ , which is soluble and therefore more available to living organisms.

#### 1.2. Iron in biology

##### 1.2.1. Biological properties of iron

Iron is a necessary element for almost all living organisms, two known exceptions being the bacteria *Borrelia burgdorferi*, which uses manganese instead (Posey and Gherardini 2000), and *Lactobacillus plantarum* (Archibald 1983). The crucial role of iron in biology is due to the very large redox potential of the  $\text{Fe}^{2+}/\text{Fe}^{3+}$  couple. Indeed, iron can serve as an electron donor and can use a large panel of ligands, which makes it a perfect fit for a plethora of proteins that are involved in biological processes such as aerobic and anaerobic respiration, tricarboxylic acid (TCA) cycle, photosynthesis, nitrogen fixation, DNA synthesis and many other processes (Chareyre and Mandin 2018). To fulfill this function, iron is mostly found as a co-factor alone or in combination with other elements such as sulfur to form iron-sulfur clusters, or as heme groups.

##### 1.2.2. Iron-sulfur clusters

In all three domains of life, most of the intracellular iron is not free but found in iron-sulfur clusters (Fe-S clusters). The Fe-S clusters are prosthetic groups necessary for the activity of the enzyme in which they are found. In nature, they exist in a variety of shapes and sizes, going from the simplest form  $2\text{Fe}-2\text{S}$  (rhombic cluster) to the most complex  $8\text{Fe}-7\text{S}$  (P-cluster). However, within proteins, Fe-S clusters are usually found in three main shapes:  $2\text{Fe}-2\text{S}$  (rhombic cluster),  $3\text{Fe}-4\text{S}$  (cuboidal cluster), and  $4\text{Fe}-4\text{S}$  (cuboidal cluster) (Esquilin-Lebron et al. 2021; Boncella et al. 2022) (**Figure 1**).

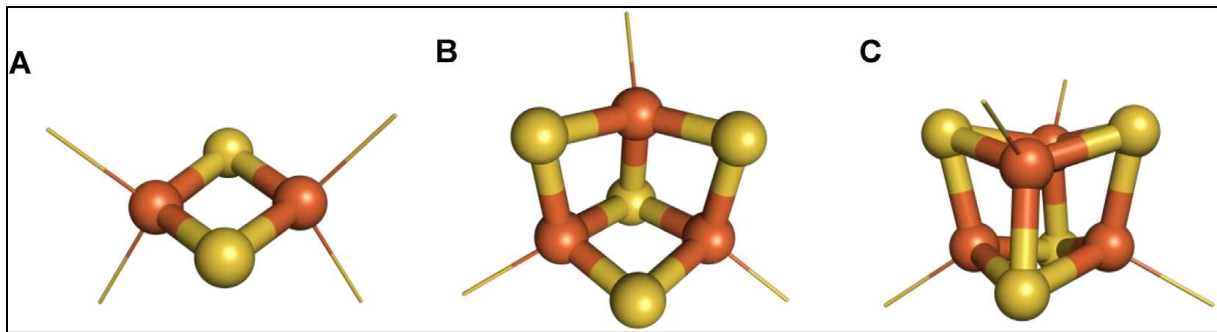


*Figure 1: Most common Fe-S clusters found in nature.*

Fe atoms are represented in orange while S atoms are represented in yellow. A) rhombic 2Fe-2S cluster; B) cuboidal 3Fe-4S cluster; C) cuboidal 4Fe-4S cluster. From (Boncella et al. 2022)

### I. Fe-S cluster biogenesis pathways in bacteria

In bacteria, three biosynthesis pathways for Fe-S clusters have been identified: Isc (Iron-Sulfur Cluster), Suf (Sulfur Formation), and Nif (Nitrogen Fixation). However, the repartition of these three systems among the bacterial kingdom is quite uneven.

The Nif system was discovered in the late '80s by the Dean's group while working on the nitrogenase maturation of the azototrophic bacteria *Azotobacter vinelandii* (Jaebson et al. 1989). Nitrogenase is a highly produced enzyme fixing nitrogen and containing iron-sulfur clusters; it was hypothesized and discovered that a specialized system dedicated to the production of the Fe-S clusters was necessary for its activity. In 1998, the same group discovered the Isc system, still in *A. vinelandii* (L. Zheng et al. 1998). While the Nif system is specific to nitrogen-fixating bacteria, Isc is a putative Fe-S biogenesis pathway that provides Fe-S clusters for other proteins. Finally, Takahashi and Tokumoto discovered the Suf system in *Escherichia coli* (Takahashi and Tokumoto 2002). It was initially thought that Suf was another system dedicated to the production of Fe-S clusters under stress conditions such as oxidative stress or iron starvation. However, recent work from the Barras's group showed that the presence of Isc and Suf in *E. coli* is exceptional and that most of the bacteria possess only one system being Suf but not Isc, even though Isc is the most studied (Garcia et al. 2022).

Although the three main Fe-S clusters biogenesis pathways are different in terms of components, the formation of Fe-S clusters follows a similar pattern in all three systems (**Figure 2**) (Roche et al. 2013; Garcia et al. 2022):

- 1) The sulfur atom is obtained via the degradation of L-cysteine into L-alanine by the action of a cysteine desulfurase (IscS, SufS, NifS)
- 2) The sulfur atom is combined with  $\text{Fe}^{2+}$  and electrons on a scaffold protein (IscU, SufB, SufC, SufD, NifU) to form a Fe-S cluster.
- 3) The Fe-S cluster is then transported and integrated into the apo-proteins by carriers (IscA, SufA), and the process is controlled by chaperones (HscA, HscB).

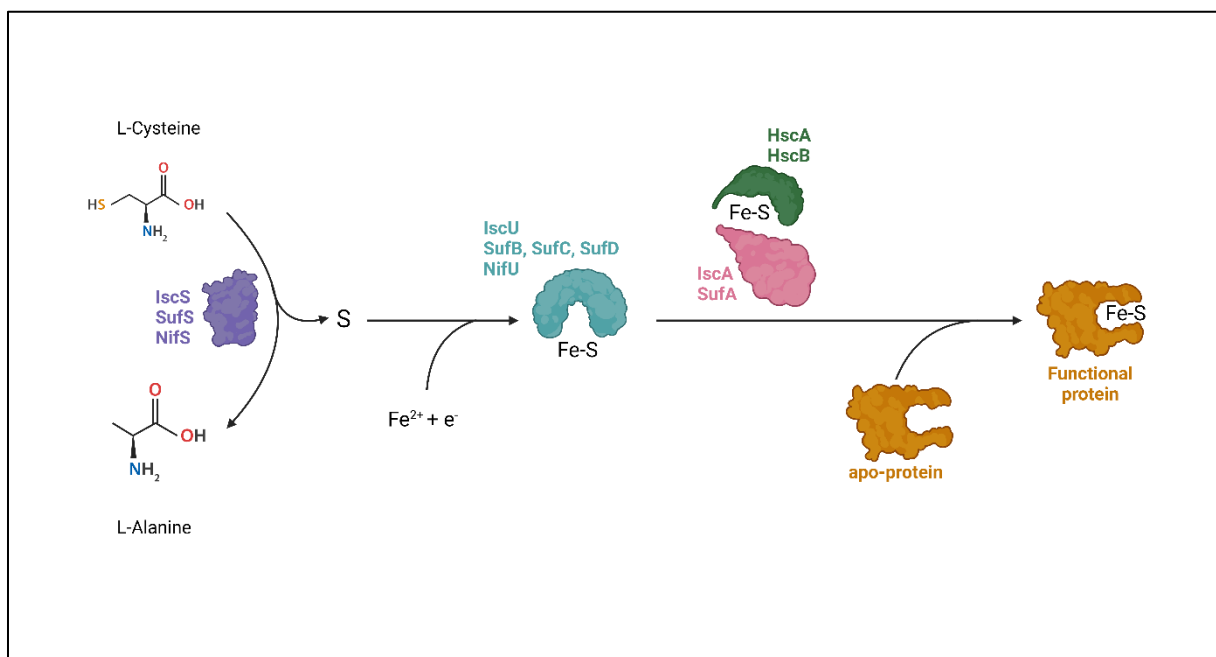


*Figure 2: Fe-S cluster biosynthesis*

L-cysteine is transformed into L-alanine via the action of a cysteine desulfurase (purple). The sulfur atom is then combined with iron and electrons to form a Fe-S cluster via a scaffold protein (light blue). The formed Fe-S cluster is then brought to apo-proteins (orange) by a carrier protein (pink), under the control of chaperones (green).

## II. Role of Fe-S clusters in bacterial metabolism

Due to their versatility in compositions and redox potential, Fe-S clusters are present in proteins with diverse functions, most of them being involved in electron transfer, catalysis, sulfur donation, and sensing (Johnson et al. 2005). For example, ferredoxins are one of the most important families of Fe-S cluster-containing proteins. Ferredoxins are small, acidic Fe-S clusters containing proteins found in all three domains of life that serve as electron carriers. The first ferredoxin has been discovered in the bacteria *Clostridium pasteurianum* (Mortenson, Valentine, and Carnahan 1962). In bacteria, ferredoxins have a 2Fe-2S, 4Fe-4S, or 4Fe-3S cluster. They serve in numerous metabolic reactions, such as pyruvate metabolism, nitrogen fixation, sulfate reduction, hydrogen production, and cytochrome P450 hydroxylation (Zanetti and Pandini 2013).

Due to their intrinsic redox potential, Fe-S cluster proteins can also be involved in gene regulation. This is for example the case of the SoxRS response in *E. coli*. Under normal conditions, the 2Fe-2S cluster of SoxR is reduced (Fe<sup>2+</sup>-Fe<sup>3+</sup> state). In the presence of oxidative stress, the reactive oxygen species (ROS) will cause oxidation of the 2Fe-2S cluster of SoxR (Fe<sup>3+</sup>-Fe<sup>3+</sup> state) that will allow it to activate the transcription of its only target *soxS* (H. Ding, Hidalgo, and Demple 1996; Gaudu and Weiss 1996; Gaudu, Moon, and Weiss 1997). *soxS* encodes a transcription factor regulating genes involved in oxidative stress resistance, such as the superoxide dismutase *sodA* or the nitroreductase *nfsA* (Pomposiello, Bennik, and Demple 2001).

In *Staphylococcus aureus*, several regulators are proteins containing Fe-S clusters, such as for example NreB, or AirS, a kinase part of a two-component system that senses oxygen (Sun et al. 2012). Under oxygen depletion, NreB is a histidine kinase that works in a two-component system with the regulator NreC by providing it phosphoryl groups for it to bind the promoter regions of nitrate and nitrite reductase to enhance their transcription (Fedtke et al. 2002). In presence of O<sub>2</sub>, the [4Fe-4S]<sup>2+</sup> cluster of NreB is first converted by oxidation into [3Fe-4S]<sup>+</sup>, which leads to the release of one ferrous ion, and later degraded by a series of oxidation events due to a prolonged exposition to oxygen (Unden and Schirawski 1997), leading to an inactive NreB that cannot activate NreC and therefore *S. aureus* lose the ability to use nitrate for respiration.

More complex Fe-S clusters also exist: [FeFe] hydrogenases possess the H-cluster that consists of a [4Fe-4S] cluster linked to [2Fe] by a cysteine (**Figure 3A**) (Bortolus et al. 2018); Nitrogenases with a P-cluster have a 8Fe-7S cluster derived from two 4Fe-4S clusters (**Figure 3B**) (Lee et al. 2009). However, these complex clusters are specific and not found for other proteins.

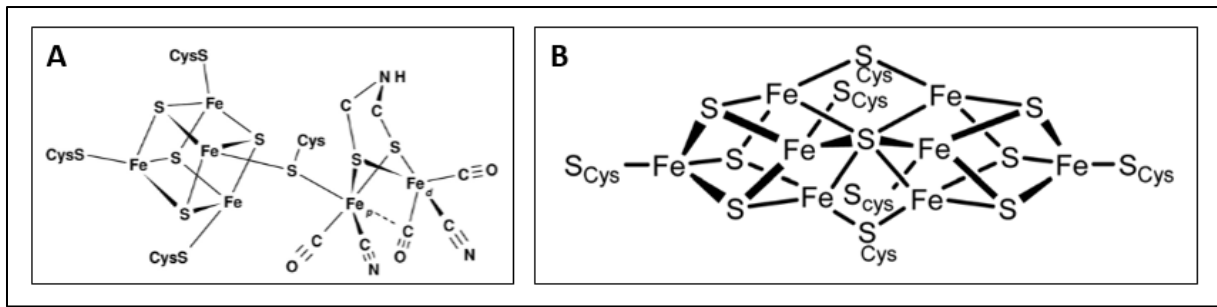


*Figure 3: Model representation of the H-cluster and the P-cluster.*

A: The H-cluster is composed of a cubane 4Fe-4S cluster (left) linked to a diiron (2Fe) cluster by a S-cysteine bridge. B: The P-cluster is formed by merging two 4Fe-4S clusters and losing an S element, which leads to forming an 8Fe-7S cluster. Adapted from (Lambertz et al. 2011) and (C.-H. Wang and DeBeer 2021).

### 1.2.3. Heme

#### I. Generalities

The total human body intracellular iron pool is approximately 4g, with about 3g found under the form of heme (Tong and Guo 2009). Heme is a cofactor containing an atom of metal, in majority iron, on the center of an organic ring called porphyrin. This iron atom can then bind diatomic gas such as dioxygen. Heme A, B and C are with different chemical formulas, with heme B being the most common type present in hemoglobin or myoglobin. Heme A and C are found in cytochromes A and C, respectively. Proteins in which the heme group is a cofactor are known as hemoproteins and serve for a large panel of functions such as electron transfer, substrate oxidation, metal ion storage, ligand sensing, and transport (Reedy and Gibney 2004). Hemoproteins are found in bacteria, eukaryotes, and archaea highlighting the biological importance of heme groups.

Heme is also a signaling molecule, by binding or dissociating from a protein. In humans, heme regulation affects transcription factors, translational activators, and other regulatory elements to control pathways such as oxidative stress response, circadian rhythm, and cell proliferation (Chambers et al. 2021).

In bacteria, heme is present in essential proteins such as cytochromes involved in the respiratory chain. Therefore, many bacteria possess a heme synthesis pathway (Gruss, Borezée-Durant, and Lechardeur 2012). Heme biosynthesis begins with a glutamyl-tRNA followed by different steps depending on the type of bacteria: Gram-negative bacteria use a "classical" pathway identical to Eukaryotes, while Gram-positive bacteria use a "non-canonical" pathway (Choby and Skaar 2016) (**Figure 4**). In addition, many pathogenic bacteria possess systems for the acquisition of exogenous heme (see page 18).

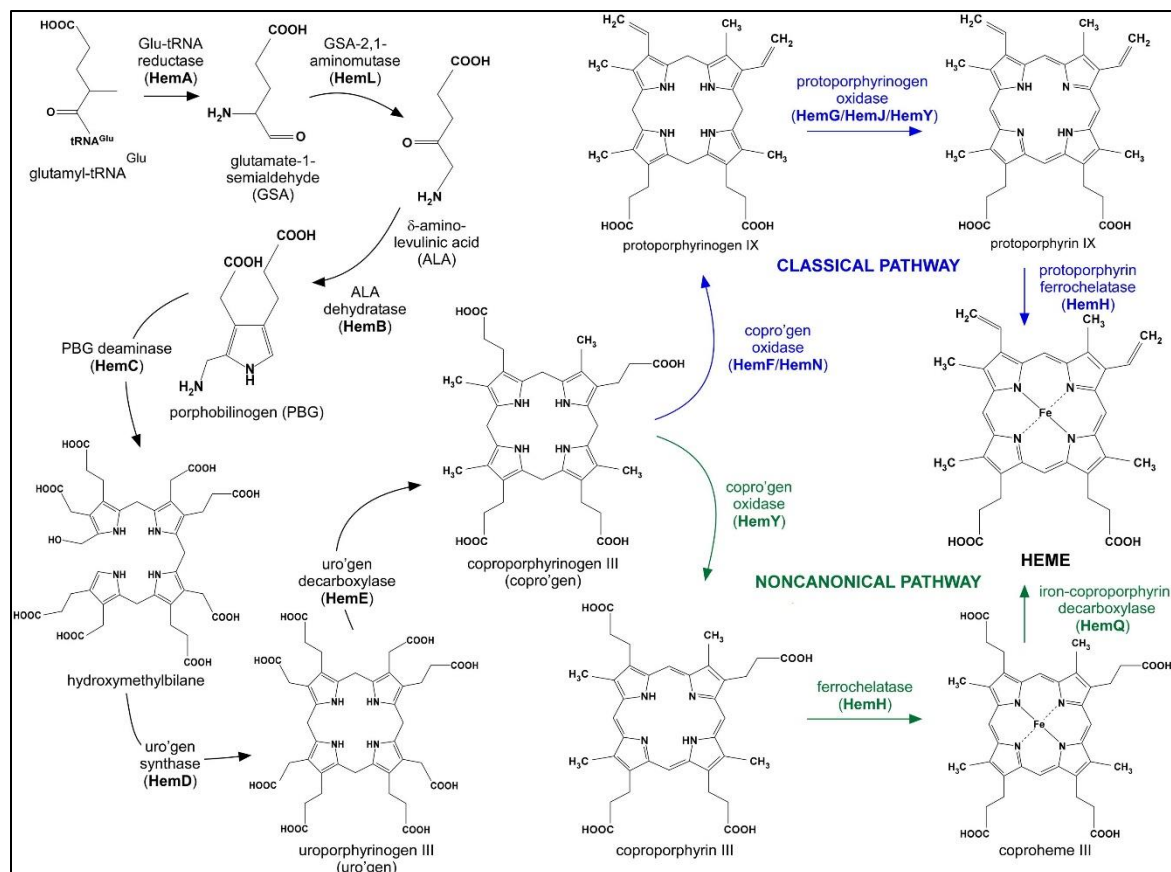


**Figure 4: Heme synthesis pathways in bacteria**

The formation of heme starts with a molecule of glutamyl-tRNA, which is transformed sequentially into coproporphyrinogen III by HemA, HemL, HemB, HemC, HemD, and HemE. In Gram-negative bacteria and Eukaryotes, the coproporphyrinogen III molecule is transformed into heme via the “classical pathway” (in blue) with an intermediate reaction to form protoporphyrin IX. In Gram-positive bacteria, heme is formed by the “non-canonical” pathway (in green) via the formation of coproheme III. From (Choby and Skaar 2016).

### 1.3. Iron homeostasis within the bacteria

Bacteria, like most living organisms, need iron to survive. For example, *E. coli* has up to  $10^6$  atoms of iron per cell (Andrews, Robinson, and Rodríguez-Quñones 2003). This concentration is similar in other bacteria but can go up to  $10^7$  atoms per cell in magnetotactic bacteria such as *Magnetospirillum magneticum* (Amor et al. 2020). Thus, iron starvation is often a growth-limiting factor. However, iron concentration within the cell has to be tightly regulated, since high concentrations cause the production of ROS via the Fenton and the Haber-Weiss reactions which can affect several processes such as protein or DNA integrity (Cornelis et al. 2011; Seixas et al. 2022). Oxidative stress can also affect the activity of some enzymes by promoting their mismetallation (Gu and Imlay 2013). Therefore, bacteria have acquired different systems to sense the intracellular iron concentration and adapt in order to survive.

### 1.3.1. The ferric uptake regulator (Fur)

The ferric uptake regulator (Fur) was first identified in 1981 from an *E. coli* mutant in which the siderophore production pathways were constitutively expressed (Hantke 1981). Its existence was predicted since it was already known that a low level of intracellular  $\text{Fe}^{2+}$  induces siderophore production in *E. coli* (Brot and Goodwin 1968). Fur is present in most prokaryotes, with the exception of the genus *Lactobacillus*. The different Fur proteins are grouped a superfamily of metallo-regulators, the FUR family, which includes Zur, Nur, Mur, and PerR associated respectively with the zinc uptake, nickel uptake, manganese uptake, and peroxide stress response (Steingard and Helmann 2023; Fillat 2014).

Fur is a DNA-binding protein. *In vitro*, it can use  $\text{Fe}^{2+}$ ,  $\text{Mn}^{2+}$ ,  $\text{Co}^{2+}$ ,  $\text{Zn}^{2+}$  and  $\text{Cd}^{2+}$  as cofactor. However, only  $\text{Fe}^{2+}$ ,  $\text{Mn}^{2+}$ , and  $\text{Co}^{2+}$  can regulate gene expression *in vivo*. Under normal conditions, the Fur- $\text{Fe}^{2+}$  complex is organized in homodimer, and each one of the two protomers possesses an iron-binding site. It binds to specific DNA sequences called Fur boxes, usually located within the promoter region of iron-regulated genes, thus preventing the binding of the RNA polymerase and gene transcription (Troxell and Hassan 2013). When intracellular  $\text{Fe}^{2+}$  levels are low, the Fur- $\text{Fe}^{2+}$  complex is dismantled from the Fur box and RNA polymerase can transcribe of the iron-regulated genes (**Figure 5**).

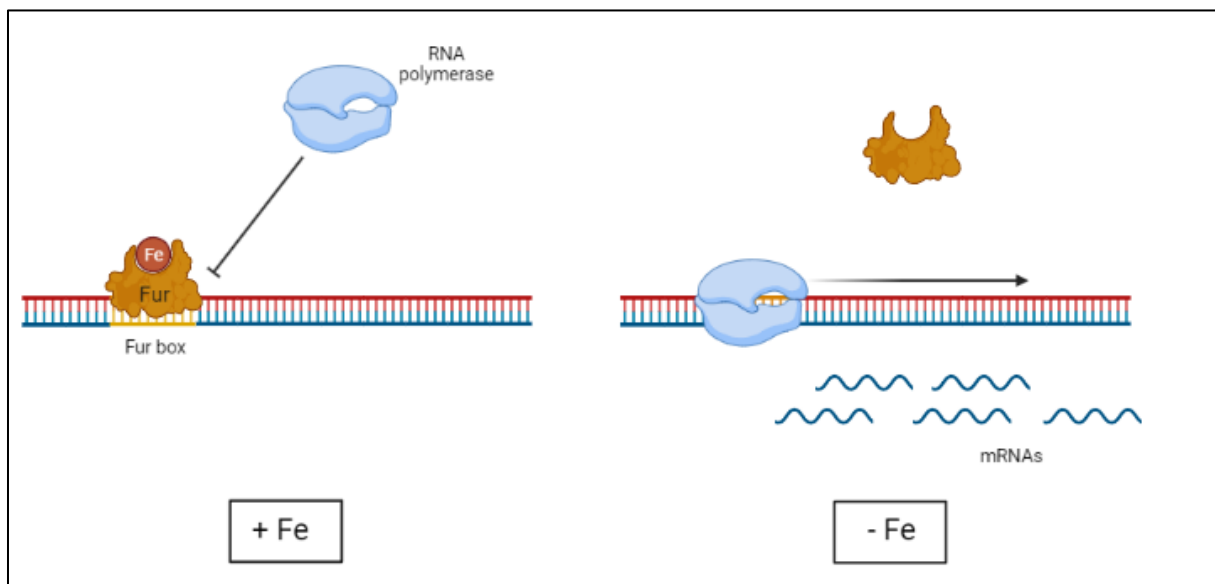


*Figure 5: Fur regulation*

Under iron-rich conditions,  $\text{Fe}^{2+}$  contributes to the stability of Fur (orange) homodimer, which in turn recognizes and binds to Fur boxes (yellow). The Fur complex on DNA prevents the RNA polymerase (blue) from binding to iron-regulated promoters and thus their transcription. When intracellular iron is low, iron-free Fur cannot bind to Fur boxes, and iron-regulated promoters are transcribed.

However, recent data challenge this model in *E. coli* by showing that *in vivo*, Fur activity is likely regulated by a [2Fe-2S] cluster rather than Fe<sup>2+</sup> (Fontenot et al. 2020; Fontenot and Ding 2023)

Fur target genes involved in iron homeostasis and the most studied targets of Fur are genes involved in iron acquisition systems such as siderophore synthesis. Fur also represses genes that are not directly involved in iron homeostasis. For example, in *E. coli* or *Vibrio parahaemolyticus*, Fur represses genes involved in flagellum assembly, so that the expression of the flagella is diminished in presence of iron, probably to prevent bacteria from moving to a more hostile environment (McCarter and Silverman 1989).

In some cases, Fur can also act as an activator. For example, in *Salmonella typhimurium*, the expression of Fur is necessary for the expression of key acid shock proteins (Hall and Foster 1996). However, these positive regulations can be indirect: in *E. coli*, Fur indirectly activate *sodB* expression by preventing *sodB* mRNA degradation normally induced by the RyhB sRNA (Masse and Gottesman 2002)

### 1.3.2. Iron import systems

When intracellular iron concentration is too low, the bacteria have to find a way to acquire iron from the environment. For this, bacteria have systems to extract and incorporate iron under different forms, which are active according to growth conditions.

#### I. Siderophores

The most studied iron acquisition pathway in bacteria is the production of siderophores. Under many growth conditions, free iron barely exists, and most of the iron is found in the insoluble Fe<sup>3+</sup>. Siderophores are secondary metabolites secreted into the environment to scavenge Fe<sup>3+</sup> to bacterial cells. The incorporation into the cell can be done directly via transporter specific for Fe<sup>3+</sup>, or the siderophore-bound Fe<sup>3+</sup> can be reduced into Fe<sup>2+</sup> by a ferric-chelate reductase present in extracellular media or anchored to the membrane of the bacteria (Miethke and Marahiel 2007). Almost all known bacteria produce at least one siderophore, meaning that siderophores probably represent the most important iron acquisition mechanism for bacteria (Kramer, Özkaya, and Kümmerli 2020).

In pathogens, conserved transcriptional regulators controlling iron homeostasis also regulate siderophore production. Siderophore production is therefore induced upon iron starvation. In Firmicutes such as *Staphylococcus* spp, *Bacillus* Spp and *Listeria monocytogenes*, this regulator is Fur. In other bacteria iron homeostasis can be regulated by the DtxR, MtsR, and SloR regulators, which are also functional and structural homologs of Fur (Sheldon and Heinrichs 2015).

The vast majority of known siderophores can be classified into four families, depending on the moiety donating the oxygen ligand used for Fe<sup>3+</sup> coordination. These molecules can be catecholate, phenolates, hydroxamates, or carboxylates deriving from either citrate or 2-oxo-glutarate (**Figure 6**). However, this classification is now more complex due to the fact that "mixed-type" siderophores that contain at least two classes of moieties in the same molecule have been discovered (Miethke and Marahiel 2007).

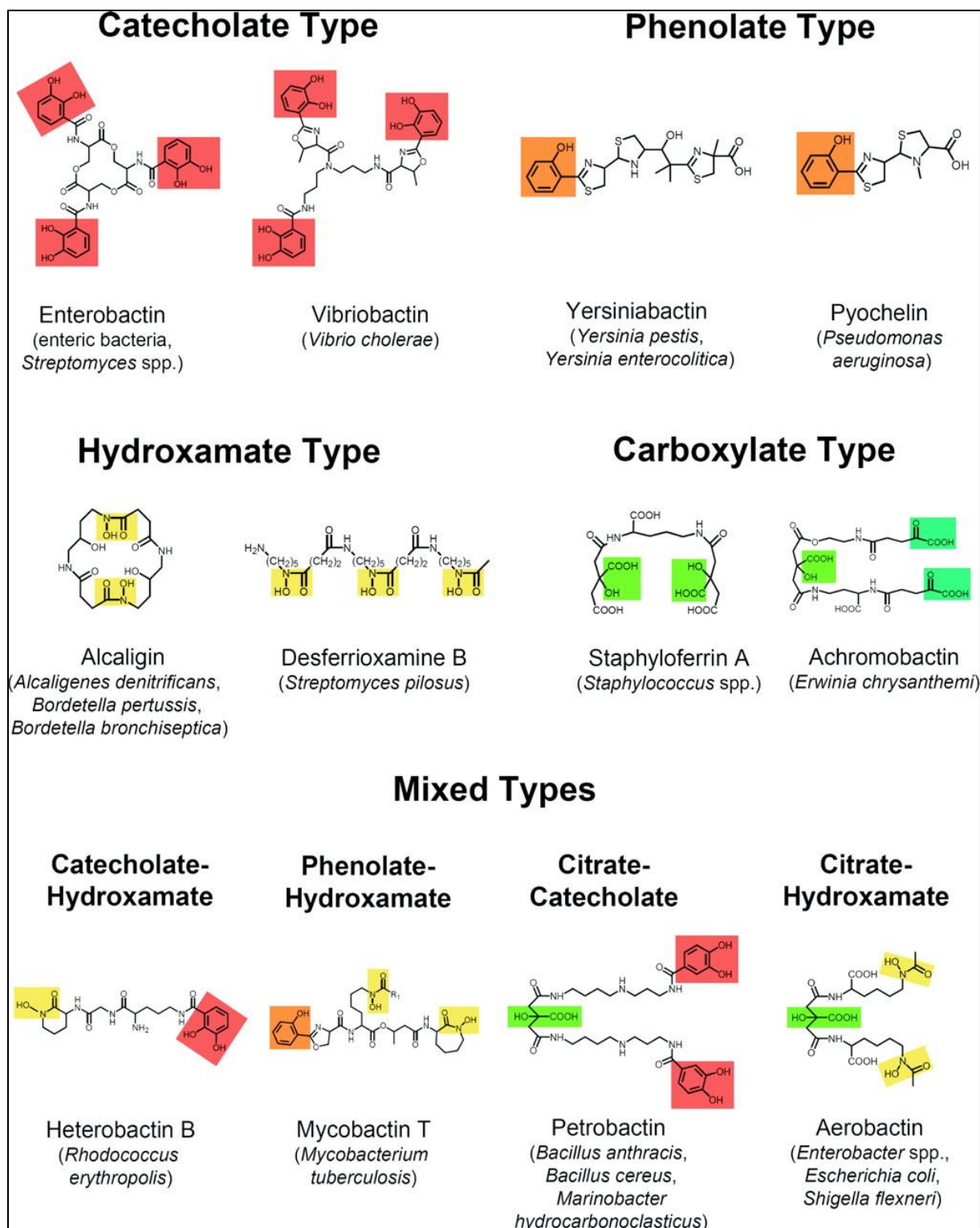


Figure 6: Examples of different families of siderophores

The moieties involved in iron coordination have been highlighted as indicated: catecholates in red, phenolates in orange, hydroxamates in yellow, carboxylates deriving from citrate in green, and carboxylates deriving from 2-oxo-glutarate in light blue. From (Miethke and Marahiel 2007).

Siderophores are molecules of less than 1 kDa that have an affinity of up to  $10^{-52}$  M for  $\text{Fe}^{3+}$ . This exceptionally high affinity enables them to scavenge iron directly from host proteins such as transferrins or lactoferrins, which generally have an affinity around  $10^{-20}$  (Baker and Baker 2004; Steere et al. 2012). However, the host can sequester siderophores using siderocalin, a protein secreted by neutrophils that bind specifically to negatively charged siderophores like the catecholate to prevent their iron-scavenging activity (Goetz et al. 2002). Therefore, most pathogens evolved by producing several types of siderophores, one being susceptible to siderocalin (usually a catecholate) and one immune. For example, some pathogenic strains of *Bacillus anthracis* or *Bacillus cereus* produce both bacillibactin (catecholate, susceptible to siderocalin) and petrobactin (citrate-catecholate, resistant to siderocalin) (Hotta et al. 2010).

Finally, some bacteria are also able to use siderophores produced by other bacteria for themselves, which are then called xenosiderophores. Their use is possible by the presence on the recipient bacteria of a transporter with broad specificity. The use of xenosiderophores provides a great advantage for growth in a mixed population, since these bacteria can use siderophores without having to spend energy to produce them (D'Onofrio et al. 2010). This hijacking can also be more specific; for example, *Staphylococcus lugdunensis* is not able to synthesize staphyloferrin A and B, but it can incorporate them because it possesses the HtsABC and SirABC transporters. Therefore, in co-culture with *S. aureus*, it will use the staphyloferrin A and B produced by this latter to enhance its growth (Brozyna, Sheldon, and Heinrichs 2014).

## II. Heme acquisition systems

Heme represents the greatest source of iron from the host. Heme groups are present in a great variety of proteins called hemoproteins, the most important being the hemoglobin, located within the erythrocytes. Hemoglobin contains about two-thirds of the total human iron, and one erythrocyte can contain about 280 million molecules of hemoglobin (Choby and Skaar 2016). Therefore, most pathogenic bacteria, such as *S. aureus*, have a preference for heme-based iron and have evolved to acquire it from the host (Skaar et al. 2004).

Since most of the heme is not free but rather in association with hemoproteins inside various cells, the first step of its acquisition is to degrade them by the action of hemolysins. These hemolysins are pore-forming toxins (PFTs) and are found in a large number of pathogens such as *Streptococcus pneumoniae*, *S. aureus*, *E. coli*, and *Mycobacterium tuberculosis*. They usually act by binding to a specific receptor and formation of multimers which will cause the formation of a pore in the membrane (Los et al. 2013).

After being damaged, the cells (for example erythrocytes) will release dissociated heme but also hemoglobin. The heme groups will then be scavenged by proteins secreted or present at the surface of the pathogens called hemophores (Sheldon, Laakso, and Heinrichs 2016; Contreras et al. 2014).

In Gram-negative bacteria, these hemophores are part of the HasA (heme acquisition system) family and were first isolated in *Serratia marcescens* before being found in several pathogens like *Pseudomonas aeruginosa* or *Yersinia pestis*. HasA-like hemophores are small proteins that are secreted through a type I secretion system. HasA-like hemophores are able to scavenge heme from a broad range of hemoproteins (Wandersman and Delepelaire 2012). Once bound to heme, HasA will recognize and bind to an outer membrane receptor protein, HasR, and will transfer the heme to it so it can be internalized (**Figure 7**).

In Gram-positive bacteria, the hemophores are not secreted proteins but rather cell-surface associated proteins (IsdABH) containing a NEAT domain, which are part of the iron-regulated surface determinant (Isd) pathway, which has been studied extensively in *S. aureus*. These proteins can bind hemoproteins and transmit heme to different transporters (IsdCDEF) that will allow them to be transported across the cell wall (**Figure 7**) (Skaar and Schneewind 2004). Once in the cytoplasm, heme is then dissociated by heme oxygenases (IsdGI) to recover only  $Fe^{2+}$ .

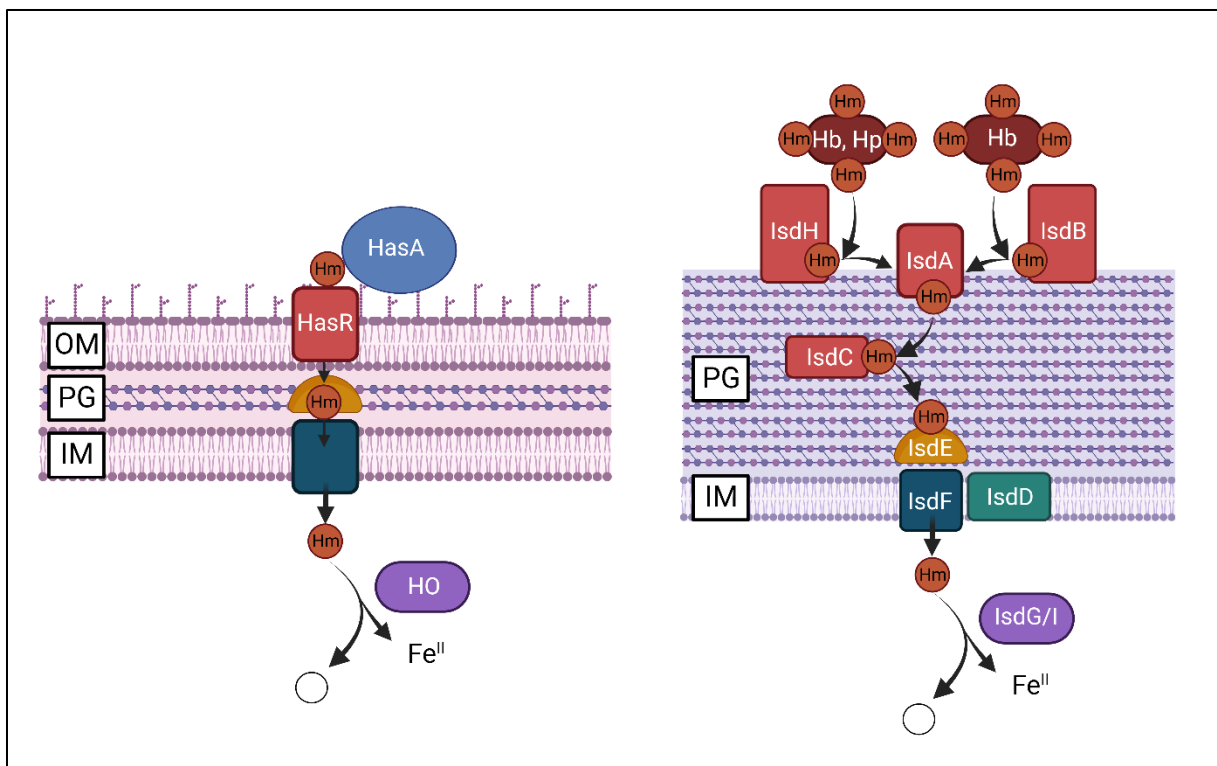


Figure 7: Heme acquisition pathways in Gram-negative (left) and Gram-positive (right) bacteria.

Organization and the localization of the two main heme acquisition systems in bacteria. OM: outer membrane; PG: peptidoglycan; IM: innner membrane; Hm: heme; Hb: hemoglo- bin; Hp: haptoglobin

### III. Inorganic iron uptake

In anoxic or acidic environments, most of the available is under the  $Fe^{2+}$  state. Bacteria have thus developed several systems that allow them to directly acquire available iron through the use of transport systems, even though their use is minor compared to the importance of siderophores and heme acquisition systems. These systems for the acquisition of inorganic iron are widely conserved in Gram-negative and Gram-positive bacteria and the most studied is the ferrous iron transport system present in the *feo* operon.

The *feo* operon, discovered in 1987 in *E. coli*, is composed of three genes *feoA*, *feoB*, and *feoC* (Hantke 1987). It is controlled by Fur, therefore repressed in presence of iron, and Fnr, a transcriptional activator active under anaerobic growth conditions. The *feoABC* operon is always expressed, but its expression increases by three-fold in the absence of oxygen. Homologs of the *feo* operon have been found in many Gram-negative and few Gram-positive bacteria (**figure 8**) (Lau, Krewulak, and Vogel 2016).

The *feoABC* operon consists of an iron permease, encoded by *feoB*, which possesses a G protein domain in the N-ter region, located in the cytoplasm. FeoA and FeoC are two small hydrophilic and cytoplasmic proteins. While FeoA is necessary for FeoB activity, FeoC is not always present (**figure 8**) and is required only in certain species such as *Vibrio cholerae* (Carpenter and Payne 2014).



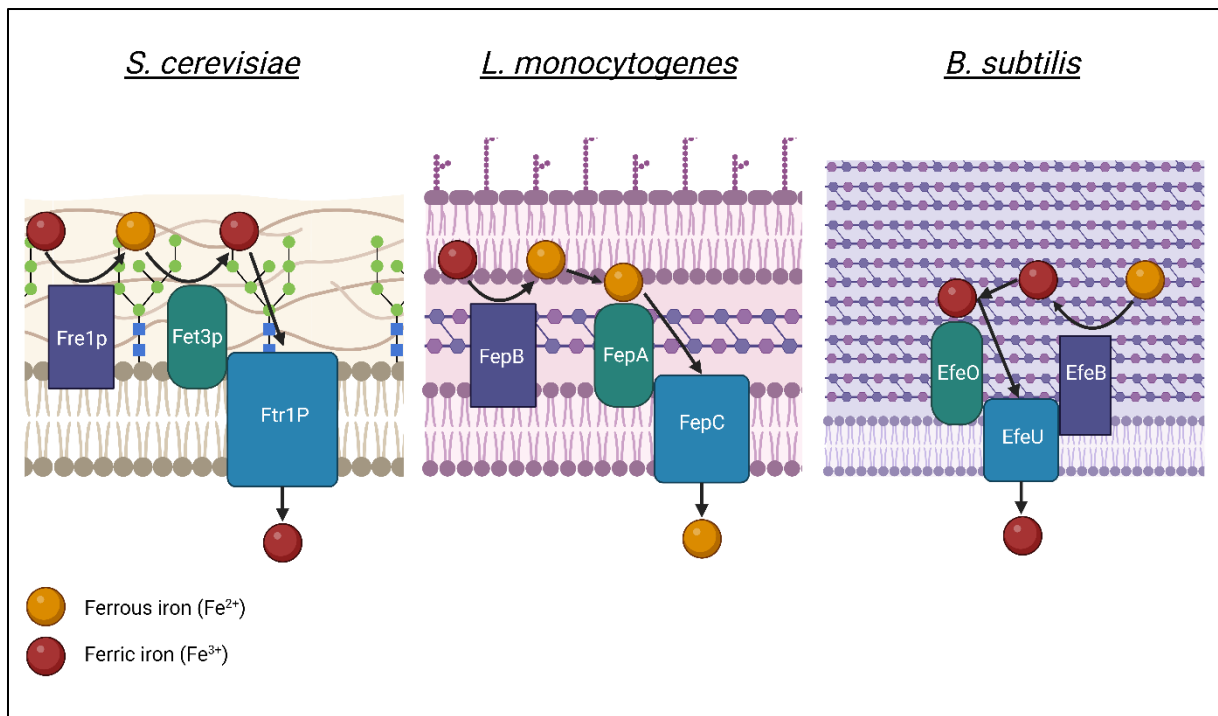


*Figure 9: Overview of inorganic iron acquisition pathways in S. cerevisiae, L. monocytogenes, and B. subtilis*

Homologs of the permease are in light blue, homologs of the imelysin-like protein are in green, and homologs of the reductase are in purple.

### 1.3.3. Iron efflux and storage systems

#### I. Iron efflux systems

As mentioned previously, iron is toxic at high concentrations because of its ability to form ROS via the Fenton reaction. Therefore, most prokaryotes possess one or several systems that allow them to either export iron or store it in specialized compartments. Usually, the expression of these systems is under the control of transcriptional regulators sensitive to oxidative stress, in such a way that a rise in the intracellular  $\text{H}_2\text{O}_2$  concentration will trigger the expression of iron-sequestering proteins and iron efflux systems (Pi and Helmann 2017). Several bacterial iron efflux systems have been discovered and are summarized in **Figure 10**.

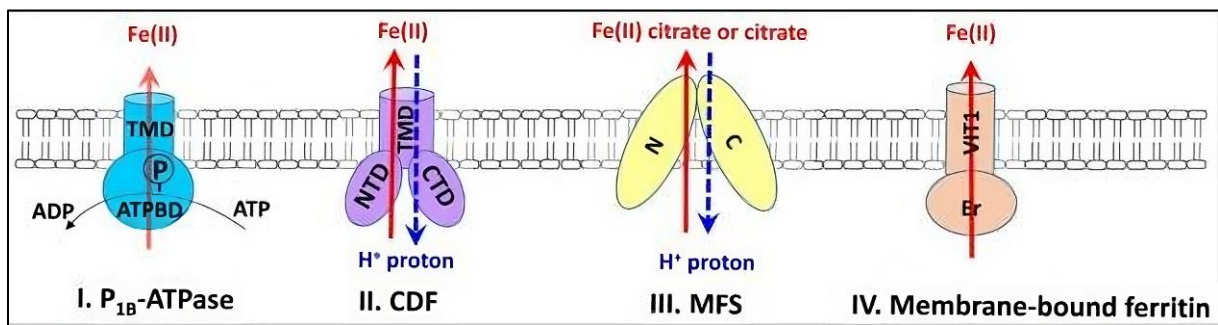


*Figure 10: Different families of bacterial iron efflux systems*

I) P1B-ATPase possesses a transmembrane domain (TMD) and an ATP binding domain (ATPBD). Hydrolysis of ATP into ADP provides the energy sufficient for  $\text{Fe}^{2+}$  efflux. II) Cation diffusor facilitators (CDF) are transmembrane proteins that use proton motive force to export  $\text{Fe}^{2+}$ . III) Major facilitator superfamily (MFS) transporters are composed of two transmembrane domains that use proton motive force to transport a substrate, which is usually ferrous citrate or citrate alone. IV) Membrane-bound ferritin possesses a ferritin-like domain (Er) and a vacuolar iron transporter domain (Vit1) located in the membrane that allows binding and transfer of  $\text{Fe}^{2+}$ . From (Pi and Helmann 2017).

P-type ATPases are transmembrane proteins, present in all domains of life, which can transport different ions or lipids through the membrane of the cell using the energy from ATP hydrolysis. P-type ATPases have been divided into five families according to their sequence, but we will focus here on type I ATPases that regroups the ones dedicated to the transport of transition metals. Type I ATPases are subdivided into two groups. Type 1A ATPases are ion pumps that import ions into the cells while type 1B-ATPases are the ones implicated in the efflux of metal ions (Kühlbrandt 2004). One example of a P1B-ATPase involved in iron efflux is the PerR-regulated transporter PmtA from the *Streptococcus* genus, in which a  $\Delta pmtA$  mutant shows greater concentrations of intracellular iron and increased resistance to streptonigrin, a  $\text{Fe}^{2+}$ -activated antibiotic (C. Zheng et al. 2019). It has also been shown that PmtA prevents the mismetallation of SodA by Fe during oxidative stress (Turner et al. 2019). Other known P1-type ATPases involved in iron efflux are PfeT in *B. subtilis*, DR1440 in *Deinococcus radiodurans*, and FrvA in *L. monocytogenes* (Guan et al. 2015; Dai et al. 2018; Pi et al. 2016).

Cation diffusion facilitators (CDFs) are transmembrane proteins found in all three domains of life that are able to transport heavy metal ions across the cellular membrane using the proton motive force. All CDFs have the same organization, with a transmembrane domain and at least an N-ter cytoplasmic domain, which may be in charge of metal selectivity, even though this aspect is still poorly understood (Kolaj-Robin et al. 2015). Interestingly, CDFs are ubiquitous and do not respond to Fur regulation. The most studied bacterial CDF is FieF in *E. coli*, where a  $\Delta fieF$  mutant shows a decreased iron tolerance upon *fur* deletion that causes an excess of intracellular  $\text{Fe}^{2+}$  (Grass et al. 2005). Other bacterial CDFs are AitP in *P. aeruginosa*, where its deletion

leads to an increased sensitivity to  $\text{Fe}^{2+}$  and  $\text{Co}^{2+}$ , and FeoE in *Shewanella oneidensis* (Salusso and Raimunda 2017; Bennett, Brutinel, and Gralnick 2015)

The Major facilitator superfamily (MFS) is a family of membrane proteins that can transport small molecules using the proton motive force (Kumar et al. 2020). The MFS contains symporters, uniporters, and antiporters, but we will focus on antiporters since they are the ones involved in iron efflux systems. All the MFS are composed of two transmembrane domains that contain each six transmembrane helix and the substrate binds at the interface between these two domains (Yan 2015). One known example of an MFS involved in iron homeostasis is the IceT transporter from *S. typhimurium*. IceT was discovered using a transposon library looking for mutations that increased sensitivity for streptonigrin and transport  $\text{Fe}^{2+}$ -citrate out of the cell. The *iceT* gene is part of an operon whose expression is induced by nitric oxide and modification of iron homeostasis not mediated by Fur (Frawley et al. 2013). Interestingly, the authors also show that *iceT* expression increases resistance to clinical antibiotics such as ampicillin or ciprofloxacin. This resistance is probably due to the redirection of citrate from the TCA cycle that causes a reduction of the growth rate, as shown in *M. tuberculosis* (Baek, Li, and Sasseti 2011).

Membrane-bound ferritin A (MBFa) is a transmembrane protein that has been discovered for the first time in plants pathogens such as *Agrobacterium tumefaciens* or *Bradyrhizobium japonicum* (Bhubhanil et al. 2014). MBFa proteins are composed of a C-terminal domain located in the membrane and similar to the VIT1 domain of *Arabidopsis thaliana* that transport iron into vacuoles, and an N-terminal domain which is ferritin-like (Bhubhanil et al. 2014). In *A. tumefaciens*, *mbfA* expression is repressed by Irr, a transcriptional regulator that represses genes involved in iron storage when iron levels are low (Ruangkiattikul et al. 2012).

## II. Iron storage systems

To ensure their viability, bacteria maintain a pool of available intracellular iron. Typically, this iron pool will serve for the metalation of iron-containing proteins, which represent 60% of the intracellular iron in cells in *E. coli* (Hristova et al. 2008). However, because of the danger that iron represents for the bacteria, this iron pool is not maintained free but rather stored by dedicated proteins.

The main bacterial iron storage proteins belong to the ferritin family. Among them are bacterial homologs of eukaryotic ferritins called (Ftns), heme-containing ferritins (Bfrs), and mini ferritins. These ferritin homologs have the same goal: sequester  $\text{Fe}^{2+}$  by first oxidizing it into  $\text{Fe}^{3+}$  and storing it inside a cavity (Bradley et al. 2020). Usually, the expression of mini-ferritins is regulated by transcriptional regulators sensitive to oxidative stress such as OxyR, whereas Ftn and Bfr protein expression is

rather controlled by repression under iron-rich conditions. In *E. coli*, the *ftn* and *bfr* genes are repressed by the small regulatory RNA RyhB, which is only expressed under iron starvation conditions (Haikarainen and Papageorgiou 2010; Masse and Gottesman 2002).

In the past few years, a novel class of storage systems has gained interest: the encapsulins. They are icosahedral, self-assembling nano-compartments with a diameter between 25 and 42 nm that were initially found in culture of *Brevibacterium linens*, but were also observed in *M. tuberculosis*, *Thermotoga maritima*, and *Streptomyces* (Gabashvili et al. 2020). Encapsulins were initially misidentified as bacteriocins due to their specific form or thought to be secreted proteases (Giessen 2022). Encapsulins can store different kinds of proteins, including those involved in iron storage such as ferritin-like proteins (Flps). In *Micrococcus xanthus*, the proteins necessary for the encapsulin are expressed but the assembly of the encapsulin only happens upon starvation conditions; The encapsulins are loaded with iron (about 28500 Fe atoms per compartment) and protect the cells from oxidative stress (McHugh et al. 2014)

## 1.4. Iron homeostasis within the host

### 1.4.1. Repartition and acquisition of iron

As mentioned in page 5, an average body is estimated to contain approximately 4g of iron, and about 70% of it is used by red blood cells for tissue oxygenation. The rest is either found in macrophages degrading senescent red blood cells, in myoglobin for muscle oxygenation, or in iron-containing proteins. The leftover iron not used is stored in the liver where it is bound to a protein called ferritin (Gkouvatsos, Papanikolaou, and Pantopoulos 2012). Each day, around 30 mg of iron is transported from the liver to the bone marrow by plasma transferrin (Tfn) where it is used for heme biosynthesis and the production of new erythrocytes.

Dietary iron absorption incorporates between 1 and 2 mg of iron per day, which is far less than what is needed for the renewal of erythrocytes. Therefore, the biggest iron source is not our diet, but rather the recycling of pre-existing iron. Indeed, when blood cells enter into senescence, they are phagocytosed by macrophages through a process called erythrophagocytosis. During this process, the heme groups are degraded by heme oxygenases (HO-1 or HO-2) that produce CO, biliverdin, and inorganic ferrous iron, which is then exported to the plasma transferrin through a specific transmembrane transporter ferroportin (Ftn) to be reused (Gkouvatsos, Papanikolaou, and Pantopoulos 2012; Galaris, Barbouti, and Pantopoulos 2019) (**Figure 11**).

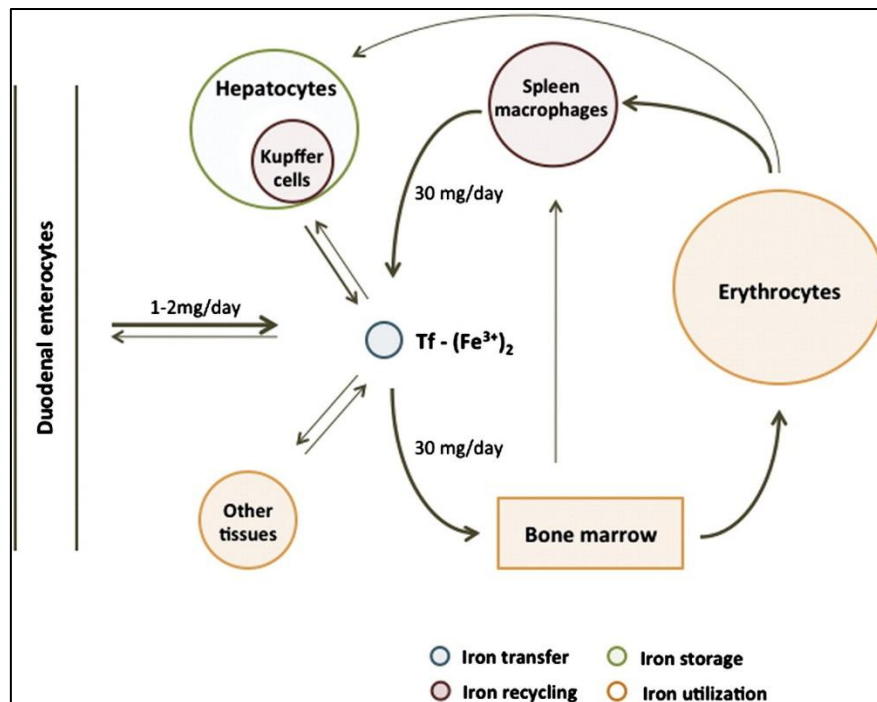


*Figure 11: Utilization and renewal of the iron pool in the human body*

More than 30 mg of iron is needed per day for erythrocytes and other cells. Iron is brought into the bone marrow by transferrin for the formation of new erythrocytes. Senescent erythrocytes are degraded by spleen macrophages; released  $\text{Fe}^{2+}$  binds to transferrin to be recycled. From (Gkouvatsos, Papanikolaou, and Pantopoulos 2012)

#### 1.4.2. Mechanisms of regulation of iron homeostasis

Regulation of the iron levels is necessary for the correct functioning of the cells, but also in the case of infection where iron restriction is part of the defense response called nutritional immunity (see page 28). Therefore, elaborated mechanisms were acquired during the evolution to sense and regulate intracellular iron levels. Iron homeostasis is mostly maintained at the intracellular and systemic levels (Bogdan et al. 2016).

At the intracellular level, regulation of iron levels is made via iron responsive elements (IREs) and iron regulatory proteins (IRPs). The IRP response is mediated by two iron regulatory proteins called IRP1 and IRP2. IRP1, also named ACO1, is bifunctional protein. When iron is abundant, ACO1 is a functional aconitase. However, upon iron starvation, ACO1 loses its Fe-S cluster and becomes the apoprotein IRP1. Even though IRP2 has a 79% sequence homology with IRP1, it is not a functional enzyme and is able to bind IREs constitutively. However, IRP2 possesses a signal that promotes its degradation by the proteasome upon iron-rich conditions (Hentze et al. 2010). IRP1/2 regulates the expression of genes involved in iron uptake or storage/export by binding on IREs, which are specific RNA stem-loops located either

in 5' or 3' of the mRNA targets. If the IRE is in 5', binding of the IRP prevents the translation of the target mRNA. If the binding is on 3', then binding of the IRP prevents the degradation of the mRNA by endonucleases. Usually, IRPs bind on the 5' region of genes involved in iron export or iron storage (*e.g.* ferritin) and bind on the 3' region of genes involved in iron uptake (*e.g.* transferrin receptor) (Bogdan et al. 2016; Wallace 2016) (**figure 12**). This double regulation allows for a simultaneous downregulation of genes preventing iron utilization and upregulation of genes involved in iron uptake.

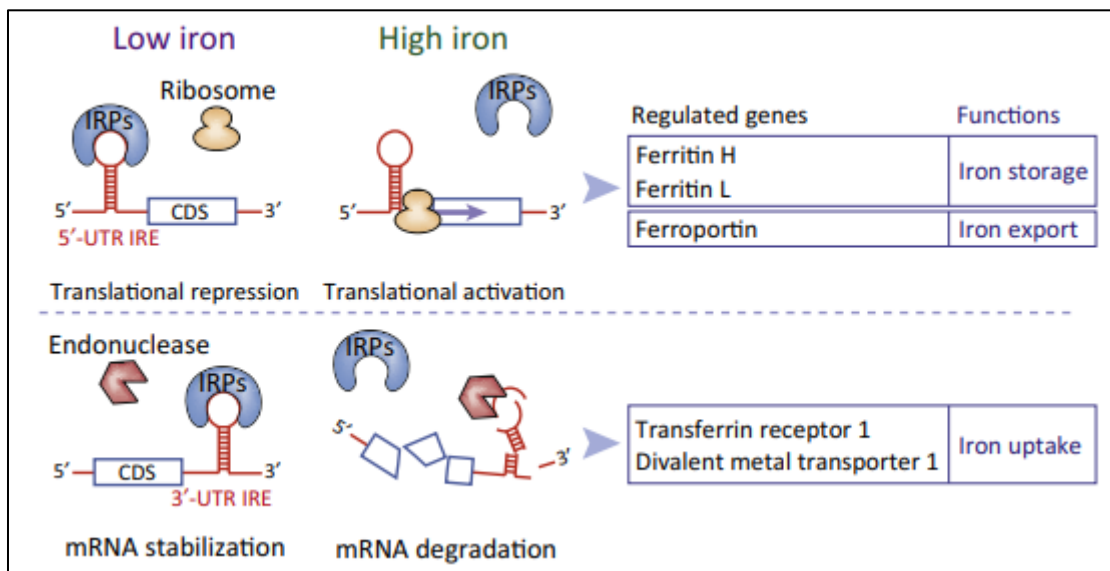


Figure 12: Functioning of the IRE-IRP response

IRPs regulate either the translation or the stability of target mRNAs depending on the localization of the IRE. If the IRE is in the 5'UTR, the translation is impaired by iron starvation. If the IRE is in the 3'UTR, the stability of targeted mRNAs is increased by iron starvation. From (Bogdan et al. 2016).

At the systemic level, iron homeostasis is maintained by two important proteins: hepcidin and ferroportin. Hepcidin is a small hormone (25 amino acids, 2.7 kDa) produced by the liver. Ferroportin is a specific iron transporter present at the surface of macrophages and hepatocytes, in charge of releasing iron resulting from dietary absorption, storage, or recycling by macrophages into the blood plasma. Hepcidin is produced and secreted in response to high iron concentration and inflammatory stimuli. It then binds to the extracellular binding loop of the ferroportin transporter and triggers its degradation by the ubiquitination system, thus reducing the rate of iron transfer to transferrin (Hentze et al. 2010; Ganz 2013).

#### 1.4.3. Human diseases linked to iron metabolism

Disruption of iron homeostasis leads to iron deficiency or overload. It can be transient or the result of chronic conditions caused by genetic diseases.

Iron-deficiency anemia (IDA) is the most common nutritional deficiency in the world, with an estimated 30% of the population affected according to the World Health Organization (WHO) (Kumar et al. 2022). IDA is a global health issue, predominantly in third-world countries. 2 to 9% of people have IDA in USA or Canada whereas this number increases up to 60% in sub-Saharan Africa (Kassebaum et al. 2014). IDA is caused by a large panel of physiological factors, such as pregnancy or menstruation. However, it can also be the result of pathological conditions like surgery or the use of aspirin (Lopez et al. 2016).

Conversely, iron overload is also deleterious, and can be caused by several factors, most of them being genetic disorders. Hemochromatosis is a common disease associated with iron overload. It can result from mutations in genes involved in hepcidin synthesis or maturation. As a result, hepcidin levels decrease and an excess of iron is released into the blood plasma by ferroportin. In other types of hemochromatosis, mutations affects the ferroportin transporter, resulting in reduced secreted iron and thus its accumulation within cells (Siddique and Kowdley 2012). Iron-loading anemia is another iron disorder caused by a massive erythropoiesis and therefore stimulates iron absorption. Examples of iron-loading anemias are sideroblastic anemia, thalassemia, and congenital dyserythropoietic anemia (Jr Benz 2015).

Iron homeostasis disorders have a crucial role in bacterial infections since an excess of iron within the host facilitates the growth of pathogenic bacteria. Therefore, humans have developed several strategies in order to prevent bacteria from acquiring the circulating iron through a series of processes called nutritional immunity.

## **1.5. Nutritional immunity**

The concept of nutritional immunity was first used in 1975 as a series of mechanisms by which the host is going to defend itself against bacterial infection by sequestering trace metals in order to prevent microbial growth (Weinberg 1975). Even though most of the studies about nutritional immunity are focused on iron, nutritional immunity also englobes the sequestration of zinc and magnesium (Murdoch and Skaar 2022; Hood and Skaar 2012). Different processes involved in nutritional immunity ensure that no iron is scavenged by pathogens:

In response to bacterial infection, hosts produces different inflammatory signals such as IL1-like and IL-2 cytokines. These cytokines are recognized by the hepatocytes and trigger a signaling cascade that leads to hepcidin production. Hepcidin binds to ferroportin and promotes its degradation, causing a loss of iron efflux and its accumulation inside macrophages. This process, called hypoferremia of infection, allows for a 30% reduction of serum iron concentration (Lokken, Tsohis, and Bäumlner

2014; Nemeth et al. 2003).

- Some bacteria scavenge iron from heme. Upon infection, red blood cells are lysed releasing hemoglobin and heme. In response, hosts secrete haptoglobin and hemopexin that capture hemoglobin and heme, respectively (Choby and Skaar 2016).
- All circulating iron that is not part of heme groups is bound to transferrin, which makes it available for bacteria that do not possess iron acquisition systems such as siderophores.
- Macrophages can be the targets of several intracellular pathogens, such as *M. tuberculosis* or *S. enterica*. In response to infection, they will use the natural resistance-associated macrophage protein 1 (NRAMP1) to export all nutrients from the lysosome to the cytoplasm (Brenz et al. 2017).
- Neutrophils will secrete lactoferrin, calprotectin, and siderocalin. Lactoferrin and calprotectin are Fe-scavenging proteins and siderocalin can bind to bacterial siderophores, thus preventing their activity (Murdoch and Skaar 2022).

## 2. The role of citrate metabolism in bacteria

Citrate, or citric acid, is an organic, weak acid. Its name comes from the fact that it was discovered initially in fruits from the *Citrus* family. Citrate is commonly used in the industry as a flavoring or an acidifier, but it is mostly known for being the first intermediate of the tricarboxylic acid (TCA) cycle, a metabolic pathway found in all aerobic organisms that provide energy for the cell. However, the acquisition, synthesis, and utilization of citrate within the cell is not dedicated only to the production of energy but covers several aspects of bacterial metabolism.

### 2.1. Synthesis of citrate: The citrate synthase

Citrate is formed by the irreversible condensation of oxaloacetate and acetyl-CoA in the first step of the TCA cycle. This reaction is catalyzed by an enzyme called citrate synthase (CS). CSs represent a family of enzymes present in all three domains of life but are classified into two types, I and II, according to their oligomerization. Type I CSs are organized in dimers found in eukaryotes, Gram-positive bacteria, and archaea. Type II CSs found in Gram-negative bacteria have a higher molecular weight and are organized in hexamers (Wiegand and Remington 1986).

Another difference between type I and type II CSs is their regulation. Since CSs are producing energy, their expression is regulated by the level of energy present in the cell, which is represented by ATP and NADH. Therefore, high levels of ATP to ADP

and NADH to NAD<sup>+</sup>, which represent a high-energy supply within the cell, are inhibitors of CSs, unlike the presence of ADP. However, while inactivation by ATP and NADH is isosteric (in the same interaction site as the acetyl-CoA) for type I CS, the inhibition of type II CS by NADH is allosteric (NADH binds on a different site than the one that binds acetyl-CoA) (Harford and Weitzman 1975).

The role of CSs is to provide citrate to the TCA cycle to perpetuate the cycle and produce energy. However, recent studies have shown that CSs could also have other roles. For example, in *Caulobacter crescentus*, CS CitA could act as a moonlighting protein and serve to control the cell cycle via the transcriptional regulator CtrA (Bergé et al. 2020). Some bacteria have also developed a second citrate synthase to fulfill their needs. For example, in addition to CitZ, *S. aureus* possesses SbnG which is expressed only upon iron starvation and whose role is to provide citrate for the synthesis of staphyloferrin, a *S. aureus* siderophore (Sheldon, Marolda, and Heinrichs 2014).

## 2.2. Acquisition of exogenous citrate

Even if bacteria can synthesize citrate through the TCA cycle, they can also acquire it from the environment. Most of the citrate found in exogenous media is complexed with metal ions. Therefore, its acquisition is via the use of specific transporters dedicated to the transport of complexed citrate. These transporters belong to the vast majority of the superfamily of CitMHS transporters. Most of the bacterial citrate transporters known to date are symporters that use the energy of protons or sodium ions to import citrate complexed with divalent ions (Sobczak and Lolkema 2005). However, in some cases, citrate transporters are antiporters, such as CitW from *Klebsiella pneumoniae* that antiports citrate with acetate (Kastner et al. 2002), or CitT from *E. coli* that antiports citrate with succinate, fumarate or tartrate (Pos, Dimroth, and Bott 1998).

The most studied citrate transporters are CitM and CitH from *B. subtilis*. Interestingly, even though both transport metal-citrate, they both have an affinity for specific metal ions (see **Figure 13**) (Krom et al. 2000). Since then, homologs from CitM and CitH have been found in *Streptomyces coelicolor*, *Campylobacter jejuni*, and *Neisseria meningitidis*. So far, no free citrate transporter has been found in bacteria. One explanation is that citrate which has a high affinity for metals is mainly found in this form in the environment. Furthermore incorporating metal-citrate provides simultaneously energy and metal (Huta et al. 2012).

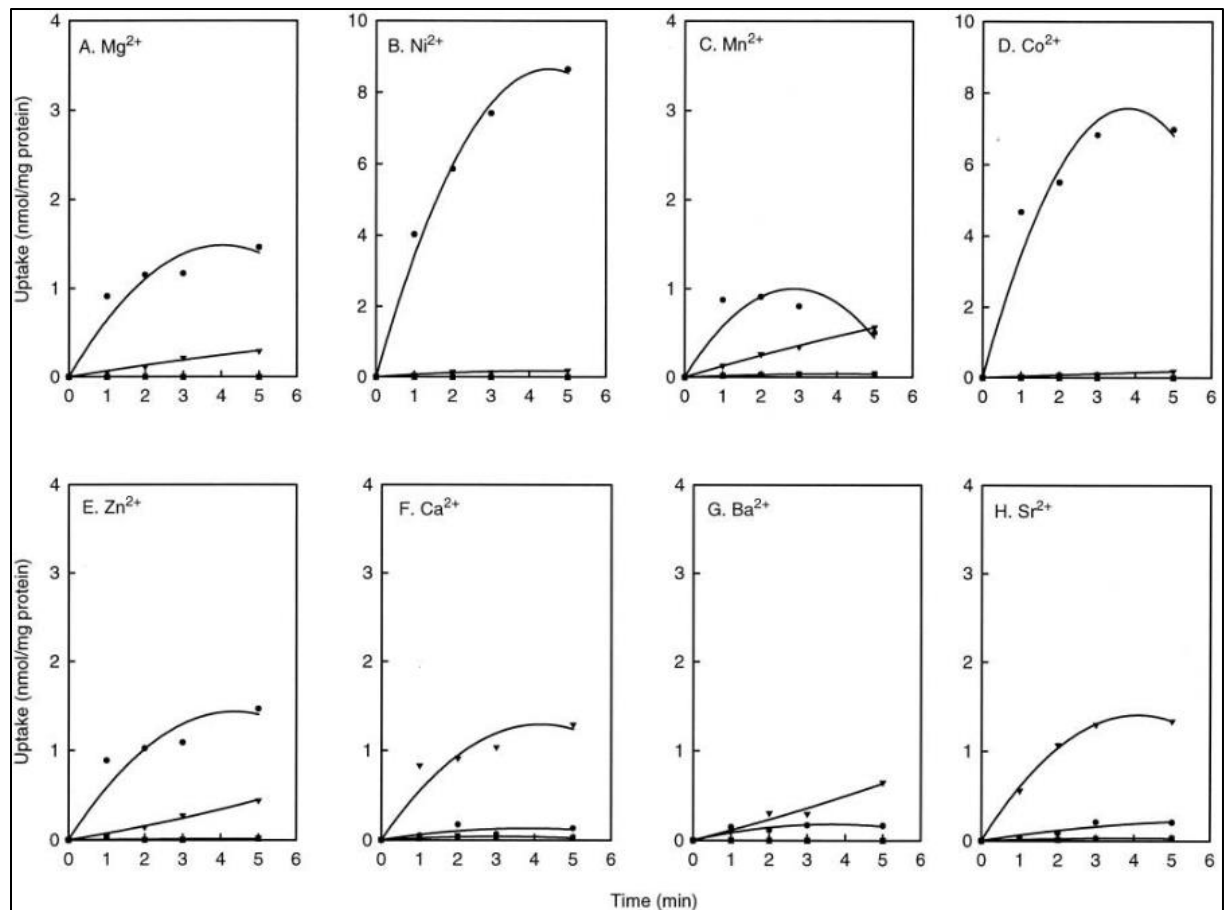


*Figure 13: Metal ion specificity of CitM and CitH*

Measurement of [<sup>14</sup>C] citrate uptake in *E. coli* harboring an empty plasmid (■), a plasmid expressing CitM (●), or a plasmid expressing CitH (▼) in the presence of 1 mM Mg<sup>2+</sup> (A), Ni<sup>2+</sup> (B), Mn<sup>2+</sup> (C), Co<sup>2+</sup> (D), Zn<sup>2+</sup> (E), Ca<sup>2+</sup> (F), Ba<sup>2+</sup> (G), Sr<sup>2+</sup> (H). From (Krom et al. 2000).

### 2.3. Citrate as a carbon source

Citrate is one of the intermediates of the TCA cycle, which is widely conserved in organisms able to grow in the presence of oxygen. However, bacteria that grow in anaerobic conditions have to develop alternative metabolic pathways as they cannot use the TCA cycle due to the necessity of the NADH and FADH<sub>2</sub> produced to transfer their electrons. One of these alternatives is the use of citrate as a carbon source through citrate fermentation, also called the reverse TCA (rTCA) cycle. Citrate fermentation occurs in anaerobic organisms, but it can also happen in the presence of oxygen when the bacteria do not possess a fully functional TCA cycle (for example lactic acid bacteria) or when citrate is present in the growth media. Citrate fermentation allows the production of the energy necessary for cell metabolism (Garcia, Blancato, and Repizo 2008). For citrate fermentation to occur, three steps are necessary:

- 1) Import of citrate into the cell through citrate permeases: Most citrate permeases allow the import of citrate in symport with a metal ion thanks to transporters that are part of the CitMHS family (discussed in part I). However, other families of citrate permeases are more specific of bacteria able to exert citrate fermentation:
- The citrate-cation symporters (CCS) family: One of the best examples of this type of transporter is the CitT transporter of *E. coli*. CitT is an antiport that imports citrate while exporting succinate, which is the end-product of citrate metabolism under anaerobic conditions (Pos, Dimroth, and Bott 1998).
  - The 2-hydroxy-carboxylate transporters (2-HCT): This family of transporters uses di or tri-carboxylic acids to import citrate. The most studied 2-HCT citrate permease is the CitP transporter, present and conserved in several lactic acid bacteria (LAB). CitP is an antiport that incorporates citrate while exporting lactate (Drider, Bekal, and Prévost 2004). Another known 2-HCT transporter is CitS from *K. pneumoniae*, which is a symporter between citrate and  $\text{Na}^{2+}$  (Van Der Rest, Molenaar, and Konings 1992). Interestingly, while CitS is located on the chromosome of *K. pneumoniae*, all sequences of CitP present in Lactococcus are located on unrelated plasmids and share 99% homology, suggesting a recent acquisition by horizontal transfer (Drider, Bekal, and Prévost 2004).
  - The Metabolite:  $\text{H}^+$  symporters (MHS): This family of transporters belongs to the major facilitator superfamily (MFS). They group citrate permeases from Enterobacteriaceae that import citrate in symport with protons (1 molecule of citrate for 3 protons). Among them are the transporter CitH from *K. pneumoniae* and CitA from *Salmonella typhimurium* (Van Der Rest, Molenaar, and Konings 1992; Shimamoto et al. 1991)
- 2) Transformation of citrate into oxaloacetate by a citrate lyase: Once citrate is inside the cell, it will be converted into oxaloacetate and acetate by the action of a citrate lyase (CL). CLs constitute a family of proteins found across the tree of life that conserved the same organization. CLs are enzymatic complexes constituted of three subunits  $\alpha$ ,  $\beta$  and  $\gamma$  present in equal stoichiometry, which forms an  $\alpha_6\beta_6\gamma_6$  complex (Garcia, Blancato, and Repizo 2008). Only the  $\alpha$  and  $\beta$  subunits have an enzymatic activity, the  $\gamma$  subunit being used only for the transport of the prosthetic group (triphosphoribosyldephospho-coenzyme A). In bacteria, most of the work on citrate lyase has been conducted on the pathogen *K. pneumoniae* (Michael Bott and Dimroth 1994). In this bacteria, the three subunits are encoded by the genes *citD*, *citE*, and *citF*, respectively. The details of the reactions that lead to the conversion of citrate into oxaloacetate are detailed in **Figure 14**. Briefly, the  $\gamma$  subunit, an acyl carrier protein (ACP), carries acetyl-S-CoA. In a first reaction, the  $\alpha$  subunit, a citrate:acetyl-ACP transferase, exchanges the acetyl group from acetyl-S-CoA and the citryl group from citrate to give citryl-

S-CoA and acetate. In a second reaction, the  $\beta$  subunit (a citryl-CoA oxaloacetate lyase) regenerates Acetyl-S-CoA from citryl-S-CoA and releases oxaloacetate.

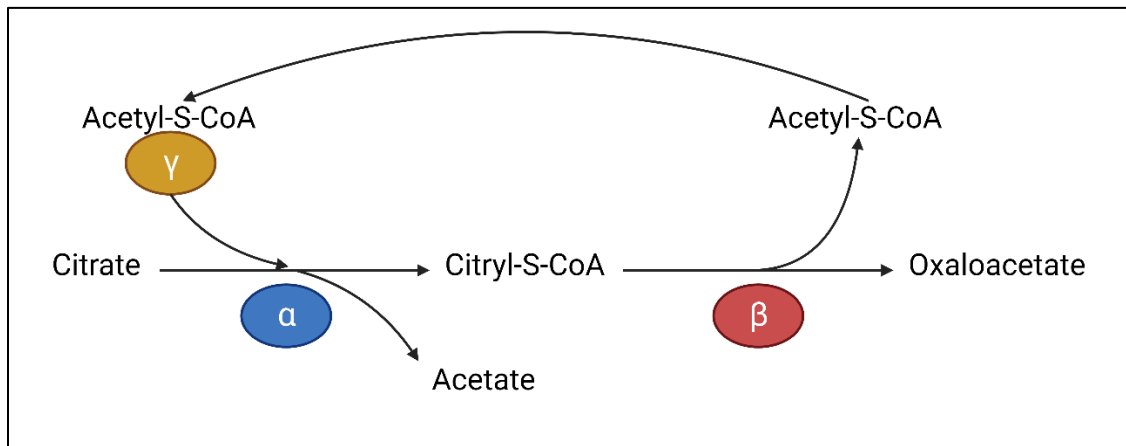


*Figure 14: Transformation of citrate into oxaloacetate by the citrate lyase enzymatic complex*

In a first reaction, the  $\alpha$  subunit (in blue) exchanges the citryl group from citrate and the acetyl group from acetyl-S-CoA (brought by the  $\gamma$  subunit, in orange), which leads to the formation of citryl-S-CoA and acetate. In a second reaction, the  $\beta$  subunit (in red) regenerates acetyl-S-CoA, which liberates one molecule of oxaloacetate. The newly formed acetyl-S-CoA can then be reused by the ACP.

Interestingly, the activity of the CL complex in bacteria relies on  $Mg^{2+}$  but not ATP, which is necessary for the activity of eukaryotic CL. However, in *M. tuberculosis*, the CL activity is inhibited by ATP, which suggests that the ATP concentration allows the bacteria to control its metabolism by using citrate either in the TCA cycle or the rTCA cycle depending on growth conditions (Hu et al. 2020).

- 3) Transformation of oxaloacetate into pyruvate by an oxaloacetate decarboxylase (OAD): The formation of pyruvate by oxaloacetate is mediated by the activity of an OAD, which generates one molecule of  $CO_2$  as a by-product. Like the CL the OAD is not an enzyme but an enzymatic complex, located on the membrane. The OAD complex is composed of three subunits  $\alpha$ ,  $\beta$ , and  $\gamma$ . Only the  $\beta$  and  $\gamma$  subunits are fully inserted into the membrane. The  $\alpha$  subunit is a carboxyltransferase, the  $\beta$  is a decarboxylase and the  $\gamma$  subunit has no catalytic role but is essential for the formation of the complex. The details of the reactions that lead to the formation of pyruvate are detailed in **figure 15**. Briefly, a first reaction occurs in the  $\alpha$  subunit where the carboxyl group of oxaloacetate is transferred to a molecule of biotin, which leads to the formation of pyruvate and carboxybiotin. In a second time, the carboxybiotin group is transferred into the  $\beta$  subunit via the  $\gamma$  subunit to be decarboxylated, producing one molecule of carbon dioxide and a new molecule of biotin that can be reused. The decarboxylation

reaction is  $\text{Na}^{2+}$ -dependent, therefore one proton from the periplasm is consumed and two sodium ions are exported when it occurs (Dimroth and Von Ballmoos 2007).

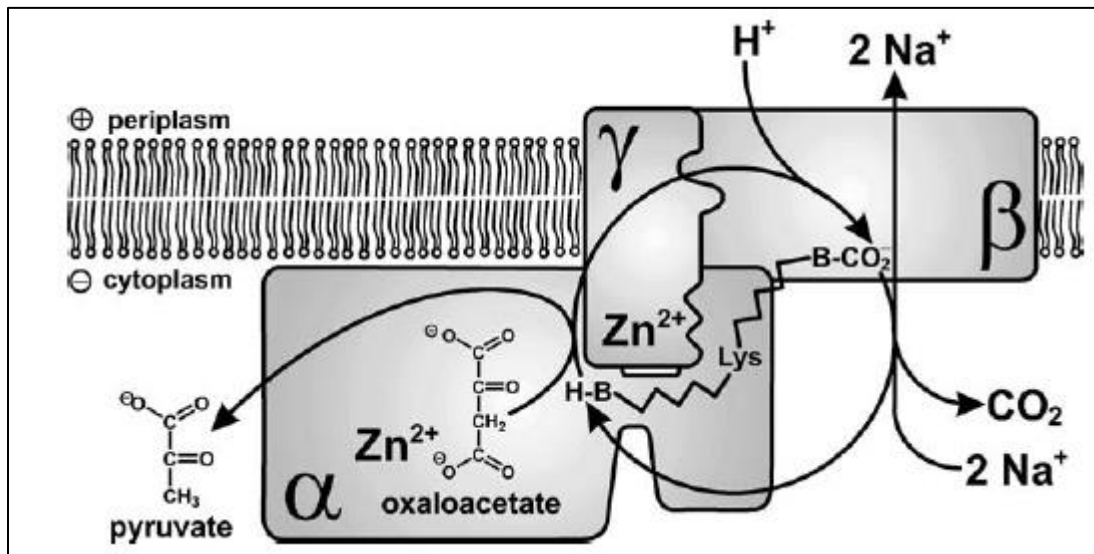


*Figure 15: Formation of pyruvate by the OAD enzymatic complex*

H-B: Biotin, B-CO<sub>2</sub>: Carboxybiotin; From (Dimroth and Von Ballmoos 2007).

Once pyruvate is formed, it is metabolized via different pathways depending on organisms and growth conditions. In anaerobic conditions, pyruvate is used for a variety of fermentative pathways leading to the production of one or several products. For example, in *K. pneumoniae* and *S. typhimurium*, pyruvate fermentation produces formate and acetate (M. Bott 1997). Under aerobic conditions, pyruvate is transformed into acetyl-CoA by the pyruvate dehydrogenase. The newly formed acetyl-CoA can then be used in the TCA cycle, for acetate production or fatty acid synthesis.

Interestingly, all the genes that encode the proteins necessary for citrate fermentation (citrate permease, citrate lyase, and oxaloacetate decarboxylase) are grouped in a gene cluster found in a variety of bacteria able to use citrate as a carbon source (**Figure 16**). However, it is now known that the regulations involved in the transcription of this cluster differs according to bacteria.



mediated by a two component system (TCS), but by a transcriptional regulator called CitI from the SorC family. The presence of citrate induces the auto-stimulation of *citI* transcription, and CitI will then bind to an A-T-rich region located between the *citI* locus and the *citMCDEFGRP* operon. The binding of CitI on DNA enhances the recruitment of RNA polymerases and thus the transcription of the *cit* operon (Martin et al. 2005). In *Enterococcus faecalis*, *Streptococcus mutans*, *Streptococcus pyogenes*, *Lactobacillus casei*, and *Lactobacillus sakei*, the transcriptional regulator is not CitI but CitO, which is part of the GntR family (Blancato et al. 2008).

## 2.4. Citrate in the TCA cycle: the moonlighting role of aconitase

### 2.4.1. The enzymatic activity of aconitase

In the TCA cycle, citrate is transformed into aconitate and then isocitrate by an enzyme called aconitase. The aconitase possesses a  $[4\text{Fe-4S}]^{2+}$  cluster which is necessary for its enzymatic activity. Indeed, one of the iron ions present in the cluster is exposed in the active site and binds to the oxygen atoms from substrates to react with them. During the conversion of citrate into isocitrate, a first reaction of dehydration will occur where the aconitase will remove a hydroxyl group and hydrogen from the citrate molecule bound to it, thus forming *cis*-aconitate and liberating one molecule of water. The newly-formed *cis*-aconitate molecule is then released, and a new molecule of *cis*-aconitate binds to the cluster in order for the second reaction to occur. In a second step, a hydration reaction that uses one molecule of water allows for the re-insertion of hydrogen and a hydroxyl group, thus forming isocitrate (**Figure 17**) (Castro et al. 2019). The utility of the conversion of citrate into isocitrate can seem questionable, but citrate (a tertiary alcohol) cannot be oxidized to form  $\alpha$ -ketoglutarate, so it has to be transformed into isocitrate which is a secondary alcohol and can be oxidized.

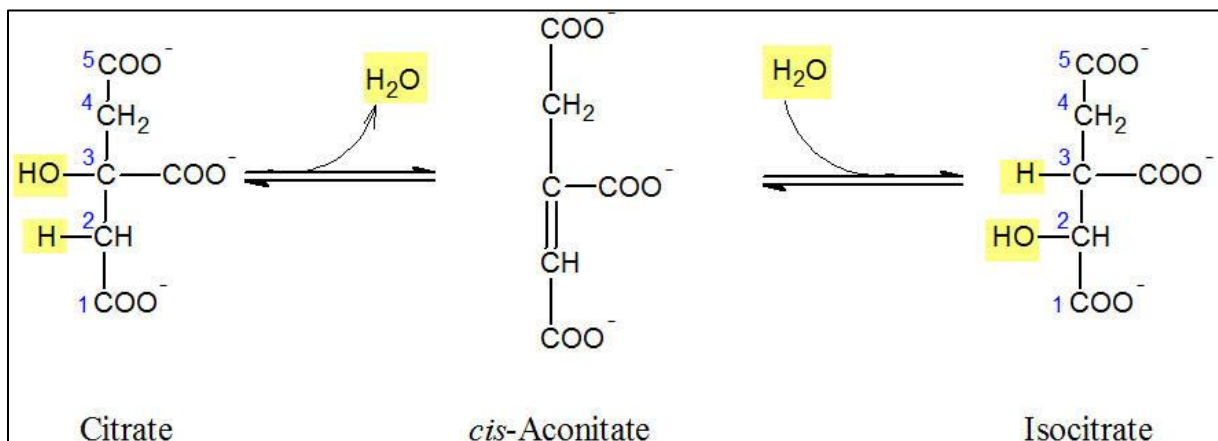


*Figure 17: Isomerization of citrate into isocitrate by aconitase*

In the first reaction of dehydration, one hydrogen from C2 and one hydroxyl group from C3 are removed from the citrate molecule to form cis-aconitate. In a second reaction of hydration, one hydrogen is added to C3, and one hydroxyl group is added to C2, forming isocitrate. From <https://proteopedia.org>.

#### 2.4.2. Moonlighting activity of aconitase as an RNA-binding protein

Aconitase is a protein widely conserved into the three domains of life. In Eukaryotes, two types of aconitase exist, a mitochondrial one (m-Acn) and a cytosolic one (c-Acn or IRP1). In bacteria, only one aconitase exists named AcnA or CitB. A known exception is *E. coli*, which possesses two aconitases, AcnA, and AcnB (Gruer and Guest 1994). AcnB is the major enzyme of the TCA cycle, while AcnA is only induced upon stress during stationary phase (Cunningham, Gruer, and Guest 1997). Remarkably, all known aconitases except m-Acn in eukaryotes share one characteristic, which is their moonlighting activity upon iron starvation. The moonlighting activity of aconitase in bacteria has been first reported in the two model bacteria *E. coli* and *B. subtilis* (Tang and Guest 1999; Alen and Sonenshein 1999). Since then, the moonlighting activity of aconitase has been observed or suspected in several bacteria, including animal and plant pathogens (**Table 2**).

| Organism                    | Gene       | Reference                         |
|-----------------------------|------------|-----------------------------------|
| <i>E. coli</i>              | AcnA, AcnB | (Tang and Guest 1999)             |
| <i>B. subtilis</i>          | CitB       | (Alen and Sonenshein 1999)        |
| <i>H. pylori</i>            | AcnB       | (Austin, Wang, and Maier 2015)    |
| <i>M. tuberculosis</i>      | Acn        | (Banerjee et al. 2007)            |
| <i>S. viridochromogenes</i> | AcnA       | (Michta et al. 2012)              |
| <i>S. enterica</i>          | AcnA       | (Baothman, Rolfe, and Green 2013) |

*Table 1: Confirmed bifunctional aconitases in bacteria*

As mentioned previously, aconitase possesses a  $[4\text{Fe-4S}]^{2+}$  cluster necessary for its enzymatic activity. In favor of iron starvation, or under the action of oxidative stress, the cluster is degraded and aconitase loses its enzymatic activity. The loss of the cluster induces a conformational change in aconitase. Upon unstress conditions, aconitase is compacted and the Fe-S cluster is hidden in the active site, with only one iron ion serving as a ligand. Upon iron starvation or oxidative stress, the disassembly of the Fe-S cluster provokes a conformational change of the apo-aconitase, which is more open allowing an interaction with RNA sequences (Walden et al. 2006) (**Figure 18**).

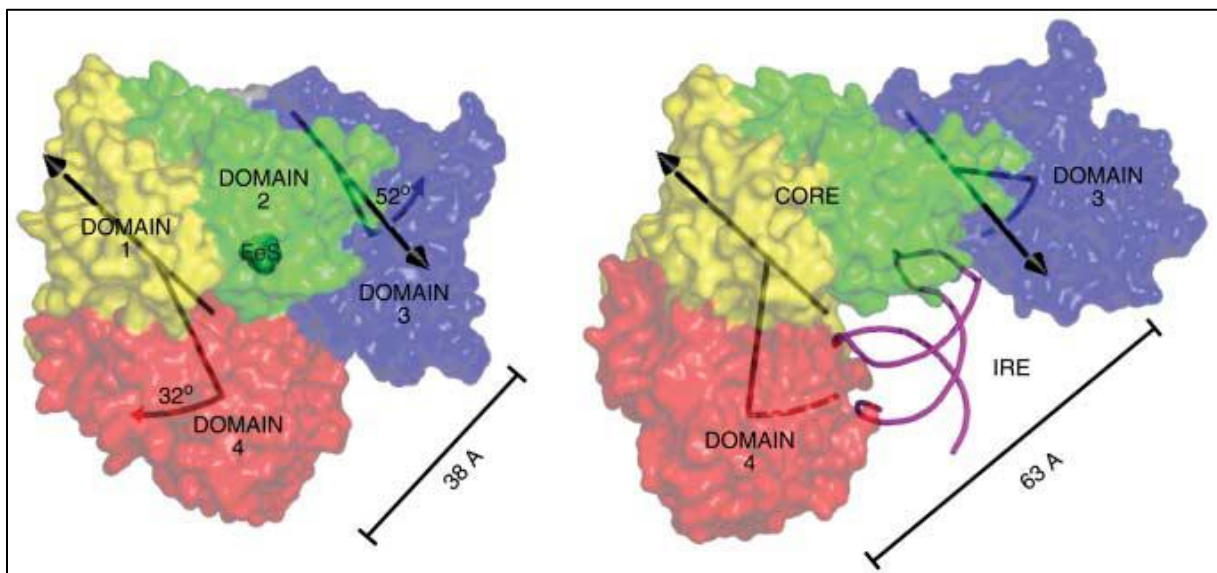


*Figure 18: Conformational change of cytoplasmic aconitase (c-Acn) upon iron starvation*

Left image: c-Acn in normal conditions; Right image: c-Acn during iron starvation. RNA is indicated by the purple helix. IRE: Iron Responsive Element. From (Walden et al. 2006).

The interaction of apo-aconitase with RNA is not random. Indeed, apo-aconitase binds specifically to RNA sequences called iron-responsive elements (IRE). The IREs are located in genes implicated in the regulation of iron homeostasis. In Eukaryotes, they are conserved in terms of sequence and structure. An IRE is made of a  $\approx 30$ -nt long stem-loop with a CAGUG motif on the top of the stem, which is necessary for the recognition and binding of IRP-1 (Walden et al. 2006). However, all the existing IRE do not bind with IRP with the same affinity and that the regions adjacent to the stem-loop also play a role in binding affinity, highlighting the fact that it is rather the secondary structure and not the sequence which is important (Goforth et al. 2010).

Aconitase being in charge of maintaining iron homeostasis in case of iron starvation, a few studies have pointed out the relation between its RNA-binding activity and the modification of the bacterial metabolism in certain bacteria, including the potential effects on host colonization.

- In *B. subtilis*, a strain deficient for the RBP activity of aconitase is defective for sporulation (Serio, Pechter, and Sonenshein 2006). The sporulation process necessary for disseminating the bacteria is highly regulated by a series of regulators that allow for a temporal expression of different sets of genes, such as  $\sigma^K$  and GerE. In the late-sporulation stage, apo-CitB normally binds to *gerE* mRNA on the 3' region and stabilizes it, thus allowing for higher protein concentration and its action as a repressor of sporulation.
- In *S. enterica*, it has been shown that apo-AcnB was able to interact with the 5' UTR of *ftsH* mRNA (Tang et al. 2004), which encodes a protease (Herman et al. 1993). By binding to the 5' UTR, apo-AcnB represses translation of *ftsH* mRNA, reducing FtsH levels and therefore increasing the levels of  $\sigma^{32}$ , which is normally degraded by FtsH (Herman et al. 1995). Increased levels of  $\sigma^{32}$  lead to an enhanced production of the transcriptional activator DnaK, which will in turn enhance the production of the flagella protein FliC. Therefore, the inactivation of AcnB leads to an hyper-production of FtsH, which degrades  $\sigma^{32}$  and thus indirectly represses FliC production, leading to a defect in motility (Tang et al. 2004).
- A proteomic analysis of *H. pylori* to detect differentially expressed proteins in  $\Delta acnB$  strain compared to WT indicates several downregulated and upregulated targets of apo-AcnB (Austin, Wang, and Maier 2015). Interestingly, most downregulated genes in the  $\Delta acnB$  mutant are involved in the resistance to oxidative stress (e.g. superoxide dismutase and catalase), but several virulence factors such as ureases or flagellum protein were also found. These findings were confirmed by the fact that the  $\Delta acnB$  strain has a higher sensitivity to oxygen and, as in *S. enterica*, a loss of motility (Austin, Wang, and Maier 2015).

### 2.4.3. Regulators of the aconitase

#### I. Transcriptional regulators:

Since the aconitase is part of the TCA cycle, a key point for bacterial metabolism, its expression is tightly regulated by different transcriptional regulators responding to different environmental stimuli (reviewed by (Sonenshein 2007)).

In rich media, when a rapidly usable carbon source and a source of  $\alpha$ -ketoglutarate are both present, the transcription of *citB* is low. To activate *citB* expression, a novel carbon source, such as citrate, has to be present, but it is also necessary that no glucose remains, which indicates that *citB* is subject to a regulation by carbon catabolite repression (Rosenkrantz, Dingman, and Sonenshein 1985). In *B. subtilis* and *L. monocytogenes*, *citB* and *citZ* (citrate synthase) are under the control of CcpC, a LysR regulator sensitive to citrate. CcpC usually represses the transcription of both *citZ* and *citB* as well as its own gene. When citrate is present, it binds to CcpC inducing a conformational change that alleviates repression (Jourlin-Castelli et al. 2000; Kim et al. 2002; Pechter et al. 2013a). In addition, in the presence of high citrate concentrations, CcpC is an activator of *citB* (Mittal et al. 2013). It should be noted that CcpC is present in *S. aureus*, but named CcpE (Hartmann et al. 2013; Y. Ding et al. 2014).

*citB* is also regulated by CcpA, another carbon catabolite repressor from the LacI/GalR family. In the presence of glucose, CcpA represses the transcription of genes implicated in the utilization of other carbon sources. CcpA has numerous targets including *citZ* encoding citrate synthase and CcpC (Kim, Roux, and Sonenshein 2002; Kim et al. 2002). Therefore, glucose prevents *citB* expression by CcpA-dependent *ccpC* repression. Besides carbon catabolite repression, *citB* expression is also negatively regulated by CodY, a global regulator sensitive to the concentration of GTP and branched-chain amino acids (BCAA) that regulates the metabolic switch between the exponential and stationary phase. However, CcpC and CodY do not bind at the same positions and can act simultaneously. Taken together, these results imply that in order to have a full expression of *citB*, bacteria has to use the available glucose to prevent CcpA activity, to accumulate citrate to activate CcpC, and have a low concentration of GTP and BCAA to inactivate CodY (Kim, Kim, et al. 2003) (**Figure 19**).

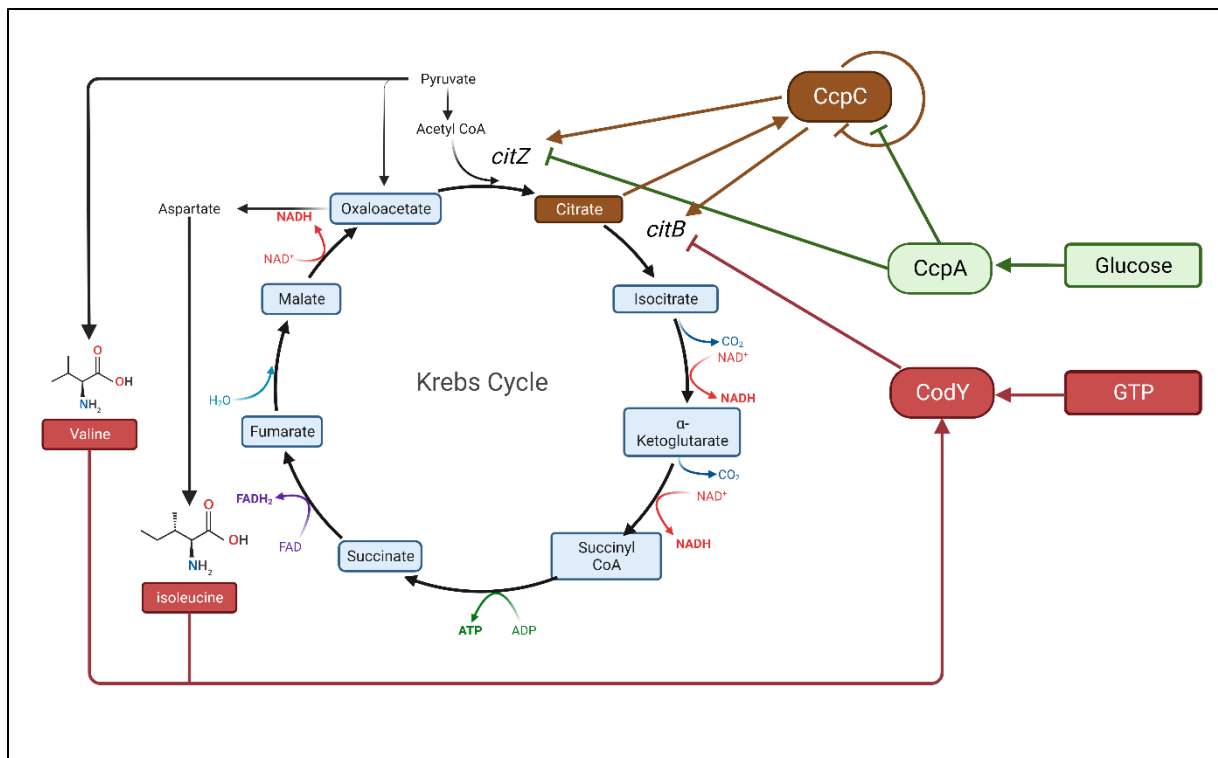


*Figure 19: Regulation of citB expression by metabolic regulators*

In brown: Regulation by CcpC. In the presence of citrate, CcpC activates the transcription of its own mRNA as well as *citZ* and *citB* mRNAs. In green: Regulation by CcpA. In the presence of glucose, CcpA represses *citZ* and *ccpC*, which indirectly represses *citB*. In red: Regulation by CodY. In the presence of GTP or BCAA, CodY represses *citB* transcription.

## II. Regulatory RNAs:

In addition to its regulation by transcriptional regulators, aconitase is often subject to regulation by regulatory RNAs that allow the cell to fine-tune its expression depending on the environmental conditions.

In *E. coli*, the *acnB* aconitase mRNA is a target of RyhB, a sRNA regulated by Fur whose expression is induced upon iron starvation. RyhB down-regulates genes encoding for non-essential iron-using proteins (Massé, Vanderpool, and Gottesman 2005). However, as mentioned before, upon iron starvation, aconitase loses its Fe-S cluster and switches from an enzymatic to an RNA-binding activity. Interestingly, the apo-aconitase can bind on an IRE located on the 3' region of its own mRNA, and this binding prevents the mRNA degradation induced by RyhB (Benjamin and Massé 2014) (**Figure 20**). The regulation of aconitase by sRNAs involved in iron homeostasis was also demonstrated in other bacteria (Vasil 2007; Gaballa et al. 2008), but so far the link between this regulation and the apo-aconitase is specific to *E. coli*.

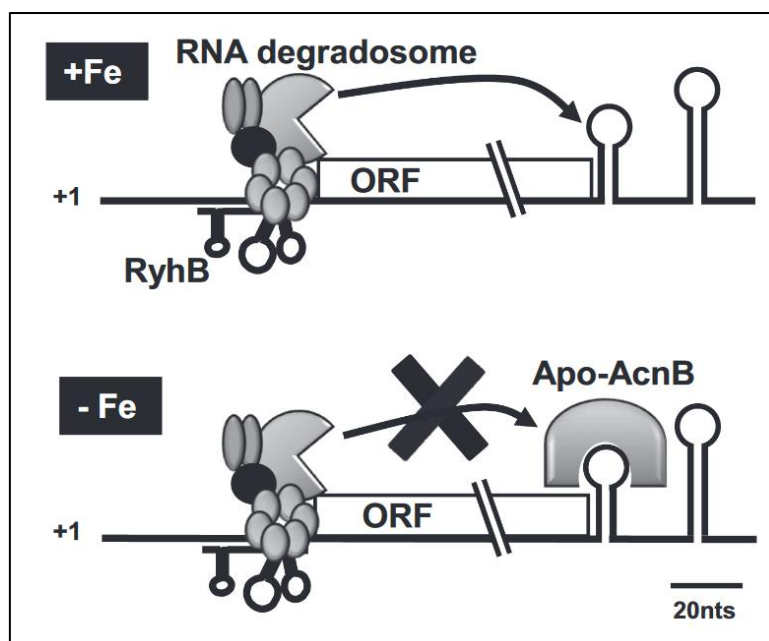


*Figure 20: Role of apo-aconitase in the protection of acnB mRNA*

In the presence of iron, RyhB (expressed from a plasmid via an arabinose-inducible promoter) binds on the 5' region of *acnB* mRNA and recruits the RNA degradosome that binds on a stem-loop located in 3' and induces the mRNA cleavage. In the absence of iron, RyhB is naturally induced and binds on *acnB* mRNA to induce its degradation, however, the stem-loop recognized by the degradosome contains an IRE and is hidden by the apo-AcnB, thus protecting *acnB* mRNA from degradation. From (Benjamin and Massé 2014).

The regulation of aconitase activity by a sRNA expressed upon iron starvation is not specific to *E. coli*. Indeed, in *B. subtilis*, *citB* is a target of FsrA, a RyhB functional homolog (Smaldone et al. 2012). In *P. aeruginosa*, the two aconitase genes *acnA* and *acnB* are both regulated by Prf1 and Prf2, which are also RyhB functional homologs (Oglesby et al. 2008).

In *S. aureus*, aconitase is possibly the target of at least two sRNAs:

- IsrR, a newly-discovered Fur-regulated sRNA of *S. aureus* involved in the response to iron starvation (Coronel-Tellez et al. 2022).
- RsaE is a sRNA expressed in the mid or late exponential phase known to repress several genes involved in the TCA cycle and amino acid catabolism (Bohn et al. 2010; Rochat et al. 2018a). Interestingly, aconitase is also predicted to be a target for RoxS, the RsaE homolog in *B. subtilis* (Allouche et al. 2023).

It is worth noting that even though aconitase or citrate synthase are the targets of many regulatory RNAs, they are always part of a larger regulon that contains other

targets involved in the TCA cycle. The regulation of citrate-related enzymes is not specific but is rather part of a larger mechanism that aims to redirect central metabolism of the bacteria.

### 3. Regulatory RNAs in bacteria

Regulatory RNAs are molecules that exert a regulatory activity in a wide variety of cellular processes without being translated. The first mention of a bacterial regulatory RNA dates back to 1981, with the discovery in *E. coli* of an untranslated RNA called RNAI, which prevented the replication of ColE1 plasmids (Stougaard, Molin, and Nordström 1981). Two years later, it was demonstrated that an RNA transcribed from the Tn10 transposon promoter was capable of repressing transposition by preventing the translation of the transposase mRNA (Simons and Kleckner 1983). Since then, and thanks to technological advances in the field of RNA biology (*e.g.* tiling array and next-generation sequencing), a large number of regulatory RNAs were discovered in different bacterial species. In *E. coli*, for example, around 80 sRNAs were identified, representing a 2% increase in the number of total genes (Waters and Storz 2009).

Regulatory RNAs exert their activity through various mechanisms, such as preventing mRNA transcription or translation, altering mRNA stability, or even sponging other sRNAs (Dutta and Srivastava 2018; Wagner and Romby 2015). In order to achieve their role, they bind either to RNA or proteins.

Before examining the roles of regulatory RNAs in more detail, it is worth defining the term sRNA:

- sRNA refers to small regulatory RNA because the majority of characterized regulatory RNAs, which are not UTRs, are between 100 and 150 nucleotide (nt) long. However, in some cases, sRNAs are much longer. The best examples for *S. aureus* are RNA III (Benito et al. 2000) and SSR42 (Horn et al. 2018), which are 514 and 1,232 nt long, respectively.
- Regulatory RNAs are often not translated, but there are exceptions. For example, RNA III possesses a small ORF that encodes the  $\delta$ -hemolysin (Novick and Geisinger 2008). In *E. coli*, the sRNA SgrS, which represses the translation of *ptsG* mRNA, also encodes the SgrT protein (Wadler and Vanderpool 2007). ncRNA, for non-coding RNA, is a term mainly used in eukaryotes while sRNA is more commonly used for regulatory RNAs in prokaryotes.
- Regulatory RNAs are classified as *cis*- or *trans*-encoded according to their transcription loci to their targets and *cis*- or *trans*-acting according to their mode of action (see below).

### 3.1. *Cis*-acting regulatory RNAs

*Cis*-acting regulatory RNAs are RNA molecules located on the same RNA strand as their mRNA target. The best examples of this type of regulatory RNAs are the riboswitches, which are usually 5'UTR of mRNAs responding to the presence of specific ligands. Riboswitches are composed of two domains: a ligand-binding sequence called aptamer and an expression platform that modulates gene expression. The binding of specific molecules to aptamers alters their conformation, which in turn affect the activity of expression platforms. The results is a modified stability or translation of downstream mRNAs (Ariza-Mateos, Nuthanakanti, and Serganov 2021) (**Figure 21**).

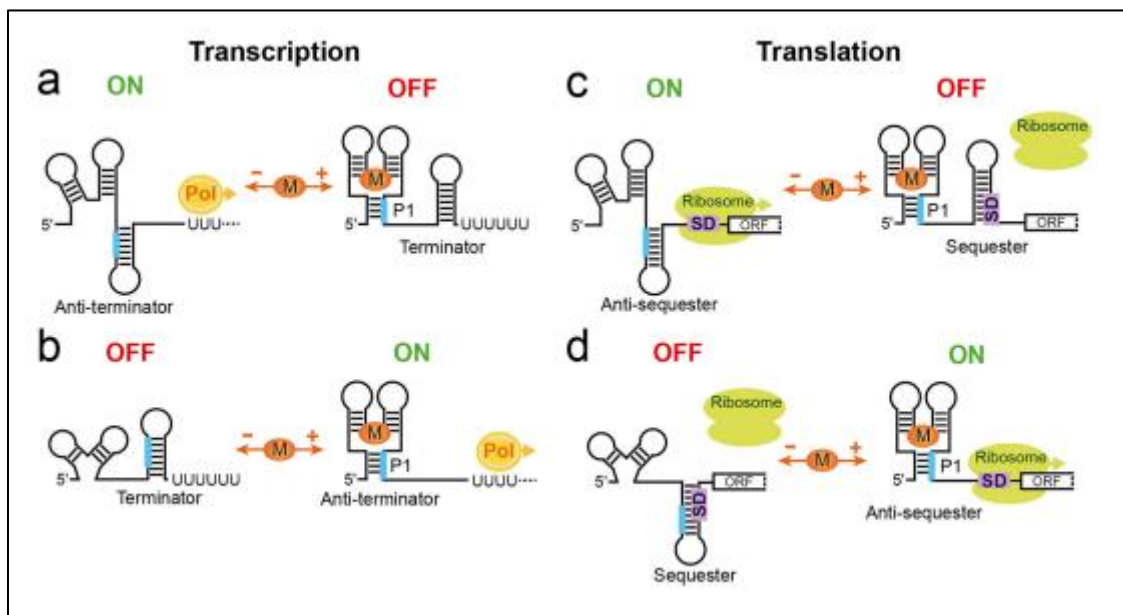


*Figure 21: Mode of action of riboswitches*

A: Transcription inactivation. In presence of the metabolite (orange), the aptamer forms a terminator that leads to premature termination of transcription. B: Transcription activation. In presence of the metabolite, the terminator formed by the aptamer is released and transcription is activated. C: Translation inactivation. In presence of the metabolite, the aptamer adopts a secondary structure that sequesters the Shine-Dalgarno sequence (purple), thus blocking translation. D: Translation activation. The SD sequence is sequestered by the aptamer. In the presence of the metabolite, the secondary structure adopted by the aptamer releases the SD sequence and allows the translation of the mRNA. From (Ariza-Mateos, Nuthanakanti, and Serganov 2021).

Although riboswitches and other *cis*-acting RNAs can respond to a plethora of environmental stimuli and are of crucial importance to bacterial metabolism, they are outside the scope of this thesis and will therefore not be discussed further.

## 3.2. *Trans-acting regulatory RNAs*

*Trans-acting regulatory RNAs* are RNAs that interact with proteins or RNA molecules distinct from them.

### 3.2.1. Regulatory RNAs interacting with proteins

There are only a few examples of RNAs interacting with proteins that are not RNA chaperones. The best-studied examples of this category are tmRNA, 6S RNA, CsrB, and CsrC from *E. coli*.

Transfer-messenger RNA (tmRNA, also called SsrA) is highly conserved among bacteria with a tRNA-like domain and a small ORF. The tRNA-like domain act as a tRNA transferring an alanine while the ORF generates the SsrA-tag to proteins being synthesized. This dual activity contributes to protein quality control (Moore and Sauer 2007). Charged cognate tRNA deficiency, mRNA missing stop codon (Keiler, Waller, and Sauer 1996), weak translational termination (Collier, Binet, and Bouloc 2002) or exit tunnel jamming (Collier, Bohn, and Bouloc 2004) are conditions leading to ribosome stalling during translation and leading to tmRNA recruitment by ribosomes at the acceptor site. tmRNA activity releases a protein containing a SsrA-tag at its C-terminus and therefore frees the ribosomes. The SsrA-tag allows the recognition of the hybrid protein by proteases to prevent accumulation of faulty polypeptides (Keiler, Waller, and Sauer 1996; Herman et al. 1998; Bohn, Binet, and Bouloc 2002). The loss of tmRNA leads to different phenotypes according to species: increased sensitivity to miscoding antibiotics in *E. coli*, temperature sensitivity in *B. subtilis* and virulence defect in *Francisella tularensis* (Abo et al. 2002; Shin and Price 2007; Svetlanov et al. 2012).

6S RNA discovered in *E. coli* (Hindley 1967) is conserved among bacteria. It accumulates in stationary phase and contributes to reprogramming gene expression by blocking the activity of RNA polymerase containing a vegetative  $\sigma$  factor ( $\sigma^A$  or  $\sigma^{70}$ ). Consequently, transcription is driven by RNA polymerase containing other sigma factors allowing the adaptation to the environmental conditions. 6S RNA expression increases upon certain stress conditions, highlighting its role as a stress response regulator (Wassarman 2018). For example, 6S RNA promotes butanol resistance in *C. acetobutylicum*, while 6S RNA deletion is associated with an increased susceptibility to antibiotics targeting RNA polymerase in *S. aureus* (Jones, Venkataramanan, and Papoutsakis 2016; Esberard et al. 2022).

CsrA is a RNA-binding protein that regulates the stability and the translation of several genes involved in carbon metabolism virulence, motility, and biofilm formation. CsrB and CsrC are two sRNAs binding to CsrA and thus preventing CsrA activity (reviewed by Pourciau et al. 2020). The transcription of CsrB and CsrC is activated by the two-component system BarA-UvrY and is sensitive to formate and acetate.

### 3.2.2. Regulatory RNAs interacting in *trans* with RNAs

#### I. asRNA

asRNA are RNA molecules that are encoded on the opposite strand of their target. These regulatory RNAs are likely targeting the RNA encoded on the opposite strand, with which they share a perfect complementarity. Consequently, they can form long double strand RNA structures and are expected to affect mRNA stability or translation (Georg and Hess 2018).

Part of characterized asRNAs to this date are originating from accessory DNA elements, such as plasmids, phages, or transposons. In the case of these asRNAs, their function is to regulate the replication or conjugation of plasmids, the transposition, or the switch between lysis and lysogeny in bacteriophages (Brantl 2002). Another group of asRNAs are acting as antitoxins in plasmids type I toxin/antitoxin systems, and repress the translation of toxic proteins in order to kill only the cell that has lost the mobile element.

However, recent advances in genome-wide sequencing shed light on chromosomally-encoded asRNAs. Some of these asRNAs are encoded in the complementary region between two ORFs and can regulate simultaneously two adjacent genes. For example, in *B. subtilis*, expression of the asRNA SR6 affects the two adjacent genes *yoyJ* and *yonT*, by inhibiting *yoyJ* translation and initiating *yonT* degradation, respectively (Reif, Löser, and Brantl 2018) (**Figure 22**).

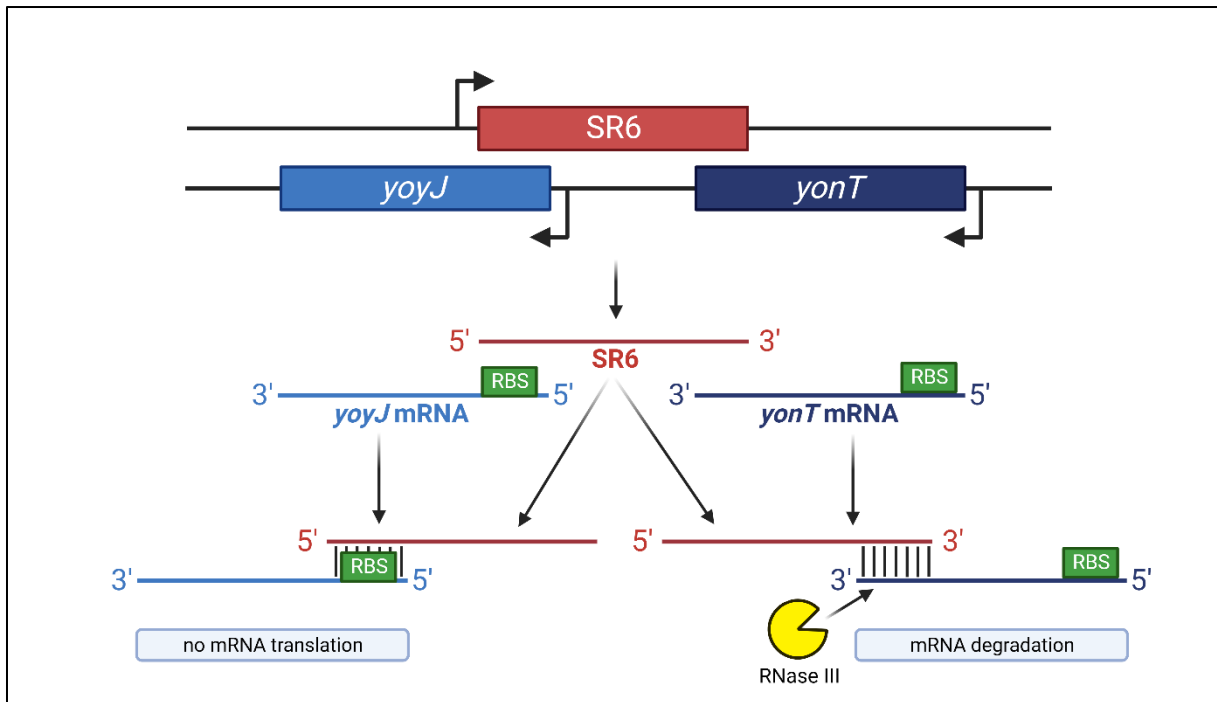


*Figure 22: Regulation of yoyJ and yonT mRNAs by SR6*

SR6 (in red) is located on the opposite strand at the level of the intergenic region between *yoyJ* (light blue) and *yonT* (dark blue). Therefore, SR6 has homologous regions to *yoyJ* and *yonT*. When SR6 is expressed, it represses simultaneously *yoyJ* and *yonT* mRNAs by binding on their 5' and 3' regions, respectively. The binding of SR6 on *yoyJ* mRNA at the level of the RBS prevents translation while binding on *yonT* mRNA induces its degradation by the recruitment of RNase III (in yellow). Adapted from (Brantl and Müller 2021).

## II. sRNA

By definition, we call sRNAs trans-acting RNA, which are not asRNA. Most sRNAs are *trans*-encoded regulatory RNAs as their corresponding gene is often distant from their target gene. Unlike asRNAs, sRNAs bind to their mRNA targets via short, partial complementary sequences. Most sRNAs act by base-pairing to the RBS of their mRNA targets, resulting in translational inhibition. In some cases, whether or not associated with translational inhibition, sRNA recruits an RNase that promotes mRNA degradation. However, the sRNA binding to an mRNA can enhance target expressions by disrupting a secondary structure that previously sequestered an RBS (Waters and Storz 2009) (**Figure 23**).

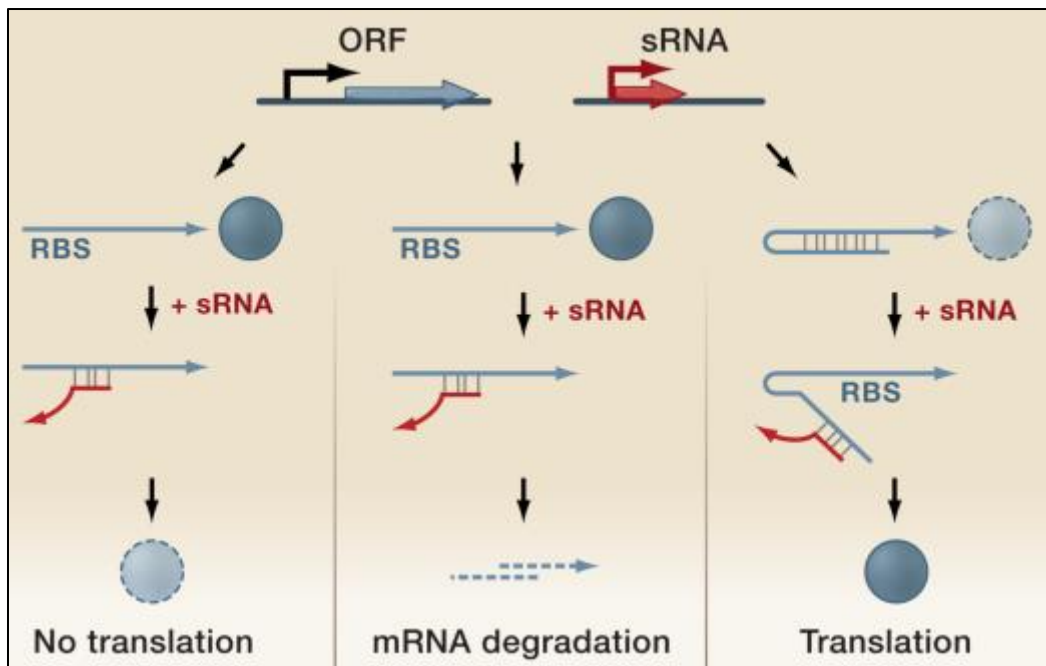


*Figure 23: Regulatory functions of sRNAs*

Trans-encoded sRNAs (in red) can act negatively by binding to the 5' UTR of their mRNA targets (in blue) and blocking ribosome binding (left panel) or they can recruit RNases for mRNA degradation (middle panel). sRNAs can also act positively by preventing the formation of a secondary structure that sequesters the RBS (right panel). From (Waters and Storz 2009).

Many sRNA genes possess their own promoter and for most of them, their expression is specific to environmental conditions as illustrated with the following examples. In *B. subtilis*, *roxS* (*rsaE* in *S. aureus*) expression is under the control of the ResDE two-component system and is induced in the presence of nitric oxide (Durand et al. 2015). In *E. coli*, *ryhB* is repressed by Fur and induced upon iron starvation (Massé and Gottesman 2002); this regulation is conserved for all *ryhB* homologs. Still in *E. coli*, Spot42 is accumulated under high glucose concentrations, *oxyR* is activated by OxyS under oxidative stress (Altuvia et al. 1997) and MicA/RybB accumulates upon outer membrane stress due to a  $\sigma^E$  regulation of their genes (Gogol et al. 2011). In *S. aureus*, the accumulation of RNAIII is Agr-dependent, a quorum sensing regulator, whereas *rsaA*, is induced by  $\sigma^B$  (Novick et al. 1993; Romilly et al. 2014). In summary, any transcriptional factor can regulate the expression of a sRNA.

Since sRNA/mRNA target base-pairing involves short complementary sequences, sRNAs may regulate many genes, which are often involved in the same metabolic process. Consequently, sRNAs can modulate adaptive responses similarly to a transcriptional factor but by acting at the post-transcriptional level. For example, *E. coli* RyhB down-regulates the amount of enzymes containing iron-sulfur clusters under iron-starved growth conditions, while MicA and RybB repress membrane porins upon

membrane stress. sRNAs are usually involved in negative feedback loops, in such a way that their expression remains temporary. For example, RyhB accumulates during iron starvation to favor iron uptake which in turn represses the expression of its corresponding gene.

Even if sRNAs bind to their targets through complementary sequences, the whole sequence is not entirely necessary for the regulation. Indeed, in some cases, only a few bases are necessary for the sRNA activity. For example, SgrS pairing with *ptsG* mRNA involves 23 bases, but mutations in only four of them are sufficient to affect SgrS activity (Kawamoto et al. 2006). In Firmicutes, including *S. aureus*, most of the sRNAs that repress translation of their mRNA targets, including RsaE, act through exposed and single-stranded C-rich regions (**Figure 24**). These regions bind to G-rich regions which are located on the ribosome binding sites of their targets (Geissmann et al. 2009; Rochat et al. 2018).

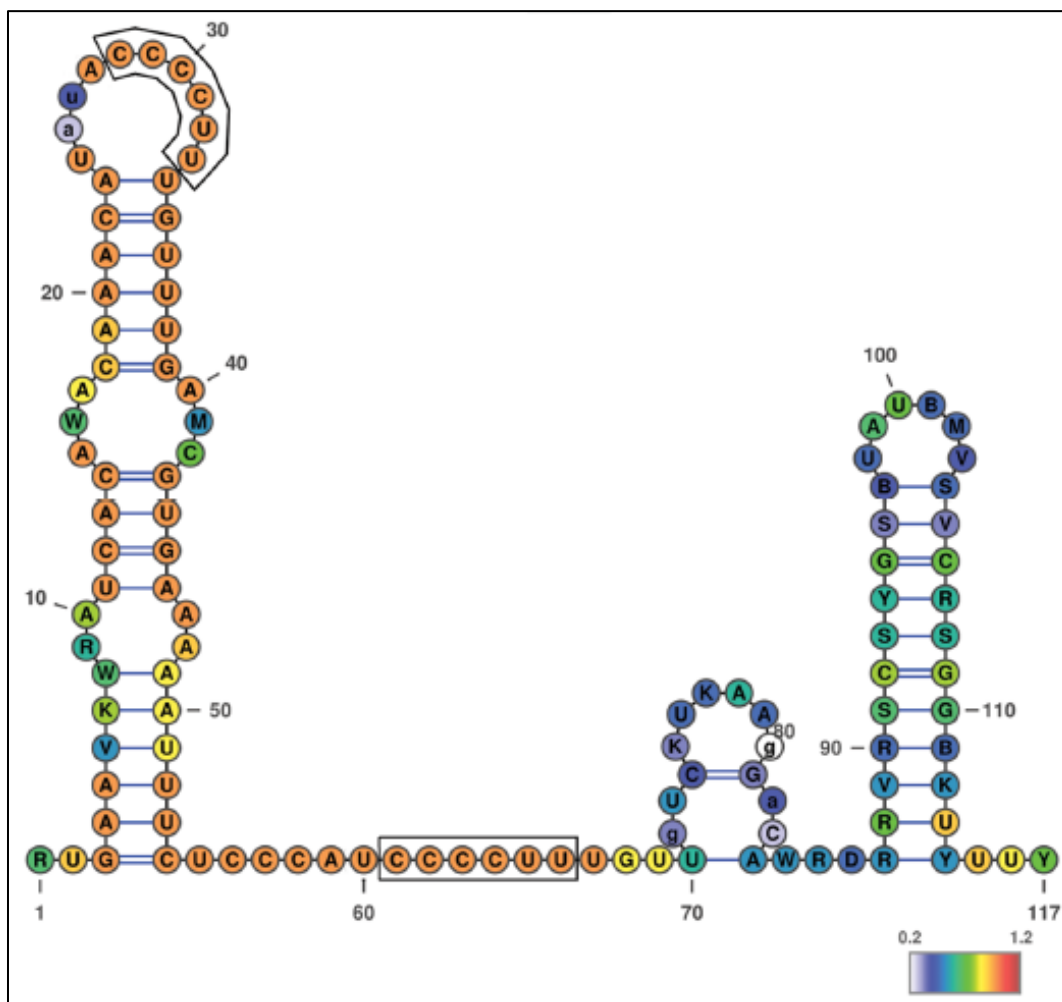


*Figure 24: Secondary structure of RsaE*

The secondary structure has been predicted using LocaRNA. The two C-rich regions (black boxes) are located on unpaired regions and pair with the RBS of the mRNA targets to inhibit their translation. From (Rochat et al. 2018).

### 3.3. RNA chaperones

The sRNA/mRNA target pairing involves a recognition step between two unpaired regions via seed motifs leading to the formation of a kissing complex. The interaction between the two molecules then expands beyond the seed motifs and requires the unfolding of intramolecular pairings. In many cases, these different steps require the activity of an RNA chaperone. The most studied RNA chaperone in prokaryotes is Hfq, which is widely conserved among bacteria. However, other RNA chaperones, such as ProQ or CsrA are also involved in the maintenance of sRNA-mRNA interactions.

#### 3.3.1. Hfq

Hfq is one, if not the most conserved RNA chaperone in bacteria. Hfq belongs to the family of Sm-like (LSm) proteins, a protein family found in all three domains of life suggesting that Hfq originates from the common ancestor to bacteria, archaea, and Eukaryotes (Vogel and Luisi 2011). Hfq acts as a homohexamer organized in a ring. Hfq possesses four regions that can bind RNAs according to their sequence (Updegrave, Zhang, and Storz 2016). This flexibility allows Hfq to interact with sRNAs and their target mRNAs at the same time. Hfq can bind and stabilize sRNAs, mRNAs, and sRNA-mRNA duplexes or target them for degradation by ribonucleases. Hfq is necessary in many species for sRNAs to exert their activities (**Figure 25**).

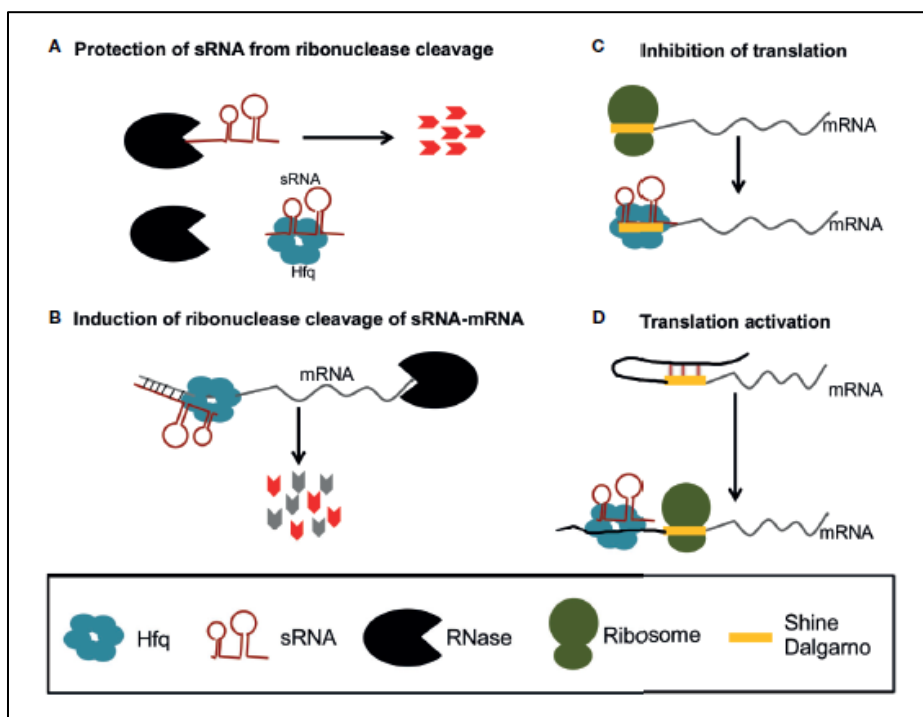


### Figure 25: Roles of Hfq in gene regulation in bacteria

A: Hfq can protect sRNAs from degradation (A) or recruit RNases to degrade the sRNA-mRNA duplex (B). Hfq can also promote sRNA binding on the mRNA in order to inhibit (C) or promote (D) its translation. From (Djapgne and Oglesby 2021).

Hfq is necessary for the action of sRNAs in many pathogenic bacteria (reviewed by Djapgne and Oglesby 2021). In Enterobacteriaceae, Hfq is necessary for the activity of RyhB and MicA, sRNAs involved in the regulation of iron homeostasis and adaptation to membrane stress, respectively. In *Shigella sonnei*, a  $\Delta hfq$  mutant is more sensitive to antibiotics and less virulent (Y. Wang et al. 2023). However, the function of Hfq remains elusive in some bacterial species. In *Clostridioides difficile*, Hfq seems to be involved in key metabolic pathways during infection such as sporulation, stress response or biofilm formation (Boudry et al. 2014; Soutourina 2017). Up to now, no sRNA-dependent phenotype seems associated with the absence of Hfq in *B. subtilis* (Hämmerle et al. 2014; Rochat et al. 2015) or in *S. aureus* (Bohn, Rigoulay, and Bouloc 2007; Rochat et al. 2012; Liu et al. 2020).

#### 3.3.2. Other RNA chaperones

Several studies have identified additional sRNA chaperones, diminishing the unique role of Hfq in sRNA regulation. In 2011, ProQ was identified as an RNA chaperone in *E. coli* (G. Chaulk et al. 2011). However, the first paper showing the link between ProQ and sRNAs was published a few years ago in *Salmonella* (Smirnov et al. 2016). ProQ is part of the FinO domain protein family, FinO being an RNA chaperone that controls plasmid conjugation in *E. coli* by stabilization of the pairing between FinP sRNA and *traJ* mRNA (Arthur et al. 2011). Homologs of ProQ have been found in several Gram-negative species, such as *E. coli*, *L. pneumophila*, and *Salmonella*, where it has been shown to control many sRNA networks and is involved in antibiotic persistence and virulence (Smirnov et al. 2016; Rizvanovic et al. 2022; Westermann et al. 2019). The link between ProQ and sRNAs has been well established among Gram-negative species and even revealed overlapping targets with Hfq (Silva et al. 2019; Melamed et al. 2020). Note that ProQ is absent in Gram-positive bacteria.

CsrA was initially annotated as a regulator of carbon storage that was acting as a homodimer at the post-transcriptional level of many mRNAs involved in carbon metabolism, motility, virulence iron homeostasis, biofilm formation, and cell envelope integrity (Katsuya-Gaviria et al. 2022). In contrast to Hfq which is widely present in eubacteria, the distribution of CsrA is more heterogeneous. Indeed, CsrA is absent in several Firmicutes, such as *Streptococcus*, *Staphylococcus*, *Listeria*, and is present in more than 50% of *Bacillus* species (Sobrero and Valverde 2020). The action of CsrA is often mediated by sRNAs, which will bind to it and prevent its action, acting like sponges (Pourciau et al. 2020). A recent paper in *B. subtilis* showed that CsrA was also

able to promote the interaction between SR1 sRNA and its mRNA target *ahrC* (Müller et al. 2019).

Other proteins also exert an RNA chaperone activity at a more specific level. For example, in *S. aureus*, CspA (cold-shock protein A), one of the most abundant proteins in the cytoplasm and a major regulator, can bind its own mRNA to protect it from RNase III degradation (Caballero et al. 2018). In *B. subtilis* the small iron-regulated proteins FbpA, FbpB, and FbpC interact with FsrA sRNA (Gaballa et al. 2008; Smaldone et al. 2012). It is important to note that FsrA acts in an Hfq-independent manner, in opposition to its homolog RyhB, highlighting the fact that they are not orthologs but rather functional homologs.

### 3.4. RyhB

RyhB was first identified in *E. coli* (Massé and Gottesman 2002). It is 90-nt long with three stem-loops, and its expression is regulated by Fur. The *ryhB* gene, as well as its location between *yhhX* and *yhhY*, is conserved in *E. coli*, *Salmonella*, and *Klebsiella*, and to a lesser extent in *Y. pestis* and *V. cholerae*. In some species (e.g., *Salmonella* and *Yersinia*), a second *ryhB*-like sequence is present suggesting the existence of two RyhB-like sRNAs (Ellermeier and Slauch 2008; Deng et al. 2012). As discussed above, RyhB activity is Hfq-dependent (Wassarman et al. 2001) (**Figure 26**). The regulation network of RyhB covers several aspects of bacterial metabolism, which are all connected towards the survival upon iron starvation and that will be discussed in the following paragraphs.

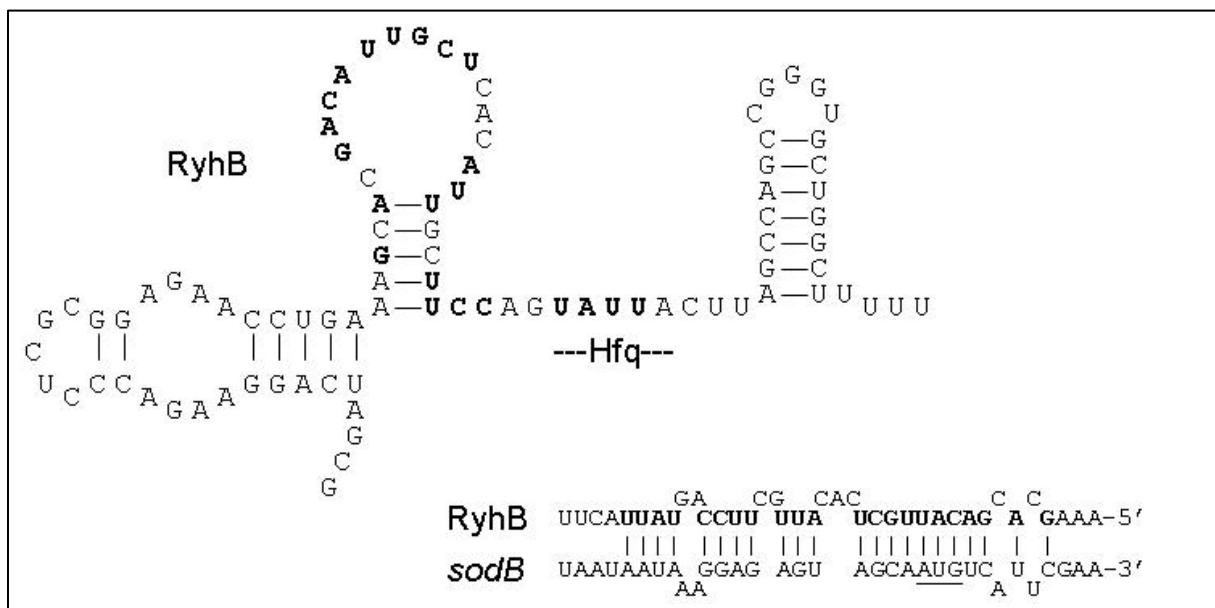


Figure 26: Secondary structure of RyhB

Top: RyhB binds to target mRNAs through nucleotides located on unpaired regions. Hfq binding site is indicated. Bottom: predicted pairing between RyhB and *sodB* mRNA. Nucleotides involved in the pairing are indicated in bold. From (Tjaden et al. 2006)

#### 3.4.1. Regulation of the TCA cycle

*sdhCDAB* operon mRNA (encoding succinate dehydrogenase) and *fumA* mRNA (encoding fumarase) are RyhB targets. A  $\Delta fur$  mutant has a growth defect on succinate or fumarate as a sole carbon source (Massé and Gottesman 2002). The phenotype is due to the constitutive expression of RyhB in a  $\Delta fur$  mutant, preventing the translation of mRNAs associated with the succinate and fumarate catabolism. Other confirmed RyhB targets include *acnA* mRNA (aconitase), *bfr* mRNA (bacterial ferritin), *ftn* mRNA (ferritin), and *sodB* mRNA (superoxide dismutase). Note that all these targets encode proteins involved in iron storage or containing Fe-S clusters. Furthermore, three of these targets (*acnA*, *fumA* and *sdhCDAB* mRNAs) are involved in TCA cycle. However, other TCA cycle enzymes that do not contain Fe-S clusters are not regulated by RyhB (Massé and Gottesman 2002). Other studies identified new RyhB targets, most of them being mRNAs encoding proteins with Fe-S clusters (Massé, Vanderpool, and Gottesman 2005). Taken together, these results imply that RyhB regulates intracellular iron utilization by repression of the TCA cycle, a non-essential metabolic pathway that needs several iron-containing enzymes.

#### 3.4.2. RyhB and Fe-S clusters synthesis

Another target of RyhB is the *iscRSUA* operon mRNA, which is involved in the synthesis of Fe-S clusters via the *isc* system. In presence of iron, IscR possess a Fe-S cluster and represses expression of the *iscRSUA* operon. In absence of iron, Apo-IscR alleviates its repression on *iscRSUA* operon and also activates transcription of the *suf* operon, the second Fe-S cluster machinery expressed upon iron starvation (Outten, Djaman, and Storz 2004; Yeo et al. 2006). Interestingly, RyhB targets the *iscRSUA* operon but only downstream of *iscR*, which leads to expression of IscR and cleavage of the *iscSUA* mRNA (Desnoyers et al. 2009). RyhB also targets *erpA* mRNA encoding for an acyl-carrier protein, which is repressed by IscR under presence of iron (Mandin, Chareyre, and Barras 2016). Taken together, these two results shows that bimodal regulation of the *iscRSUA* operon and regulation of *erpA* mRNA promote the switch from the *isc* to the *suf* system and ensure that ErpA can bring Fe-S clusters only when it is necessary.

#### 3.4.3. Siderophore production

Interestingly, some RyhB targets such as *shiA* mRNA are positively regulated by RyhB. *shiA* encodes a permease of shikimate, a precursor for the biosynthesis of enterobactin and salmochelin siderophores. *shiA* mRNA is poorly translated because

of the presence of an inhibitory secondary structure on its 5' region that hides the RBS. By binding to the *shiA* 5' UTR, RyhB prevents the formation of this structure and activates *shiA* translation (Prévost et al. 2007). Further studies showed that globally,  $\Delta$ *ryhB* mutants produce less siderophores and are less virulent than WT strains (Porcheron et al. 2014).

Taken together, analysis of RyhB targets reveal its dual role: on one side, RyhB improves the fitness of bacteria by repressing non-essential genes that contains Fe-S cluster to spare iron for essential proteins, on the other side, RyhB promotes iron acquisition to recover a normal intracellular iron concentration. Regulation of iron homeostasis by a Fur-regulated sRNA seems an optimum solution for bacteria. Indeed, it is economical in terms of energy, efficient and it can evolve to downregulate new targets.

#### 3.4.4. RyhB and Hfq

Like many sRNAs, RyhB binds to RBSs, using Hfq to stabilize the interactions. Binding of RyhB to *sodB* mRNA lead to recruitment of RNase E with the degradation of both *sodB* mRNA and RyhB (Massé, Escorcia, and Gottesman 2003). The degradation of mRNAs by RyhB is independent of the translational repression (Prévost et al. 2011). This mechanism is the same for all mRNA targets of RyhB except for *acnB* mRNA, which encodes for the major aconitase of *E. coli*. In the case of *acnB* mRNA, RNase-E-induced degradation by RyhB is prevented by the binding of Apo-AcnB (which acts as an RNA-binding protein) on the cleavage site (Benjamin and Massé 2014). Recent work by David Lalaouna showed that many *E. coli* sRNAs (including RyhB) are actually able to bind mRNAs even in the absence of Hfq. However, mRNAs bound by RyhB without Hfq were not degraded, meaning that the ternary complex formed by sRNA, a target mRNA, and Hfq is necessary for the recruitment of RNase E (Lalaouna et al. 2021).

#### 3.4.5. Other RyhB functional homologs in bacteria

Over the years, many RyhB orthologs and functional homologs were discovered in different species. This confirms the hypothesis that having a sRNA-mediated response to iron starvation confers a great advantage and has been naturally selected over the course of the evolution.

As mentioned previously, Enterobacteriaceae may have paralogs of RyhB. In addition, functional homologs of RyhB have also been found in bacteria which are evolutionary distant from *E. coli* (Table 2). These homologs do not share the same sequence nor the same need for RNA chaperone, but they are all induced upon iron starvation and repress iron-containing proteins.

| Name         | Bacteria  | Reference                    |
|--------------|---|------------------------------|
| FsrA         | <i>Bacillus subtilis</i>  | (Gaballa et al. 2008)        |
| Prrf1, Prrf2 | <i>Pseudomonas aeruginosa</i>                                   | (Wilderman et al. 2004)      |
| NrrF         | <i>Neisseria meningitidis</i> ,<br><i>Neisseria gonorrhoeae</i> | (Mellin et al. 2007)         |
| ArrF         | <i>Azotobacter vinelandii</i>                                   | (Jung and Kwon 2008)         |
| MrsI         | <i>Mycobacterium tuberculosis</i>                               | (Gerrick et al. 2018)        |
| IsrR         | <i>Staphylococcus aureus</i>                                    | (Coronel-Tellez et al. 2022) |

Table 2: Functional homologs of RyhB in other bacteria

The fact that orthologs or functional homologs of RyhB are found in many different bacteria confirms that this mechanism of response to iron starvation was not acquired through horizontal transfer but rather emerged through evolutive convergence, showing that response to iron starvation is critical for the survival of the bacteria. Regulation of iron homeostasis by a Fur-regulated sRNA seems an optimum solution, because it is economical in terms of energy, efficient and it can evolve to downregulate new targets.

## **4. *Staphylococcus aureus***

### **4.1. Generalities and pathogenicity of *S. aureus***

*S. aureus* is a Gram-positive, rod-shaped bacterium. It is a member of the Bacillota, formerly called Firmicutes. *S. aureus* is a non-motile, facultative anaerobe, non-sporulating bacterium, and able to obtain energy from nitrate reduction (Pantel et al. 1998). Its name comes from the fact that *S. aureus* colonies are golden yellow due to the production of a specific pigment, staphyloxanthin.

*S. aureus* is a human commensal with an estimated 30% of the population carrying it in their nares (Krismer et al. 2017). It can be an opportunistic pathogen favored by immunodepression, following surgery or an antibiotic treatment, for example. Some studies reported that deaths caused by *S. aureus* in the U.S.A. accounted for around 20,000 people, more than AIDS, tuberculosis, and viral hepatitis deaths combined (Kourtis et al. 2019; Van Hal et al. 2012). A recent paper showed that *S. aureus* was the leading cause of death by bacterial infections in the world in 2019,

and the most deadly bacterial pathogen in 135 countries (Figure 27) (Ikuta et al. 2022). *S. aureus* infections have become a real issue due to the emergence of antibiotic multi-resistance, especially with the apparition of the multiresistant methicillin-resistant *S. aureus* (MRSA) and vancomycin-resistant *S. aureus* (VRSA). In 2019, multiresistant strains of *S. aureus* were responsible for more than 80000 deaths, and more than 50,000 people died from infections caused by MRSA (Mestrovic et al. 2022). Even if nosocomial-related MRSA infections are decreasing in developed countries, they are still rising in developing countries (Cheung, Bae, and Otto 2021).

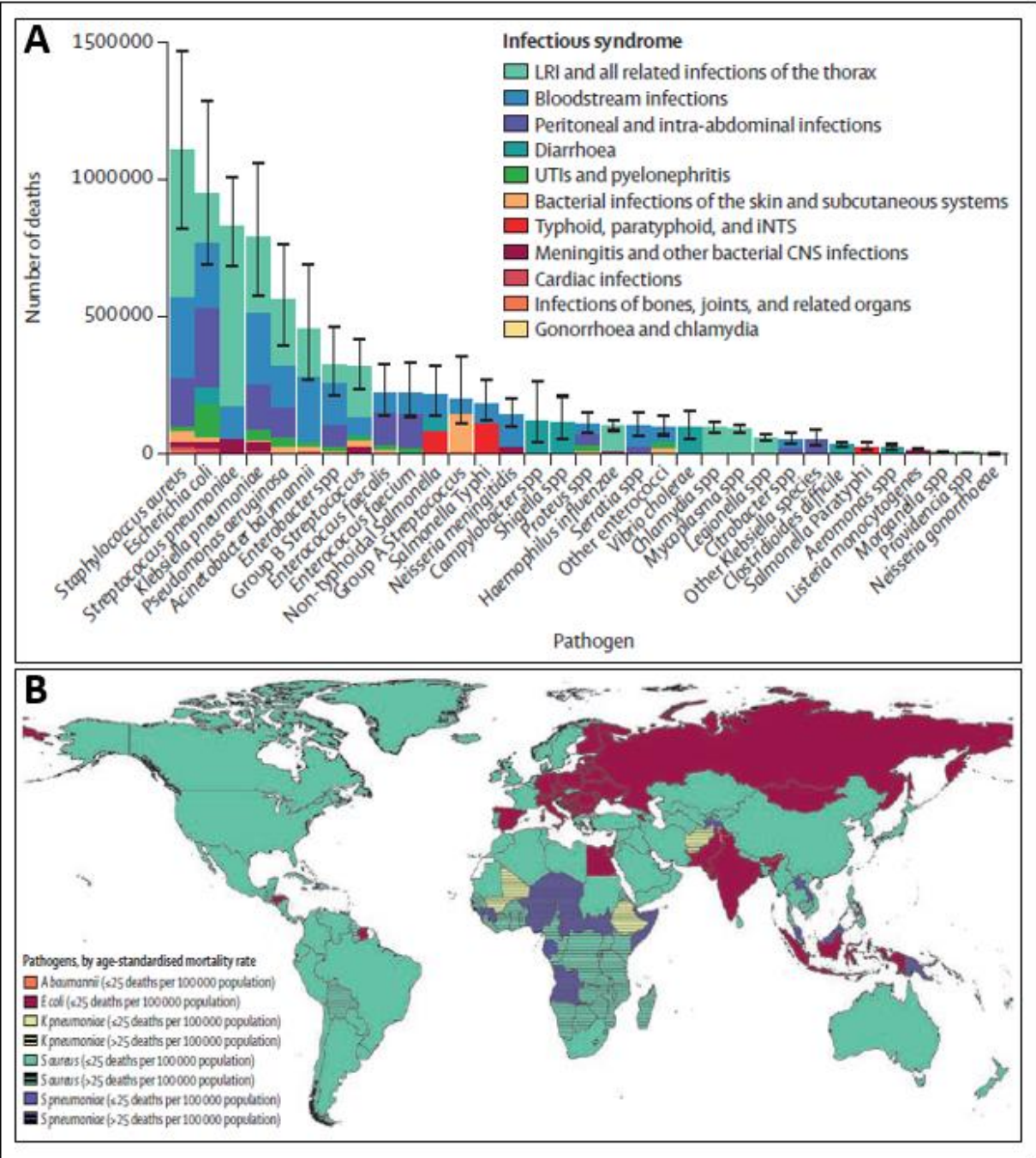


*Figure 27: S. aureus is the leading cause of bacterial infections in the world*

A: Global number of deaths by pathogen and infectious syndrome in 2019. LRI = Lower respiratory infections; UTI = Urinary tract infections; iNTS: invasive non-typhoidal Salmonella. B: Pathogen responsible for the highest age-standardized mortality per 100,000 inhabitants and country in 2019. From (Ikuta et al. 2022).

*S. aureus* can cause a large panel of infections, ranging from minor skin infections such as furuncles, panariciums, or abscesses to more severe and possibly lethal infections such as pneumonia, bloodstream infections, endocarditis, or intoxication during toxic shock syndrome or food poisoning. *S. aureus* skin infections usually originate from asymptomatic contamination or by skin-to-skin contact if there is the presence of an entry point, which can be a minor scratch in the skin. Nosocomial infections, or toxic shock syndrome, are caused by an infection of internal tissues or organs by *S. aureus* through individuals or infected fomites. In the case of food poisoning, the infection is not due to *S. aureus* itself but by the ingestion of contaminated food that contains staphylococcal enterotoxins that will trigger an excessive immune response. The pathogenicity and the wide range of *S. aureus* infections are due to the presence of numerous virulence factors that enable it to adapt to various environmental conditions and survive within the host.

## **4.2. Virulence factors of *S. aureus***

### **4.2.1 Biofilms**

*S. aureus* has the ability to form biofilms on many surfaces, such as pacemakers, urinary catheters, or prostheses. Biofilms can also appear on biological tissues, such as heart valves in the case of endocarditis. They represent a great virulence factor, as their structure allows the bacteria to survive and multiply while resisting host defenses and antibiotic treatment. Plus, the behavior of the cells within biofilms is modified and leads to the appearance of persisters (Mah and O'Toole 2001).

The formation of a biofilm starts with the attachment of the cells to a surface, usually the host matrix composed of fibronectin, fibrinogen, etc. *S. aureus* possesses about 20 microbial surface components recognizing adhesive matrix molecules (MSCRAMM), which include two clumping factors (ClfA and ClfB) and two fibronectin-binding proteins (FnBPA, FnBPB), as well as several secretable expanded repertoire adhesive molecules (SERAM) (Clarke and Foster 2006). All these proteins are used by the bacteria to anchor to the host matrix. The proliferation and shaping of the 3D structure of the biofilm are ensured by the production of polysaccharide intercellular adhesion (PIA), which binds the cells together, and the production of two phenol-soluble modulins (PSMs) and ten exoproteins that shape and degrade the biofilm

(Boles and Horswill 2011). The regulation of genes involved in biofilm formation depends on several factors, such as the global regulator SarA and the quorum sensing system Agr (Otto 2018).

#### 4.2.2 Escaping host immunity

To be phagocytosed by macrophages or neutrophils, the bacteria must be opsonized, *i.e.* labeled with antibodies to be recognized. *S. aureus* has developed several mechanisms to avoid opsonization, the most studied being the production of protein A. Protein A is secreted and binds to the IgG and IgM, thus providing camouflage to the bacteria while promoting apoptosis of B cells (Falugi et al. 2013).

*S. aureus* is also able to directly lyse white blood cells using a leukotoxin called Panton-Valentine leukocidin (PVL). This toxin targets different receptors on immune cells and forms pores, which induces their lysis. Other leukotoxins exist, such as LukAB and LukDE, but PVL is the most cytotoxic (Ahmad-Mansour et al. 2021). The destruction of the host immune cells is also mediated by PSMs that can attach to the receptor FPR2 and attract innate immune cells to lyse them (Cheung et al. 2014).

#### 4.2.3 Hemolysins

Hemolysins are used by *S. aureus* to penetrate the epithelial barrier and destroy erythrocytes. *S. aureus* encodes  $\alpha$ -,  $\beta$ -,  $\gamma$ -, and  $\delta$ -hemolysins, all four being regulated by Agr. The most studied hemolysin is  $\alpha$ -hemolysin, encoded by the *hla* gene. This hemolysin targets a large variety of cells, in which it will assemble as an homoheptamer on the ADAM10 receptor to create an aqueous channel that will lead to cell lysis (Divyakolu et al. 2019). Interestingly, even though 95% of *S. aureus* strains encode *hla*, the most pathogenic strains (*e.g.* USA300) have a significant increase in *hla* expression than the others, linking *hla* expression and pathogenicity (Montgomery et al. 2008).

$\beta$ -hemolysin, also called hot-cold hemolysin due to its enhanced activity after a switch of temperature from 37°C to 10°C, is a Mg<sup>2+</sup>-dependent sphingomyelinase able to lyse erythrocytes by cleaving sphingomyelin into phosphorylcholine and ceramide. Even though erythrocytes are not highly sensitive to  $\beta$ -hemolysin, its activity enhances the activity of  $\alpha$ -hemolysin and PVL, and the production of ceramide triggers MAP kinases and apoptosis (Futerman and Hannun 2004).

$\Gamma$ -hemolysin is a type of bi-component leukocidin that shares structure similarity with  $\alpha$ -hemolysin and PVL (Gouaux, Hobaugh, and Song 2008). Like PVL and  $\alpha$ -hemolysin, it is a pore-forming toxin that exerts its activity by associating in oligomers on the surface of target cells and inducing their lysis.

$\delta$ -hemolysin is produced from the sRNA RNAlII, which is under the control of Agr. It is expressed preferentially in the post-exponential phase. Unlike other *S. aureus*

hemolysins,  $\delta$ -hemolysin acts by first forming pores on the membrane, but it then acts as a surfactant to destabilize it and induce lysis (Verdon et al. 2009).

#### 4.2.4 *S. aureus* toxins

*S. aureus* encodes several toxins that are superantigens. These toxins can interact with T cells and trigger a strong immunity response that can lead to multiple organ failure. In *S. aureus*, two types of toxins are produced: The staphylococcal enterotoxins (SE) and the toxic shock syndrome toxin 1 (TSST-1). There are more than 20 SEs, and some of them are involved in food poisoning, such as SEA, SEB, and SED. SEs can cross the epithelial barrier and bind to class II MHC molecules, which triggers a strong inflammatory response causing nausea, vomiting, abdominal pain, and diarrhea (Pinchuk, Beswick, and Reyes 2010; Balaban and Rasooly 2000). TSST-A, encoded by the gene *tstH* located on a pathogenicity island, is also able to cross the epithelial barrier and interact with class II MHC. The massive cytokine liberation causes fever, rash, desquamation, and hypotension, and can lead to multi-organ failure (McCormick, Yarwood, and Schlievert 2001).

#### 4.2.5 Resistance to oxidative stress

When neutrophils phagocyte *S. aureus*, they produce reactive oxygen species (ROS) that attack its membrane and DNA. *S. aureus* has developed mechanisms to survive in these conditions, which mainly rely on the ability to convert ROS into inoffensive species (**Figure 28**).

One mechanism is the production of staphyloxanthin. Indeed, the carotenoid pigment that gives the golden color to the cells serves as an antioxidant by binding radicals onto a series of conjugated double bonds (Clauditz et al. 2006). In addition to staphyloxanthin, *S. aureus* possesses enzymes to detoxify oxygen radicals. *S. aureus* encodes for two superoxide dismutases, SodA and SodM that catalyze the dismutation of  $O_2^-$  into oxygen and hydrogen peroxide ( $H_2O_2$ ). Hydrogen peroxide can be further reduced into water and oxygen by the action of a catalase (KatA) or an alkyl hydroperoxide reductase (AhpC). However,  $H_2O_2$  can also react with  $Cl^-$  to form hypochlorite via the action of myeloperoxidase (MPO). Fortunately, MPO activity is inhibited by the staphylococcal peroxidase inhibitor (SPIN). The neutrophils can also produce  $ONOO^-$  by combining  $O_2^-$  and nitric oxide (NO), but the activity of superoxide dismutases greatly represses its production (Cheung, Bae, and Otto 2021; Gaupp, Ledala, and Somerville 2012).

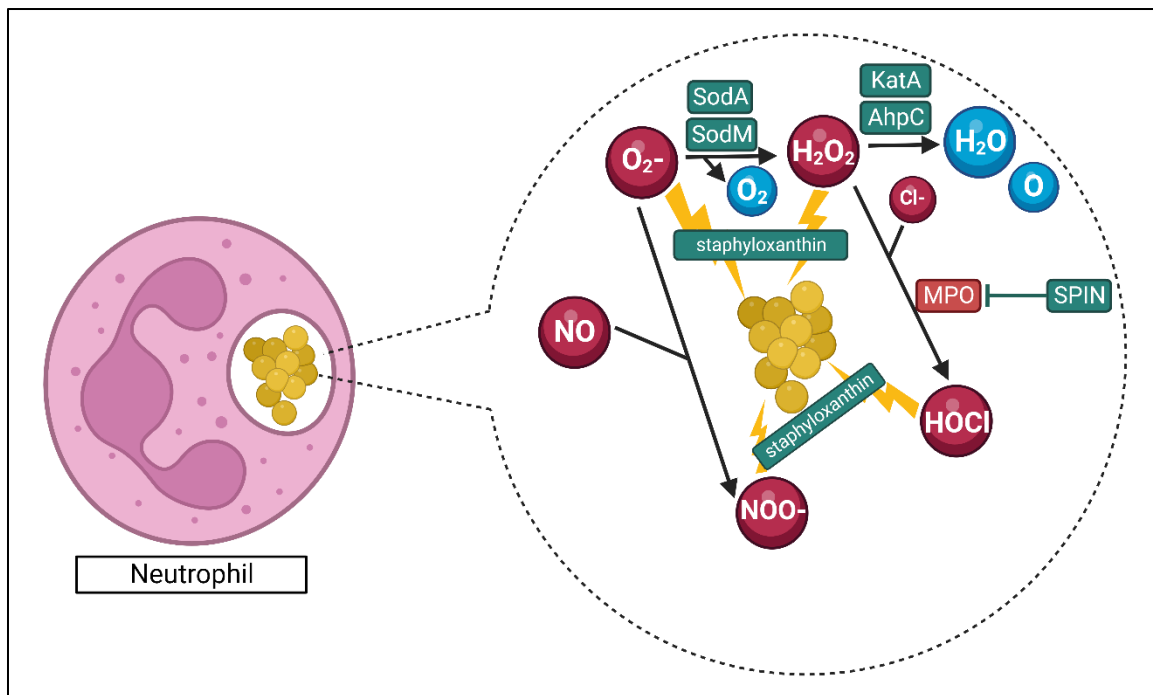


*Figure 28: S. aureus resistance to oxidative stress inside neutrophils*

Reactive oxygen species and neutrophil proteins are indicated in red. Staphylococcal proteins are indicated in green. SodA/SodM: Superoxide dismutase A/M; KatA: Catalase; AhpC: Alkyl hydroperoxide reductase; SPIN: Staphylococcal peroxidase inhibitor; MPO: myeloperoxidase.

This list of virulence factors is not exhaustive, as *S. aureus* possesses dozens of mechanisms that allow its survival in a large panel of conditions. Among them, the most important is the multitude of iron acquisition systems that permit the bacteria to acquire iron from various sources.

### 4.3 Iron acquisition systems in *S. aureus*

Iron acquisition by *S. aureus* relies on a variety of systems that allow it to recover free iron, but also iron complexed to host proteins, such as transferrins, lactoferrins or calprotectin, and even iron found within heme groups. All these systems are under the control of Fur (**Figure 29**).

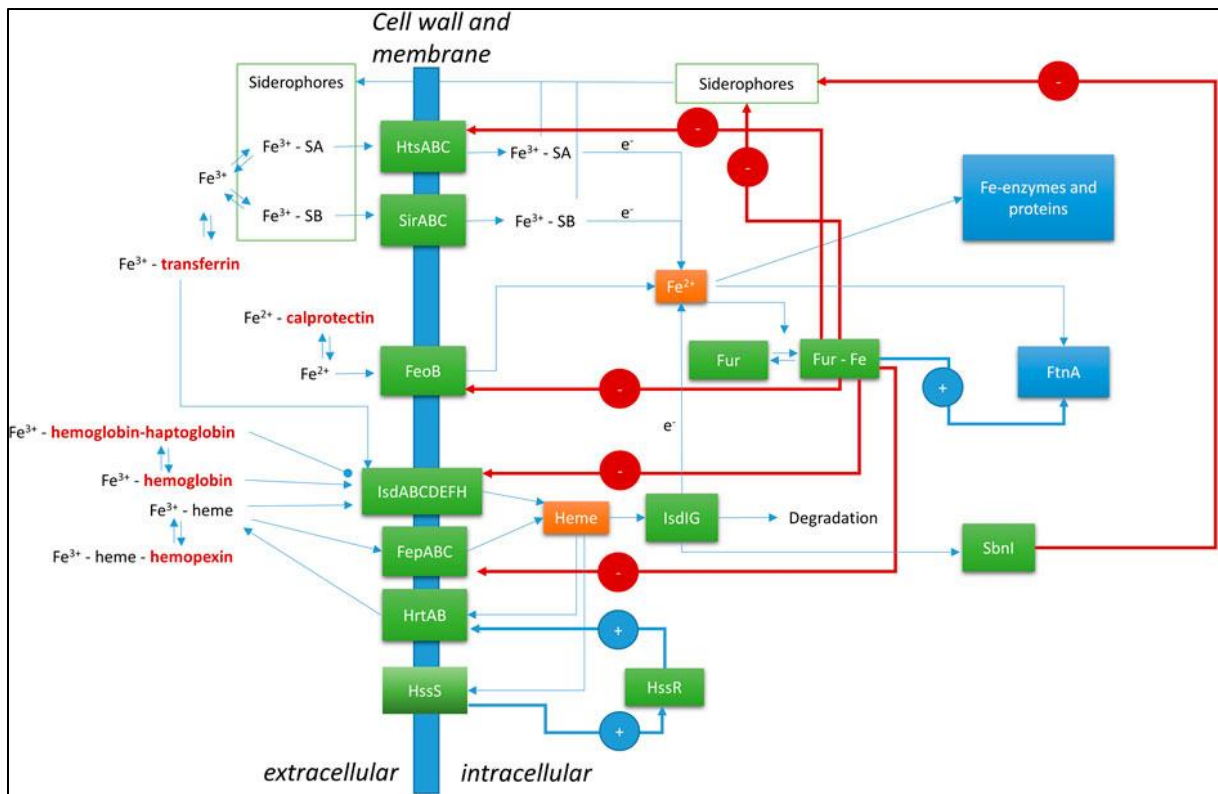


Figure 29: Different iron acquisition systems in *S. aureus*

FeoB, ferrous Fe transporter; FepABC, Fe dependent peroxidase transporter; FtnA, ferritin; Fur, ferric uptake regulator; HrtAB, heme regulator transporter efflux pump; HssR, heme sensing two-component regulator regulatory protein; HssS, heme sensing two-component regulator sensor protein; HtsABC, heme transport system involved in Fe-SA uptake; IsdABCDEFH, iron-regulated surface determinant system; SA, Staphyloferrin A; SB, Staphyloferrin B; SbnI, L-serine kinase and heme responsive regulator of SB biosynthesis. Human (host) proteins are in bold and dark red font. From (Van Dijk, De Kruijff, and Hagedoorn 2022).

#### 4.3.1 Acquisition of free iron

*S. aureus* can acquire iron through two different systems. The first system uses the FeoB iron transporter. FeoB is part of the FeoABC system, an iron transporter system widespread among bacteria and mostly studied in Gram-negative bacteria. In *S. aureus*, only FeoB is present and is sufficient for the transport of ferrous iron, free or coming from calprotectin, into the cell. However, recent studies showed that FeoB is probably important for the pathogenicity of *S. aureus* since inhibition of FeoB reduced intracellular iron concentration and prevented resistance to gentamicin (Shin et al. 2021).

The second system used by *S. aureus* to incorporate free iron is the FepABC (Fe-dependent peroxidase) transporter. FepABC from *S. aureus* has not been well characterized yet but seems to be a homolog of *E. coli efeUOB* (see page 21). FepABC

is encoded in an operon and is composed of an iron permease (FepC), an iron-binding protein (FepA), and an iron-dependent peroxidase (FepB) (Sheldon and Heinrichs 2015). The role of FepB is not clear yet, but studies showed that FepB is transported across the membrane through the twin-arginine translocation (Tat) pathway and is also able to bind heme groups in order to extract iron from it (Biswas et al. 2009; Turlin et al. 2013). FepABC is therefore able to scavenge free iron from the media as well as iron coming from heme groups.

#### 4.3.2 Acquisition of heme by the Isd system

In the host, the vast majority of available iron is present in the form of heme. Interestingly, heme is the preferred iron source for *S. aureus* (Skaar et al. 2004) and therefore, it has developed an efficient way to acquire it through the Isd system (see page 19, Figure 7). IsdB and IsdH, which are both anchored to the membrane by sortase A, are both able to bind host hemoproteins, such as methemoglobin, hemoglobin, and haptoglobin (Conroy et al. 2019). However, IsdB seems to be the primary receptor of hemoglobin since  $\Delta isdB$  mutants are not growing in the presence of heme as the sole iron source and display decreased virulence in a murine model (Torres et al. 2006).

It is important to note that several studies showed an interplay between iron acquisition pathways through heme and siderophores. Indeed, SbnI, the regulator of the *sbn* operon that controls the synthesis of staphyloferrin B, can be repressed by heme binding from the heme-degrading protein IsdI. Heme binding causes repression of staphyloferrin B production when heme is present (Laakso et al. 2016; Verstraete et al. 2019). Another example of interaction between siderophore and heme utilization pathways is the role of the oxidoreductases IruO and NtrA, that release ferrous iron from hydroxamates siderophores and staphyloferrin A, respectively. Indeed, IruO and NtrA are also needed for the release of ferric iron by IsdI/G (Hannauer, Arifin, and Heinrichs 2015). Finally, some studies also mentioned that the staphyloferrin A transporter HtsBC could be a heme permease (Skaar et al. 2004). This claim was invalidated later, but the authors showed that a  $\Delta isdE\Delta htsA$  mutant of *S. aureus* was still able to acquire heme, suggesting the presence of another and still unknown heme acquisition system (Wright and Nair 2012).

#### 4.3.3 Iron acquisition by siderophores

*S. aureus* can scavenge iron complexed to host proteins, such as transferrin or lactoferrin, by the production of two siderophores: staphyloferrin A (SA) and staphyloferrin B (SB). Both siderophores are part of the carboxylate family and are therefore resistant to siderocalin. They are both synthesized through the non-ribosomal peptide synthesis independent siderophore (NIS) pathway, meaning that they are synthesized by enzymes that condensate alternating subunits or dicarboxylic

acids (in the case of SA and SB, citrate) with diamines, amino alcohols and alcohols (Conroy et al. 2019). SA is synthesized and exported by proteins encoded from the *sfa* locus, and imported by the HtsABC transporter. Interestingly, the *hts* and *sfa* loci are located next to each other. The same observation exists for the loci responsible for the synthesis and the import of SB (*sbn* and *sir*, respectively) (**Figure 30**). All the genes encoding for biosynthesis and uptake of siderophores are under the control of Fur.

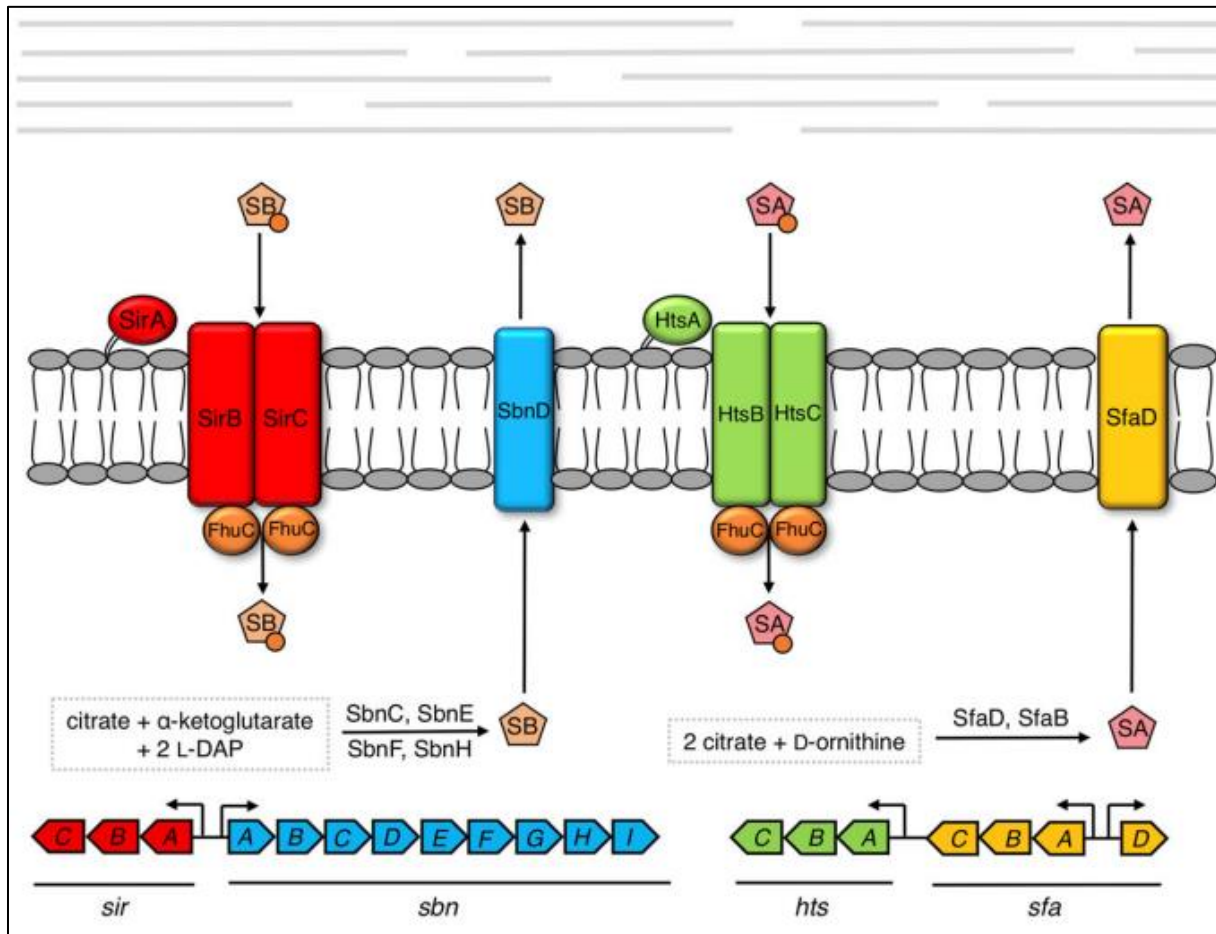


*Figure 30: SA and SB biosynthesis and uptake systems in S. aureus*

Proteins involved in the biosynthesis and export of staphyloferrin A (SA) and staphyloferrin B (SB) are encoded in the *sfa* and *sbn* loci, respectively. The siderophore uptake systems HtsABC and SirABC facilitate the transport of SA and SB, respectively. Orange spheres indicate ferric iron. From (Conroy et al. 2019).

Besides the production of SA and SB, *S. aureus* is also able to use xenosiderophores (siderophores produced by other microorganisms) (**Figure 31**). While it does not produce hydroxamate siderophores, *S. aureus* is able to use some of them, such as aerobactin, rhodotorulic acid, and ferrichrome using the ferric hydroxamate uptake (Fhu) system. The Fhu system is encoded by *fhuD* and *fhuCBG*. FhuD is a hydroxamate receptor, FhuB and FhuG are transmembrane proteins and FhuC is an ATP-binding protein. Interestingly, there are two paralogs of Fhu encoded by

*fhuD1* and *fhuD2*. FhuD2 is present in all *S. aureus* strains and has a better affinity and a wider range of hydroxamate targets than FhuD1, which is found in variable locations on the genome or can be absent (Sebulsky et al. 2004). *S. aureus* also incorporates catechol siderophores thanks to the *staphylococcal siderophore transporter* (Sst). Sst is encoded by the *sstABCD* operon encoding the transmembrane proteins (SstA and SstB), the ATP-binding protein (SstC), and the siderophore-binding protein (SstD) (Beasley et al. 2011). Sst is necessary for the import of enterobactin and bacillibactin, but it is also able to incorporate catecholamine-iron complexes (such as epinephrine-iron complexes) that can be used as an iron source by *S. aureus*. All the genes encoding the Fhu and Sst systems are under the control of Fur.

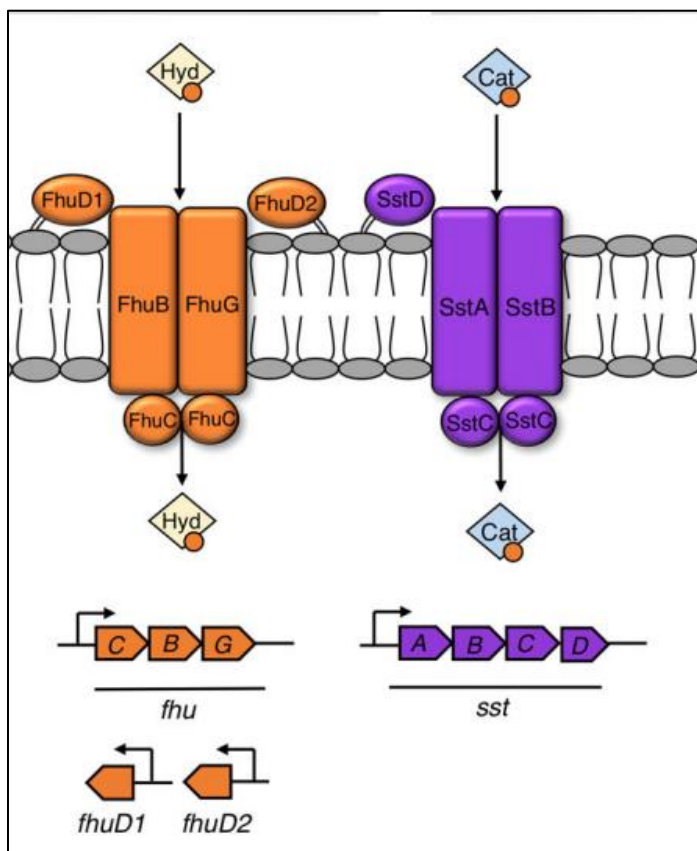


*Figure 31: Xenosiderophores uptake systems in S. aureus*

Proteins of the Fhu systems implicated in the incorporation of hydroxamates siderophores are indicated in orange. Proteins of the Sst system involved in the incorporation of catecholates are indicated in purple. Hyd: hydroxamates; Cat: catecholates; orange sphere: ferric iron. From (Conroy et al. 2019).

## 4.4 Citrate metabolism of *S. aureus*

*S. aureus* is not able to use citrate as a carbon source, and so far no citrate transporter has been properly described. Citrate is produced from the conversion of oxaloacetate and acetyl-CoA by the citrate synthase CitZ. It is then converted first into cis-aconitate, and then into isocitrate by the aconitase CitB. *citB* is under the control of the carbon catabolite protein E (CcpE), which is itself sensitive to the intracellular citrate concentration and activates the transcription of *citB* and *citZ* mRNAs (Hartmann et al. 2013; Y. Ding et al. 2014). Therefore, CitB and CcpE are part of an autoregulatory feedback loop: when citrate is produced, it activates CcpE which in turn activates the transcription of both CitZ and CitB, leading to an activation of the TCA cycle (**Figure 21**).

Surprisingly, *S. aureus* possesses a second citrate synthase, encoded by the *sbnG* gene. *sbnG* is part of the operon that encodes for staphyloferrin B and serves for the production of citrate as a precursor of SB when the bacteria is grown in iron-restricted media containing glucose (Sheldon, Marolda, and Heinrichs 2014);

While citrate can be found in the environment, isocitrate has to be synthesized by aconitase to pursue the TCA cycle activity. This has been confirmed, as a *B. subtilis*  $\Delta$ *citB* mutant is an auxotroph for glutamate, which cannot be synthesized since it is made from  $\alpha$ -ketoglutarate, produced from isocitrate (Pechter et al. 2013).

## 4.5 IsrR

IsrR (Iron-sparing response regulator) is a 174-nt long *trans*-encoded sRNA conserved among the *Staphylococci* and is involved in the response to iron starvation and the virulence in *S. aureus* (Coronel-Tellez et al. 2022). IsrR expression is controlled by Fur via two Fur boxes. Therefore, it is expressed during iron starvation and constitutively in a  $\Delta$ *fur* mutant. IsrR possesses three stem-loops and has its own terminator, as well as three C-rich regions (CRR). These later regions are important for staphylococcal sRNA activities (*e.g.* Geissmann et al. 2009; Rochat et al. 2018) (**Figure 32**).

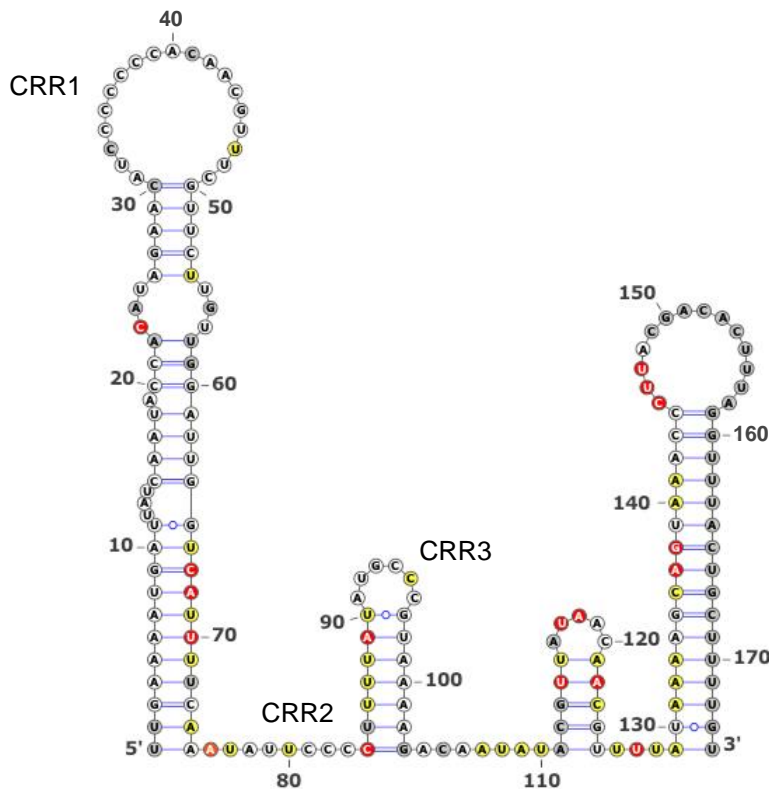


*Figure 32: Secondary structure of IsrR*

The secondary structure of IsrR was obtained by SHAPE analysis and bioinformatics studies. Each base is colored depending on its reactivity to 1M7, which cleaves unpaired regions of the RNA. Grey: Not determined; White: Low reactivity; Yellow: Medium reactivity; Red: High reactivity. Stem loops are indicated by H1, H2, and H3. Terminator is indicated by T. C-rich regions (CRR) are indicated in red boxes. From (Coronel-Tellez et al. 2022)

IsrR acts by repressing the translation of several non-essential proteins containing Fe-S clusters in order to spare residual iron for essential processes only. On the list of the 23 most probable targets of IsrR, seven are mRNAs encoding for proteins containing Fe-S clusters. IsrR binds to the 5' UTR of its mRNA targets through its CRRs and thus prevents ribosome attachment. Interestingly, several confirmed targets of IsrR to this date are genes involved in nitrate respiration (*fdhA*, *narG*, *nasD*, and *gltB2* mRNAs). However, other putative targets of IsrR are involved in other aspects of *S. aureus* metabolism, such as citrate utilization.

## D: Outline

---

The concept of using regulatory RNAs as mechanisms to overcome iron starvation is well-described in bacteria (Chareyre and Mandin 2018). The idea is that during iron starvation, regulatory RNAs repress non-essential genes encoding for proteins that contain iron to spare the remaining iron for its reallocation to essential processes, such as respiration or DNA synthesis. This phenomenon has been investigated in depth in *E. coli*, with the description of RyhB. However, until recently, the adaptation of *S. aureus* to iron-starved growth conditions was not associated with any regulatory RNA (Price and Boyd 2020). Thanks to a method developed for screening sRNA phenotypes in our laboratory (Le Lam et al. 2017), IsrR, a sRNA required for improved fitness in iron-depleted media was discovered. This functional homolog, but not ortholog, of RyhB in *S. aureus* is expressed under iron starvation and is involved in virulence.

During the first year of my thesis project, I had the opportunity to participate in the first characterization of IsrR. In particular, I contributed in obtaining the secondary structure of IsrR alone and in interaction with *fdhA* and *gltB* mRNAs by SHAPE. I also contributed to *in vitro* studies showing the interactions of IsrR with its mRNA targets by gel retardation. These results are within a publication I co-authored ((Coronel-Tellez et al. 2022), chapter F).

IsrR was shown to repress nitrate respiration, but bio-computing data suggested that IsrR had numerous other targets and was possibly associated with the regulation of several metabolic pathways. I pursued the characterization of IsrR with the identification of new targets. I notably discovered that IsrR was regulating the citrate metabolism by repressing aconitase and its transcriptional activator (chapter G).

MiaB is a tRNA modification enzyme containing [Fe-S] clusters. With Elise Leclair, a Master student that I co-trained, we showed that *miaB* expression is down-regulated by IsrR (chapter H). This work highlights the specificity role of CRR domains in translational regulations.

# **E: sRNA-controlled iron sparing response in Staphylococci**

---

# sRNA-controlled iron sparing response in Staphylococci

Rodrigo H. Coronel-Tellez<sup>1</sup>, Mateusz Pospiech<sup>2</sup>, Maxime Barrault<sup>1</sup>, Wenfeng Liu<sup>1</sup>, Valérie Bordeau<sup>3</sup>, Christelle Vasnier<sup>2</sup>, Brice Felden<sup>3,†</sup>, Bruno Sargueil<sup>2</sup> and Philippe Bouloc<sup>1,\*</sup>

<sup>1</sup>Université Paris-Saclay, CEA, CNRS, Institute for Integrative Biology of the Cell (I2BC) 91198, Gif-sur-Yvette, France, <sup>2</sup>CNRS UMR 8038, CitCoM, Université Paris Cité 75006, Paris, France and <sup>3</sup>Université de Rennes 1, BRM (Bacterial regulatory RNAs and Medicine) UMR.S 1230 35000, Rennes, France

Received November 10, 2021; Revised July 06, 2022; Editorial Decision July 07, 2022; Accepted July 19, 2022

## ABSTRACT

*Staphylococcus aureus*, a human opportunist pathogen, adjusts its metabolism to cope with iron deprivation within the host. We investigated the potential role of small non-coding RNAs (sRNAs) in dictating this process. A single sRNA, named here *IsrR*, emerged from a competition assay with tagged-mutant libraries as being required during iron starvation. *IsrR* is iron-repressed and predicted to target mRNAs expressing iron-containing enzymes. Among them, we demonstrated that *IsrR* down-regulates the translation of mRNAs of enzymes that catalyze anaerobic nitrate respiration. The *IsrR* sequence reveals three single-stranded C-rich regions (CRRs). Mutational and structural analysis indicated a differential contribution of these CRRs according to targets. We also report that *IsrR* is required for full lethality of *S. aureus* in a mouse septicemia model, underscoring its role as a major contributor to the iron-sparing response for bacterial survival during infection. *IsrR* is conserved among staphylococci, but it is not ortholog to the proteobacterial sRNA *RyhB*, nor to other characterized sRNAs down-regulating mRNAs of iron-containing enzymes. Remarkably, these distinct sRNAs regulate common targets, illustrating that RNA-based regulation provides optimal evolutionary solutions to improve bacterial fitness when iron is scarce.

## INTRODUCTION

Iron is essential for numerous enzymatic processes that use its redox properties, notably in respiration. Despite being one of the most abundant elements on earth, iron bioavail-

ability can be limiting. The mammalian host may prevent pathogen proliferation by restricting access to free iron, creating a nutritional immunity. In parallel, pathogens have developed complex systems for iron assimilation leading to a ‘battle for iron’ (1–4). While iron is required for growth, its excess is toxic. Indeed, ferrous iron decomposes hydrogen peroxide via the Fenton reaction into oxygen radical species that are highly reactive and oxidize a wide range of substrates, including bacterial macromolecules (DNAs, RNAs, proteins and lipids). Since most living organisms need iron but are sensitive to its excess, strict regulation of iron uptake and iron-containing enzymes is necessary (5,6).

For many bacteria, the main contributor to iron homeostasis is the transcriptional regulator *Fur* (7). In the presence of iron, *Fur* acts as a repressor targeting genes involved in iron acquisition, thereby ensuring a feedback regulation to maintain homeostasis of intracellular iron. In *Escherichia coli*, the absence of *Fur* leads to repression of a subset of genes using iron as a cofactor by an indirect effect. The mystery of this apparent paradox was solved by the discovery of a small regulatory RNA (sRNA) repressed by *Fur*, *RyhB* (8). In low iron conditions, *RyhB*, assisted by the RNA chaperone *Hfq*, accumulates and pairs to mRNAs, preventing the expression of iron-containing proteins and inducing an iron-sparing response (9). *RyhB* orthologs are present in many species from the *Enterobacteriaceae* family where they contribute to adaptation to low iron conditions (5,10). In *Pseudomonas* species, a major contributor to this adaptation is *PrrF*, a sRNA down-regulated by *Fur* contributing to iron homeostasis (11). Of note, the corresponding *ryhB* and *prrF* genes are duplicated in some species. Surprisingly, much less is known concerning Gram-positive bacteria where, so far, *RyhB* and *PrrF* orthologs were not found. sRNAs can nevertheless be regulators of the iron-sparing response. In *Bacillus subtilis*, *FsrA* sRNA is down-regulated by *Fur*, and with the help of three RNA chaperones, *FbpABC*, it prevents the expression of iron-

\*To whom correspondence should be addressed. Tel: +33 1 69 82 62 17; Email: philippe.bouloc@i2bc.paris-saclay.fr

†This work is dedicated to the memory of our colleague Brice Felden who died unexpectedly on 5 March 2021.

© The Author(s) 2022. Published by Oxford University Press on behalf of Nucleic Acids Research.

This is an Open Access article distributed under the terms of the Creative Commons Attribution License (<http://creativecommons.org/licenses/by/4.0/>), which permits unrestricted reuse, distribution, and reproduction in any medium, provided the original work is properly cited.

containing enzymes (12–14). In *Mycobacterium tuberculosis*, the sRNA MrsI is predicted to be down-regulated by IdeR, a functional homolog of Fur, and to exert a similar iron-sparing response. Interestingly, this bacterium does not possess Hfq (15).

*Staphylococcus aureus* is a human and animal opportunistic pathogen and a leading cause of nosocomial and community-acquired infections (16,17). Its success as a pathogen relies on the expression of numerous virulence factors and its adaptability to various environmental conditions including metal starvation. Indeed, iron limitation in the host is counteracted by alleviation of Fur repression, leading to the production of iron-scavenging siderophores (18). In this condition, *S. aureus* should down-regulate non-essential iron-containing enzymes to preserve iron for vital processes. However, despite significant research efforts devoted to the characterization of this major pathogen, no such system has been characterized to date (18).

As sRNAs are major regulators of iron homeostasis in several species, we designed a selection assay to identify staphylococcal sRNAs that could be involved in this process. We established a collection of *S. aureus* sRNA gene mutants that was used in fitness assays during iron starvation conditions. A single sRNA emerged as being essential for optimum growth when iron becomes scarce. We named it IsrR for ‘iron-sparing response regulator’, an acronym reflecting its function uncovered by the present study. In anaerobic conditions, expression of *isrR* prevented nitrate respiration, a non-essential metabolic pathway involving several iron-containing enzymes. IsrR is required for full lethality in an animal septicemia model of infection.

This study uncovers an iron-sparing response in *S. aureus*, dictated by a regulatory RNA, IsrR, which reallocates iron to essential processes when it is scarce.

## MATERIALS AND METHODS

### Bacterial strains, plasmids and growth conditions

Bacterial strains used for this study are described in Supplementary Table S1. Most of the work was performed with HG003, a *S. aureus* model strain widely used for regulation studies (19). Gene annotations refer to NCTC8325 nomenclature (file CP00025.1) retrieved from Genbank and Aureowiki (20). Plasmids were engineered by Gibson assembly (21) in *Escherichia coli* IM08B (22) as described (Supplementary Table S2), using the indicated appropriate primers (Supplementary Table S3) for PCR amplification. Plasmids expressing sGFP were constructed in MG1655Z1 *penB*::Km, a strain that decreases ColE1 plasmid copy number and therefore reduces toxic effects produced by high amounts of certain proteins in *E. coli*. MG1655Z1 *penB*::Km was constructed by the introduction of the *penB*::Km allele (23) in MG1655Z1 (24) by P1-mediated transduction.

Plasmids were verified by DNA sequencing and transferred into HG003, 8325-4, RN4220, or their derivatives. Chromosomal mutants (deletions and insertions) were either reported (25) or constructed for this study (Supplementary Table S1) using pIMAY derivatives as described (25), except for the *fur*::*tet* allele which was transferred

from MJH010 (26) to HG003 and HG003  $\Delta$ *isrR*::tag135 by phage-mediated transduction.

Staphylococcal strains were routinely grown in Brain Heart Infusion (BHI) broth at 37°C aerobically or anaerobically under anaerobic conditions (5% H<sub>2</sub>, 5% CO<sub>2</sub>, and 90% N<sub>2</sub>) in an anaerobic chamber (Jacomex).  $\Delta$ *fur* *S. aureus* derivatives in anaerobic conditions were grown in Tryptic Soy Broth (TSB). *E. coli* strains were grown aerobically in Luria-Bertani (LB) broth at 37°C. Antibiotics were added to media as needed: ampicillin 100 µg/ml and chloramphenicol 20 µg/ml for *E. coli*; chloramphenicol 5 µg/ml and kanamycin 60 µg/ml for *S. aureus*. Iron-depleted media was obtained by the addition of either DIP (2,2'-dipyridyl) 1.25 mM, unless stated otherwise; or EDDHA (ethylenediamine-*N,N'*-bis(2-hydroxyphenylacetic acid)) 0.7 mM and incubated for 30 min prior to the addition of bacteria.

### Fitness assay

Mutants with altered fitness in the presence of iron chelators were identified and analyzed using a reported strategy (25) with three independent libraries containing 48 mutants (Supplementary Table S4). The libraries were grown at 37°C in BHI, BHI DIP 1.25 mM, and BHI EDDHA 0.7 mM for 3 days. Overnight cultures were diluted 1000 times in fresh pre-warmed medium. Samples were withdrawn at OD<sub>600</sub> 1 and overnight as indicated (Figure 1A).

### Spot tests

Strain plating efficiency was visualized by spot tests. 5 µl of 10-fold serial dilutions of overnight cultures were spotted on plates containing either BHI, BHI DIP 1.25 mM or BHI EDDHA 0.7mM. Plates were supplemented with chloramphenicol 5 µg/ml when strains with plasmids were tested. BHI plates were incubated overnight at 37°C while BHI DIP and BHI EDDHA were incubated for 24h.

### Northern blots

Total RNA preparations and Northern blots were performed as previously described (27). 10 µg of total RNA samples were separated either by agarose (1.3%) or acrylamide (8%) gel electrophoresis. Membranes were probed with primers <sup>32</sup>P-labelled with [alpha-P32]Deoxycytidine 5'-triphosphate (dCTP) using Megaprime DNA labelling system (GE Healthcare) (for primers, see Supplementary Table S3) and scanned using the Amersham Typhoon imager.

### Rifampicin assay

Bacteria were cultured overnight in BHI. Then, 200 µl of cultures were transferred into 60 ml of fresh BHI or BHI supplemented with DIP 1.4 mM and grown at 37°C. At OD<sub>600</sub> 1.5 (*t*<sub>0</sub>), rifampicin was added to a final concentration of 200 µg/ml. Six ml of cultures were harvested at *t*<sub>0</sub> and 1, 3, 5, 10 and 20 min after the addition of rifampicin and transferred to tubes in liquid nitrogen to stop bacterial growth. RNA was extracted as described (27) and Northern blots were performed as described above. tmRNA was used as RNA loading control.

### Biocomputing analysis

DNA-seq data from fitness experiments were analyzed using a reported pipeline (25). *isrR* orthologs were identified thanks to the sRNA homolog finder GLASSgo (28) with *isrR* (174nt) as input using the default parameters. Fur boxes were detected using the motif finder FIMO (29) with *isrR* sequences retrieved from GLASSgo (option including 100nt upstream *isrR* sequences) and *S. aureus* NCTC8325 Fur consensus motifs from RegPrecise (30). IsrR secondary structure was modelled with LocARNA (31) with 18 IsrR orthologs with non-identical sequences using default parameters. Putative IsrR targets were found by CopraRNA (32) set with default parameters and *isrR* orthologs from *S. aureus* NCTC8325 (NC.007795), *S. epidermidis* RP62A (NC.002976), *S. lugdunensis* HKU09-01 (NC.013893), *Staphylococcus pseudintermedius* HKU10-03 (NC.014925), *Staphylococcus pseudintermedius* ED99 (NC.017568), *Staphylococcus xylosus* (NZ\_CP008724), *Staphylococcus warneri* SG1 (NC.020164), *Staphylococcus pasteurii* SP1 (NC.022737), *Staphylococcus hyicus* (NZ\_CP008747), *Staphylococcus xylosus* (NZ\_CP007208), *Staphylococcus argenteus* (NC.016941), *Staphylococcus carnosus* TM300 (NC.012121), *Staphylococcus cohnii* (NZ\_LT963440), *Staphylococcus succinus* (NZ\_CP018199), *Staphylococcus agnetis* (NZ\_CP009623), *Staphylococcus piscifermentans* (NZ\_LT906447), *Staphylococcus stepanovicii* (NZ\_LT906462), *Staphylococcus equorum* (NZ\_CP013980), *Staphylococcus nepalensis* (NZ\_CP017460), *Staphylococcus lutrae* (NZ\_CP020773), *Staphylococcus muscae* (NZ\_LT906464), *Staphylococcus simulans* (NZ\_CP023497).

### Probability calculation

For a set of  $N$  objects (number of *S. aureus* mRNAs = 2889) with  $m$  different objects (number of mRNA expressing Fe–S containing proteins = 32 (estimated number in *S. aureus* [Table S6, (33,34)], the probability of drawing  $n$  objects (23 targets proposed by CopraRNA) and to have among  $k$  differentiated objects (mRNA expressing Fe–S containing proteins = 7) is given the following equation  $p(X = k) = \frac{C_m^{n-k} C_{N-m}^k}{C_N^n}$ , where  $C$  represents a combination operator (<https://www.dcode.fr/picking-probabilities>).

### Electrophoretic mobility shift assay

RNAs were transcribed from PCR products (for primers, see Supplementary Table S3) using T7 RNA polymerase and purified by ethanol precipitation. Wild-type alleles were generated from HG003 genomic DNA and mutated alleles from gBlock DNAs (Integrated DNA Technologies) containing the desired mutations. Gel-shift assays were performed as described (35) with the following modifications: RNAs were denatured in 50 mM Tris pH 7.5, 50 mM NaCl for 2 min at 80°C, followed by refolding for 20 min at 25°C after adding MgCl<sub>2</sub> at final concentration of 5 mM. The binding reactions were performed in 50 mM Tris–HCl (pH 7.5), 50 mM NaCl, 5 mM MgCl<sub>2</sub> for 30 min at 37°C. About 0.25 pmol of labeled IsrR or IsrRmut were incubated with various concentrations of *fdhA* mRNA or *fdhA*mut mRNA. Samples were supplemented with 10% glycerol and

were loaded on a native 8% polyacrylamide gel containing 5% glycerol. Gels were dried and visualized by autoradiography.

### Fur boxes reporter assay

Fluorescent tests to evaluate the contribution of Fur boxes were performed with 8325-4, a ‘pigment-less’ strain (36) containing either pP<sub>isrR</sub>::*gfp*, pP<sub>isrR1</sub>::*gfp*, pP<sub>isrR2</sub>::*gfp* or pP<sub>isrR1&2</sub>::*gfp* (Supplementary Table S2). Overnight cultures were diluted 100 times, sonicated for 30 seconds, and fixated with ethanol 70% and PBS 1×. Fluorescence was detected using a Partec Cube 6 flow cytometer with ≈500 000 cells for each measure, with 488 and 532 nm wavelength filters for excitation and emission, respectively.

### Quantification of nitrite

*S. aureus* cultures were grown aerobically overnight, diluted 1000 times in fresh media and grown anaerobically overnight. They were then diluted to OD<sub>600</sub> 0.01, after 2 hours of incubation at 37°C, NaNO<sub>3</sub> 20 mM was added. 150 or 240 min after, samples were recovered and nitrite in supernatant was determined using the Griess Reagent System (Promega) according to the manufacturer’s instructions. OD<sub>600</sub> and OD<sub>540</sub> were determined with a microtiter plate reader (CLARIOstar).

### 5′/3′ RACE mapping

5′/3′ RACE was performed as previously described (37) with some modifications. Total RNA (6 μg) from HG003 Δ*fur* was treated with TAP (Epicentre) for 1 h at 37°C. After phenol/chloroform extraction followed by ethanol precipitation, RNA was circularized using T4 RNA ligase (Thermo Scientific) overnight at 16°C. Circularized RNA was once more extracted with phenol/chloroform, ethanol precipitated, and reverse transcribed using primer 2728 (Supplementary Table S3). A first PCR across the 5′/3′ junction was performed using primers 2729/2730, followed by a nested PCR with primers 2731/2732. The PCR products were cloned using the pJET1.2/blunt system (Thermo Scientific) within *E. coli* and 20 samples were sequenced.

### sRNA activity reporter assay

The principle of a reporter assay for sRNA activity was described for Enterobacteria (38) and Gram-positive bacteria (39). The effect of sRNAs on targets is determined via the quantification of leader reporter fusions. The latter results from in-frame cloning of *gfp* downstream of 5′UTRs and first codons of target genes. sRNAs and reporter genes are both on plasmids. We developed a similar system to test IsrR activity against its putative substrates.

Plasmids driving constitutive expression of *isrR* (pRMC2ΔR-IsrR) and its derivatives with CRR deletions (pRMC2ΔR-IsrRΔCRR1, pRMC2ΔR-IsrRΔCRR2, and pRMC2ΔR-IsrRΔCRR3 expressing *isrR*ΔCRR1, *isrR*ΔCRR2 and *isrR*ΔCRR3, respectively) were constructed and introduced in HG003 Δ*isrR* (Supplementary

Tables S1 and S2). These strains were subsequently transformed with p5'FdhA-GFP, p5'NarG-GFP, p5'NasD-GFP and p5'GltB2-GFP reporting the activity of IsrR on *fdhA*, *narG*, *nasD* and *gltB2* mRNAs, respectively (Supplementary Tables S1 and S2). The latter plasmids express the complete interaction region with IsrR of each mRNA target predicted by IntaRNA plus 10 additional codons in frame with the sGFP coding sequence. Each gene fusion is under the control of the *sarA* promoter. Of note, the four reporter plasmids were constructed in MG1655Z1 *pcnB::Km*. Fluorescence on solid medium was visualized from overnight cultures that were streaked on plates supplemented with chloramphenicol 5 µg/ml and kanamycin 60 µg/ml. Fluorescence was detected using Amersham Typhoon scanner at 488 nm and 525 nm wavelengths for excitation and emission, respectively. Fluorescence in liquid was visualized from overnight cultures diluted 1000-fold in TSB supplemented with chloramphenicol 5 µg/ml and kanamycin 60 µg/ml, and grown in microtiter plates. Fluorescence was measured after six hours of growth using a microtiter plate reader (CLARIOstar), normalized to OD<sub>600</sub>, and set at 1 for the strains with the control plasmid (pRMC2ΔR).

### SHAPE experiments

Synthetic genes placing *isrR* and, portions of *fdhA*, *narG*, *nasD* and *gltB2* under the transcriptional control of the T7 RNA polymerase were constructed by PCR on HG003 genomic DNA using primers indicated in Supplementary Table S3. The resulting synthetic genes were *in vitro* transcribed using T7 RNA polymerase (40). RNA integrity and folding homogeneity were assessed by agarose gel electrophoresis.

RNAs were probed in the presence and absence of 5 mM Mg<sup>2+</sup> using methyl-7-nitroisatoic anhydride (1M7) and modifications were revealed by selective 2'-hydroxyl acylation and analyzed by primer extension (SHAPE) as described (41,42) with slight modifications. Briefly, 12 pmoles of RNA (*isrR*, *fdhA*, *narG*, *nasD* and *gltB2*) were diluted in 64 µl of water and denatured for 5 min at 85°C. Then, 16 µl of pre-warmed (37°C) folding buffer (final conc. 40 mM HEPES pH 7.5, 150 mM KCl with/without 5 mM MgCl<sub>2</sub>) were added, and the solution was cooled down to room temperature for 7 min. Samples were then incubated for 5 min in a dry bath set at 37°C.

Similarly, when investigating interactions, RNAs were refolded in separate tubes (12 pmol of IsrR and 60 pmol of target RNA or the opposite) as described above, then mixed and incubated for 20 min at 37°C.

Refolded RNAs were split in two and either 1M7 (final concentration of 4 mM) or DMSO was added and incubated at 37°C for 5 min. Probed RNAs were precipitated in ethanol in the presence of ammonium acetate 0.5 M, ethanol, and 20 µg of glycogen. The pellets were washed twice with 70% ethanol, air-dried, and resuspended in 10 µl of water.

Modifications were revealed by elongating fluorescent primers (WellRed D2 or D4 fluorophore from Sigma, for sequences, see Supplementary Table S3) using MMLV re-

verse transcriptase RNase H Minus (Promega). Purified resuspended cDNAs were sequenced on a CEQ 8000 capillary electrophoresis sequencer (9+). The resulting traces were analyzed using QuSHAPE (43). Reactivity was obtained from at least three independent replicates. Reactivity value was set arbitrarily to -10 for the nucleotides for which it could not be determined (intrinsic RT stops). Secondary structures were modeled using IPANEMAP (44) and drawn with VaRNA (45). Probing profiles were compared as described (40).

### Animal studies

Female Swiss mice (Janvier Labs), 6–8 weeks old and weighing ~30 g were used for the septicemia model. Experiments were monitored in the ARCHE-BIOSIT animal lab in Rennes, and were performed in biological duplicates. We used groups of 5 mice for the mild septicemia model. Mice were infected intravenously by the tail vein with 200 µl of suspensions in 0.9% NaCl containing 3 × 10<sup>8</sup> bacteria with either HG003, HG003 Δ*isrR*, or HG003 Δ*isrR* locus2::*isrR*<sup>+</sup> strains. Mouse survival was monitored for 8 days, and the statistical significance of difference(s) between groups was evaluated using the Mantel-Cox test. A *p* value < 0.05 was considered as significant. All experimental protocols were approved by the Adaptive Therapeutics Animal Care and Use Committee (APAFiS #2123–2015100214568502v4).

## RESULTS

### IsrR is an sRNA required for growth in iron-depleted media

Iron is essential for *S. aureus* pathogenicity (46) and sRNAs are ubiquitous regulators for adaptation (47); we asked whether sRNAs are required in this bacterium to adapt to low iron availability, a condition encountered during infection. To address this question, we took advantage of a strategy that we recently developed, based on a competitive fitness evaluation of sRNA mutant libraries (25,48). A library of DNA-tagged deletion mutants was constructed in the HG003 strain (Supplementary Table S1); three independent mutants were constructed for each locus, to be subsequently used to constitute three independent libraries (Supplementary Table S4). Gene deletions of sRNAs corresponding to UTR regions or antisense from coding sequences more likely lead to phenotypes due to their associated coding genes; such mutations would interfere with the screening procedure designed to uncover the fine-tuning activity of sRNAs. We therefore restricted our collection to 48 mutants corresponding to nearly all known HG003 'bona fide sRNAs', defined as those that are genetically independent with their own promoter and terminator (49). Deletion and substitution of these genes by tag sequences were designed to avoid interference with the expression of adjacent genes. The deleted region of each mutant was replaced by a specific DNA tag, which allowed us to count each mutant and therefore evaluate their proportion within a population of mutant strains. Using an indexed PCR primer pair, up to 40 samples can be tested in one DNA-seq run (25). Mutants that disappeared or accumulated in

a given stress condition indicated a functional role of the corresponding sRNAs with respect to the imposed growth conditions.

The triplicate libraries were challenged to iron depletion by the addition of iron chelators, 2,2'-dipyridyl (DIP) and ethylenediamine-N,N'-bis(2-hydroxyphenyl)acetic acid (EDDHA) to growth media. The proportion of each mutant within the population was determined at different growth steps over 3 days (Figure 1A). Results were normalized to the same medium without iron chelator. Among 48 tested mutants, the strain with tag135 bearing a tagged deletion between the *arlR* and *pgpB* operons had a significant fitness disadvantage with each of the two tested iron chelators (Figure 1B); after about 28 generations, its distribution compared to the control condition decreased more than 10- and 1000-fold in DIP and EDDHA, respectively.

The deletion associated with tag135 inactivated an sRNA reported in two global studies under the names S596 (50) and Tsr25 (51). It is renamed here IsrR for iron-sparing response regulator. Neither *malIII*, *rsaA*, *rsaC*, *rsaD*, *rsaE*, *rsaG*, *rsaOG*, *ssr42* nor *ssrS* deletion mutants (49) present in the tested libraries were impacted by the presence of either DIP or EDDHA, indicating that their corresponding sRNAs do not significantly contribute to adaptation to low iron conditions in the tested conditions.

The HG003  $\Delta$ *isrR* strain had no apparent growth defect in rich medium compared to its parental strain (Figure 1C and Supplementary Figure S1). However, by spot tests, a  $\Delta$ *isrR* mutant displayed reduced colony size in the presence of DIP and EDDHA, supporting the fitness experiment results and evidencing that the individual  $\Delta$ *isrR* mutant, in the absence of the other 47 mutants, is required for optimal growth when the iron supply is limited (Figure 1C and Supplementary Figure S1). Of note, the slight growth retardation of  $\Delta$ *isrR* observed on iron-depleted plates or in liquid cultures corresponds to a drastic fitness cost when in competition with other bacteria. To confirm that the phenotype was solely due to the absence of IsrR, a copy of *isrR* with its endogenous promoter was inserted in the chromosome of the  $\Delta$ *isrR* strain at two different loci, leading to either  $\Delta$ *isrR* locus2::*isrR*<sup>+</sup> or  $\Delta$ *isrR* locus3::*isrR*<sup>+</sup> strains (Supplementary Figure S2A). Loci 2 and 3 were chosen since these regions were located between two terminators and seemed not to be transcribed. *isrR* expression from loci 2 and 3 was confirmed by Northern blot (Supplementary Figure S2B). The two  $\Delta$ *isrR* strains carrying a single copy of the *isrR* gene had plating efficiencies equivalent to that of the isogenic parental strain when grown with DIP or EDDHA, with colony sizes similar to those of the parental strain. These results confirm that the observed  $\Delta$ *isrR* phenotype was strictly dependent on *isrR* (Figure 1C and Supplementary Figure S2C). Of note, HG003 carrying *pIsrR* (IsrR expressed from its endogenous promoter) leads to a 100-fold reduced ability to form colonies on iron-depleted media compared to the strain carrying a control vector (Figure 1D). Multicopy *isrR* expression is deleterious for *S. aureus*, possibly due to the disruption of important metabolic pathways; thus, we cannot rule out that the effect is due to an IsrR off-target activity. We conclude that the absence of IsrR is detrimental to *S. aureus* growth under iron-depleted conditions.

### IsrR expression is repressed by the ferric uptake regulator Fur

Extremities of IsrR were determined by 5'/3'RACE experiments after circularization of total RNAs (Supplementary Figure S3A). *isrR* transcription starts at position 1362894 and terminates at position 1363067 on the NCTC8325 genome map, generating a 174 nucleotide-long sRNA (Figure 2A) in agreement with tiling array data (50). *isrR* is preceded by a  $\sigma^A$ -dependent promoter and ends with a rho-independent terminator (50). Its high expression in a chemically-defined medium and the presence of a putative Fur-box within the promoter region suggested iron-dependent expression of *isrR* (50). Fur-dependence of *isrR* regulation was verified in a HG003  $\Delta$ *fur* mutant (Supplementary Table S1). In rich medium, IsrR was not detected by Northern blotting in the parental strain but strongly accumulated in the  $\Delta$ *fur* mutant, demonstrating that Fur negatively controls *isrR* expression (Figure 2B). The *isrR* gene is predicted to be controlled by two Fur-boxes, one within the promoter region and the second immediately downstream of the transcriptional start site (Figure 2A). To test their relative contributions, a plasmid-based transcriptional reporter system placing a *gfp* gene under the control of the *isrR* promoter was constructed ( $P_{isrR}::gfp$ ) (Supplementary Table S2). The contribution of each predicted Fur box was tested by targeted mutagenesis altering either the first ( $P_{isrR1}::gfp$ ), the second ( $P_{isrR2}::gfp$ ), or both ( $P_{isrR1\&2}::gfp$ ) Fur-binding motifs (Figure 2C). As expected, the transcriptional reporter generated no fluorescence in a *fur*<sup>+</sup> strain (Figure 2D). Alteration of the upstream box led to strong fluorescence, which was even more intense when both boxes were mutated. In contrast, mutations only in the downstream Fur motif had no effect on the expression of the reporter fusion. We concluded that both sites contribute to efficient *isrR* Fur-dependent repression, the first one being epistatic over the second.

### IsrR and its regulation by Fur are conserved in the Staphylococcus genus

Most *trans*-acting bacterial sRNAs are poorly conserved across species (52,53), including among the staphylococci (49,54). However, the *isrR* gene was detected in all screened genomes from the *Staphylococcus* genus (Figure 3A and Supplementary Table S5). Sequence conservation includes the two Fur boxes, which were detected for all *isrR* gene sequences of the different *Staphylococcus* species. And indeed, the expression and iron dependency of IsrR were experimentally confirmed for *S. haemolyticus*, *S. epidermidis*, and *S. lugdunensis* (Figure 3). Our results suggest that IsrR has an important function related to iron metabolism that is conserved throughout the *Staphylococcus* genus.

IsrR orthologs from different species of the *Staphylococcus* genus were used to feed LocARNA, a software for multiple alignments of RNAs that generates secondary structure predictions and highlights conserved pairing regions (31). The proposed IsrR structure includes three stem-loops (H1 to 3) and a canonical Rho-independent terminator (T) (Supplementary Figure S3B). Three conserved C-rich regions, named here CRR1 to 3, are predicted to be single-stranded. CRR1 and 3 are within the loops of stem-loop

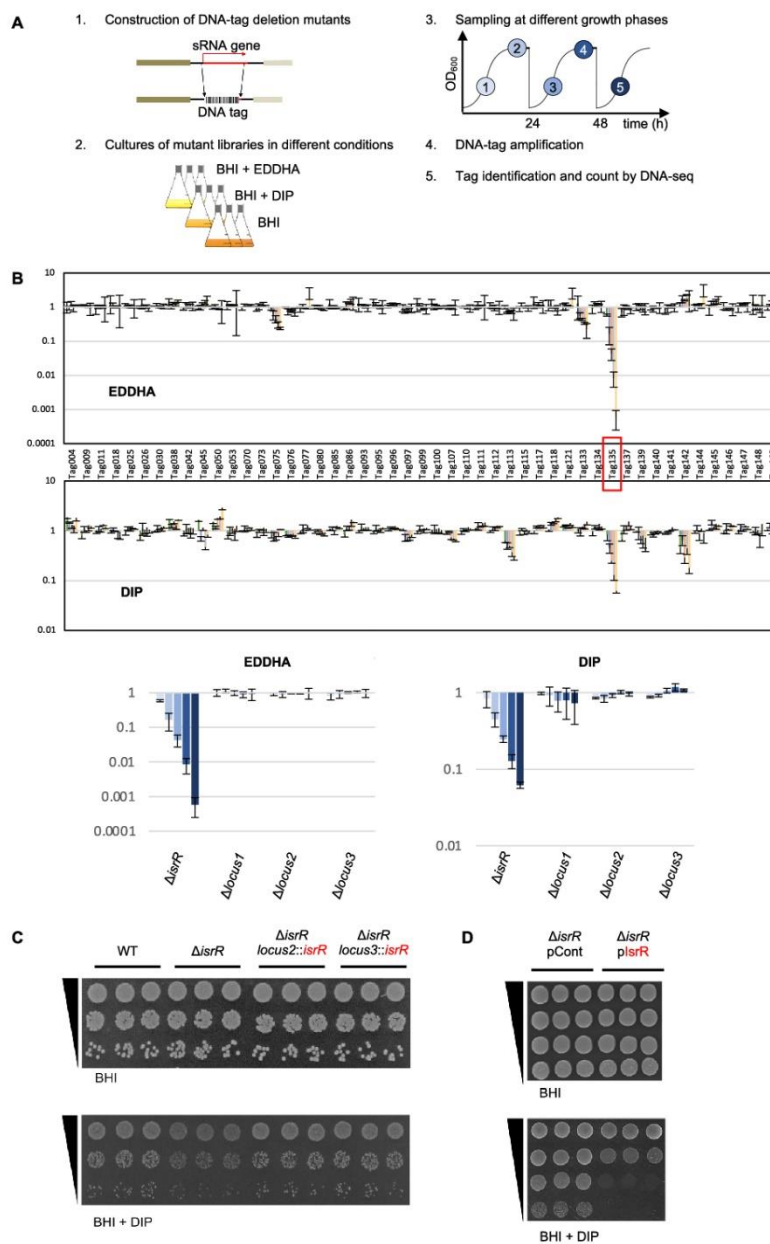


**Figure 1.** *S. aureus* *IsrR* sRNA is required for optimal growth when iron is scarce. (A) Experimental protocol scheme to select mutants with altered fitness in media containing iron chelators. (B) Evolution of mutant proportions in libraries (for composition, see Supplementary Table S4) grown in the presence of EDDHA 0.7 mM or DIP 1.25 mM normalized to the same libraries grown in the absence of iron chelators. Error bars indicate the standard deviation from three independent libraries. Upper parts; data with the complete 48 mutant libraries. Tag135 corresponding to the *IsrR* mutant is highlighted by a red box. For Tag/mutant correspondence, see Supplementary Table S1. Note that Tag145 and Tag149 are in a single strain, which corresponds to a double mutant ( $\Delta sprX2 \Delta sprX1$ ). Lower parts, selected data (enlargement):  $\Delta IsrR$  and three other tagged regions are shown. Loci 1, 2 and 3 correspond to tag insertions in non-transcribed regions expected not to affect bacterial growth. Histogram color code corresponds to sampling time color code from (A). (C)  $\Delta IsrR$  growth defect in iron-depleted media is complemented by an *IsrR* ectopic chromosomal copy. For strain constructions see Supplementary Table S1 and Supplementary Figure S2A. Plating efficiency of indicated strains on BHI medium without (upper panels) or with (lower panels) DIP 1.25mM. Three independent biological clones are shown for each strain. For results with EDDHA, see Supplementary Figure S2C. (D) Multicopy *IsrR* is toxic in iron-depleted media. Experiments were performed as for Figure 1C. pCont, pCN38; plsR, pCN38-*IsrR*. For strain and plasmid constructions see Supplementary Tables S1 and S2.

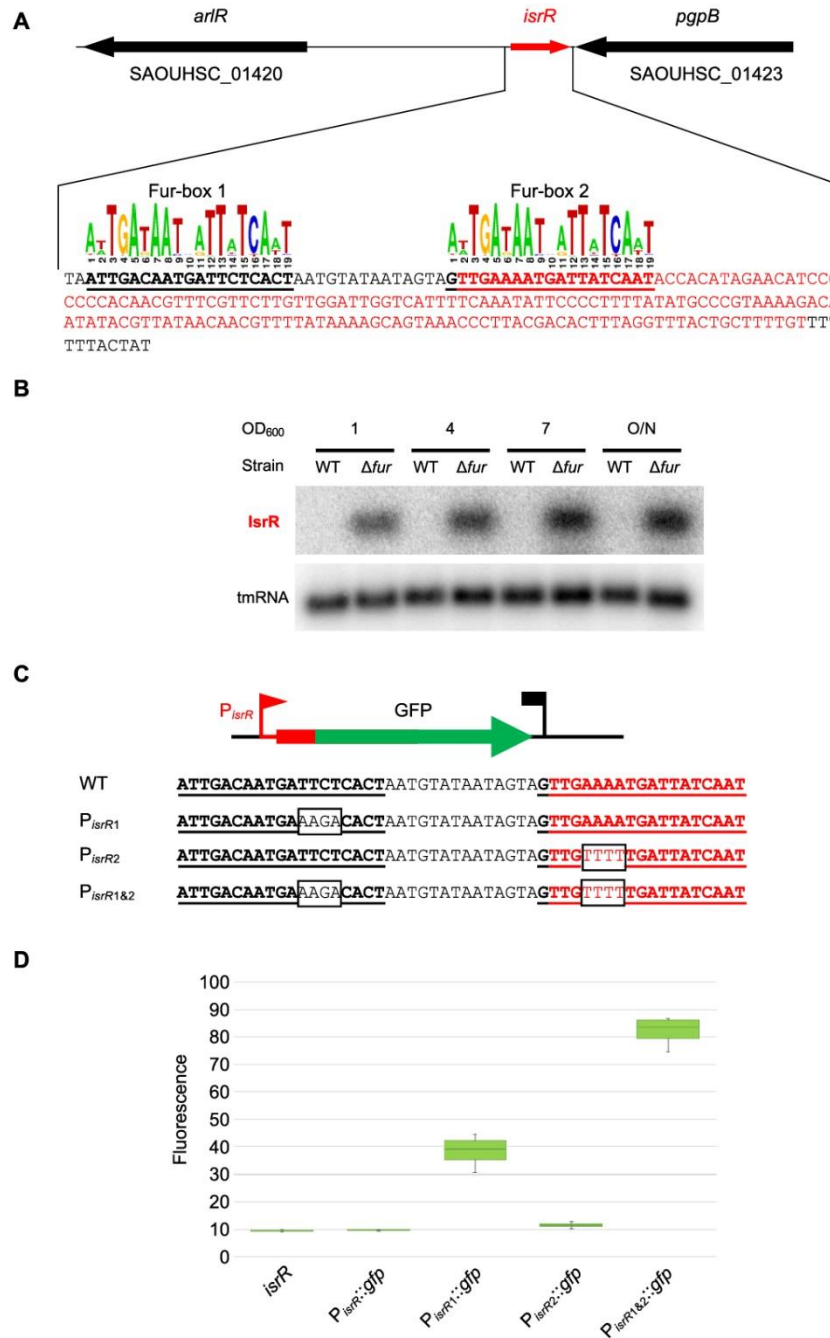


**Figure 2.** *isrR* is regulated by Fur. (A) *isrR* genetic locus. The transcribed region is in red. For *isrR* 3'-5'RACE mapping results, see Supplementary Figure S3A. Predicted Fur boxes are bold and underlined. The staphylococcal Fur box consensus is taken from the RegPrecise database (30). (B) Northern blot experiment with HG003 and its *fur* derivative sampled at the indicated OD<sub>600</sub> and probed for *IsrR* and tmRNA (control) ( $n = 2$ ). (C) *isrR* Fur box sequence (WT) and its mutant derivatives ( $P_{isrR1}$ ,  $P_{isrR2}$  and  $P_{isrR1\&2}$ ). Mutations altering the Fur boxes are shown in black boxes. (D) Fluorescence of transcriptional fusions placing *gfp* under the control of the *isrR* promoter and its mutant derivatives (as indicated) measured by flow cytometry, ( $n = 5$ ). The first strain indicated '*isrR*' is a control strain in which the *isrR* gene is not fused to *gfp*.

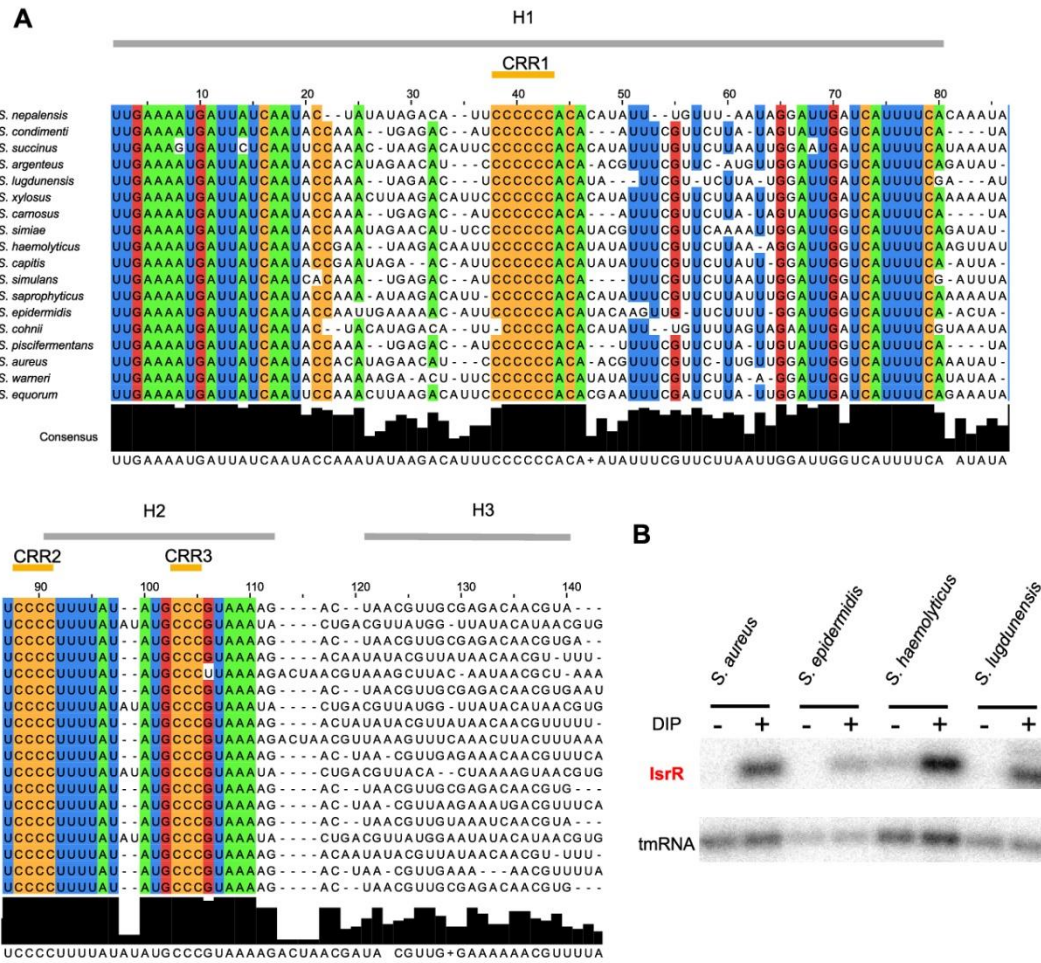


**Figure 3.** *IsrR* is conserved and Fur-regulated within the *Staphylococcus* genus. (A) Sequence conservation. The alignment was obtained using LocARNA (31) with *IsrR* sequences from indicated strains generated by GLASSgo (28) as inputs. 80% conserved nucleotides within the tested sequences are colored (green, A; blue, U; red, G; other, C). Sequences shown are limited to the three first stem-loops (H1 to H3). There is poor nucleotide sequence conservation for H3 and the transcriptional terminator. Three C-rich regions are indicated (CRR1 to CRR3). (B) Northern blot probed for *IsrR* in *S. aureus* HG003, *S. epidermidis* ATCC 12228, *S. haemolyticus* JCS1435, and *S. lugdunensis* N920143. Bacteria were grown in BHI or BHI supplemented with DIP 1.25 mM and were withdrawn at OD<sub>600</sub> 1 (n = 2).

structures H1 and H2, while CRR2 is at the 5'-end abutting stem H2. CRR1 is four to seven C-long, according to the species considered. C-rich motifs are important for sRNA/target recognition in *S. aureus* (55–57). This feature efficiently discriminates targets in staphylococcal strains, since their genomes are ~70% AT-rich, and G-rich stretches are infrequent except within Shine-Dalgarno sequences. Two first stems, H1 and H2, have conserved primary sequences with little covariation, indicating the importance of each nucleotide, possibly for an interaction with a yet unknown protein. Of note, single-stranded regions adjacent to CRR and within the loops are more variable than H1 and H2. To confirm experimentally its secondary structure, *IsrR* was subjected to SHAPE chemical probing, a technol-

ogy revealing single-stranded nucleotides. RNAs were incubated with 1-Methyl-7-nitroisatoic anhydride (1M7), which specifically reacts with flexible nucleotides (58,59). Reactivity data was implemented into the IPANEMAP workflow to predict *IsrR* secondary structure according to thermodynamics and probabilistic calculations balanced with the experimental data (44). The experimental model obtained (Figure 4) is identical to the one obtained using the phylogenetic approach described above. Most nucleotides with high reactivity were identified in predicted single-stranded regions. However, several nucleotides with medium to high reactivity are in predicted double-stranded regions probably reflecting the poor stability of such A–U rich structures. Surprisingly, CCR1 is weakly reactive, and CRR2 and

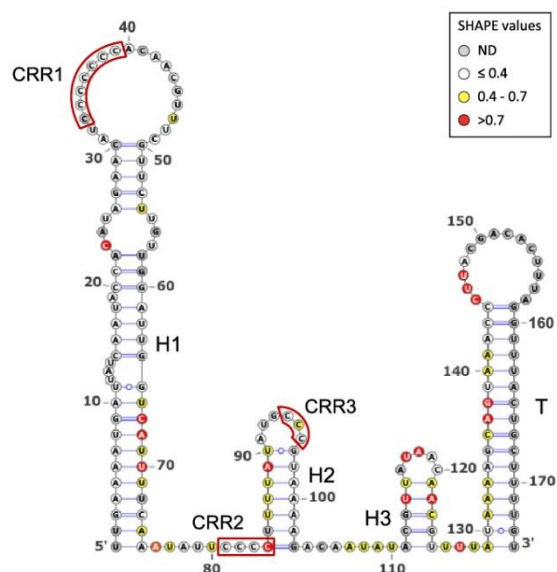


**Figure 4.** IsrR secondary structure model obtained using IPANEMAP. IsrR was probed with 1M7 at 37°C in 40 mM HEPES pH 7.5, 150 mM KCl with/without 5 mM MgCl<sub>2</sub>. White: low reactivity to 1M7, yellow: moderate reactivity, red: high reactivity. Nucleotides in grey denote undetermined reactivity. Specific regions of the IsrR structure are indicated: Three stem-loop structures (H1 to H3), a rho-independent transcription terminator (T), and three C-rich regions (CRR1 to CRR3).

CRR3 are only mildly reactive, suggesting that although modeled in single-stranded regions, these Cs are involved in some interactions. As IsrR does not feature any stretches of G, Cs from the CRRs might be involved in yet to be identified non-canonical interactions. Of note, such interactions could actually expose the C's Watson-Crick face to the solvent making them available for an intermolecular interaction. To detect divalent ion-dependent tertiary folding, IsrR was probed in the presence or absence of Mg<sup>2+</sup> ions (Supplementary Figure S3C). Only a few significant local reactivity changes located after CRR1 stem-loop were observed suggesting that this region of IsrR does not adopt an extensive tertiary structure (60).

The presence of CRRs suggests that IsrR is likely a conserved *trans*-acting small regulatory RNA.

#### Bioinformatics predictions indicate that IsrR targets mRNAs encoding enzymes with Fe–S clusters

As *trans*-acting bacterial sRNAs base-pair to RNAs, it is possible to predict their putative targets by bioinformatics; however, some predictive programs generate false positive candidates (61). We used CopraRNA, a comparative prediction algorithm for small RNA targets, which takes into account RNA sequence accessibility within sRNA structures and the evolutionary conservation of the pairings (32). It is reportedly an efficient sRNA-target predictor when ortholog sRNA sequences are detected among different species, especially when they are phylogenetically distant (61). As IsrR is a conserved sRNA in the *Staphy-*

*lococcus* genus, IsrR ortholog sequences were used as input for CopraRNA. Results indicated a functional convergence of the proposed targets (Supplementary Figure S4). Among the 23 top candidates with the best e-values on pairings, seven are mRNAs that encode iron-sulfur (Fe–S)-containing proteins (NasD, MiaB, GltB2, FdhA, CitB, NarG and SAOUHSC\_01062). Several of these IsrR putative targets were previously proposed by Mäder et al. using the same approach (50). Considering 32 different Fe–S containing proteins in *S. aureus* identified by manually curated *in silico* analyses (detailed in Supplementary Table S6), the probability of identifying seven mRNAs encoding Fe–S containing proteins by chance is  $2 \times 10^{-9}$  (see Materials and Methods). This remarkably low probability allows one to state with high confidence that Copra RNA identified relevant IsrR targets. Other putative targets, such as *moaD* and *nreC* mRNAs, are also associated with Fe–S containing complexes (62,63). It is therefore likely that most, if not all, predicted targets associated with Fe–S clusters are direct IsrR targets. Remarkably, nitrate reductase, nitrite reductase, glutamate synthase, formate dehydrogenase, aconitase, and hydratase methionine sulfoxide reductase, which are all putatively affected by IsrR (Supplementary Figure S4), also correspond to either putative or demonstrated enzymes affected by RyhB (5,64) suggesting a striking functional convergence between these two sRNAs.

#### IsrR targets mRNA encoding nitrate-related enzymes

In the absence of oxygen, *S. aureus* uses nitrate, if available, as an electron acceptor of the respiratory chain (65). Nitrate is converted to nitrite by nitrate reductase encoded by the *nar* operon (Supplementary Figure S5). In a second step, nitrite is converted to ammonium by nitrite reductase encoded by the *nas* operon. Ammonium is then used by glutamate synthase encoded by the *gltB2* gene. Transcription of *nar* and *nas* operons depends on the NreABC regulatory system, whose activity requires the presence of nitrate and the absence of oxygen (63). Strikingly, *narG* (nitrate reductase subunit  $\alpha$ ), *nasD* (nitrite reductase large subunit), and *gltB2* mRNAs are IsrR putative targets, suggesting that IsrR could affect all steps of nitrate to glutamate conversion.

In *E. coli*, the *fdhF* gene encoding a molybdenum-dependent formate dehydrogenase is regulated by nitrate (66). A strain with a mutated *fdhF* allele lacks nitrate reductase activity (67), suggesting that FdhF is associated with the nitrate dissimilatory pathway. Interestingly, the *fdhF* ortholog in *S. aureus*, *fdhA*, is also predicted to be an IsrR target.

To assess IsrR targets associated with the nitrate reduction pathway, we selected *fdhA*, *narG*, *nasD* and *gltB2* mRNAs. Detection of long transcripts by Northern blot is often not possible in *S. aureus*. For this reason, the effect of IsrR on the amount of its targets was tested by Northern blots solely for *fdhA* and *gltB2* mRNAs, which are expressed from short operons (bi- and mono-cistronic, respectively). In many cases, the interaction of an sRNA with its mRNA target results in the destabilization of transcripts. Consequently, we questioned whether IsrR would affect *fdhA* and *gltB2* mRNA stability. RNA stability was evaluated upon

transcription inhibition by rifampicin, where the variations in RNA quantities are assumed to reflect their degradation. This classical approach should nevertheless be interpreted cautiously since i) stability of sRNA and mRNA targets depends on their base pairing and that ii) rifampicin prevents the synthesis of both partners, one of them being possibly limiting (68). In HG003 and its  $\Delta isrR$  derivative, *fdhA* and *gltB2* mRNAs were unstable in rich medium. Addition of DIP to the growth media resulted in a minor increase of both mRNAs in HG003 and  $\Delta isrR$  strain (Figure 5). However, IsrR does not have a significant effect on *fdhA* and *gltB2* mRNA stability, with the caveat associated with the possible limitation of using rifampicin to assess regulatory RNA activities.

We used the SHAPE technology to probe and model the secondary structure of *fdhA*, *gltB2*, *narG* and *nasD* 5'UTR as well as the heteroduplex they form with IsrR. To this end, RNA either corresponding to the four 5'UTR alone or in complex with IsrR were submitted to a SHAPE probing experiment with 1M7 (IsrR structure probing and modelling is reported above). These experiments were carried out in triplicate and the results were used as constraints to model RNA secondary structure according to the IPANEMAP workflow (43). IPANEMAP yielded secondary structure models very consistent with the SHAPE probing data for *fdhA*, *gltB2* (Figure 6) and *nasD* (Supplementary Figure S7) mRNAs, whereas the *narG* mRNA reactivity map did not allow modelling of a stable structure, suggesting it does not adopt one. Interestingly, *fdhA* Shine-Dalgarno sequence is embedded in a stable structure whereas the initiation codon is highly reactive while the opposite is observed for *gltB2* mRNA. The limited availability of either of these sequence elements suggests that the expression of these two genes is regulated by their own RNA structure.

Statistically significant reactivity variations for specific nucleotides were observed for IsrR and each of its mRNA targets when incubated alone or as an IsrR/5' UTR target pair (Supplementary Figures S6 and S7). Such data strongly support an interaction of IsrR with the four putative mRNA targets tested. Nucleotides for which reactivity decreases are likely to be involved in base pairing between IsrR and a target mRNA, whereas an increase of reactivity probably reflects the destabilization of a structure upon formation of the sRNA/mRNA heterodimer (e.g. the initiation codon of *fdhA* and the region including the Shine-Dalgarno of *gltB2*, which were highly reactive in the absence of IsrR, present a significantly decreased reactivity in the presence of IsrR). Interestingly, no significant differences are observed in IsrR 50 first nucleotides, suggesting that CCR1 is not involved in the interaction with the mRNA targets. These data were used as constraints for IPANEMAP to model the interaction between IsrR and *fdhA*, *gltB2* and *nasD* mRNAs. The interactions proposed include IsrR CRR2 and CCR3 as well as the Shine-Dalgarno and the AUG initiator codon on the mRNA target side, suggesting that IsrR impairs translation of its targets.

The binding of IsrR to one putative nitrate-related target, *fdhA* mRNA, was tested by electrophoretic mobility shift assay (EMSA). An IsrR band shift was observed in the presence of *fdhA* mRNA. The specificity of bind-

ing was challenged with a specific competitor (unlabelled IsrR) and a nonspecific competitor (polyU) (Supplementary Figure S8A). As expected, unlabelled IsrR, but not polyU, displaced the interaction, confirming the specificity of the IsrR/*fdhA* RNA duplex. To identify nucleotides contributing to the complex formation, EMSA was performed with IsrR and *fdhA* mRNA harbouring point mutations in the predicted interaction zone (Supplementary Figure S8B). Because the interaction between IsrR and *fdhA* mRNA involves likely 31 base-pairs, the replacement of several nucleotides was necessary. The presence of seven point mutations altering either IsrR or *fdhA* mRNA prevented band shifts when associated with their corresponding wild-type partner. However, when the mutated IsrR was incubated with *fdhA* mRNA harbouring compensatory mutations restoring the pairing, a band shift was observed (Supplementary Figure S8C). The decreased amount of RNA duplex with both mutated RNAs can be explained by a less stable complex as predicted by IntaRNA software (69) ( $\Delta G = -16.98$  kcal/mol for WT IsrR/*fdhA* duplex versus  $\Delta G = -12.8$  kcal/mol for mutated IsrR/*fdhA* duplex). Our data support a direct interaction of IsrR and mRNAs associated with nitrate metabolism.

#### Translational control by IsrR

Our *in vitro* experiments indicate a direct interaction of IsrR with its targets. However, at least in the case of *fdhA* and *gltB2* mRNAs, this pairing does not trigger mRNA degradation, therefore, suggesting that IsrR can act on translation without affecting the stability of targeted mRNAs. To support this hypothesis, translation reporter systems were constructed. 5'UTR sequences of predicted mRNA targets of IsrR were fused to a reporter gene. For these experiments, sequences corresponding to the 5'UTRs and the first codons of mRNA targets were cloned under the control of the P1 *sarA* promoter in frame with the GFP coding sequence (p5'FdhA-GFP, p5'NarG-GFP, p5'NasD-GFP, p5'GltB2-GFP; Supplementary Figure S9A). The cloned regions comprise the sequences predicted to pair with IsrR. Note that transcription of the 5'UTRs from P1 *sarA* promoter is likely constitutive and IsrR-independent. The *isrR* gene was placed under the control of the P<sub>let</sub> promoter on a multicopy plasmid (pRMC2 $\Delta$ R-IsrR), and mutants lacking either the first, second or third C-rich motif were constructed, leading to pRMC2 $\Delta$ R-IsrR $\Delta$ CRR1, pRMC2 $\Delta$ R-IsrR $\Delta$ CRR2, and pRMC2 $\Delta$ R-IsrR $\Delta$ CRR3, respectively (Supplementary Table S1). The  $\Delta isrR$  strains containing the different reporters were transformed with pRMC2 $\Delta$ R (control plasmid), pRMC2 $\Delta$ R-IsrR, and its derivatives. We confirmed that *isrR* and its  $\Delta$ CRR derivatives were constitutively expressed (Supplementary Figure S9B). For each strain containing one of the four reporter genes, expression of IsrR led to reduced fluorescence (Figure 7 and Supplementary Figure S10). The integrity of CRR1 was required for the IsrR activity against *fdhA* and *gltB2* reporter fusions. However, CRR1, despite being the largest CRR, was dispensable for IsrR activity against *narG* and *nasD* reporter fusions (Supplementary Figure S10). Interestingly, CRR2 was necessary for IsrR activity against all four reporter fusions. The observations are supported

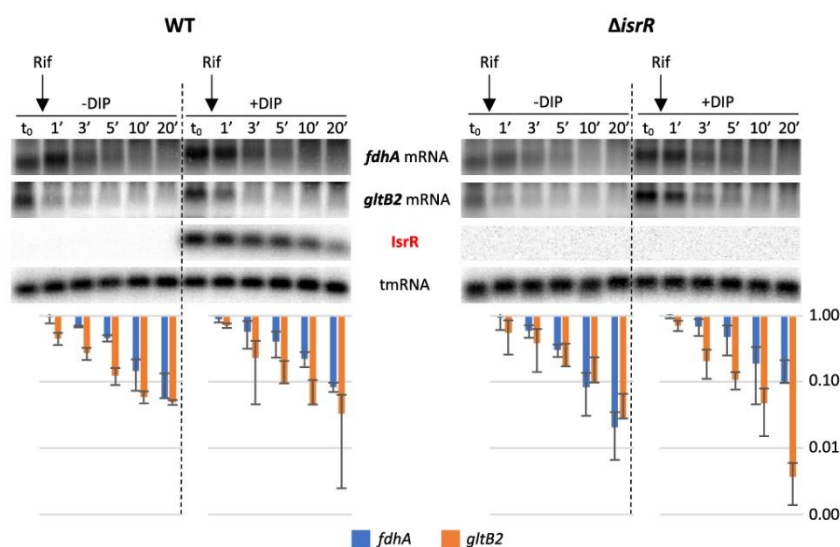


**Figure 5.** Stability of *fdhA* and *gltB2* mRNAs is not significantly affected by IsrR. HG003 (left panel) and its isogenic  $\Delta$ *ISR* derivative (right panel) were grown in rich medium with or without the addition of DIP (as indicated). At  $t_0$ , rifampicin (Rif) was added to the growth medium. Cultures were sampled at  $t_0$ , 1, 3, 5, 10 and 20 min after addition of rifampicin, total RNA was extracted, and the amounts of *fdhA* mRNA, *gltB2* mRNA, tmRNA (loading control), and IsrR were assessed by Northern blot. Histograms show the quantification of *fdhA* and *gltB2* mRNAs normalized to  $t_0$  from two rifampicin assays as shown in the upper panel. Vertical axis, arbitrary units. Error bars indicate the standard deviation from two independent experiments ( $n = 2$ ).

by SHAPE data. The integrity of at least two IsrR CRRs was required for activity against the four targets. These observations revealed that all CRRs are needed to mount the complete IsrR response, but differentially affect activity according to the given mRNA target.

#### IsrR down-regulates nitrate metabolism

To determine if IsrR could indeed interfere with nitrate respiration, the amount of nitrite in anaerobic cultures upon addition of nitrate was measured in strains with either no IsrR or overexpressing IsrR. Two systems were used: (i)  $\Delta$ *ISR* carrying a plasmid control (pCont) compared to the same strain with a plasmid expressing IsrR (p-IsrR) and (ii)  $\Delta$ *fur* compared to  $\Delta$ *fur*  $\Delta$ *ISR* strains (Figure 8). Note that *ISR* is constitutively expressed in the  $\Delta$ *fur* background. In both systems, IsrR accumulation prevented nitrite production, as expected if nitrate reductase (*narG*) is indeed down-regulated by IsrR.

#### IsrR activity is Hfq independent

In Enterobacteriaceae, Hfq is an RNA chaperone required for sRNA-mediated regulations (70). However, it does not seem to be the case in *S. aureus* (71–73), nor for *B. subtilis* (74–76) where its function remains enigmatic. Since RyhB activity is Hfq-dependent in *E. coli* (8), we asked whether IsrR would require a functional Hfq in *S. aureus*. The *fdhA*, *nasD*, *narG*, and *gltB2* translation reporter genes described above were introduced into  $\Delta$ *hfq* strains containing either a control plasmid or a plasmid constitutively expressing IsrR. As with the parental strain (Figure 7 and Supplementary Figure S10), the reporter fusions were downregulated

by IsrR despite the absence of Hfq (Supplementary Figure S11A). It was conceivable that *ISR* cloned on a multi-copy plasmid produced high levels of sRNA that would bypass the need for Hfq. We therefore introduced the *fdhA* translation reporter in HG003, HG003  $\Delta$ *hfq*, and HG003  $\Delta$ *ISR*. When present, *ISR* expression was induced from its endogenous locus by the addition of DIP to the medium. On DIP-containing plates, the reporter fusion showed reduced activity in the parental and  $\Delta$ *hfq* strain compared to the strain lacking IsrR (Supplementary Figure S11B). Additionally, *in vivo* nitrite production in anaerobiosis was compared qualitatively between a HG003 WT strain and its  $\Delta$ *hfq* derivative containing either a control plasmid or a plasmid constitutively expressing IsrR. 150 minutes after the addition of nitrate ( $\text{NaNO}_3$ ), the  $\Delta$ *hfq* strain expressing IsrR efficiently inhibited nitrite production as observed with the parental strain (Supplementary Figure S11C). Of note, IsrR induction through the addition of DIP was not used in this case since under anaerobic conditions, iron starvation results in severe growth arrest of the strains. We conclude that IsrR activity does not require Hfq for the tested phenotypes.

#### IsrR RNA is required for *S. aureus* virulence

Host iron scavenging plays a crucial role in *S. aureus* infection (4,77). As the  $\Delta$ *ISR* mutant has altered fitness in iron-restricted environments, we postulated that it could also impact virulence. We compared the virulence of  $\Delta$ *ISR*,  $\Delta$ *ISR* *locus2::ISR*<sup>+</sup> and parental (HG003) strains injected intravenously in a mouse septicemia model (78). Of note, the absence of *ISR* does not alter *in vitro* growth in rich media (Figure 1 and Supplementary Figure S1) and IsrR is expressed in the  $\Delta$ *ISR* *locus2::ISR*<sup>+</sup> strain (Supplementary

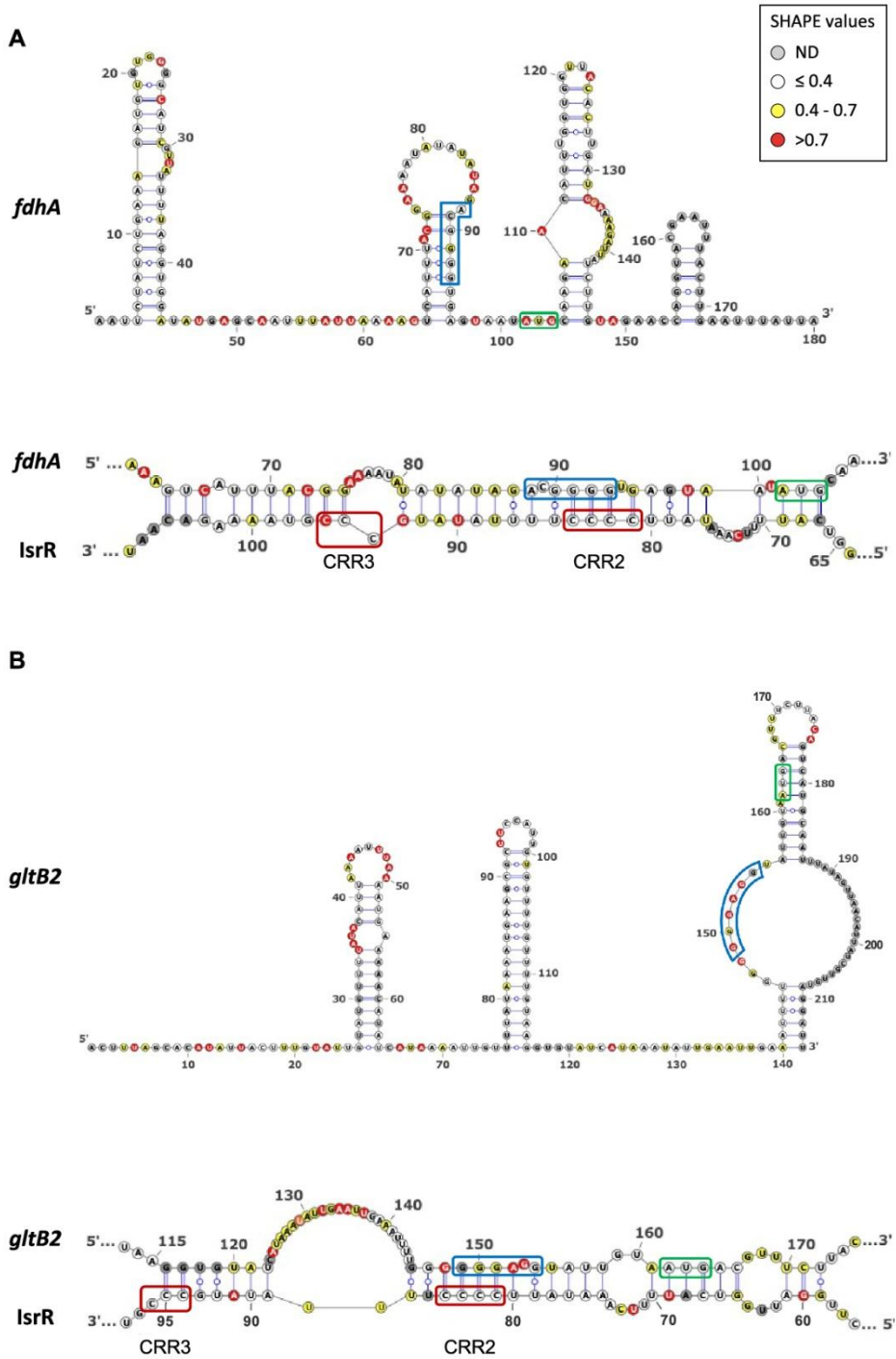


**Figure 6.** Secondary structure models for *fdhA* and *gltB2* 5'UTR alone or in interaction with IsrR. Top panels: Secondary structure model obtained with IPANEMAP for *fdhA* (A) and *gltB2* (B) 5'UTRs using 1M7 reactivity as constraints. Nucleotides are coloured according to their reactivity in the absence of IsrR with the indicated colour code. ND, not determined. Bottom panels: model for interaction between IsrR and *fdhA* (A) and *gltB2* (B) mRNAs based on changes in reactivity in the presence of IsrR. mRNA Shine-Dalgarno sequence is shown in a blue rectangle and the start codon in a green rectangle; IsrR C-rich regions are shown in red rectangles.

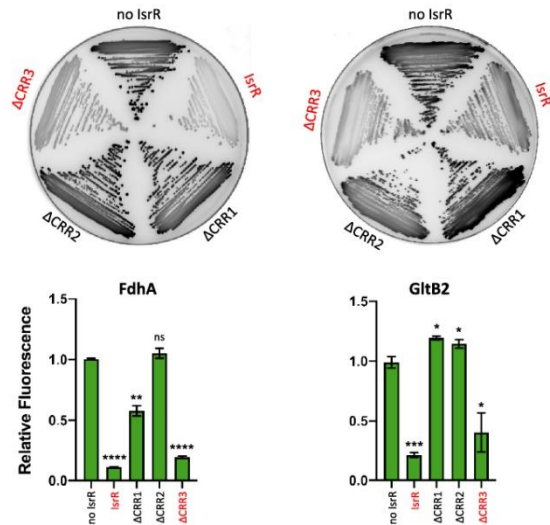


**Figure 7.** Translational down-regulation by IsrR and the CRR contribution. Leader fusions between the first codons of *fdhA* or *gltB2* and GFP were constructed (Supplementary Figure S9 and Table S2). The cloned fragments include the interaction regions with IsrR as described (Figure 6). HG003  $\Delta$ *isrR* derivatives with either a control plasmid (no IsrR; pRMC2 $\Delta$ R), or plasmids expressing IsrR (pRMC2 $\Delta$ R-*isrR*), IsrR $\Delta$ CRR1 (pRMC2 $\Delta$ R-*isrR* $\Delta$ CRR1), IsrR $\Delta$ CRR2 (pRMC2 $\Delta$ R-*isrR* $\Delta$ CRR2), IsrR $\Delta$ CRR3 (pRMC2 $\Delta$ R-*isrR* $\Delta$ CRR3) were transformed with each engineered reporter gene fusion. Translational activity from the reporters in the presence of the different *isrR* derivatives were evaluated by fluorescence scanning of streaked clones on plates ( $n = 3$ ). Fully active IsrR derivatives are shown in red. Translational activity of the reporter genes with the different *isrR* derivatives was also determined in liquid culture. Fluorescence of the strains was measured in 6 h cultures using a microtiter plate reader. Results are normalized to 1 for each fusion with the control plasmid. Error bars indicate the standard deviation from three independent experiments ( $n = 3$ ). Statistical analyses were performed using a *t*-test with Welch's correction: \*\*\*\* represents *P*-value < 0.0001, \*\*\* represents *P*-value of 0.0003, \*\* represents *P*-value of 0.0029, \* represents *P*-value between 0.0111–0.0184.

Figure S2B). Most mice inoculated with strains expressing a functional *isrR* (HG003 and  $\Delta$ *isrR* locus2::*isrR*) were dead within 8 days (Figure 9). In striking contrast, the lack of IsrR expression significantly reduced HG003 virulence, demonstrating the important role of this regulatory RNA during *S. aureus* infection in this model.

## DISCUSSION

The link between *S. aureus* pathogenicity and its iron status is established (79). The host exerts nutritional immunity that depletes iron in response to invading bacteria as a means to restrict infection. Here, we identified IsrR as the only sRNA, from 45 tested, required for optimum *S. aureus* growth in iron-restricted conditions and indeed, its absence attenuates *S. aureus* virulence.

IsrR was previously reported in a large-scale transcriptome study performed in numerous growth conditions (50), and was also observed to be the most highly upregulated sRNA when *S. aureus* growth in human serum was compared to that in a rich laboratory medium (51). Environ-

ments that failed to provide free iron, such as serum, promoted the induction of iron-repressed genes in infecting bacteria (80,81). Our findings on *isrR* regulation identify iron starvation as the signal for IsrR induction. RsaOG, RsaG, Tegl6, SsrS and RsaD sRNAs were reported as upregulated in serum (51), but they do not contribute to *S. aureus* optimized fitness in the iron-starved conditions we tested. Supporting our observation, their corresponding genes are not preceded by Fur boxes (49,50) and their susceptibility to serum is likely not related to iron starvation. RsaC is an *S. aureus* sRNA produced in response to manganese (Mn) starvation that inhibits the synthesis of the superoxide dismutase SodA, a Mn-containing enzyme (82). RsaC is possibly the Mn counterpart of IsrR for iron and may contribute to adaptation to metal-dependent nutritional immunity. However, while putative RsaC targets are also associated with iron homeostasis, the *rsaC* mutant was not significantly affected by the chelating conditions tested here. IsrR is the only sRNA tested affected by both DIP and EDDHA and it is Fur regulated.

Inactivation of the Fur repressor leads to down-regulation of numerous genes (83,84). This paradoxical regulation could be achieved by a Fur-dependent expression of negative regulators, which act as ‘inverters’ of the Fur response, with IsrR being an *S. aureus* Fur inverter. Of note, several genes reported down-regulated upon iron starvation in *S. aureus* (85) are IsrR targets predicted by Copra RNA, including *narG* and *nasD*.

In the absence of oxygen, Staphylococci use nitrate and nitrite as electron acceptors of the anaerobic respiratory chain (86). These products are provided to humans by nutrients and are also generated by the oxidation of endogenous NO synthase products (87,88). Nitrate and nitrite reductases are expressed when needed, *i.e.* in anaerobic conditions when nitrate is present. Their expression is controlled by the staphylococcal transcriptional regulator NreABC (89–91). IsrR provides an additional checkpoint to nitrate respiration by linking transcription of *narGHJ* and *nirR nasDEF* operons to the presence of iron, an essential element of these encoded respiratory chain components (Figure 10). When iron is limiting, IsrR targets various mRNAs expressing iron-containing proteins that are not essential for growth. The dissimilatory nitrate reduction pathway is inactivated, while *S. aureus* can still grow by fermentation in anaerobic conditions. Biocomputing analysis (Supplementary Figure S4) suggests that IsrR targets *nreC* mRNA; if so, the expression of the nitrogen respiration pathway would be simultaneously downregulated by targeting mRNAs encoding dissimilatory nitrate reduction enzymes and their transcriptional activator. sRNAs that directly affect nitrogen metabolism have been characterized in Alphaproteobacteria, Gammaproteobacteria and Cyanobacteria (92–94); in several cases, the sRNAs directly downregulate regulators of nitrogen respiratory pathways. To our knowledge, IsrR would be the first sRNA example from the Firmicutes phylum.

A characteristic feature of sRNAs in Firmicutes and in particular in *S. aureus* is the presence of one or several exposed CRRs that can act on the G-rich region like those of the Shine Dalgarno sequences. The interaction models proposed from the probing experiments indicate that CRR2

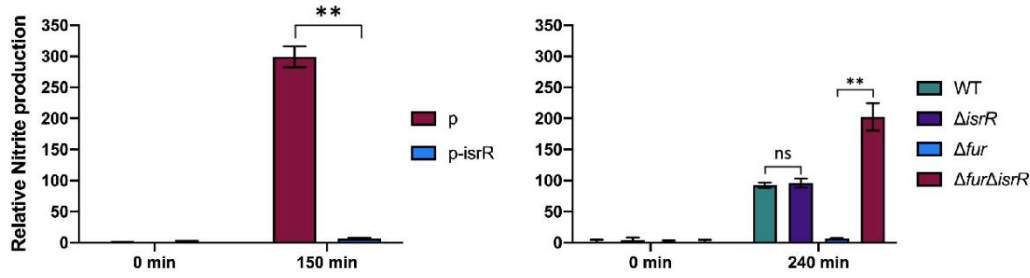


**Figure 8.** IsrR controls nitrite production. IsrR prevents nitrate conversion to nitrite. Strains were grown in anaerobic conditions for two hours and nitrate (20 mM) was added to cultures. Growth media: left panel, BHI; right panel, TSB. TSB medium was used here since we observed that  $\Delta fur$  mutants grow poorly in BHI under anaerobic conditions. Samples for nitrite measurement were withdrawn at times 0 and 150 (left panel) or 240 min (right panel) upon nitrate addition. p, pRMC2 $\Delta$ R; p-IsrR, pRMC2 $\Delta$ R-IsrR. Histograms represent the relative nitrite concentration (Griess assay, OD<sub>540</sub>) normalized to the bacterial mass (OD<sub>600</sub>). Results are normalized to 1 for  $\Delta isrR$  p (left panel) and WT (right panel) samples prior to nitrate addition. Error bars indicate the standard deviation from three independent experiments ( $n = 3$ ). Statistical analyses were performed using a  $t$ -test with Welch's correction: \*\* represents  $P$ -value between 0.001–0.004; ns, non-significant.

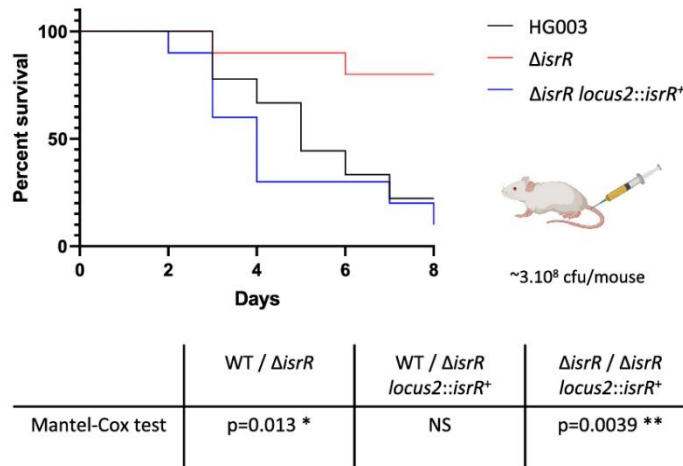


**Figure 9.** IsrR is required for *S. aureus* full virulence. Kaplan–Meier survival probability plots in a septicemia model of mice infected with either HG003 (WT, black), HG003  $\Delta isrR$  (red) and HG003  $\Delta isrR$  locus2:: $isrR^+$  ( $\Delta isrR$  complemented, blue). Survival was monitored for 8 days post-infection. Results shown are from 10 mice per group; the experiment was performed twice, and data combined. The Mantel-Cox test was used to determine  $P$  values. NS, non-significant.

and to a lesser extent CCR3 are involved in the base pairing of IsrR with *fdhA*, *gltB2* and *nasD* mRNAs. Translational activity assays with a reporter fusion system further confirmed the CRR2 requirement to regulate expression of the mRNA targets. The results of the SHAPE footprinting do not suggest the involvement of CCR1 in the interaction with the mRNAs, although it appears important but not crucial for *fdhA* regulation. It should be noted that this assay only detects state-changing nucleotides and cannot detect those not reactive when the RNA is incubated alone, for example, CCR1 nucleotides. Therefore, it could be possible that the performed footprinting assay does not reveal an existing interaction involving CCR1. However, we did not observe any significant changes in IsrR 50 first nucleotides, suggesting that the long hairpin harboring CCR1 is not destabilized upon the interaction. We therefore suggest that the CCR1

role is not to base pair with the target. The complex models include both the SD sequence and the initiation codon further suggesting that IsrR acts primarily on translation rather than on mRNA stability.

Most staphylococcal sRNAs are poorly conserved across different species (49). One explanation is that the *trans*-acting sRNAs mostly act by imperfect pairing to untranslated regions (i.e. sRNAs and targeted UTRs); unlike ORFs, these sequences are prone to numerous inconsequential mutations and thus subject to rapid evolutionary changes. However, *isrR* and its Fur regulation are conserved throughout the *Staphylococcus* genus. This less-common interspecies conservation (another example in *S. aureus* is RsaE (95)) reveals a selective pressure to maintain IsrR sequence, structure, and regulation intact. IsrR pairs with several mRNA targets related to important functions, such as

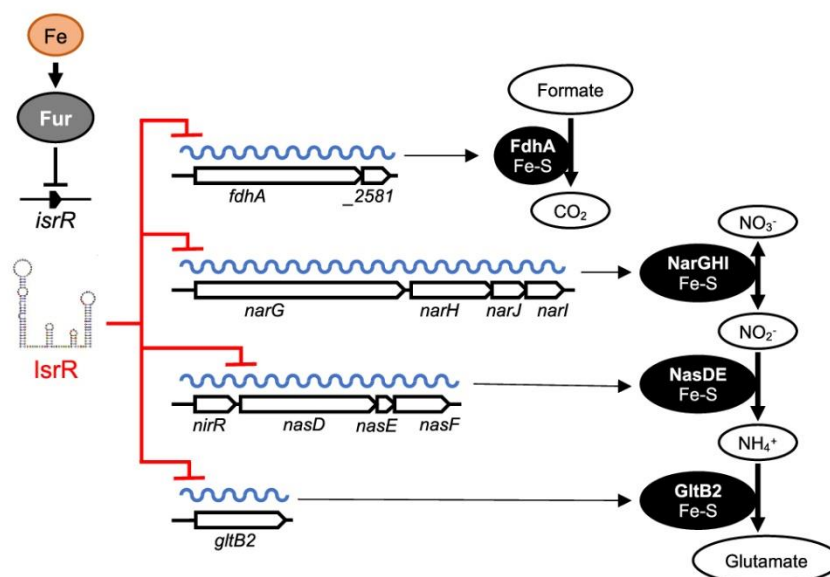


**Figure 10.** IsrR control of dissimilatory nitrate reduction. *isrR* is Fur-regulated. Its expression is induced in iron-free growth conditions. IsrR base pairs to SDs of mRNAs encoding components of formate dehydrogenase, nitrate reductase, nitrite reductase and glutamate synthase, thus preventing translation of the encoded iron-sulfur containing enzymes and nitrate dissimilatory reduction.

iron homeostasis, which may explain this conservation; the occurrence of random *isrR* mutations would affect iron-related metabolism, and therefore be counter-selected.

sRNAs that down-regulate mRNAs encoding iron-sulfur clusters are found in Gram-positive and Gram-negative bacteria. In addition to IsrR, these include RyhB in enteric bacteria (5), the paralogs PrrF1 and PrrF2 in *P. aeruginosa* (11), Mrsl in *M. tuberculosis* (15) and FsrA sRNA in *B. subtilis* (96). Remarkably, none of these sRNAs share the same RNA chaperone dependency (e.g. Hfq for RyhB and PrrF1/PrrF2; FbpA, FbpB and FbpC for FsrA) with IsrR, and their genes share neither synteny nor sequence homology. FsrA, but not the other sRNAs, binds to the Shine-Dalgarno sequence via a C-rich motif (96), but requires three chaperone functions. These sRNAs are therefore not IsrR orthologs. Nevertheless, they do share several target mRNAs encoding the same iron-sulfur-containing enzymes (Supplementary Table S7). Indeed, the iron-sparing response of these sRNAs includes targets involved in nitrate metabolism and the TCA cycle. The TCA cycle mRNA encoding aconitase (*acnA/citB*) is targeted by all the sRNAs discussed above.

The common regulation of these sRNAs by iron and their shared targets suggest convergent evolution, which can be reasonably explained as follows: The accumulation of non-essential iron-containing enzymes is deleterious in iron-scarce environments; however, an sRNA induced during iron starvation that mutates to pair with these transcripts provides an immediate selective advantage, more energetically efficient than the production of specialized regulatory proteins. Since Fur is a widely conserved iron-dependent repressor in bacteria, any Fur-regulated sRNAs, possibly

originating from spurious transcriptions, can be recruited to fulfill this task. RNAs responsive to Fe (rrF) are indeed common in bacteria (5,93). The long-term evolution of some rrFs is expected to lead *in fine* to the birth of IsrR/RyhB functional analogs.

#### DATA AVAILABILITY

Data generated or analyzed during this study are presented. Strains and plasmids are available from the corresponding author on request.

#### SUPPLEMENTARY DATA

Supplementary Data are available at NAR Online.

#### ACKNOWLEDGEMENTS

We are grateful to our colleagues, Sandy Gruss (INRAE, MICALIS) for critical reading of the manuscript, Cintia Gonzalez (UMR\_S 1230) and Svetlana Chabelskaia (UMR\_S 1230) for assistance with animal model experiments, Elise Borezée-Durant (INRAE, MICALIS) for the gift of staphylococcal strains, Aurélie Jaffrenou (I2BC) and Pierre Boudry (I2BC) for the gift of plasmids, Isabelle Hatin (I2BC) for the use of a flow cytometer, Olga Soutourina (I2BC) for access to an anaerobic chamber, Kam Pou Ha (I2BC) for the help with statistical analysis and Béatrice Py (LCB, UMR 7283) for her expertise to identify proteins containing iron-sulfur clusters in *S. aureus* presented in Supplementary Table S6. We thank our lab colleagues and Paul Aner for helpful discussions, technical help, and

warm support. We acknowledge the high-throughput sequencing facility of I2BC for its sequencing and bioinformatics expertise and for its contribution to this study (<http://www.i2bc.paris-saclay.fr>), and the animal core facility ARCHE (ARCHE/SFR BIOSIT, Université Rennes 1, France) for animal experiments.

**Author contributions:** P.B. conceived the project. R.H.C.T., W. L., M. B. and P.B. designed experiments and interpreted the data. V.B. and B.F. designed, performed the animal experiments, EMSAs and interpreted the data. M.P., C.V. and B.S. designed, performed experiments, and interpreted the data to determine RNA structures and interactions. R.H.C.T. and P.B. wrote the manuscript. R.H.C.T., B.F., M.P., B.S. and P.B. edited the paper.

## FUNDING

Research in P.B. and B.F. laboratories was supported by CNRS/Université Paris-Saclay and INSERM/Université Rennes 1, respectively; ‘Agence Nationale de la Recherche’ (ANR) [ANR-15-CE12-0003-01 (sRNA-Fit)]; ‘Fondation pour la Recherche Médicale’ (FRM) [DBF20160635724]; research in P.B. laboratory was also supported by the ANR grant [ANR-19-CE12-0006-01 (sRNA-RRARE)]; research in B.S. laboratory was supported by CNRS; Université de Paris; ANR [ANR-19-CE45-0023-02]; R.H.C.T. was the recipient of a scholarship from the ‘Consejo Nacional de Ciencia y Tecnología’ (CONACyT); M.P. was the recipient of the ‘Agence Nationale de la Recherche contre le SIDA fellowship’ [ANRS-A02019-2 ECTZ108689]. Funding for open access charge: Agence Nationale de la Recherche. **Conflict of interest statement.** None declared.

## REFERENCES

- Troxell, B. and Hassan, H.M. (2013) Transcriptional regulation by ferric uptake regulator (Fur) in pathogenic bacteria. *Front. Cell Infect. Microbiol.*, **3**, 59.
- Sheldon, J.R., Laakso, H.A. and Heinrichs, D.E. (2016) Iron acquisition strategies of bacterial pathogens. *Microbiol. Spectr.*, **45**, 43–85.
- Skaar, E.P. (2010) The battle for iron between bacterial pathogens and their vertebrate hosts. *PLoS Pathog.*, **6**, e1000949.
- Murdoch, C.C. and Skaar, E.P. (2022) Nutritional immunity: the battle for nutrient metals at the host-pathogen interface. *Nat. Rev. Microbiol.*, **10**, <https://doi.org/10.1038/nrmicro2836>.
- Chareyre, S. and Mandin, P. (2018) Bacterial iron homeostasis regulation by sRNAs. *Microbiol. Spectr.*, **6**, 267–281.
- Jordan, M.R., Wang, J., Capdevila, D.A. and Giedroc, D.P. (2020) Multi-metal nutrient restriction and crosstalk in metallostasis systems in microbial pathogens. *Curr. Opin. Microbiol.*, **55**, 17–25.
- Escobar, L., Perez-Martin, J. and de Lorenzo, V. (1999) Opening the iron box: transcriptional metalloregulation by the fur protein. *J. Bacteriol.*, **181**, 6223–6229.
- Masse, E. and Gottesman, S. (2002) A small RNA regulates the expression of genes involved in iron metabolism in *Escherichia coli*. *Proc. Nat. Acad. Sci. U.S.A.*, **99**, 4620–4625.
- Masse, E., Vanderpool, C.K. and Gottesman, S. (2005) Effect of RyhB small RNA on global iron use in *Escherichia coli*. *J. Bacteriol.*, **187**, 6962–6971.
- Oglesby-Sherroue, A.G. and Murphy, E.R. (2013) Iron-responsive bacterial small RNAs: variations on a theme. *Metalloids*, **5**, 276–286.
- Wilderman, P.J., Sowa, N.A., FitzGerald, D.J., FitzGerald, P.C., Gottesman, S., Ochsner, U.A. and Vasil, M.L. (2004) Identification of tandem duplicate regulatory small RNAs in *Pseudomonas aeruginosa* involved in iron homeostasis. *Proc. Nat. Acad. Sci. U.S.A.*, **101**, 9792–9797.
- Pi, H. and Helmann, J.D. (2017) Sequential induction of Fur-regulated genes in response to iron limitation in *Bacillus subtilis*. *Proc. Nat. Acad. Sci. U.S.A.*, **114**, 12785–12790.
- Smaldone, G.T., Revelles, O., Gaballa, A., Sauer, U., Antelmann, H. and Helmann, J.D. (2012) A global investigation of the *Bacillus subtilis* iron-sparing response identifies major changes in metabolism. *J. Bacteriol.*, **194**, 2594–2605.
- Gaballa, A. and Helmann, J.D. (2007) Substrate induction of siderophore transport in *Bacillus subtilis* mediated by a novel one-component regulator. *Mol. Microbiol.*, **66**, 164–173.
- Gerrick, E.R., Barbier, T., Chase, M.R., Xu, R., Francois, J., Lin, V.H., Szucs, M.J., Rock, J.M., Ahmad, R., Tjaden, B. *et al.* (2018) Small RNA profiling in *Mycobacterium tuberculosis* identifies MsrI as necessary for an anticipatory iron sparing response. *Proc. Nat. Acad. Sci. U.S.A.*, **115**, 6464–6469.
- Tong, S.Y., Davis, J.S., Eichenberger, E., Holland, T.L. and Fowler, V.G. Jr (2015) *Staphylococcus aureus* infections: epidemiology, pathophysiology, clinical manifestations, and management. *Clin. Microbiol. Rev.*, **28**, 603–661.
- Haag, A.F., Fitzgerald, J.R. and Penades, J.R. (2019) *Staphylococcus aureus* in animals. *Microbiol. Spectr.*, **7**, <https://doi.org/10.1128/microbiolspec.GPP3-0060-2019>.
- Price, E.E. and Boyd, J.M. (2020) Genetic regulation of metal ion homeostasis in *Staphylococcus aureus*. *Trends Microbiol.*, **28**, 821–831.
- Herbert, S., Ziebandt, A.K., Ohlsen, K., Schafer, T., Hecker, M., Albrecht, D., Novick, R. and Gotz, F. (2010) Repair of global regulators in *Staphylococcus aureus* 8325 and comparative analysis with other clinical isolates. *Infect. Immun.*, **78**, 2877–2889.
- Fuchs, S., Mehlan, H., Bernhardt, J., Hennig, A., Michalik, S., Surmann, K., Pane-Farre, J., Giese, A., Weiss, S., Backert, L. *et al.* (2018) AureoWiki the repository of the *Staphylococcus aureus* research and annotation community. *Int. J. Med. Microbiol.*, **308**, 558–568.
- Gibson, D.G., Young, L., Chuang, R.Y., Venter, J.C., Hutchison, C.A. 3rd and Smith, H.O. (2009) Enzymatic assembly of DNA molecules up to several hundred kilobases. *Nat. Methods*, **6**, 343–345.
- Monk, I.R., Tree, J.J., Howden, B.P., Stinear, T.P. and Foster, T.J. (2015) Complete bypass of restriction systems for major *Staphylococcus aureus* lineages. *Mbio*, **6**, e00308–e00315.
- March, J.B., Colloms, M.D., Hart-Davis, D., Oliver, I.R. and Masters, M. (1989) Cloning and characterization of an *Escherichia coli* gene, *penB*, affecting plasmid copy number. *Mol. Microbiol.*, **3**, 903–910.
- Bohn, C., Collier, J. and Boulou, P. (2004) Dispensable PDZ domain of *Escherichia coli* YaeL essential protease. *Mol. Microbiol.*, **52**, 427–435.
- Le Lam, T.N., Morvan, C., Liu, W., Bohn, C., Jaszczyszyn, Y. and Boulou, P. (2017) Finding sRNA-associated phenotypes by competition assays: an example with *Staphylococcus aureus*. *Methods*, **117**, 21–27.
- Horsburgh, M.J., Clements, M.O., Crossley, H., Ingham, E. and Foster, S.J. (2001) PerR controls oxidative stress resistance and iron storage proteins and is required for virulence in *Staphylococcus aureus*. *Infect. Immun.*, **69**, 3744–3754.
- Marchais, A., Naville, M., Bohn, C., Boulou, P. and Gautheret, D. (2009) Single-pass classification of all noncoding sequences in a bacterial genome using phylogenetic profiles. *Genome Res.*, **19**, 1084–1092.
- Lott, S.C., Schäfer, R.A., Mann, M., Backofen, R., Hess, W.R., Voß, B. and Georg, J. (2018) GLASSgo – automated and reliable detection of sRNA homologs from a single input sequence. *Front. Genet.*, **9**, 124.
- Grant, C.E., Bailey, T.L. and Noble, W.S. (2011) FIMO: scanning for occurrences of a given motif. *Bioinformatics*, **27**, 1017–1018.
- Novichkov, P.S., Kazakov, A.E., Ravcheev, D.A., Leyn, S.A., Kovaleva, G.Y., Sutormin, R.A., Kazanov, M.D., Riehl, W., Arkin, A.P., Dubchak, I. *et al.* (2013) RegPrecise 3.0 – a resource for genome-scale exploration of transcriptional regulation in bacteria. *BMC Genomics*, **14**, 745.
- Will, S., Joshi, T., Hofacker, I.L., Stadler, P.F. and Backofen, R. (2012) LocARNA-P: accurate boundary prediction and improved detection of structural RNAs. *RNA*, **18**, 900–914.
- Wright, P.R., Georg, J., Mann, M., Sorescu, D.A., Richter, A.S., Lott, S., Kleinkauf, R., Hess, W.R. and Backofen, R. (2014) CopraRNA and

- intarna: predicting small RNA targets, networks and interaction domains. *Nucleic Acids Res.*, **42**, W119–W123.
33. Py, B. and Barras, F. (2010) Building Fe-S proteins: bacterial strategies. *Nat. Rev. Microbiol.*, **8**, 436–446.
  34. Duverger, Y. and Py, B. (2021) Molecular biology and genetic tools to investigate functional redundancy among Fe-S cluster carriers in *E. coli*. *Methods Mol. Biol.*, **2353**, 3–36.
  35. Le Huyen, K.B., Gonzalez, C.D., Pascreau, G., Bordeau, V., Cattoir, V., Liu, W., Boulouc, P., Felden, B. and Chabelskaya, S. (2021) A small regulatory RNA alters *Staphylococcus aureus* virulence by titrating RNAPIII activity. *Nucleic Acids Res.*, **49**, 10644–10656.
  36. Liu, W., Boudry, P., Bohn, C. and Boulouc, P. (2020) *Staphylococcus aureus* pigmentation is not controlled by Hfq. *BMC Res Notes*, **13**, 63.
  37. Soutourina, O.A., Monot, M., Boudry, P., Saujet, L., Pichon, C., Sismeiro, O., Semenova, E., Severinov, K., Le Bouguenec, C., Coppee, J.Y. et al. (2013) Genome-wide identification of regulatory RNAs in the human pathogen *Clostridium difficile*. *PLoS Genet.*, **9**, e1003493.
  38. Urban, J.H. and Vogel, J. (2007) Translational control and target recognition by *Escherichia coli* small RNAs in vivo. *Nucleic Acids Res.*, **35**, 1018–1037.
  39. Ivain, L., Bordeau, V., Eyraud, A., Hallier, M., Dreano, S., Tattevin, P., Felden, B. and Chabelskaya, S. (2017) An in vivo reporter assay for sRNA-directed gene control in Gram-positive bacteria: identifying a novel sRNA target in *Staphylococcus aureus*. *Nucleic Acids Res.*, **45**, 4994–5007.
  40. De Bisschop, G. and Sargueil, B. (2021) RNA footprinting using small chemical reagents. *Methods Mol. Biol.*, **2323**, 13–23.
  41. Deforges, J., Chamond, N. and Sargueil, B. (2012) Structural investigation of HIV-1 genomic RNA dimerization process reveals a role for the major Splice-site donor stem loop. *Biochimie*, **94**, 1481–1489.
  42. Deforges, J., de Breyne, S., Ameur, M., Ulryck, N., Chamond, N., Saaidi, A., Ponty, Y., Ohlmann, T. and Sargueil, B. (2017) Two ribosome recruitment sites direct multiple translation events within HIV1 GAG open reading frame. *Nucleic Acids Res.*, **45**, 7382–7400.
  43. Karabiber, F., McGinnis, J.L., Favorov, O.V. and Weeks, K.M. (2013) QuShape: rapid, accurate, and best-practices quantification of nucleic acid probing information, resolved by capillary electrophoresis. *RNA*, **19**, 63–73.
  44. Saaidi, A., Allouche, D., Regnier, M., Sargueil, B. and Ponty, Y. (2020) IPANEMAP: integrative probing analysis of nucleic acids empowered by multiple accessibility profiles. *Nucleic Acids Res.*, **48**, 8276–8289.
  45. Darty, K., Denise, A. and Ponty, Y. (2009) VARNA: interactive drawing and editing of the RNA secondary structure. *Bioinformatics*, **25**, 1974–1975.
  46. Haley, K.P. and Skaar, E.P. (2012) A battle for iron: host sequestration and *Staphylococcus aureus* acquisition. *Microbes Infect.*, **14**, 217–227.
  47. Storz, G., Vogel, J. and Wassarman, K.M. (2011) Regulation by small RNAs in bacteria: expanding frontiers. *Mol. Cell*, **43**, 880–891.
  48. Esberard, M., Hallier, M., Liu, W., Morvan, C., Bossi, L., Figueroa-Bossi, N., Felden, B. and Boulouc, P. (2022) 6S RNA-Dependent susceptibility to RNA polymerase inhibitors. *Antimicrob. Agents Chemother.*, **66**, e0243521.
  49. Liu, W., Rochat, T., Toffano-Nioche, C., Le Lam, T.N., Boulouc, P. and Morvan, C. (2018) Assessment of bona fide sRNAs in *Staphylococcus aureus*. *Front. Microbiol.*, **9**, 228.
  50. Mader, U., Nicolas, P., Depke, M., Pane-Farre, J., Debarbouille, M., van der Kooi-Pol, M.M., Guerin, C., Derozier, S., Hiron, A., Jarmer, H. et al. (2016) *Staphylococcus aureus* transcriptome architecture: from laboratory to infection-mimicking conditions. *PLoS Genet.*, **12**, e1005962.
  51. Carroll, R.K., Weiss, A., Broach, W.H., Wiemels, R.E., Mogen, A.B., Rice, K.C. and Shaw, L.N. (2016) Genome-wide annotation, identification, and global transcriptomic analysis of regulatory or small RNA gene expression in *Staphylococcus aureus*. *Mbio*, **7**, e01990-15.
  52. Wagner, E.G.H. and Romby, P. (2015) Small RNAs in bacteria and archaea: who they are, what they do, and how they do it. *Adv. Genet.*, **90**, 133–208.
  53. Dutcher, H.A. and Raghavan, R. (2018) Origin, evolution, and loss of bacterial small RNAs. *Microbiol. Spectr.*, **6**, 289–313.
  54. Sassi, M., Augagneur, Y., Mauro, T., Ivain, L., Chabelskaya, S., Hallier, M., Sallou, O. and Felden, B. (2015) SRD: a *Staphylococcus* regulatory RNA database. *RNA*, **21**, 1005–1017.
  55. Geissmann, T., Chevalier, C., Cros, M.J., Boisset, S., Fechter, P., Noirot, C., Schrenzel, J., Francois, P., Vandenesch, F., Gaspin, C. et al. (2009) A search for small noncoding RNAs in *Staphylococcus aureus* reveals a conserved sequence motif for regulation. *Nucleic Acids Res.*, **37**, 7239–7257.
  56. Rochat, T., Bohn, C., Morvan, C., Le Lam, T.N., Razvi, F., Pain, A., Toffano-Nioche, C., Ponien, P., Jacq, A., Jacquet, E. et al. (2018) The conserved regulatory RNA RsaE down-regulates the arginine degradation pathway in *Staphylococcus aureus*. *Nucleic Acids Res.*, **46**, 8803–8816.
  57. Benito, Y., Kolb, F.A., Romby, P., Lina, G., Etienne, J. and Vandenesch, F. (2000) Probing the structure of RNAPIII, the *Staphylococcus aureus* agr regulatory RNA, and identification of the RNA domain involved in repression of protein expression. *RNA*, **6**, 668–679.
  58. Low, J.T. and Weeks, K.M. (2010) SHAPE-directed RNA secondary structure prediction. *Methods*, **52**, 150–158.
  59. Frezza, E., Courban, A., Allouche, D., Sargueil, B. and Pasquali, S. (2019) The interplay between molecular flexibility and RNA chemical probing reactivities analyzed at the nucleotide level via an extensive molecular dynamics study. *Methods*, **162–163**, 108–127.
  60. de Bisschop, G., Allouche, D., Frezza, E., Masquida, B., Ponty, Y., Will, S. and Sargueil, B. (2021) Progress toward SHAPE constrained computational prediction of tertiary interactions in RNA structure. *Non-Coding RNA*, **7**, 71.
  61. Pain, A., Ott, A., Amine, H., Rochat, T., Boulouc, P. and Gautheret, D. (2015) An assessment of bacterial small RNA target prediction programs. *RNA Biol.*, **12**, 509–513.
  62. Zupok, A., Iobbi-Nivol, C., Mejean, V. and Leimkuhler, S. (2019) The regulation of moco biosynthesis and molybdoenzyme gene expression by molybdenum and iron in bacteria. *Metallomics*, **11**, 1602–1624.
  63. Schlag, S., Fuchs, S., Nerz, C., Gaupp, R., Engelmann, S., Liebecke, M., Lalk, M., Hecker, M. and Gotz, F. (2008) Characterization of the oxygen-responsive NreABC regulon of *Staphylococcus aureus*. *J. Bacteriol.*, **190**, 7847–7858.
  64. Wright, P.R., Richter, A.S., Papenfort, K., Mann, M., Vogel, J., Hess, W.R., Backofen, R. and Georg, J. (2013) Comparative genomics boosts target prediction for bacterial small RNAs. *Proc. Nat. Acad. Sci. U.S.A.*, **110**, E3487–E3496.
  65. Fuchs, S., Pane-Farre, J., Kohler, C., Hecker, M. and Engelmann, S. (2007) Anaerobic gene expression in *Staphylococcus aureus*. *J. Bacteriol.*, **189**, 4275–4289.
  66. Wang, H. and Gunsalus, R.P. (2003) Coordinate regulation of the *Escherichia coli* formate dehydrogenase *fdnGHI* and *fdhF* genes in response to nitrate, nitrite, and formate: roles for NarL and NarP. *J. Bacteriol.*, **185**, 5076–5085.
  67. Glaser, J.H. and DeMoss, J.A. (1972) Comparison of nitrate reductase mutants of *Escherichia coli* selected by alternative procedures. *Mol. Gen. Genet.*, **116**, 1–10.
  68. Masse, E., Escorcia, F.E. and Gottesman, S. (2003) Coupled degradation of a small regulatory RNA and its mRNA targets in *Escherichia coli*. *Genes Dev.*, **17**, 2374–2383.
  69. Mann, M., Wright, P.R. and Backofen, R. (2017) IntaRNA 2.0: enhanced and customizable prediction of RNA-RNA interactions. *Nucleic Acids Res.*, **45**, W435–W439.
  70. Vogel, J. and Luisi, B.F. (2011) Hfq and its constellation of RNA. *Nat. Rev. Microbiol.*, **9**, 578–589.
  71. Bohn, C., Rigoulay, C. and Boulouc, P. (2007) No detectable effect of RNA-binding protein hfq absence in *Staphylococcus aureus*. *BMC Microbiol.*, **7**, 10.
  72. Boulouc, P. and Repoila, F. (2016) Fresh layers of RNA-mediated regulation in Gram-positive bacteria. *Curr. Opin. Microbiol.*, **30**, 30–35.
  73. Jousselin, A., Metzinger, L. and Felden, B. (2009) On the facultative requirement of the bacterial RNA chaperone, hfq. *Trends Microbiol.*, **17**, 399–405.
  74. Rochat, T., Boulouc, P., Yang, Q., Bossi, L. and Figueroa-Bossi, N. (2012) Lack of interchangeability of Hfq-like proteins. *Biochimie*, **94**, 1554–1559.

75. Rochat, T., Delumeau, O., Figueroa-Bossi, N., Noirot, P., Bossi, L., Dervyn, E. and Bouloc, P. (2015) Tracking the elusive function of *Bacillus subtilis* hfq. *PLoS One*, **10**, e0124977.
76. Hammerle, H., Amman, F., Vecerek, B., Stulke, J., Hofacker, I. and Blasi, U. (2014) Impact of hfq on the *Bacillus subtilis* transcriptome. *PLoS One*, **9**, e98661.
77. Bullen, J.J., Rogers, H.J., Spalding, P.B. and Ward, C.G. (2005) Iron and infection: the heart of the matter. *FEMS Immunol. Med. Microbiol.*, **43**, 325–330.
78. Kim, H.K., Missiakas, D. and Schneewind, O. (2014) Mouse models for infectious diseases caused by *Staphylococcus aureus*. *J. Immunol. Methods*, **410**, 88–99.
79. Marchetti, M., De Bei, O., Bettati, S., Campanini, B., Kovachka, S., Gianquinto, E., Spyrikis, F. and Ronda, L. (2020) Iron metabolism at the interface between host and pathogen: from nutritional immunity to antibacterial development. *Int. J. Mol. Sci.*, **21**, 2145.
80. Oogai, Y., Matsuo, M., Hashimoto, M., Kato, F., Sugai, M. and Komatsuzawa, H. (2011) Expression of virulence factors by *Staphylococcus aureus* grown in serum. *Appl. Environ. Microbiol.*, **77**, 8097–8105.
81. Malachowa, N., Whitney, A.R., Kobayashi, S.D., Sturdevant, D.E., Kennedy, A.D., Braughton, K.R., Shabb, D.W., Diep, B.A., Chambers, H.F., Otto, M. *et al.* (2011) Global changes in *Staphylococcus aureus* gene expression in human blood. *PLoS One*, **6**, e18617.
82. Lalaoua, D., Baude, J., Wu, Z., Tomasini, A., Chicher, J., Marzi, S., Vandenesch, F., Romby, P., Caldelari, I. and Moreau, K. (2019) RsaC sRNA modulates the oxidative stress response of *Staphylococcus aureus* during manganese starvation. *Nucleic Acids Res.*, **47**, 9871–9887.
83. Horsburgh, M.J., Ingham, E. and Foster, S.J. (2001) In *Staphylococcus aureus*, fur is an interactive regulator with PerR, contributes to virulence, and is necessary for oxidative stress resistance through positive regulation of catalase and iron homeostasis. *J. Bacteriol.*, **183**, 468–475.
84. Torres, V.J., Attia, A.S., Mason, W.J., Hood, M.I., Corbin, B.D., Beasley, F.C., Anderson, K.L., Stauff, D.L., McDonald, W.H., Zimmerman, L.J. *et al.* (2010) *Staphylococcus aureus* fur regulates the expression of virulence factors that contribute to the pathogenesis of pneumonia. *Infect. Immun.*, **78**, 1618–1628.
85. Allard, M., Moisan, H., Brouillette, E., Gervais, A.L., Jacques, M., Lacasse, P., Diarra, M.S. and Malouin, F. (2006) Transcriptional modulation of some *Staphylococcus aureus* iron-regulated genes during growth in vitro and in a tissue cage model in vivo. *Microbes Infect.*, **8**, 1679–1690.
86. Burke, K.A. and Lascelles, J. (1975) Nitrate reductase system in *Staphylococcus aureus* wild type and mutants. *J. Bacteriol.*, **123**, 308–316.
87. Lundberg, J.O., Weitzberg, E. and Gladwin, M.T. (2008) The nitrate-nitrite-nitric oxide pathway in physiology and therapeutics. *Nat. Rev. Drug Discov.*, **7**, 156–167.
88. Ma, L., Hu, L., Feng, X. and Wang, S. (2018) Nitrate and nitrite in health and disease. *Aging Dis.*, **9**, 938–945.
89. Kamps, A., Achebach, S., Fedtke, I., Uden, G. and Gotz, F. (2004) Staphylococcal nreB: an O(2)-sensing histidine protein kinase with an O(2)-labile iron-sulphur cluster of the FNR type. *Mol. Microbiol.*, **52**, 713–723.
90. Nilkens, S., Koch-Singenstreu, M., Niemann, V., Gotz, F., Stehle, T. and Uden, G. (2014) Nitrate/oxygen co-sensing by an NreA/NreB sensor complex of *Staphylococcus carnosus*. *Mol. Microbiol.*, **91**, 381–393.
91. Niemann, V., Koch-Singenstreu, M., Neu, A., Nilkens, S., Gotz, F., Uden, G. and Stehle, T. (2014) The NreA protein functions as a nitrate receptor in the staphylococcal nitrate regulation system. *J. Mol. Biol.*, **426**, 1539–1553.
92. Prasse, D. and Schmitz, R.A. (2018) Small RNAs involved in regulation of nitrogen metabolism. *Microbiol. Spectr.*, **6**, <https://doi.org/10.1128/microbiolspec.RWR-0018-2018>.
93. Muro-Pastor, A.M. and Hess, W.R. (2019) Regulatory RNA at the crossroads of carbon and nitrogen metabolism in photosynthetic cyanobacteria. *Biochim. Biophys. Acta Gene Regul. Mech.*, **1863**, 194477.
94. Durand, S. and Guillier, M. (2021) Transcriptional and Post-transcriptional control of the nitrate respiration in bacteria. *Front. Mol. Biosci.*, **8**, 667758.
95. Bohn, C., Rigoulay, C., Chabelskaya, S., Sharma, C.M., Marchais, A., Skorski, P., Borezee-Durant, E., Barbet, R., Jacquet, E., Jacq, A. *et al.* (2010) Experimental discovery of small RNAs in *Staphylococcus aureus* reveals a riboregulator of central metabolism. *Nucleic Acids Res.*, **38**, 6620–6636.
96. Gaballa, A., Antelmann, H., Aguilar, C., Khakh, S.K., Song, K.B., Smaldone, G.T. and Helmann, J.D. (2008) The *Bacillus subtilis* iron-sparing response is mediated by a Fur-regulated small RNA and three small, basic proteins. *Proc. Nat. Acad. Sci. U.S.A.*, **105**, 11927–11932.



## SUPPLEMENTARY DATA

### **sRNA-controlled iron sparing response in Staphylococci**

Rodrigo H. Coronel-Tellez<sup>1</sup>, Mateusz Pospiech<sup>2</sup>, Maxime Barrault<sup>1</sup>, Wenfeng Liu<sup>1</sup>, Valérie

Bordeau<sup>3</sup>, Christelle Vasnier<sup>2</sup>, Brice Felden<sup>3</sup>, Bruno Sargueil<sup>2</sup> and Philippe Bouloc<sup>1</sup>

<sup>1</sup>Université Paris-Saclay, CEA, CNRS, Institute for Integrative Biology of the Cell (I2BC), 91198 Gif-sur-Yvette, France

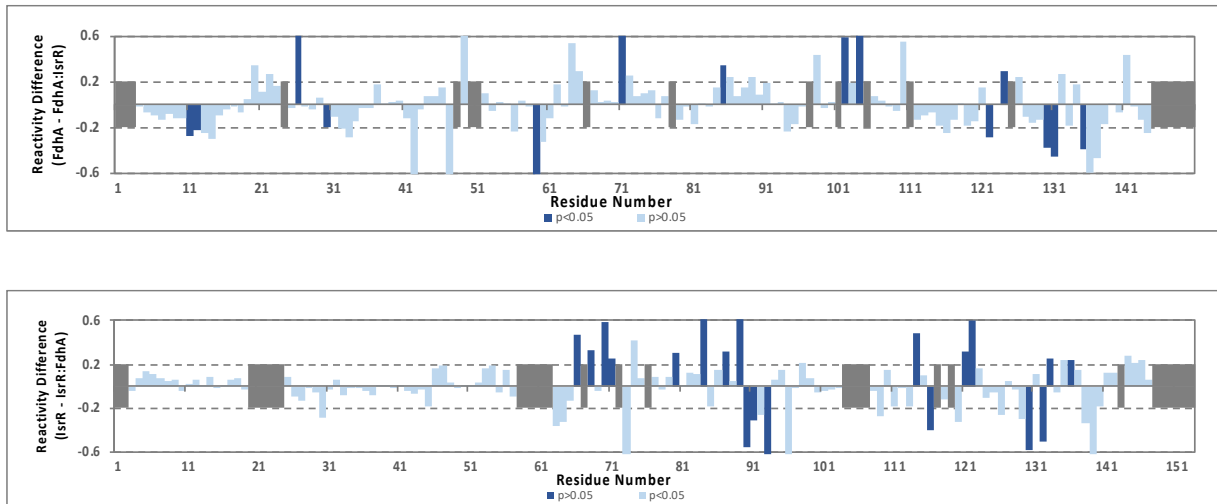
<sup>2</sup>CNRS UMR 8038, CitCoM, Université de Paris, 75006 Paris, France

<sup>3</sup>Université de Rennes 1, BRM (Bacterial regulatory RNAs and Medicine) UMR\_S 1230, 35000 Rennes, France

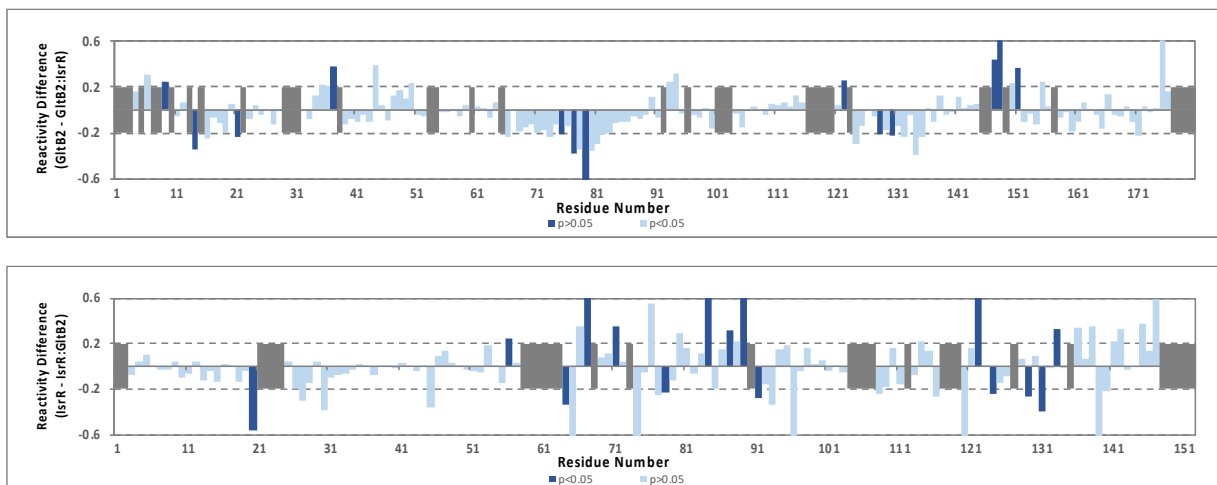
The supplementary data presented here are only the ones related to the experiments in which I participated. Full supplementary data are accessible through this link: [10.1093/nar/gkac648](https://doi.org/10.1093/nar/gkac648)

Figure S6. Comparison of *fdhA* and *gltB2* mRNAs reactivity to 1M7 obtained in the presence/absence of IsrR

**A**

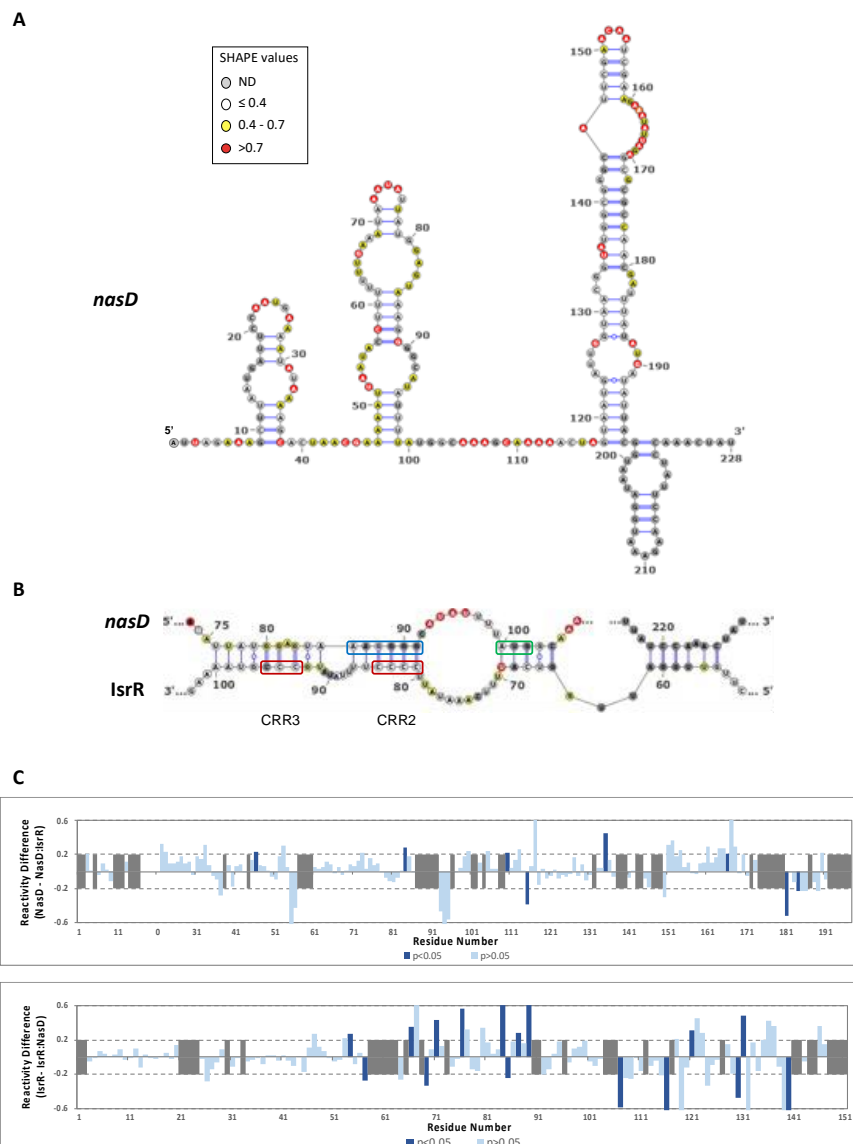


**B**



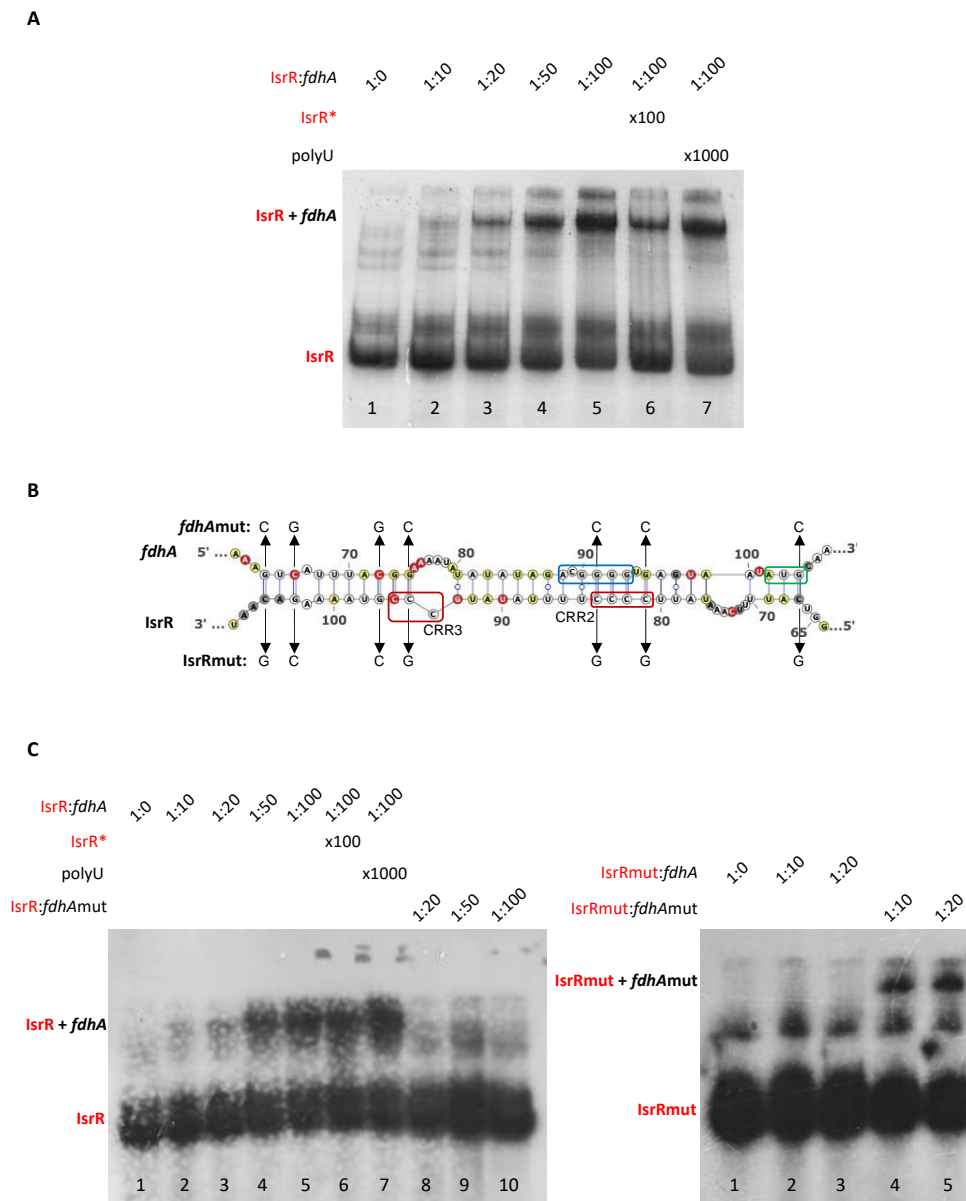
(A) Top panel: difference of reactivity to 1M7 for each nucleotide of *fdhA* mRNA when IsrR was added. Bottom panel: difference of reactivity to 1M7 for each nucleotide of IsrR when *fdhA* mRNA was added; nucleotides in intense blue presented a significant difference while those in light blue did not. (B) Top panel: difference of reactivity to 1M7 for each nucleotide of *gltB2* mRNA when IsrR was added. Bottom panel: difference of reactivity to 1M7 for each nucleotide of IsrR when *gltB2* mRNA was added; nucleotides in intense blue presented a significant difference while those in light blue did not.

Figure S7. Comparison of *nasD* mRNA reactivity obtained to 1M7 in the presence/absence of IsrR with proposed interaction model



(A) Secondary structure model obtained with IPANEMAP for *nasD* 5'UTR using 1M7 reactivity as constraints. Nucleotides are coloured according to their reactivity in the absence of IsrR with the indicated colour code. ND, not determined. (B) Model for interaction between *nasD* mRNA and IsrR based on changes in reactivity in the presence of IsrR. mRNA Shine-Dalgarno sequence is shown in a blue rectangle and the start codon in a green rectangle; IsrR C-rich regions are shown in red rectangles. (C) Top panel: difference of reactivity to 1M7 for each nucleotide of *nasD* mRNA when IsrR was added. Bottom panel: difference of reactivity to 1M7 for each nucleotide of IsrR when *nasD* mRNA was added; nucleotides in intense blue presented a significant difference while those in light blue did not.

Figure S8. Electrophoretic mobility shift assay of IsrR in the presence of *fdhA* mRNA



- (A) Electrophoretic mobility shift assay (EMSA) with labelled IsrR. Constant amounts of IsrR (0.25 pmol) were mixed with increasing amounts of *fdhA* mRNA in the indicated proportions (columns 1-5). A specific competitor (unlabelled IsrR\*, column 6) and a nonspecific competitor (polyU, column 7) were used as controls. (B) Predicted interaction between IsrR and *fdhA* mRNA as shown in Figure 6. Inserted point mutations ( $G \leftrightarrow C$ ) are indicated with an arrow, resulting in IsrRmut and *fdhAmut*. (C) Left panel: EMSA with labelled IsrR as in (A) (columns 1-7) or mixed with increasing amounts of *fdhA* mRNAmut (columns 8-10). Right panel: EMSA with labelled IsrRmut. Constant amounts of IsrRmut were mixed with increasing amounts of *fdhA* mRNA (columns 1-3) or *fdhA* mRNAmut (columns 4-5) in the indicated proportions.



## **F: Regulation of staphylococcal aconitase expression in iron deficiency: Control by sRNA-driven feedforward loop and moonlighting activity**

---

# **sRNA-driven feedforward loop and moonlighting activity control staphylococcal aconitase expression during iron deficiency**

Maxime Barrault<sup>1</sup>, Svetlana Chabelskaya<sup>2</sup>, Rodrigo H. Coronel-Tellez<sup>1</sup>, Claire Toffano-Nioche<sup>1</sup> and Philippe Bouloc<sup>1\*</sup>

<sup>1</sup>Université Paris-Saclay, CEA, CNRS, Institute for Integrative Biology of the Cell (I2BC), 91198 Gif-sur-Yvette, France

<sup>2</sup>Université de Rennes 1, BRM (Bacterial regulatory RNAs and Medicine) UMR\_S 1230, 35000 Rennes, France

Running Head: Aconitase post-transcriptional controls in *S. aureus*

\* To whom correspondence should be addressed.

Tel: +33 1 69 82 62 17; Email: [philippe.bouloc@i2bc.paris-saclay.fr](mailto:philippe.bouloc@i2bc.paris-saclay.fr)

## **ABSTRACT**

IsrR is a regulatory RNA (sRNA) whose activity is decisive for *S. aureus* optimum fitness upon iron starvation and its full virulence. IsrR down-regulates several genes coding iron-containing enzymes to spare iron for essential processes. Here, we report the role of IsrR in regulating citrate metabolism through the control of aconitase, CitB, and its transcriptional regulator, CcpE. We show that IsrR binds to the Shine-Dalgarno sequences of *citB* and *ccpE* mRNAs through its C-rich regions thus preventing their translation. This IsrR-dependent dual-regulatory mechanism provides a feedforward loop control over aconitase underscoring the intricate role played by IsrR in shaping citrate metabolism. We also uncover a noteworthy regulatory activity of *S. aureus* aconitase, mirroring its multifunctional role observed in other species during iron starvation. Beyond its canonical role, aconitase not only negatively regulates its expression but also impacts the enzymes involved in both its substrate supply and product utilization. Intriguingly, this moonlighting activity concurrently upregulates pyruvate carboxylase expression, potentially compensating for the tricarboxylic acid (TCA) cycle deficiency associated with iron scarcity.

**Keywords:** *Staphylococcus aureus*, IsrR, regulatory RNA, Iron-sulfur clusters, aconitase, citrate

## INTRODUCTION

The transition from oxidized to reduced state of iron generates a redox potential couple that is utilized by enzymes to transfer energy. Therefore, iron is an essential compound for sustaining life. Mammals use this dependence on iron in response to infections through a defense mechanism called nutritional immunity, whereby they sequester metal ions to inhibit pathogen growth. (1). Bacteria adapt to iron-depleted environments such as within the host with sophisticated systems to capture and import iron using siderophores and dedicated transporters. However, an excess of iron is also toxic due to its oxidized state, which generates harmful reactive oxygen species (ROS) that can damage macromolecular compounds. Balancing the iron content is therefore crucial for living organisms to optimize their fitness, as they must navigate between the necessity of iron and its potential toxicity. Many bacteria address this challenge by regulating the expression of iron import through the ferric uptake regulator (Fur). This protein acts as a repressor that is fully active in iron-replete cells but becomes inactivated under conditions of iron starvation (2,3). By modulating the expression of iron import, bacteria can carefully manage their iron levels to ensure proper function and minimize the detrimental effects of excess iron.

Bacterial small regulatory RNAs (sRNAs) typically bind to mRNA molecules through base-pairing interactions, thereby modulating their activity. These sRNAs play a role in maintaining general homeostasis and facilitating adaptation to fluctuating growth conditions (4). In this context, sRNAs provide an additional layer of regulation that is essential for optimal fitness and adaptation to variations in iron availability. A commonly observed strategy, conserved among both Gram-positive and Gram-negative bacteria, is the production of sRNAs under iron-starved conditions. These sRNAs act by downregulating mRNAs encoding non-essential enzymes that require iron (5). By doing so, these sRNAs facilitate the conservation of iron resources, ensuring its allocation to essential cellular processes.

*Staphylococcus aureus*, a pathogen capable of infecting both humans and livestock,

exhibits remarkable adaptability to diverse ecological niches and is responsible for numerous diseases. In a recent study, we identified IsrR, an sRNA that is repressed by Fur (6). IsrR forms base-pairing interactions with mRNAs predominantly involved in the expression of iron-containing enzymes, thereby preventing their translation. The primary function of IsrR is presumed to be conserving iron in environments lacking it, ensuring its availability for essential cellular processes.

The absence of IsrR significantly diminishes the virulence of *S. aureus* (6). This outcome aligns with expectations, as the pathogen loses its ability to adapt to hosts that sequester iron. Furthermore, we demonstrated that in anaerobic growth conditions, IsrR modulates nitrate respiration by targeting mRNAs associated with this metabolic pathway. Through bioinformatics analysis, numerous potential targets of IsrR were identified indicating its potential role as a global regulator capable of reshaping metabolic pathways in response to iron starvation (6,7). Notably, some of these targets are associated with citrate metabolism.

Citrate is a key compound linking synthesis and degradation metabolic pathways, including those of carbohydrates, fatty acids, and amino acids. It is the initial molecule synthesized in the tricarboxylic acid (TCA) cycle, formed through the condensation of oxaloacetate and acetyl-CoA by the enzyme citrate synthase. Additionally, citrate acts as a regulator for various enzymatic reactions (8). Given its central position in metabolism, enzymes associated with citrate are tightly regulated at multiple levels.

One example of such regulation involves aconitase, a moonlighting enzyme responsible for the isomerization of citrate to isocitrate within the TCA cycle. In several species, it has been observed that growth conditions characterized by iron deprivation lead to aconitase assuming a regulatory role, exerting feedback control over its own expression (9,10). In *S. aureus*, the gene *citB*, encoding aconitase, is positively regulated by the transcriptional activator CppE, which has been reported to be responsive to citrate levels (11,12).

In this study, we present evidence demonstrating the involvement of IsrR in the downregulation of aconitase in *S. aureus* during iron starvation. Our findings reveal that IsrR exerts regulatory control through both direct and indirect mechanisms. We also document the *S. aureus* aconitase moonlighting activity, showing that in iron-starved conditions, its RNA binding activity down-regulates mRNA encoding TCA-cycle enzymes. These observations provide an understanding of the intricate and multifaceted regulatory mechanisms that operate during iron starvation in *S. aureus*.

## **MATERIAL AND METHODS**

### **Bacterial strains, plasmids, and growth conditions**

The bacterial strains used for this study are described in Supplementary Table S1. The work was performed with *S. aureus* HG003 strain (13). Gene annotations refer to NCTC8325 nomenclature (file CP00025.1) retrieved from Genbank and Aureowiki (14). Plasmids were engineered by Gibson assembly (15) in *Escherichia coli* IM08B (16) as described (Supplementary Table S2), using the indicated appropriate primers (Supplementary Table S3) for PCR amplification. Plasmids were verified by DNA sequencing and transferred into HG003 or derivatives. Chromosomal mutants (deletions and insertions) were either reported or constructed for this study (Supplementary Table S1) using pIMAY derivatives as described (17). Staphylococcal strains were routinely grown in Brain Heart Infusion (BHI) broth at 37°C aerobically. *E. coli* strains were grown aerobically in Luria-Bertani (LB) broth at 37°C. Antibiotics were added to media as needed: ampicillin 100 µg/ml and chloramphenicol 20 µg/ml for *E. coli*; chloramphenicol 5 µg/ml, erythromycin 1µ/ml and kanamycin 60 µg/ml for *S. aureus*. Iron-depleted media was obtained by the addition of 2,2'-dipyridyl (DIP) at a concentration of 0.5 mM and incubation for 30 min prior to the addition of bacteria.

### **Biocomputing analysis**

Pairing predictions between IsrR and the mRNA targets were made using intaRNA (18) set with default parameters except for suboptimal interaction overlap set to "can overlap in both". The sequences used for IsrR and mRNA targets were extracted from the *S. aureus* NCTC8325 strain (NCBI RefSeq NC\_007795.1). For the mRNA targets, the sequences used started at the TSS when known (e.g., EMOTE (19)) or were arbitrarily made to start at nucleotide -60 with respect to the +1 of translation. The sequences contain the 5' UTR and the 13 first codons of the CDS. For transcription analysis, see below the dedicated section. Statistical analyses were made using a t-test. Error bars represent the 95% confidence interval following a Student test.

## Western blotting

Protein extracts were prepared by growing cells overnight, centrifugation (5 min, 4500 RPM, 4°C), and resuspension of the pellet in 400 µL of 50 mM Tris-HCl. Cells were disrupted using Fast-Prep (MP Biomedicals) and protein extracts were recovered after centrifugation (15 min, 15000 RPM, 4°C). Protein concentrations of each extract were determined by Bradford and 10 µg of proteins were loaded on a NuPAGE 4%-12% Bis-Tris gel before migration at 150V for 45min. Proteins were transferred from the gel to a PVDF membrane using the iBind system (Invitrogen). Immunolabeling was made overnight using a rabbit anti-Flag antibody and an anti-rabbit IgG HRP-conjugated antibody (Promega) in the iBlot system (Invitrogen). Images were obtained using a Chemidoc MP (Bio-Rad) and quantified using the ImageLab software.

## Translational reporter assay for sRNA activity

Translational reporter fusions were constructed using the same sequences used for the bioinformatics predictions. Briefly, 5' UTR regions and the first 13 codons of the mRNA targets were fused in frame with the CDS of the fluorescent protein mAmetrine. The 5'UTR was placed under the control of the strong promoter P1 from *sarA* (P1<sub>sarA</sub>). These constructs were engineered using the pRN112 plasmid and then inserted on the chromosome of *S. aureus* following the protocol from de Jong et al. (20). The insertions of the reporter fusions were confirmed by sequencing. Plasmids driving constitutive expression of *isrR* (pRMC2ΔR-IsrR) and its derivatives with CRR deletions (pRMC2ΔR-IsrRΔC1, pRMC2ΔR-IsrRΔC2, pRMC2ΔR-IsrRΔC3, pRMC2ΔR-IsrRΔC1C2, pRMC2ΔR-IsrRΔC1C3, pRMC2ΔR-IsrRΔC2C3, and pRMC2ΔR-IsrRΔC1C2C3 expressing *isrR*ΔC1, *isrR*ΔC2, *isrR*ΔC3, *isrR*ΔC1C2, *isrR*ΔC1C3, *isrR*ΔC2C3, and *isrR*ΔC1C2C3, respectively) were constructed and introduced in HG003 Δ*isrR* containing the reporter fusions (Supplementary Tables S1 and S2).

Strains harboring fluorescent reporter fusions were tested on solid or liquid media. For solid media, strains were tested on BHI plates supplemented or not with DIP. For liquid media, strains were grown overnight at 37°C under agitation in BHI supplemented or

not with DIP and chloramphenicol when necessary. Cultures were then washed three times with Phosphate-buffered saline (PBS, 1X) and fluorescence was measured with a microplate reader (CLARIOstar), using dichroic filters with excitation wavelength = 425 nm and emission wavelength = 525 nm. Fluorescence was normalized by subtracting the auto-fluorescence of the HG003 strain and normalizing all cultures to  $OD_{600}=1$ .

### **RNA preparation and transcriptome analysis**

Overnight cultures were diluted at  $OD_{600}=0.005$  in preheated BHI + DIP 0.5 mM (previously incubated for 30 min). Cells were grown at 37°C under agitation (200 rpm) until  $OD_{600}=1$  (exponential phase). 15 mL of culture were sampled and centrifuged (10min, 4500 rpm, 4°C), and pellets were frozen in liquid nitrogen before storage at -70°C until RNA extraction. Cell pellets were resuspended in 800  $\mu$ L of lysis buffer (sodium acetate 20 mM pH 5.5, SDS 0.5%, EDTA 1 mM) and transferred into 2 mL Lysing matrix B tubes (MP Biomedicals). Bacteria were lysed using a Fastprep (MP Biomedicals) with 3 cycles of 45s at a speed of 6.5 m/s separated by incubation on ice for 1 min between each cycle. Tubes were then centrifuged (15 min, 14000 rpm, 4°C) and the RNA was extracted from the aqueous phase using phenol/chloroform as described (21). 30  $\mu$ g RNA was treated using Turbo DNase I (Ambion) and purified using the RNA Clean-up and concentration kit (Norgen Biotek). RNA quality was assessed using an Agilent Bioanalyzer (Agilent Technologies).

Data were processed by a Snakemake workflow (22), with FastQC (v0.11.9) quality control, creation of an index from the genome of *S. aureus* NCTC 8325 Refseq NC\_007795.1, mapping of the reads onto the genome with Bowtie 2 (v2.4.1) (23), selection of the mapped reads with Samtools (v1.13) (24) and their counting by the FeatureCounts tool of the Subread package (v2.0.1) (25) on the coding sequences listed in genome annotation augmented with the list of sRNAs selected from a previous analysis (26), as well as differential gene expression analysis with the SARTools (v1.7.2) package (27) configured with the DESeq2 method (28). Volcano plots presenting fold-change vs significance were drawn using VolcanoR (29).

### **Electrophoretic mobility shift assay**

RNAs were transcribed from PCR products (for primers, see Supplementary Table S3) using T7 RNA polymerase and purified by ethanol precipitation. Wild-type alleles were generated from HG003 genomic DNA and mutated alleles from gBlock DNAs (Integrated DNA Technologies) containing the desired mutations. Gel-shift assays were performed as described (30) with modifications reported in (6).

### **Intracellular citrate quantification:**

Intracellular citrate concentration was measured using the Citrate Assay Kit (Abcam) following the manufacturer's protocol. With this kit, citrate is converted to pyruvate, the latter being quantified by a probe becoming intensely colored (570 nm).

## RESULTS

### **Iron sparing response regulator IsrR downregulates the amount of aconitase and of CcpE.**

Through CopraRNA software analysis, several putative targets of IsrR have been identified (6,7). Among these, three are associated with citrate metabolism: i) *citB* mRNA, which encodes aconitase (31), ii) *citM* mRNA, which encodes a putative transporter for citrate complexed with metal ions (32), and iii) *ccpE* which encodes a transcriptional activator of *citB* (12). These bioinformatics analyses also indicate that IsrR targeting these three substrates is a conserved feature in different staphylococcal species raising questions regarding the role of citrate in adapting to low-iron growth conditions.

IsrR is predicted by IntaRNA software (18) to associate with the 5' untranslated regions (UTRs) of these three mRNAs, with base-pairing occurring within the Shine-Dalgarno (SD) sequence for *citB* and *ccpE* mRNAs (Figures 1A and 1B). This suggests that IsrR may function as a negative regulator of *citB* and *ccpE* expression.

To investigate the potential effect of IsrR on *citB* and *ccpE* expression, we generated gene fusions, replacing the original genes with extended open reading frames expressing complete sequences along with a C-terminal Flag tag (Supplementary Table 1). The detection of Flag-tagged proteins using anti-Flag antibodies allowed us to estimate their expression levels, serving as a proxy for endogenous wild-type gene expression. Considering that the Flag peptide consists of only 8 amino acids and involves a modification of merely 24 nucleotides, we anticipate minimal or negligible effects on bacterial regulation or physiology. Subsequently, we integrated the *citB-flag* and *ccpE-flag* alleles into the chromosome of HG003, as well as its isogenic derivative HG003  $\Delta$ *isrR*, respectively. Aconitase deficient mutants have reduce growth yields when grown in rich aerated media (31); growth experiments comparing the *citB*<sup>+</sup>, *citB* (*citB*:Bursa) and *citB-flag* strains indicate that CitB-Flag is likely a functional aconitase (Figure S2). *ccpE* mutant prevent *citB* expression and expectedly also have an altered

growth yield in rich aerated media (33).

Western blot experiments revealed that the expression levels of CitB and CcpE in HG003 cultures cultivated in a nutrient-rich medium remained unaffected by the presence or absence of *isrR* as it was not expressed in iron-replete media. However, the presence of iron chelator 2,2'-dipyridyl (DIP) in the growth medium alleviates Fur repression leading to the induction of IsrR (6). Indeed, under DIP-containing conditions, we observed a significant decrease in the abundance of CitB-Flag (Figure 2A) and CcpE-Flag (Figure 2B) in the parental strain compared to its  $\Delta isrR$  derivative revealing that the presence of IsrR correlates with a decrease of CitB and CcpE.

### **IsrR does not affect mRNA quantities**

The accumulation of a specific sRNA typically leads to changes in the stability of its target mRNAs (34). As a result, a classic approach to identifying or confirming sRNA targets involves comparing the levels of specific mRNAs in the presence or absence of the studied sRNA (e.g. (35)). To support the activity of IsrR toward its citrate-related targets and to possibly find other IsrR targets, a transcriptomic analysis was conducted by comparing a parental strain with its  $\Delta isrR$  derivative. Notably, *isrR* is not expressed under standard rich media conditions, so the strains were cultivated in the presence of DIP, a potent inducer of *isrR* expression (6). These strains were cultivated in triplicate, harvested during the exponential growth phase, and total RNAs were extracted and subjected to sequencing using RNA-seq Illumina technology. Subsequent differential expression analysis using DE-seq2 (28) unveiled a surprising result: there were hardly any differentially expressed mRNAs between the parental strain and its  $\Delta isrR$  derivative, despite a marked difference in *isrR* expression levels (Figure 3, Table S4). Remarkably, only two genes, *mtlF* and *mhqD*, showed significant differential expression. However, further bioinformatics analysis did not confirm a putative IsrR/mRNA pairing suggesting an indirect effect of IsrR on these mRNAs. It is worth noting that IsrR has many putative targets, with some being confirmed (6,36). While the expression of these targets was detected, their levels remained unaffected by the presence or absence of

IsrR. This observation contrasts with the typical behavior seen in Gram-negative bacteria, where the regulatory activity of a sRNA often influences the quantity and stability of its target mRNAs [examples also exist in *S. aureus* (37)]. However, our present transcriptomic results are supported by our previous observation that IsrR inhibits the translation of *fdhA* and *gltB2* mRNAs without impacting their stability (6). These findings challenge conventional assumptions about sRNA-mediated regulation and highlights the regulatory mechanisms at play in Gram positive bacteria and more specifically in the case of IsrR.

### **IsrR targets *citB* and *ccpE* 5'UTRs**

Biocomputing data suggest that the observed IsrR-dependent downregulation of CcpE and CitB is due to posttranscriptional regulations. However, the reduced amount of aconitase could be either direct (via post-transcriptional regulation), indirect (via a reduction of CcpE) or a combination of both. To address the question of putative IsrR direct regulation on these two substrates, the *ccpE* and *citB* 5'UTR sequences were disconnected from their endogenous transcriptional regulation. The sequences corresponding to the 5'UTRs from their transcriptional start sites (TSS) to their 13<sup>th</sup> first codons were positioned under the transcriptional control of the P<sub>sarA1</sub> promoter. We used a reporter fusion to evaluate *ccpE* and *citB* expression by inserting the fluorescent protein mAmetrine gene (*mAm*) downstream and in frame with the beginning of each ORF (Figure S3). To avoid issues associated with cloned genes on plasmids, we inserted the reporter fusions on the chromosome into a neutral locus (20) of the two *S. aureus* strains, HG003 and its isogenic derivative HG003  $\Delta$ *isrR*.

In a rich medium, the fluorescence of each reporter was similar in both strains either on plates and in liquid (Figure 4). Indeed, the *isrR* gene is repressed by the ferric uptake regulator Fur and therefore not expressed when iron is available. However, when DIP was added to the growth medium, mAmetrine fluorescence was strongly reduced in HG003 but not in HG003  $\Delta$ *isrR* with both reporters (Figure 4). These results strongly support the posttranscriptional regulation of *ccpE* and *citB* by IsrR. They also confirm

that the IsrR-dependent down-regulation of *citB* is not solely due to a reduction of CcpE activity but involves likely an activity of IsrR on *citB* mRNA.

### **IsrR CRRs are required for translational regulation of *ccpE* and *citB* mRNAs**

To obtain further information on which part of IsrR was required for IsrR activity against *ccpE* and *citB* mRNAs, we transformed the HG003  $\Delta$ *isrR* strains containing the reporter fusions with plasmids leading to the production of no IsrR, IsrR and mutated IsrRs with different CRR deletions. Notably, *isrR* was cloned under the promoter tet ( $P_{tet}$ ) in the absence of the Tet repressor (TetR) and is therefore expressed with no inducer. The endogenous *isrR* gene is controlled by two Fur boxes including one within the beginning of the transcribed sequence (6). Consequently, the second Fur box is present in all *isrR* engineered genes. Therefore, to alleviate any Fur repression, the experiments were performed in the presence of DIP.

The fluorescence of  $\Delta$ *isrR* strain containing the *citB* 5'UTR reporter fusion was strongly reduced by the presence of a plasmid expressing IsrR (pRMC2 $\Delta$ R-IsrR) as compared to a controlled plasmid (pRMC2 $\Delta$ R) or a plasmid expressing IsrR with no CRR motif (pRMC2 $\Delta$ R-IsrR $\Delta$ C1C2C3). However, the deletion of the *isrR* CRR1 (pRMC2 $\Delta$ R-IsrR $\Delta$ C1) and CRR2 (pRMC2 $\Delta$ R-IsrR $\Delta$ C2) did not significantly affect IsrR activity against the *citB* 5'UTR reporter, suggesting that these motifs are not essential for this IsrR activity, or alternatively, they could substitute for each other. In contrast, the deletion of CRR3 alone (pRMC2 $\Delta$ R-IsrR $\Delta$ C3) or in combination with other CRRs (pRMC2 $\Delta$ R-IsrR $\Delta$ C1C3, pRMC2 $\Delta$ R-IsrR $\Delta$ C2C3) led to a moderate reduction of IsrR activity, but the deletion of both CRR1 and CRR2 (pRMC2 $\Delta$ R-IsrR $\Delta$ C1C2) led to a strong mAmetrine fluorescence (Figure 5A). Taken together, these results suggest that both CRR1 and CRR2 can down-regulate *citB* mRNA translation independently. This conclusion is supported by IntaRNA results predicting two IsrR/*citB* mRNA pairings, one involving CRR1 and the other CRR2 and CRR3 (Figure 1). We previously observed a similar situation where the two CRRs of the staphylococcal sRNA RsaE could act independently on *rocF* mRNA

(38). The moderate reduction associated with the absence of CRR3 in IsrR may be due to a reduced amount of IsrR $\Delta$ C3 compared to IsrR, IsrR $\Delta$ C1, and IsrR $\Delta$ C2, as reported (6).

To assess which region of IsrR was important for interaction with *ccpE* mRNA, we performed an experiment similar to that described above, transforming the  $\Delta$ *isrR* strain containing the *ccpE* 5'UTR reporter fusion with plasmids expressing IsrR or mutated IsrR derivatives. As the fluorescence signal from the *ccpE* 5'UTR reporter fusion was too weak to be observed on plates, measurements were made only using a microplate reader. Removal of CRR1 from IsrR prevented IsrR activity towards *ccpE* mRNA, while deletion of CRR2 and CRR3 had no effects (Figure 5B). These results are in line with bioinformatics predictions indicating a pairing with the CCR1 (Figure 1).

To further support or in vivo experiment, the binding of IsrR to *citB* and *ccpE* mRNAs was tested by electrophoretic mobility shift assay (EMSA). A band-shift of radio-labeled IsrR was observed when IsrR was incubating with either *citB* or *ccpE* mRNAs. Also, when a similar experiment was performed using an IsrR mutant in which the Cs of the CRR sequence were mutated to prevent the pairing, no gel shifts were observed (Figure 1C).

Overall, in vivo and in vitro data indicate that IsrR binds, via specific CRRs, to the Shine-Dalgarno sequences of *citB* and *ccpE* mRNAs to prevent translation.

### **Aconitase moonlighting activity down-regulates the TCA cycle and rebalance its metabolic consequence.**

Aconitase catalyzes the conversion of citrate to isocitrate; however, a conserved feature from bacteria to humans is the ability of aconitase to become an iron regulatory factor (IRF) by acquiring an RNA-binding protein (RBP) recognizing iron-responsive elements (IREs) when its Fe-S clusters are absent (9,10,43). We questioned if the RBP activity of the apo-protein was present in staphylococcal aconitase and could have a possible regulatory role in response to iron starvation. Essential amino acids for aconitase activities are conserved from bacteria to eukaryotes. In *B. subtilis*, aconitase mutation changing the cysteine 517 to alanine (CitB<sup>Bs</sup><sub>C517A</sub>) leads to enzymatically inactive

aconitase which still binds to iron-responsive elements (IREs) while changing the arginine 741 and glutamine 745 to glutamic acid (Cit<sup>Bs</sup><sub>R741E Q745E</sub>) leads an aconitase defective only for its RBP activity (9,44). As *B. subtilis* and *S. aureus* aconitases share 71% identity, we modified the *S. aureus citB* gene to generate an aconitase deficient for its enzymatic activity, Cit<sup>Sa</sup><sub>C450S</sub> referred to as CitB<sub>ENZ</sub>, and for its RBP activity, Cit<sup>Sa</sup><sub>R734E Q738E</sub> referred to as CitB<sub>RBP</sub> (Figure S5). To keep the endogenous regulation and expression level, the mutated alleles were introduced into HG003 chromosomal *citB* locus by gene replacement (Table S1). The absence of aconitase leads to an altered growth in stationary phase and citrate accumulation ((45) and Figure S5). As expected, the enzymatically deficient *citB*<sub>ENZ</sub> allele was responsible for an altered growth in rich media and for the accumulation of intracellular citrate, similar to a strain having no aconitase. However, in a rich medium, the *citB*<sub>RBP</sub> allele had a similar growth yield and citrate amount as the parental strain (Figures S6 and S7).

To support the putative RNA-binding deficiency of the *citB*<sub>RBP</sub> strain, and to possibly find targets of apo-aconitase, we compared the transcriptome of HG003 and its *citB*<sub>RBP</sub> derivative. As the RBP activity is revealed only in iron-restricted growth conditions, both strains were grown in the presence of DIP. Similarly to the experiments with the  $\Delta$ *isrR* mutant (Figure 3), the two strains were cultivated in triplicate, harvested during the exponential growth phase, and total RNAs were extracted and subjected to sequencing using RNA-seq Illumina technology. Note the experiments with the  $\Delta$ *isrR* and *citB*<sub>RBP</sub> mutants were done simultaneously and used the same parental strain reference. Subsequent differential expression analysis using DE-seq2 (28) highlights a striking upregulation of *citB* and *citZ-citC* mRNAs in the *citB*<sub>RBP</sub> mutant (Figure 6, Table S5). The *citB*<sub>RBP</sub> mutant, which has an efficient aconitase activity in a rich medium (Figures S6 and S7) prevents the downregulation of genes encoding citrate synthase (*citZ*), aconitase, and isocitrate dehydrogenase (*citC*). These three enzymes act one after the other one in the TCA cycle. This result first shows that the *citB*<sub>RBP</sub> mutation alters gene expression supporting the aconitase RBP activity (9,46). It shows, as observed in human

and few bacteria(9,47), that *S. aureus* aconitase is autoregulated by lowering the amount of its own mRNA *citB* but also the *citZ-citC* operon mRNA.

*pycA* mRNA encoding the pyruvate carboxylase was significantly under-represented in the *citB*<sub>RBP</sub> strain showing that during iron-starvation, this mRNA accumulates in a wild-type strain. PycA catalyzes the carboxylation of pyruvate to form oxaloacetate. Iron starvation leads to the TCA cycle downregulation and consequently lower oxaloacetate production. We propose that the apo-aconitase, by stabilizing *pycA* mRNA, contributes to maintaining the oxaloacetate pool (Figure 6B).

### **IsrR-dependent downregulation of *citB* mRNA is not dependent on moonlighting aconitase activity**

In *E. coli*, RyhB, a non-ortholog sRNA with a similar function to IsrR, targets *acnB* mRNA encoding one of its two aconitases. The regulatory mechanism involves the apo-aconitase RBP activity, which prevents the RyhB-induced degradation of *acnB* mRNA (47). We, therefore, questioned if the *S. aureus* aconitase RBP activity could interfere with the IsrR-dependent regulation of aconitase.

To test this hypothesis, in addition to the parental strain, we introduced the *citB*<sub>RBP</sub> allele into the isogenic  $\Delta$ *isrR* strain. Two *citB*<sub>RBP</sub> alleles were constructed, expressing either the CitB natural C-terminal end or the end fused to a Flag tag. The amount of CitB monitored by Western blot experiments with anti-Flag in  $\Delta$ *isrR* and its isogenic parental strain show that IsrR similarly downregulates *citB::flag* and *citB*<sub>RBP</sub>::*flag*, showing that the aconitase RBP function is likely not associated with the IsrR-dependent regulation of CitB (Figure 7). Furthermore, during iron starvation, *citB*<sub>RBP</sub>::*flag* is in a bigger amount than *citB::flag* by comparing either the two *isrR*<sup>+</sup> or  $\Delta$ *isrR* strains. This confirms that the inability of the *citB*<sub>RBP</sub> allele to downregulate its own transcript leads to the accumulation of its corresponding protein. Our results suggest that IsrR and apo-CitB act additively against *citB* mRNA.

## DISCUSSION

In response to iron-starved growth conditions, bacteria employ intricate regulatory mechanisms to optimize their survival and adapt to the challenging environment. One such adaptation involves the downregulation of iron-containing proteins, which is mediated by small non-coding RNAs induced upon iron starvation. These sRNAs, including RyhB in many Enterobacteriaceae (48), PrrFs in *Pseudomonas aeruginosa* (49), MrsI in *Mycobacterium tuberculosis* (50), IsaR1 in cyanobacterium *Synechocystis* (51), FsrA in *B. subtilis* (52) and IsrR in *S. aureus* (6), play a pivotal role in coordinating the reduction of iron-utilizing pathways, with a particular emphasis on the TCA cycle (5).

Aconitase, an abundant protein containing two [4Fe4S] clusters, stands out as a prominent iron consumer. It is no coincidence that aconitase mRNA is targeted by multiple sRNAs, including RyhB (47,48), and FsrA (53) due to its high iron demand. In this study, we uncover an additional regulatory role of IsrR in aconitase mRNA targeting, further expanding our understanding of bacterial iron homeostasis in *S. aureus*. The staphylococcal *citB* expression is activated by CcpE, a citrate-responsive transcriptional regulator controlling the expression of over 100 metabolic enzymes and virulence factors (54). The reduction of *citB* expression results in less aconitase leading to the accumulation of citrate (12) and Figure S7). This increase amount of citrate is expected to activate CcpE and consequently *citB* transcription, leading to a paradoxical situation where *citB* downregulation could lead via CcpE to its activation. In iron-starved conditions, by targeting both *citB* and *ccpE* mRNAs, IsrR prevents this loophole and maintains metabolic homeostasis. The regulatory pathway in which a three-node graph of the form A (IsrR) affects B (CcpE) and C (CitB) and B affects C is defined as a feedforward loop (Figure S8). This organization for gene control is frequent with the advantage to provide an additional input on the final regulation. As IsrR downregulates *citB* expression and of its transcriptional activator gene (*ccpE*), the loop is defined as coherent and of type 2 (55). Mathematical modeling indicates that if A is regulatory RNA as for IsrR rather than a transcriptional factor, the response to signal (accumulation

of IsrR upon iron starvation) is stronger and faster with minimized fluctuations in target protein concentrations (aconitase) (56). These properties gained with a sRNA-controlled feedforward loop are likely critical for *S. aureus* adaption to low iron growth conditions as those encountered within the host.

A third element contributing to aconitase regulation is the aconitase protein itself, which is highly conserved across species. Aconitase serves as an electron transfer donor through its [4Fe-4S] clusters, which are sensitive to iron starvation and oxidative damage. Both stress conditions can inactivate aconitase by disrupting these clusters. Oxidation of one of the [4Fe-4S] cluster into a [3Fe-4S] cluster leads to the formation of an enzymatically inactive aconitase, which is more prone to cluster disassembly, and therefore complete disappearing of the cluster (9,57). In the absence of iron, aconitase becomes an RNA-binding protein with regulatory capabilities. Mutations in the putative aconitase RBP site (CitB<sub>RBP</sub>) impair *citB* mRNA downregulation, as well as the *citZ-citC* operon, mirroring observations in *E. coli* and *B. subtilis* (9,44,47). Indeed, aconitase deficiency results in the absence of isocitrate production for the TCA cycle, rendering the synthesis of isocitrate dehydrogenase (CitC) and citrate synthase (CitZ) unnecessary.

The TCA cycle contributes to biosynthetic processes, with some of its products serving as precursors for various metabolic pathways. Anaplerotic reactions are essential for replenishing depleted elements in the TCA cycle, and among these, PycA emerges as a significant enzyme, facilitating the production of oxaloacetate (58). In addition to be a key metabolite of the TCA cycle, oxaloacetate is required for diverse biochemical pathways, including the glyoxylate cycle and amino acid synthesis. Disruptions in the levels of CitZ, CitB, and CitC adversely impact TCA-dependent oxaloacetate production. Our findings indicate that apo-aconitase plays a role in stabilizing *pycA* mRNA through a yet undiscovered mechanism. This stabilization is associated with an anticipated increase in pyruvate carboxylase activity and subsequent oxaloacetate production. Therefore, it appears that apo-aconitase, through its modulation of *pycA* mRNA

stability, contributes to the maintenance of the oxaloacetate pool for supporting various essential biochemical processes.

Apo-aconitase has been shown to bind to IREs which are stem-loop sequences with the conserved CAGUGN sequence inside the loop (9,43,46). Such a structure has not been detected in the above-mentioned main apo-aconitase substrates; their *S. aureus* equivalent remained to be found.

Our results demonstrate that *S. aureus* uses multifaceted mechanisms to adapt to iron-starved environments highlighting a complex interplay between post-transcriptional regulatory elements and metabolic pathways (Figure 8).

## REFERENCES

1. Murdoch, C.C. and Skaar, E.P. (2022) Nutritional immunity: the battle for nutrient metals at the host-pathogen interface. *Nat Rev Microbiol*, **20**, 657-670.
2. Troxell, B. and Hassan, H.M. (2013) Transcriptional regulation by Ferric Uptake Regulator (Fur) in pathogenic bacteria. *Front Cell Infect Microbiol*, **3**, 59.
3. Pinochet-Barros, A. and Helmann, J.D. (2018) Redox Sensing by Fe(2+) in Bacterial Fur Family Metalloregulators. *Antioxid Redox Signal*, **29**, 1858-1871.
4. Dutta, T. and Srivastava, S. (2018) Small RNA-mediated regulation in bacteria: A growing palette of diverse mechanisms. *Gene*, **656**, 60-72.
5. Chareyre, S. and Mandin, P. (2018) Bacterial iron homeostasis regulation by sRNAs. *Microbiol Spectr*, **6**.
6. Coronel-Tellez, R.H., Pospiech, M., Barrault, M., Liu, W., Bordeau, V., Vasnier, C., Felden, B., Sargueil, B. and Bouloc, P. (2022) sRNA-controlled iron sparing response in Staphylococci. *Nucleic Acids Research*, **50**, 8529-8546.
7. Mader, U., Nicolas, P., Depke, M., Pane-Farre, J., Debarbouille, M., van der Kooi-Pol, M.M., Guerin, C., Derozier, S., Hiron, A., Jarmer, H. *et al.* (2016) *Staphylococcus aureus* transcriptome architecture: from laboratory to infection-mimicking conditions. *PLoS Genet*, **12**, e1005962.
8. Walden, W.E. (2002) From bacteria to mitochondria: aconitase yields surprises. *Proc Natl Acad Sci U S A*, **99**, 4138-4140.
9. Pechter, K.B., Meyer, F.M., Serio, A.W., Stulke, J. and Sonenshein, A.L. (2013) Two roles for aconitase in the regulation of tricarboxylic acid branch gene expression in *Bacillus subtilis*. *J Bacteriol*, **195**, 1525-1537.
10. Tang, Y. and Guest, J.R. (1999) Direct evidence for mRNA binding and post-transcriptional regulation by *Escherichia coli* aconitases. *Microbiology (Reading)*, **145 ( Pt 11)**, 3069-3079.
11. Chen, J., Shang, F., Wang, L., Zou, L., Bu, T., Jin, L., Dong, Y., Ha, N.C., Quan, C., Nam, K.H. *et al.* (2018) Structural and Biochemical Analysis of the Citrate-Responsive Mechanism of the Regulatory Domain of Catabolite Control Protein E from *Staphylococcus aureus*. *Biochemistry*, **57**, 6054-6060.
12. Hartmann, T., Baronian, G., Nippe, N., Voss, M., Schulthess, B., Wolz, C., Eisenbeis, J., Schmidt-Hohagen, K., Gaupp, R., Sunderkotter, C. *et al.* (2014) The catabolite control protein E (CcpE) affects virulence determinant production and pathogenesis of *Staphylococcus aureus*. *J Biol Chem*, **289**, 29701-29711.
13. Herbert, S., Ziebandt, A.K., Ohlsen, K., Schafer, T., Hecker, M., Albrecht, D., Novick, R. and Gotz, F. (2010) Repair of global regulators in *Staphylococcus aureus* 8325 and comparative analysis with other clinical isolates. *Infect Immun*, **78**, 2877-2889.
14. Fuchs, S., Mehlan, H., Bernhardt, J., Hennig, A., Michalik, S., Surmann, K., Pane-Farre, J., Giese, A., Weiss, S., Backert, L. *et al.* (2018) AureoWiki the repository of the *Staphylococcus aureus* research and annotation community. *International Journal of Medical Microbiology*, **308**, 558-568.
15. Gibson, D.G. (2011) Enzymatic assembly of overlapping DNA fragments. *Methods in Enzymology*, **498**, 349-361.
16. Monk, I.R., Tree, J.J., Howden, B.P., Stinear, T.P. and Foster, T.J. (2015) Complete bypass of restriction systems for major *Staphylococcus aureus* lineages. *MBio*, **6**, e00308-00315.

17. Le Lam, T.N., Morvan, C., Liu, W., Bohn, C., Jaszczyszyn, Y. and Bouloc, P. (2017) Finding sRNA-associated phenotypes by competition assays: An example with *Staphylococcus aureus*. *Methods*, **117**, 21-27.
18. Mann, M., Wright, P.R. and Backofen, R. (2017) IntaRNA 2.0: enhanced and customizable prediction of RNA-RNA interactions. *Nucleic Acids Research*, **45**, W435-W439.
19. Prados, J., Linder, P. and Redder, P. (2016) TSS-EMOTE, a refined protocol for a more complete and less biased global mapping of transcription start sites in bacterial pathogens. *BMC Genomics*, **17**, 849.
20. de Jong, N.W., van der Horst, T., van Strijp, J.A. and Nijland, R. (2017) Fluorescent reporters for markerless genomic integration in *Staphylococcus aureus*. *Sci Rep*, **7**, 43889.
21. Oh, E.T. and So, J.S. (2003) A rapid method for RNA preparation from Gram-positive bacteria. *J Microbiol Methods*, **52**, 395-398.
22. Koster, J. and Rahmann, S. (2018) Snakemake-a scalable bioinformatics workflow engine. *Bioinformatics*, **34**, 3600.
23. Langmead, B. and Salzberg, S.L. (2012) Fast gapped-read alignment with Bowtie 2. *Nat Methods*, **9**, 357-359.
24. Li, H., Handsaker, B., Wysoker, A., Fennell, T., Ruan, J., Homer, N., Marth, G., Abecasis, G. and Durbin, R. (2009) The Sequence Alignment/Map format and SAMtools. *Bioinformatics*, **25**, 2078-2079.
25. Liao, Y., Smyth, G.K. and Shi, W. (2014) featureCounts: an efficient general purpose program for assigning sequence reads to genomic features. *Bioinformatics*, **30**, 923-930.
26. Liu, W., Rochat, T., Toffano-Nioche, C., Le Lam, T.N., Bouloc, P. and Morvan, C. (2018) Assessment of Bona Fide sRNAs in *Staphylococcus aureus*. *Frontiers in Microbiology*, **9**, 228.
27. Danecek, P., Bonfield, J.K., Liddle, J., Marshall, J., Ohan, V., Pollard, M.O., Whitwham, A., Keane, T., McCarthy, S.A., Davies, R.M. *et al.* (2021) Twelve years of SAMtools and BCFtools. *Gigascience*, **10**.
28. Love, M.I., Huber, W. and Anders, S. (2014) Moderated estimation of fold change and dispersion for RNA-seq data with DESeq2. *Genome Biology*, **15**.
29. Goedhart, J. and Luijsterburg, M.S. (2020) VolcaNoseR is a web app for creating, exploring, labeling and sharing volcano plots. *Sci Rep*, **10**, 20560.
30. Le Huyen, K.B., Gonzalez, C.D., Pascreau, G., Bordeau, V., Cattoir, V., Liu, W., Bouloc, P., Felden, B. and Chabelskaya, S. (2021) A small regulatory RNA alters *Staphylococcus aureus* virulence by titrating RNAIII activity. *Nucleic Acids Research*, **49**, 10644-10656.
31. Somerville, G.A., Chaussee, M.S., Morgan, C.I., Fitzgerald, J.R., Dorward, D.W., Reitzer, L.J. and Musser, J.M. (2002) *Staphylococcus aureus* aconitase inactivation unexpectedly inhibits post-exponential-phase growth and enhances stationary-phase survival. *Infect Immun*, **70**, 6373-6382.
32. Krom, B.P., Warner, J.B., Konings, W.N. and Lolkema, J.S. (2000) Complementary metal ion specificity of the metal-citrate transporters CitM and CitH of *Bacillus subtilis*. *J Bacteriol*, **182**, 6374-6381.
33. Hartmann, T., Zhang, B., Baronian, G., Schulthess, B., Homerova, D., Grubmuller, S., Kutzner, E., Gaupp, R., Bertram, R., Powers, R. *et al.* (2013) Catabolite control protein E (CcpE) is a LysR-type transcriptional regulator of tricarboxylic acid cycle activity in

- Staphylococcus aureus*. *J Biol Chem*, **288**, 36116-36128.
34. Chao, Y., Li, L., Girodat, D., Forstner, K.U., Said, N., Corcoran, C., Smiga, M., Papenfort, K., Reinhardt, R., Wieden, H.J. *et al.* (2017) In vivo cleavage map illuminates the central role of RNase E in coding and non-coding RNA pathways. *Mol Cell*, **65**, 39-51.
  35. Bohn, C., Rigoulay, C., Chabelskaya, S., Sharma, C.M., Marchais, A., Skorski, P., Borezee-Durant, E., Barbet, R., Jacquet, E., Jacq, A. *et al.* (2010) Experimental discovery of small RNAs in *Staphylococcus aureus* reveals a riboregulator of central metabolism. *Nucleic Acids Res*, **38**, 6620-6636.
  36. Barrault, M., Leclair, E. and Bouloc, P. (2023) Staphylococcal sRNA IsrR down-regulates methylthiotransferase MiaB under iron-deficient conditions. *bioRxiv*, 2023.2011.2009.566390.
  37. Bonnin, R.A. and Bouloc, P. (2015) RNA Degradation in *Staphylococcus aureus*: Diversity of Ribonucleases and Their Impact. *International Journal of Genomics*, **2015**, 395753.
  38. Rochat, T., Bohn, C., Morvan, C., Le Lam, T.N., Razvi, F., Pain, A., Toffano-Nioche, C., Ponien, P., Jacq, A., Jacquet, E. *et al.* (2018) The conserved regulatory RNA RsaE down-regulates the arginine degradation pathway in *Staphylococcus aureus*. *Nucleic Acids Res*, **46**, 8803-8816.
  39. Ding, X., Robbe-Masselot, C., Fu, X., Leonard, R., Marsac, B., Dauriat, C.J.G., Lepissier, A., Rytter, H., Ramond, E., Dupuis, M. *et al.* (2023) Airway environment drives the selection of quorum sensing mutants and promote *Staphylococcus aureus* chronic lifestyle. *Nat Commun*, **14**, 8135.
  40. Kalivoda, K.A., Steenbergen, S.M., Vimr, E.R. and Plumbridge, J. (2003) Regulation of sialic acid catabolism by the DNA binding protein NanR in *Escherichia coli*. *J Bacteriol*, **185**, 4806-4815.
  41. Olson, M.E., King, J.M., Yahr, T.L. and Horswill, A.R. (2013) Sialic acid catabolism in *Staphylococcus aureus*. *J Bacteriol*, **195**, 1779-1788.
  42. Sohanpal, B.K., El-Labany, S., Lahooti, M., Plumbridge, J.A. and Blomfield, I.C. (2004) Integrated regulatory responses of *fimB* to N-acetylneuraminic (sialic) acid and GlcNAc in *Escherichia coli* K-12. *Proc Natl Acad Sci U S A*, **101**, 16322-16327.
  43. Hirling, H., Henderson, B.R. and Kuhn, L.C. (1994) Mutational analysis of the [4Fe-4S]-cluster converting iron regulatory factor from its RNA-binding form to cytoplasmic aconitase. *EMBO J*, **13**, 453-461.
  44. Gao, W., Dai, S., Liu, Q., Xu, H., Bai, Y. and Qiao, M. (2010) Effect of site-directed mutagenesis of *citB* on the expression and activity of *Bacillus subtilis* aconitase. *Mikrobiologiya*, **79**, 774-778.
  45. Craig, J.E., Ford, M.J., Blaydon, D.C. and Sonenshein, A.L. (1997) A null mutation in the *Bacillus subtilis* aconitase gene causes a block in Spo0A-phosphate-dependent gene expression. *J Bacteriol*, **179**, 7351-7359.
  46. Tang, Y. and Guest, J.R. (1999) Direct evidence for mRNA binding and post-transcriptional regulation by *Escherichia coli* aconitases. *Microbiology*, **145 ( Pt 11)**, 3069-3079.
  47. Benjamin, J.A. and Masse, E. (2014) The iron-sensing aconitase B binds its own mRNA to prevent sRNA-induced mRNA cleavage. *Nucleic Acids Research*, **42**, 10023-10036.
  48. Masse, E. and Gottesman, S. (2002) A small RNA regulates the expression of genes involved in iron metabolism in *Escherichia coli*. *Proc Natl Acad Sci U S A*, **99**, 4620-4625.
  49. Wilderman, P.J., Sowa, N.A., FitzGerald, D.J., FitzGerald, P.C., Gottesman, S., Ochsner,

- U.A. and Vasil, M.L. (2004) Identification of tandem duplicate regulatory small RNAs in *Pseudomonas aeruginosa* involved in iron homeostasis. *Proc Natl Acad Sci U S A*, **101**, 9792-9797.
50. Gerrick, E.R., Barbier, T., Chase, M.R., Xu, R., Francois, J., Lin, V.H., Szucs, M.J., Rock, J.M., Ahmad, R., Tjaden, B. *et al.* (2018) Small RNA profiling in *Mycobacterium tuberculosis* identifies Mrsl as necessary for an anticipatory iron sparing response. *Proc Natl Acad Sci U S A*, **115**, 6464-6469.
51. Georg, J., Kostova, G., Vuorijoki, L., Schon, V., Kadowaki, T., Huokko, T., Baumgartner, D., Muller, M., Klahn, S., Allahverdiyeva, Y. *et al.* (2017) Acclimation of oxygenic photosynthesis to iron starvation is controlled by the sRNA IsaR1. *Curr Biol*, **27**, 1425-1436 e1427.
52. Smaldone, G.T., Antelmann, H., Gaballa, A. and Helmann, J.D. (2012) The FsrA sRNA and FbpB protein mediate the iron-dependent induction of the *Bacillus subtilis* lutABC iron-sulfur-containing oxidases. *Journal of Bacteriology*, **194**, 2586-2593.
53. Smaldone, G.T., Revelles, O., Gaballa, A., Sauer, U., Antelmann, H. and Helmann, J.D. (2012) A global investigation of the *Bacillus subtilis* iron-sparing response identifies major changes in metabolism. *J Bacteriol*, **194**, 2594-2605.
54. Ding, Y., Liu, X., Chen, F., Di, H., Xu, B., Zhou, L., Deng, X., Wu, M., Yang, C.G. and Lan, L. (2014) Metabolic sensor governing bacterial virulence in *Staphylococcus aureus*. *Proc Natl Acad Sci U S A*, **111**, E4981-4990.
55. Alon, U. (2007) Network motifs: theory and experimental approaches. *Nat Rev Genet*, **8**, 450-461.
56. Tej, S., Gaurav, K. and Mukherji, S. (2019) Small RNA driven feed-forward loop: critical role of sRNA in noise filtering. *Phys Biol*, **16**, 046008.
57. Imlay, J.A. (2006) Iron-sulphur clusters and the problem with oxygen. *Mol Microbiol*, **59**, 1073-1082.
58. Owen, O.E., Kalhan, S.C. and Hanson, R.W. (2002) The key role of anaplerosis and cataplerosis for citric acid cycle function. *J Biol Chem*, **277**, 30409-30412.

## **SUPPLEMENTARY DATA**

Supplementary Data are available online.

## **ACKNOWLEDGEMENT**

We thank our lab colleagues for helpful discussions, technical help, and Edel Weiss for warm support. We acknowledge the sequencing and bioinformatics expertise of the I2BC High-throughput sequencing facility, supported by France Génomique (funded by the French National Program "Investissement d'Avenir" ANR-10-INBS-09).

## **FUNDING**

The research was supported by the "Agence National pour la Recherche" [ANR-19-CE12-0006-01 (sRNA-RRARE)]. MB was the recipient of a scholarship from the 'SDSV' (Structure et dynamique des systèmes vivants) doctoral school. R.H.C.T. was the recipient of a scholarship from the 'Consejo Nacional de Ciencia y Tecnología' (CONACyT).

## **CONFLICT OF INTEREST**

The authors declare no competing interests.

## **AUTHOR CONTRIBUTIONS**

PB conceived the project. MB, SC, RHCT, CTN and PB designed experiments and interpreted the data. MB and PB wrote the manuscript. MB, RHCT, SC, CTN, and PB edited the paper.

## **AVAILABILITY**

Strains and plasmids are available from the corresponding author on request.

## FIGURES

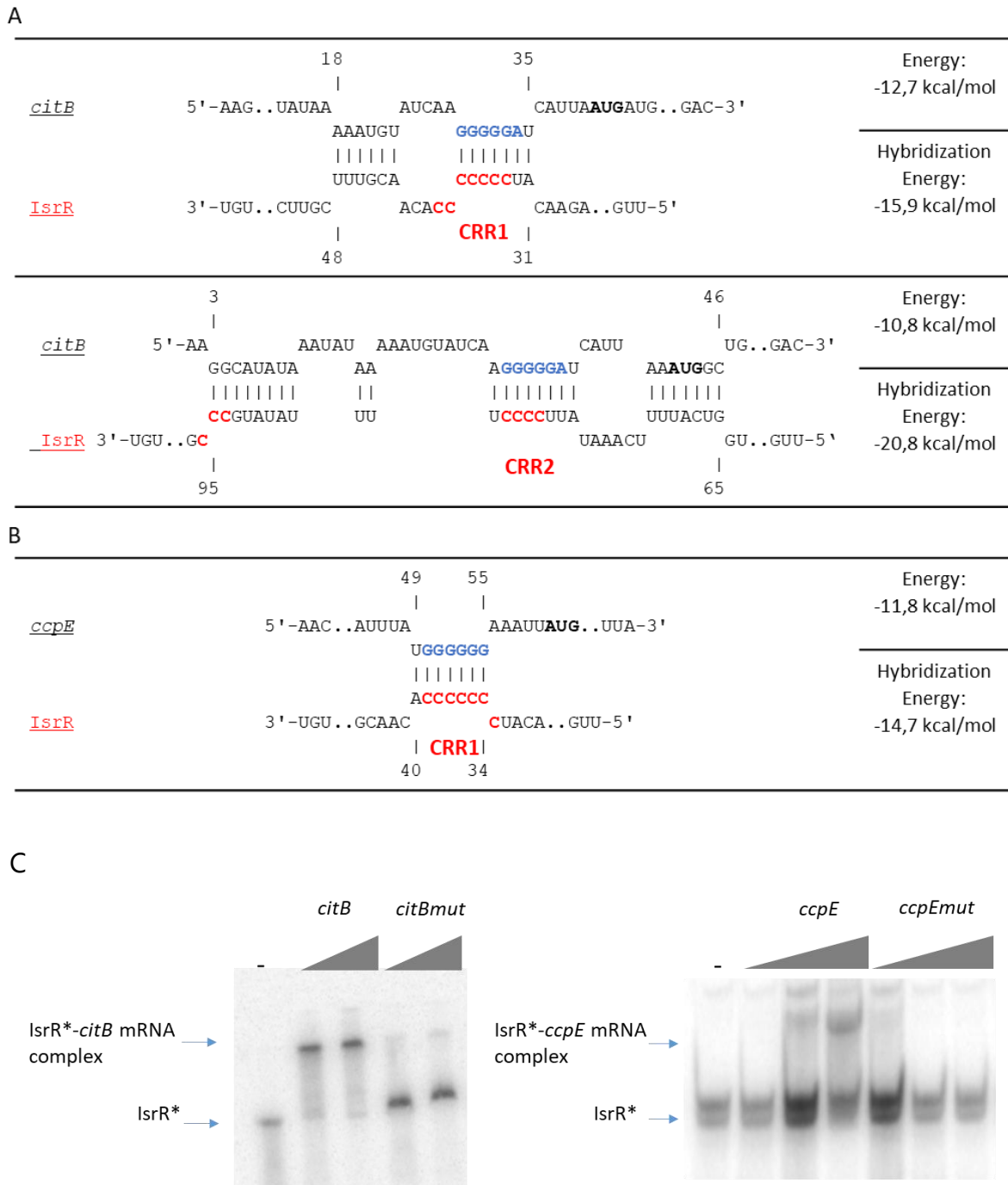


**Figure 1: Computer prediction of IsrR pairing with *citB* and *ccpE* mRNAs**

IntaRNA (18) pairing prediction A) between IsrR and *citB* mRNA, and B) between IsrR and *ccpE* mRNA. Blue sequences, SD; red sequences, CRRs; bold characters, AUG start codon. C: Gel retardation assay using radiolabeled IsrR (IsrR\*) with *citB* mRNA (left) and *ccpE* mRNA (right). RNA sequences used for gel retardation are indicated in **Figure S1**.



non-specific signal at 35kDa is also present in Flag-less strains. Below right: Histograms, ratios of *ccpE* reporter fusion production between HG003 and  $\Delta isrR$  determined as in A). \*\*\*, P-value= 0.0002.

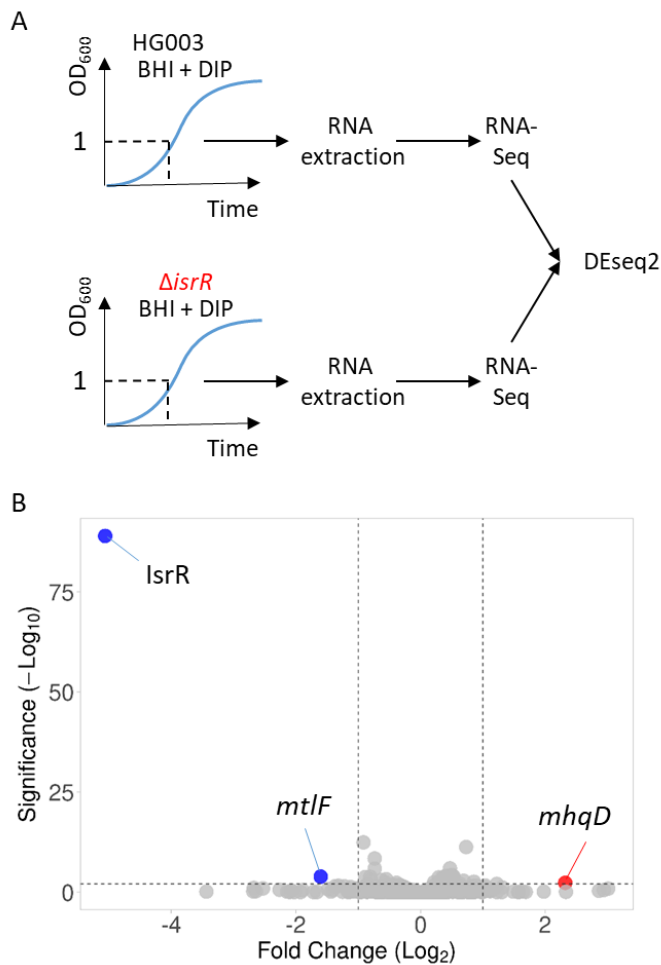


**Figure 3: RNAs significantly affected by the absence of IsrR**

A) Experimental workflow: Schematic representation of the transcriptomic experiments. HG003 and its  $\Delta isrR$  derivative were cultured overnight, followed by resuspension in fresh BHI medium supplemented with DIP. Samples were collected at an  $OD_{600}$  of 1 and RNA was extracted. Subsequently, Illumina RNA sequencing was performed, and the resulting data were analyzed using DESeq2 software. B) Volcano plot depicting significant differences in gene expression between the HG003 strain and its  $\Delta isrR$  derivative during iron starvation. Genes with reduced expression in the  $\Delta isrR$  strain are shown in blue, while those with increased expression are displayed in red. Colored spots correspond to genes with a fold-change  $< 0.5$  or  $> 2$ , a significance level with a P-adjusted value below 0.005. The analysis includes the genes with a minimum of 20 reads across at least one condition (n=3).

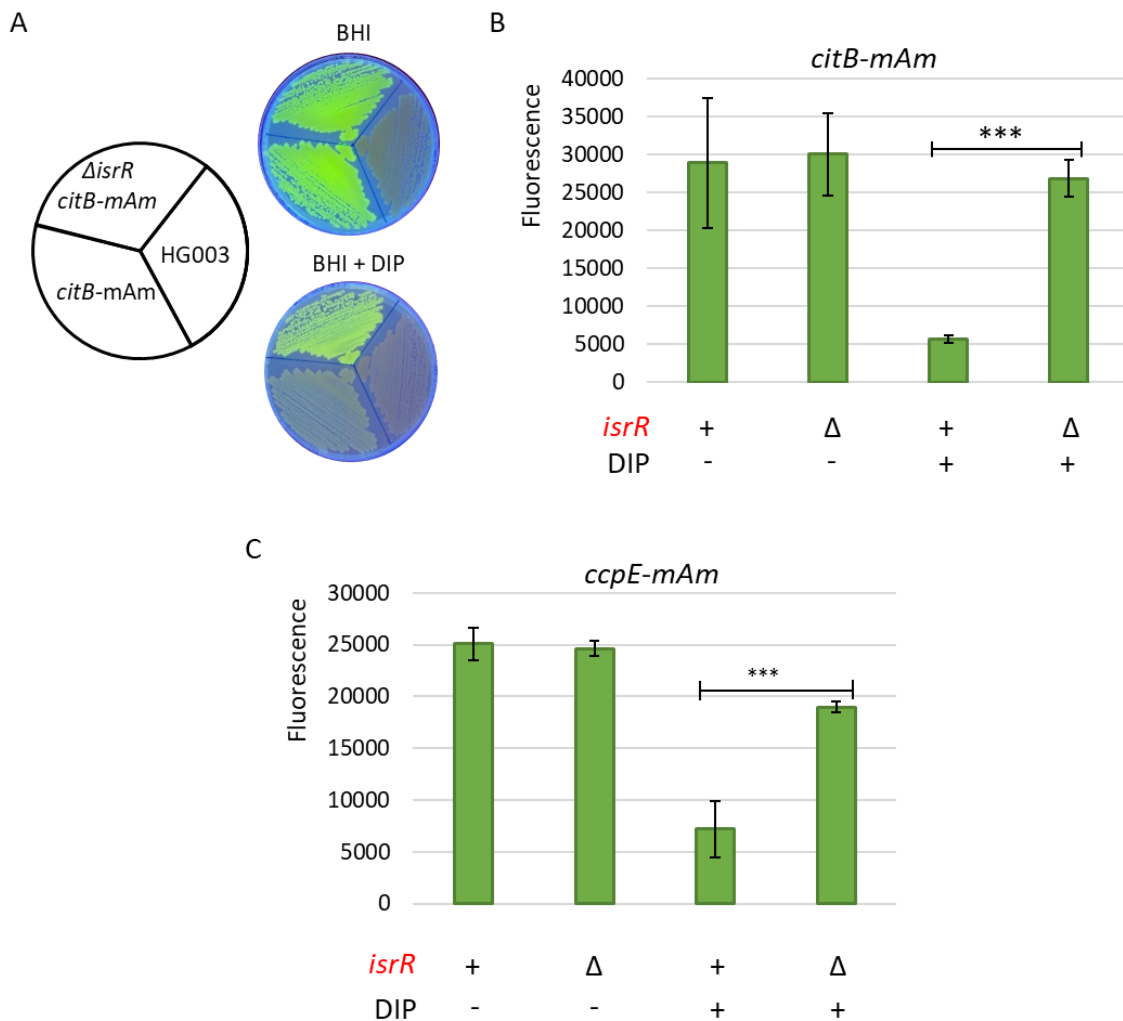


**Figure 4: Translational repression of *citB* and *ccpE* reporter by *IsrR***

A) *citB-mAm* expression on BHI and BHI supplemented with DIP plates. The relevant genotypes are indicated. B) *citB-mAm* reporter gene expression was quantified by growing overnight HG003 and  $\Delta$ *ISR* derivative harboring the fusion in BHI and BHI supplemented with DIP broths, washing them, and measuring their fluorescence on a microplate reader. Results are normalized to  $OD_{600} = 1$  ( $n = 3$ ). P-value =  $1.62 \cdot 10^{-5}$ . C) The translational activity of the *ccpE-mAm* reporter gene was quantified by growing overnight HG003 and its  $\Delta$ *ISR* derivative harboring the fusion in BHI and BHI supplemented with DIP 0.5, washing them, and measuring their fluorescence on a microplate reader. Results are normalized to  $OD_{600} = 1$  ( $n = 3$ ). P-value =  $4.7 \cdot 10^{-4}$ . The fluorescence of CcpE-mAm reporter fusions was not visible on plates.

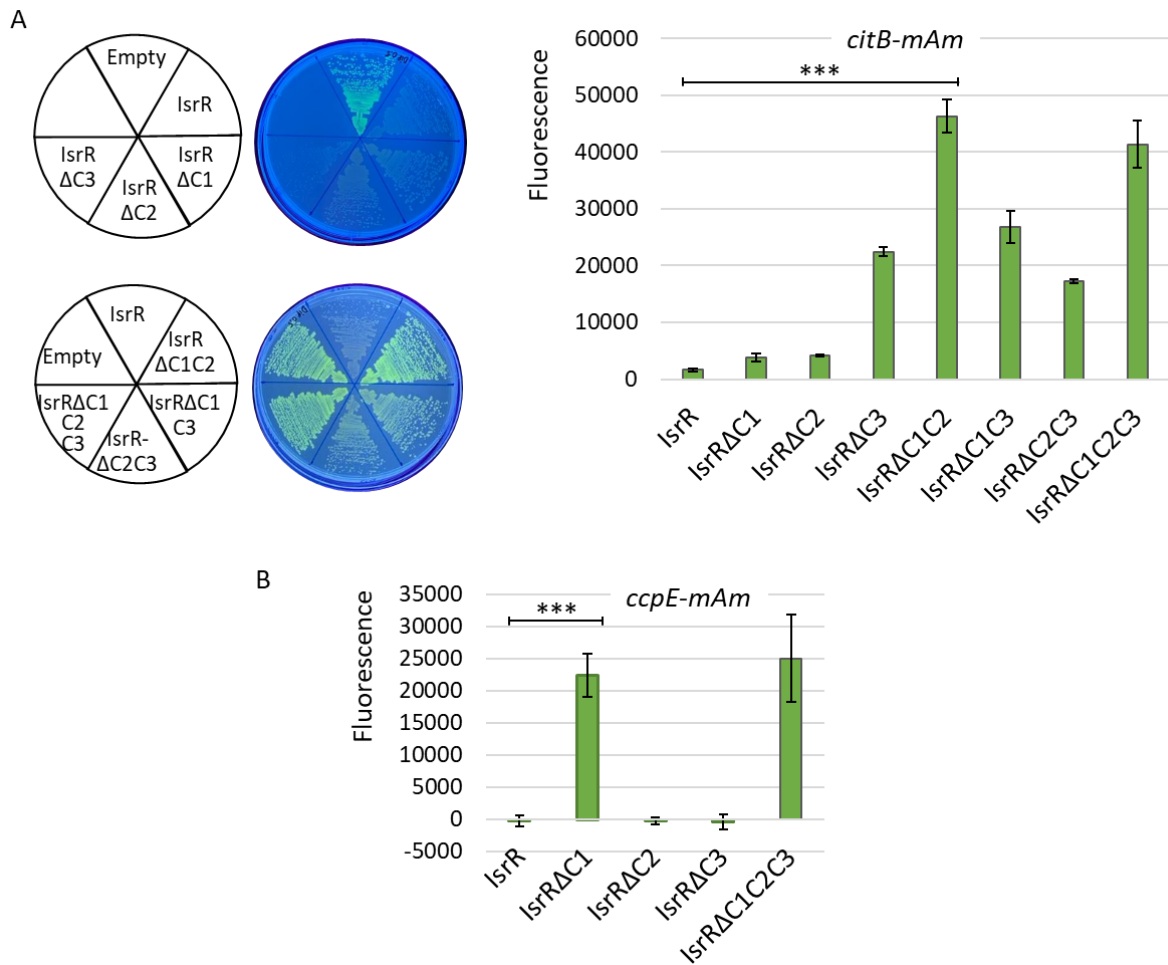


**Figure 5: IsrR CRRs required for the translational repression of *citB* and *ccpE* reporters**

A) The  $\Delta isrR$  strain harboring the *citB-mAm* reporter fusion was transformed with plasmids expressing different versions of IsrR and cultured in plates (left) or in liquid (right) in BHI supplemented with DIP. The translational activity of the *citB-mAm* reporter fusion was quantified by measuring the fluorescence of each strain on a microplate reader. Results (n=3) are normalized to  $OD_{600}=1$ . P-value= $1.1 \cdot 10^{-6}$ . B) The  $\Delta isrR$  strain harboring the *ccpE-mAm* reporter fusion was transformed with plasmids expressing different versions of IsrR and cultured overnight in BHI supplemented with DIP. The translational activity of the *ccpE-mAm* reporter fusion was quantified by measuring the fluorescence of each strain on a microplate reader. Results (n=3) are normalized to  $OD_{600}=1$ . P-value= $4.3 \cdot 10^{-5}$ .

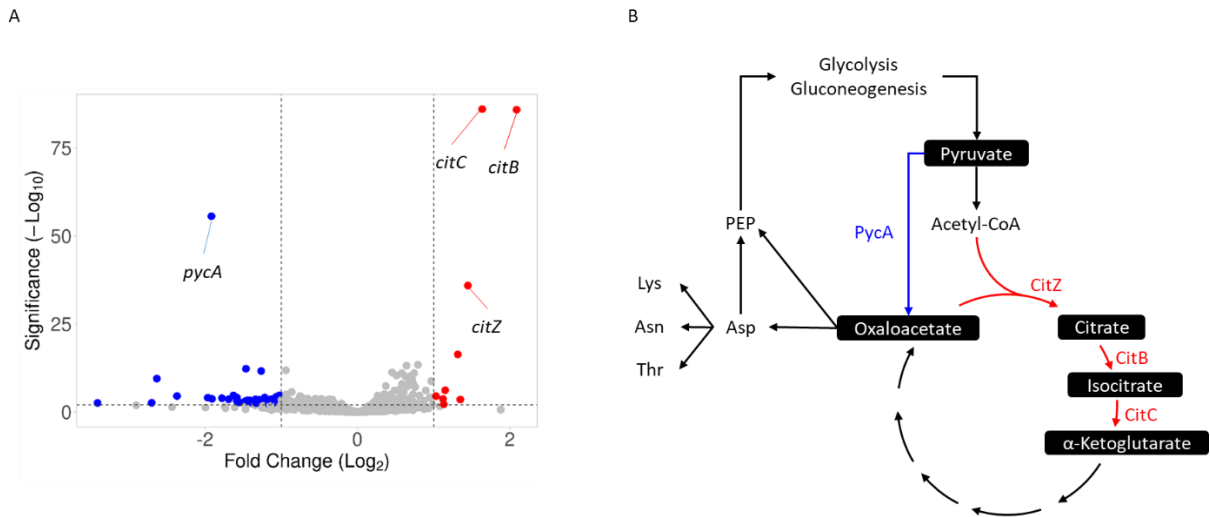


**Figure 6: RNAs significantly affected by aconitase RBP activity**

A) Volcano plot showing the relevant differences in gene expression between HG003 and *citB*<sub>RBP</sub> derivative upon iron starvation. The experimental design is the same as in Figure 3A except that the  $\Delta isrR$  allele is replaced by *citB*<sub>RBP</sub>. Blue dots, genes whose expression is decreased in *citB*<sub>RBP</sub>- strain; red dots, genes whose expression is increased in *citB*<sub>RBP</sub>- strain. For significant thresholds and fold changes, see Figure 3 (n=3). B) Metabolic regulations mediated by apo-CitB according to transcriptomic data. Red arrows, genes downregulated by apo-CitB; blue arrow, gene activated by apo-CitB; PEP, phosphoenolpyruvate; Asp, aspartate; Lys, lysine; Asn, asparagine; Thr, threonine.

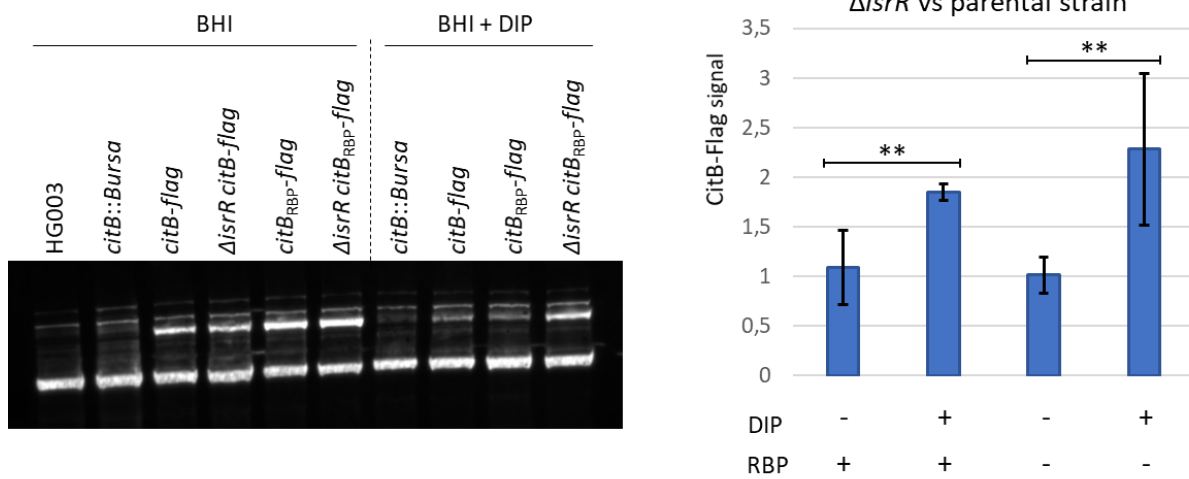


**Figure 7: CitB RBP activity and IsrR-dependent *citB* regulation**

Western-blot experiment with anti-Flag antibodies. Genotypes and growth conditions are indicated. 75 kDa, signals corresponding to CitB-Flag; 100 kDa, non-specific signal present in samples including Flag-less strains. The 75 kDa signal was used as a loading control for normalization. Histograms, ratios of reporter fusion production between HG003 and its  $\Delta$ *IsrR* derivative, each one being normalized to loading control bands. P-values < 0.01.

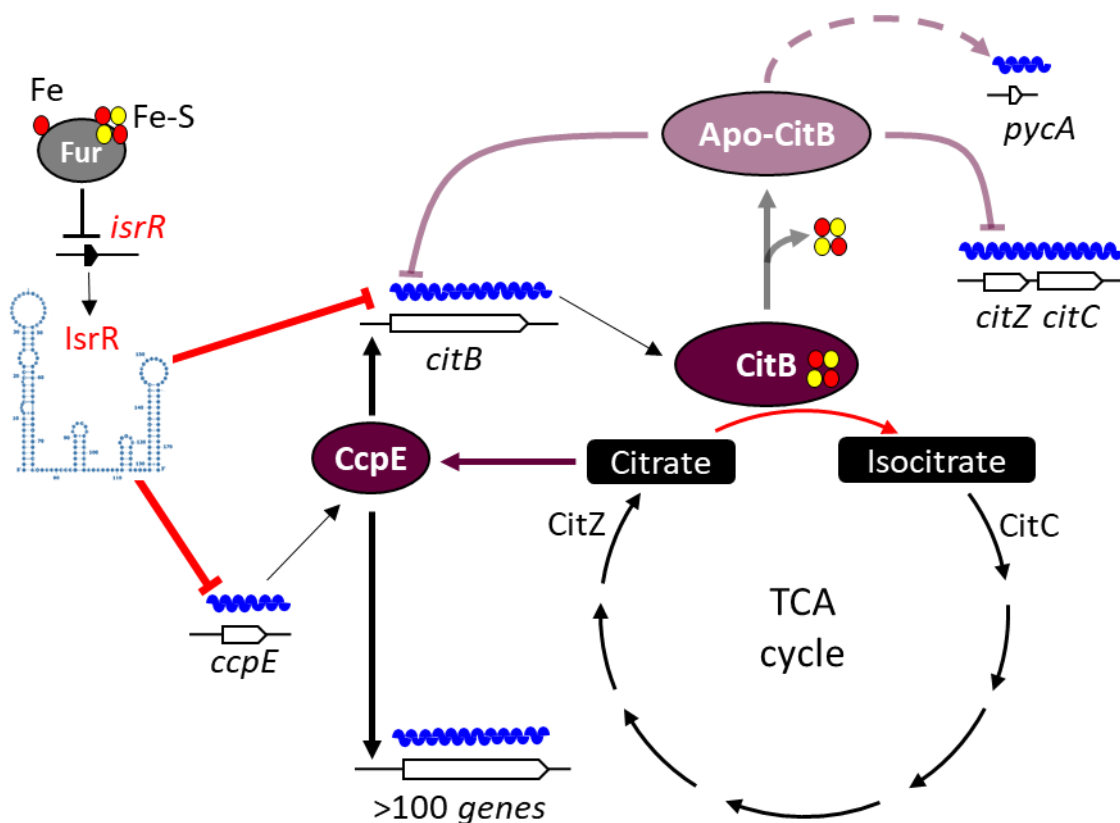


**Figure 8: IsrR and apo-CitB controlled citrate metabolism upon iron starvation**

Under iron-replete conditions, the transcription of *isrR* is repressed by Fur bound by  $\text{Fe}^{2+}$  or Fe-S clusters. Iron starvation leads to the alleviation of Fur repression, resulting in the expression of *isrR*. IsrR exerts its regulatory control on citrate metabolism by downregulating *citB* expression. This downregulation occurs through two distinct mechanisms: direct inhibition of *citB* mRNA translation and indirectly via inhibition of *ccpE* mRNA translation, CcpE being a transcriptional activator of *citB* and over a hundred other genes. Concomitantly, as iron becomes scarce, aconitase undergoes a transition from its Fe-S cluster-bound form to apo-CitB, a regulatory RNA-binding protein. Apo-CitB plays a pivotal role in the modulation of citrate metabolism, leading to the downregulation of *citZ-citC* mRNA levels and its own mRNA expression, while simultaneously promoting an increase in *pycA* mRNA levels, encoding pyruvate carboxylase.

## Supplementary data

### Regulation of staphylococcal aconitase expression in iron deficiency:

#### Control by sRNA-driven feedforward loop and moonlighting activity

Maxime Barrault<sup>1</sup>, Rodrigo H. Coronel-Tellez<sup>1</sup>, Svetlana Chabelskaya<sup>2</sup>, Claire Toffano-Nioche<sup>1</sup>

and Philippe Bouloc<sup>1\*</sup>

<sup>1</sup>Université Paris-Saclay, CEA, CNRS, Institute for Integrative Biology of the Cell (I2BC), 91198 Gif-sur-Yvette, France

<sup>2</sup>Université de Rennes 1, BRM (Bacterial regulatory RNAs and Medicine) UMR\_S 1230, 35000 Rennes, France

\* To whom correspondence should be addressed.

Tel: +33 1 69 82 62 17; Email: [philippe.bouloc@i2bc.paris-saclay.fr](mailto:philippe.bouloc@i2bc.paris-saclay.fr)

#### Table des matières

|   |     |
|---|-----|
| <a href="#">Table S2. Plasmids</a> .....  | 130 |
| <a href="#">Table S3. Primers</a> .....   | 132 |
| <a href="#">Table S4. HG003 <math>\Delta</math>isrR vs HG003 transcriptomic analysis in iron starved growth condition</a> .....                       | 136 |
| <a href="#">Table S5. HG003 <math>citB_{RBP}</math> vs HG003 transcriptomic analysis in iron starved growth condition</a> .....                       | 137 |
| <a href="#">Figure S1. RNA sequences used for gel retardation</a> .....   | 139 |
| <a href="#">Figure S2: Growth in BHI of HG003 and HG003 <math>\Delta</math>isrR with <math>citB^+</math> and <math>citB</math>-flag alleles</a> ..... | 140 |
| <a href="#">Figure S3. Chromosomal reporter fusions for detection of IsrR activity</a> .....  | 141 |
| <a href="#">Figure S4. IntaRNA pairing predictions</a> .....  | 142 |
| <a href="#">Figure S5. Enzymatic and RBP aconitase sites</a> .....  | 143 |
| <a href="#">Figure S6. Growth in BHI of HG003 and <math>citB</math> mutant derivatives</a> .....  | 144 |
| <a href="#">Figure S7. Intracellular citrate concentration in HG003 and <math>citB</math> mutant derivatives</a> .....                                | 145 |
| <a href="#">Figure S8: IsrR regulation of aconitase as a feedforward loop</a> .....   | 146 |
| <a href="#">References</a> .....  | 147 |

Table S1. *Staphylococcus aureus* strains

| Strain           | Genotype  | Construction/ Reference                                |
|------------------|---|--|
| <b>HG003</b>     | <i>rsbU</i> and <i>tcaR</i> repaired, MSSA, Agr+  | (1)  |
| <b>JE2</b>       | JE2 = USA300 cured from all plasmids  | (2)  |
| <b>NE861</b>     | USA300 <i>citB</i> ::Bursa  | (2)  |
| <b>NE1560</b>    | USA300 <i>ccpE</i> ::Bursa  | (2)  |
| <b>SAPhB1231</b> | as HG003 $\Delta$ <i>IsrR</i> ::tag135  |  |
| <b>SAPhB1755</b> | as HG003 P1 <sub>sarA</sub> _5'UTR <i>citB</i> :: <i>mAm</i> (integrated downstream of <i>sqr</i> )   | HG003 + pRN112-5' <i>citB</i>                          |
| <b>SAPhB1759</b> | as HG003 P1 <sub>sarA</sub> _5'UTR <i>ccpE</i> :: <i>mAm</i> (integrated downstream of <i>sqr</i> )   | HG003 + pRN112-5' <i>ccpE</i>                          |
| <b>SAPhB1761</b> | as HG003 $\Delta$ <i>IsrR</i> ::tag135 P1 <sub>sarA</sub> _5'UTR <i>citB</i> :: <i>mAm</i> (integrated downstream of <i>sqr</i> )   | SAPhB1231 + p RN112-5' <i>citB</i>                     |
| <b>SAPhB1765</b> | as HG003 $\Delta$ <i>IsrR</i> ::tag135 P1 <sub>sarA</sub> _5'UTR <i>ccpE</i> :: <i>mAm</i> (integrated downstream of <i>sqr</i> )   | SAPhB1231 + pRN112-5' <i>ccpE</i>                      |
| <b>SAPhB1767</b> | as HG003 $\Delta$ <i>IsrR</i> ::tag135 P1 <sub>sarA</sub> _5'UTR <i>citB</i> :: <i>mAm</i> (integrated downstream of <i>sqr</i> ) pRMC2 $\Delta$ R                          | SAPhB1761 + pRMC2 $\Delta$ R                           |
| <b>SAPhB1769</b> | as HG003 $\Delta$ <i>IsrR</i> ::tag135 <i>citB</i> - <i>mAm</i> pRMC2 $\Delta$ R- <i>IsrR</i>   | SAPhB1761 + pRMC2 $\Delta$ R- <i>IsrR</i>              |
| <b>SAPhB1771</b> | as HG003 $\Delta$ <i>IsrR</i> ::tag135 P1 <sub>sarA</sub> _5'UTR <i>citB</i> :: <i>mAm</i> (integrated downstream of <i>sqr</i> ) pRMC2 $\Delta$ R- <i>IsrR</i> $\Delta$ C1 | SAPhB1761 + pRMC2 $\Delta$ R- <i>IsrR</i> $\Delta$ C1  |
| <b>SAPhB1773</b> | as HG003 $\Delta$ <i>IsrR</i> ::tag135 P1 <sub>sarA</sub> _5'UTR <i>citB</i> :: <i>mAm</i> (integrated downstream of <i>sqr</i> ) pRMC2 $\Delta$ R- <i>IsrR</i> $\Delta$ C2 | SAPhB1761 + pRMC2 $\Delta$ R- <i>IsrR</i> $\Delta$ C2  |
| <b>SAPhB1775</b> | as HG003 $\Delta$ <i>IsrR</i> ::tag135 P1 <sub>sarA</sub> _5'UTR <i>citB</i> :: <i>mAm</i> (integrated downstream of <i>sqr</i> ) pRMC2 $\Delta$ R- <i>IsrR</i> $\Delta$ C3 | SAPhB1761 + pRMC2 $\Delta$ R- <i>IsrR</i> $\Delta$ C3  |
| <b>SAPhB1900</b> | as HG003 $\Delta$ <i>IsrR</i> ::tag135 P1 <sub>sarA</sub> _5'UTR <i>ccpE</i> :: <i>mAm</i> (integrated downstream of <i>sqr</i> ) pRMC2 $\Delta$ R                          | SAPhB1765 + pRMC2 $\Delta$ R                           |
| <b>SAPhB1902</b> | as HG003 $\Delta$ <i>IsrR</i> ::tag135 P1 <sub>sarA</sub> _5'UTR <i>ccpE</i> :: <i>mAm</i> (integrated downstream of <i>sqr</i> ) pRMC2 $\Delta$ R- <i>IsrR</i>             | SAPhB_1765 + pRMC2 $\Delta$ R- <i>IsrR</i>             |
| <b>SAPhB1904</b> | as HG003 $\Delta$ <i>IsrR</i> ::tag135 P1 <sub>sarA</sub> _5'UTR <i>ccpE</i> :: <i>mAm</i> (integrated downstream of <i>sqr</i> ) pRMC2 $\Delta$ R- <i>IsrR</i> $\Delta$ C1 | SAPhB1765 + pRMC2 $\Delta$ R- <i>IsrR</i> $\Delta$ C1  |
| <b>SAPhB1906</b> | as HG003 $\Delta$ <i>IsrR</i> ::tag135 P1 <sub>sarA</sub> _5'UTR <i>ccpE</i> :: <i>mAm</i> (integrated downstream of <i>sqr</i> ) pRMC2 $\Delta$ R- <i>IsrR</i> $\Delta$ C2 | SAPhB1765 + pRMC2 $\Delta$ R- <i>IsrR</i> $\Delta$ C2  |
| <b>SAPhB1908</b> | as HG003 $\Delta$ <i>IsrR</i> ::tag135 P1 <sub>sarA</sub> _5'UTR <i>ccpE</i> :: <i>mAm</i> (integrated downstream of <i>sqr</i> ) pRMC2 $\Delta$ R- <i>IsrR</i> $\Delta$ C3 | SAPhB_1765 + pRMC2 $\Delta$ R- <i>IsrR</i> $\Delta$ C3 |

|                  |   |                                 |
|------------------|---|---------------------------------|
| <b>SAPhB1964</b> | as HG003 <i>ΔisrR::tag135 P1<sub>sarA</sub>_5'UTRcitB::mAm</i> (integrated downstream of <i>sqr</i> ) pRMC2ΔR-IsrRΔC1C2   | SAPhB1761 + pRMC2ΔR-IsrRΔC1C2   |
| <b>SAPhB2039</b> | as HG003 <i>P1<sub>sarA</sub>_5'UTRcitB::mAm</i> (integrated downstream of <i>sqr</i> ) pRMC2ΔR-IsrRΔC1C3                 | SAPhB1231 + pRMC2ΔR-IsrRΔC1C3   |
| <b>SAPhB2041</b> | as HG003 <i>P1<sub>sarA</sub>_5'UTRcitB::mAm</i> (integrated downstream of <i>sqr</i> ) pRMC2ΔR-IsrRΔC2C3                 | SAPhB1231 + pRMC2ΔR-IsrRΔC2C3   |
| <b>SAPhB2043</b> | as HG003 <i>P1<sub>sarA</sub>_5'UTRcitB::mAm</i> (integrated downstream of <i>sqr</i> ) pRMC2ΔR-IsrRΔC1C2C3               | SAPhB1231 + pRMC2ΔR-IsrRΔC1C2C3 |
| <b>SAPhB2054</b> | as HG003 <i>ΔisrR::tag135 citB-flag</i>   | SAPhB1231 + pIMcitBflag         |
| <b>SAPhB2062</b> | as HG003 <i>ΔisrR::tag135 ccpE-flag</i>   | SAPhB1231 + pIMccpEflag         |
| <b>SAPhB2075</b> | as HG003 <i>citB-flag</i>   | HG003 + pIMcitBflag             |
| <b>SAPhB2077</b> | as HG003 <i>ccpE-flag</i>   | HG003 + pIMccpEflag             |
| <b>SAPhB2130</b> | as HG003 <i>citB::Bursa</i>   | HG003 + Φ80 lysate from NE861   |
| <b>SAPhB2133</b> | as HG003 <i>ccpE::Bursa</i>   | HG003 + Φ80 lysate from NE1560  |
| <b>SAPhB2158</b> | as HG003 <i>ΔisrR::tag135 citB<sub>RBP</sub></i>  | SAPhB1231 + pIMcitB-RBP         |
| <b>SAPhB2166</b> | as HG003 <i>citB<sub>ENZ</sub></i>  | SAPhB153 + pIMcitB-ENZ          |
| <b>SAPhB2167</b> | as HG003 <i>citB<sub>RBP</sub></i>  | SAPhB153 + pIMcitB-RBP          |
| <b>SAPhB2181</b> | as HG003 <i>ΔisrR::tag135 citB<sub>RBP</sub>-flag</i>   | SAPhB2054 + pIMcitB-RBP-flag    |
| <b>SAPhB2185</b> | as HG003 <i>citB-flag citB<sub>RBP</sub></i>  | SAPhB2075 + pIMcitB-RBP-flag    |
| <b>SAPhB2365</b> | as HG003 <i>ΔisrR::tag135 P1<sub>sarA</sub>_5'UTRcitB::mAm</i> (integrated downstream of <i>sqr</i> ) pRMC2ΔR-IsrRΔC1+2+3 | SAPhB1765 + pRMC2ΔR-IsrRΔC1C2C3 |

**Table S2. Plasmids**

| Plasmids                     | Properties   | Construction / reference                                      |
|------------------------------|--|---|
| <b>PRN112</b>                | pJB28-NWMN29-30 + SarA_P1-mAmetrine-Term   | (3)   |
| <b>pRN112-5'citB</b>         | Chromosomal integration of the <i>PsarA-5'citB-mAm</i> gene fusion between SAOUHSC_00037 and SAOUHSC_00039 | 2600/2683 on pRN112 + 2684/2685 on HG003                      |
| <b>pRN112-5'miaB</b>         | Chromosomal integration of the <i>PsarA-5'ccpE-mAm</i> gene fusion between SAOUHSC_00037 and SAOUHSC_00039 | 2600/2683 on pRN112 + 2690/2691 on HG003                      |
| <b>pIMAY</b>                 | Shuttle rep(Ts) vector in <i>S. aureus</i>   | (Monk et al. 2015)  |
| <b>pIMcitBflag</b>           | For insertion of a Flag sequence in C-ter of <i>citB</i>   | 1536/1537 on pIMAY + primers 2841/2842 and 2843/2844 on HG003 |
| <b>pIMccpEflag</b>           | For insertion of a Flag sequence in C-ter of <i>ccpE</i>   | 1536/1537 on pIMAY + primers 2849/2850 and 2851/2852 on HG003 |
| <b>PRMC2ΔR</b>               | PRMC2 derivative with a <i>tetR</i> deletion for constitutive expression                                   | (4)   |
| <b>pRMC2ΔR-IsrR</b>          | (4)  | (4)   |
| <b>pRMC2ΔR-IsrRΔC1</b>       | PRMC2ΔR derivative. Constitutive expression of IsrRΔC1   | (4)   |
| <b>pRMC2ΔR-IsrRΔC2</b>       | PRMC2ΔR derivative. Constitutive expression of IsrRΔC2   | (4)   |
| <b>pRMC2ΔR-IsrRΔC3</b>       | PRMC2ΔR derivative. Constitutive expression of IsrRΔC3   | (4)   |
| <b>pRMC2ΔR-IsrRΔC1ΔC2</b>    | PRMC2ΔR derivative. Constitutive expression of IsrRΔC1C2   | (4)   |
| <b>pRMC2ΔR-IsrRΔC1ΔC3</b>    | PRMC2ΔR derivative. Constitutive expression of IsrRΔC1C3   | 2667/2668 on pRMC2ΔR-IsrRΔC1 + Gibson assembly                |
| <b>pRMC2ΔR-IsrRΔC2ΔC3</b>    | PRMC2ΔR derivative. Constitutive expression of IsrRΔC2C3   | 2789/2790 on pRMC2ΔR-IsrRΔC2 + Gibson assembly                |
| <b>pRMC2ΔR-IsrRΔC1ΔC2ΔC3</b> | PRMC2ΔR derivative. Constitutive expression of IsrRΔC1C2C3   | 2789/2790 on pRMC2ΔR-IsrRΔC1C2 + Gibson assembly              |
| <b>pIMcitB-ENZ</b>           | For insertion of the C450S mutation to inactivate enzymatic activity of CitB                               | 1536/1537 on pIMAY + 3010/3011 and 3012/3013 on HG003         |
| <b>pIMcitB-RBP</b>           | For insertion of the R724E and Q738E mutations to inactivate RNA-binding activity of CitB                  | 1536/1537 on pIMAY + 3006/3007 and 3008/3009 on HG003         |

|                         |  |  |
|-------------------------|--|--|
| <b>pIMcitB-RBP-flag</b> | For insertion of the R724E and Q738E mutations to inactivate RNA-binding activity of CitB-Flag         | 3038/3039 on pMAY_CitB_RBP                   |
| <b>pJET1.2</b>          | Cloning vector: only recombinant plasmids are able to propagate  | Thermo Scientific                            |
| <b>pJET-T7IsrR</b>      | Plasmid with template for T7 production of IsrR RNA  | 2770/2771 on HG003 and ligation into pJET1.2 |
| <b>pJET-T7IsrR3Cmut</b> | Plasmid with template for T7 production of IsrR RNA mutated in all Cs                                  | Ligation of gBlock 3225 into pJET1.2         |
| <b>pJET-T7IsrRC1mut</b> | Plasmid with template for T7 production of IsrR RNA mutated in C1                                      | Ligation of gBlock 3226 into pJET1.2         |
| <b>pJET-T7citB</b>      | Plasmid with template for T7 production of <i>citB</i> RNA   | 3221/3222 on HG003 and ligation into pJET1.2 |
| <b>pJET-T7citBmut</b>   | Plasmid with template for T7 production of <i>citB</i> RNA with mutations complementary with IsrR3Cmut | Ligation of gBlock 3227 into pJET1.2         |
| <b>pJET-T7ccpE</b>      | Plasmid with template for T7 production of <i>ccpE</i> RNA   | 3223/3224 on HG003 and ligation into pJET1.2 |
| <b>pJET-T7ccpEmut</b>   | Plasmid with template for T7 production of <i>ccpE</i> RNA with mutations complementary with IsrRC1mut | Ligation of gBlock 3228 into pJET1.2         |

**Table S3. Primers**

| Name | Sequence  |
|------|---|
| 1536 | GGTACCCAGCTTTTGTTCCTTTAGTGAGG                                 |
| 1537 | GAGCTCCAATTCGCCCTATAGTGAGTCG                                  |
| 1538 | TACATGTCAAGAATAAACTGCCAAAGC                                   |
| 1539 | AATACCTGTGACGGAAGATCACTTCG                                    |
| 2501 | AGAAAATACCGCATCAGGCG  |
| 2502 | CCCCTTCTAAAGGGCAAAAGTG  |
| 2529 | CAGGTCGACGGTATCGATAACT  |
| 2600 | TTAGTTAATTATAACTAATTAAAAATGAGAAGTAAAC                         |
| 2666 | CCTTCACCTTCACCACGAAGTGA                                       |
| 2667 | CCCTTTTATATGGTAAAAGACAATATACGTTATAACAACG                      |
| 2668 | ATTGTCTTTTACCATATAAAAAGGGGAATATTTGAAAATGA                     |
| 2669 | ATGGAAATGAAGGCGAGGTG  |
| 2670 | CACCAACACCCCATCCTAGT  |
| 2673 | TTTGACAAAATGCAGGCACA  |
| 2674 | TCTGGCAAGATTGTAACACCT   |
| 2683 | GTTTCAAAGGTGAAGAATTATTTACA                                    |
| 2684 | TTCTCATTTTTAATTAGTTATAATTAAGTAAAAGGCATATAAAATATAAAAATGTATCAAG |
| 2685 | GTAATAAATTCCTTCACCTTTTGAACGTCAAATGTTTTTTTGATTGCT              |
| 2690 | TTCTCATTTTTAATTAGTTATAATTAAGTAAAAGTCAATGAATGCTTGTAGC          |
| 2691 | GTAATAAATTCCTTCACCTTTTGAACGTAATGTTATTAGTAAACGATAGTCTTC        |
| 2692 | GGAGGATGATTATTTTAGGTTTCAAAGGTGAAGAATTATTTAC                   |
| 2693 | TTCACCTTTTGAACCTAAAATAATCATCCTCCTAAGGTAC                      |
| 2701 | CACCACCGCATCATTTTGCACAA                                       |
| 2705 | AACGAAACGTTGTGGGGGGG  |
| 2706 | GTTATAACGTATATTGTCTTTTACGGG                                   |
| 2752 | GGATCCACTAGTTCTAGAGCGG  |
| 2753 | GGCTGCAGGAATTCGATATCAA  |
| 2754 | GATATCGAATTCCTGCAGCCATCGTCTGCACCCTAATCAAGC                    |
| 2755 | GCTCTAGAAGTGGATCCGGCGACCAAATTGACAATGCAA                       |

|             |  |
|-------------|--|
| <b>2756</b> | TCGAGGTCGACGGTATCGATAA                                     |
| <b>2757</b> | CRACTCACTATAGGGCGAATTGG                                    |
| <b>2770</b> | TAATACGACTCACTATAGTTGAAAATGATTATCAATACCACATAG              |
| <b>2771</b> | ACAAAAGCAGTAAACCTAAAGTG                                    |
| <b>2789</b> | GATTGGTCATTTTCAAATATTTTTTATATGGTAAAAGACAATATACGTTATAACAACG |
| <b>2790</b> | GTTGTTATAACGTATATTGTCTTTTACCATATAAAAAATATTTGAAAATGACCAATCC |
| <b>2830</b> | CCTTACGACACTTTATTTTTTACTATTTGGTACCG                        |
| <b>2831</b> | CCAAATAGTAAAAAATAAAGTGTCGTAAGGGTTTA                        |
| <b>2841</b> | CCTCACTAAAGGGAACAAAAGCTGGGTACCTGGAACGGTTGATATTGATTTA       |
| <b>2842</b> | CTTGTCGTCATCGTCTTTGTAGTCTTGCCTAATTTATTTCTTAA               |
| <b>2843</b> | GACTACAAAGACGATGACGACAAGTAAAAAATAGATATCACAGTAAAATTTT       |
| <b>2844</b> | CRACTCACTATAGGGCGAATTGGAGCTCATGAAATTTCTTATTCCACAAAATA      |
| <b>2849</b> | CCTCACTAAAGGGAACAAAAGCTGGGTACCCAACAACAAAAGAAAACTAAG        |
| <b>2850</b> | CTTGTCGTCATCGTCTTTGTAGTCCGCCTTTGGTTGTTCAACAAAGCTC          |
| <b>2851</b> | GACTACAAAGACGATGACGACAAGTAGTTTTAGACTAATTTAAGGTTTGTAT       |
| <b>2852</b> | CRACTCACTATAGGGCGAATTGGAGCTCTTGTCCAATGTGTAATAAAAATAAAT     |
| <b>2900</b> | CACCTTACCTGTATGATAAGTTTTGC                                 |
| <b>2901</b> | GTAAGATATGGTGGCGAATTCCAAC                                  |
| <b>2904</b> | GTAATCGTACTGCCTCTGATGTG                                    |
| <b>2905</b> | CACCTGTCCTGCTAACATCATATAGA                                 |
| <b>2926</b> | CCATCGTTCAAATTTAGTTATG                                     |
| <b>2927</b> | CATAATCCCGTGATAAATTAC                                      |
| <b>2930</b> | CGATAATTTAGAACAAGATTACC                                    |
| <b>2931</b> | GAAACATATTAGCAACAAAGAG                                     |
| <b>2941</b> | GGATCCCCTCGAGTTCATGAAAA                                    |
| <b>2942</b> | AGTGAATTCGAGCTCAGATCTGTT                                   |
| <b>2943</b> | AACAGATCTGAGCTCGAATTCACT                                   |
| <b>2944</b> | TTTTCATGAACTCGAGGGGATCC                                    |
| <b>2945</b> | TTTATATGCGCCTAAAAGAGAATATACGTTATAACAACGTT                  |
| <b>2967</b> | CCTGTACATAACCTTCGGGCATG                                    |
| <b>2968</b> | GCTTCCAAGGAGCTAAAGAGGTC                                    |
| <b>2969</b> | GTACCAGCCGTAGTTGATTTAGCTTC                                 |

|             |   |
|-------------|---|
| <b>2970</b> | CCTTGCTTAGGGGCAATGATTTTAGG                                  |
| <b>2971</b> | CGAAAACGTTACGTAAAGCGGCTG                                    |
| <b>2980</b> | CGAAGTGATTCGTAAGGACGTCTTG                                   |
| <b>2981</b> | ACCTTTTCCAATGACATCTGCAACAG                                  |
| <b>2982</b> | AGACATTAGATGTCTTACAAGAAATCGTTAAAGGC                         |
| <b>3006</b> | CTAAAGGGAACAAAAGCTGGGTACCTCTAACCCCTTATGTAATGTTAGGTGC        |
| <b>3007</b> | CTGGCGCTAATTCGTTTTTAATTTCTATATTAGCAAACGTACCTCGAACC          |
| <b>3008</b> | GTACGTTTGCTAATATAGAAATTA AAAACGAATTAGCGCCAGGTACTGAAGG       |
| <b>3009</b> | ACTATAGGGCGAATTGGAGCTCTCAGTCACAGGTGAAATGATTCC               |
| <b>3010</b> | CTAAAGGGAACAAAAGCTGGGTACCGTTTTTTAAATTGGGCAACGAAAGC          |
| <b>3011</b> | GATGTATTTGTTGATGATGTAATTGCTGCTATTGCAATATC                   |
| <b>3012</b> | GCAGCAATTACATCATCAACAAATACATCTAACCCCTTATGTAATG              |
| <b>3013</b> | ACTATAGGGCGAATTGGAGCTCTACCACGTCTTGAACCATATGAATT             |
| <b>3036</b> | GAGTATGGAGCAACTTGCGGATTCC                                   |
| <b>3037</b> | ACCATCTAGACCAAGAGAATCAGCTG                                  |
| <b>3038</b> | GACTACAAAGACGATGACGACAAGTAAAAAATAGATATCACAGTAAAATTTTAATCGG  |
| <b>3039</b> | CTTGTCGTCATCGTCTTTGTAGTCTTGGCGCTAATTTATTTCTTAAAACCA         |
| <b>3040</b> | GGTTCGTTTTGACTCACTTGTTG                                     |
| <b>3041</b> | CAAAGGTTTTGAACCGACCTATTATATC                                |
| <b>3046</b> | CTAAAGGGAACAAAAGCTGGGTACCTGTATATGACAATCTAGTAAAAAC           |
| <b>3047</b> | CTAAAATGCCTAAAATCAAATCAAATAACTAAGCTTTCATTAATTTTTCAAAGCG     |
| <b>3048</b> | CGTTTTGAAAAATTAATGAAAGCTTAGTTATTTTGATTTGATTTTAGGCATTTTAGATT |
| <b>3049</b> | CACTATAGGGCGAATTGGAGCTCCATCCTATGCTAAGAAAAAGACA              |
| <b>3050</b> | CGGTATGTTTAGCAACGCTGATTTAG                                  |
| <b>3051</b> | TGGTGTTGTTGTCATTTAATCACCCATTTTCA                            |
| <b>3052</b> | GGTGTAGATATGACAACACCTGAA                                    |
| <b>3053</b> | CTTAAATATCCAGATGGCGATTTCTG                                  |
| <b>3062</b> | TGAAAATGGGTGATTAATGACAACAACACCA                             |
| <b>3221</b> | TAATACGACTCACTATAGAAGGCATATAAATATAAAAATGTATC                |
| <b>3222</b> | AAACTTTAGTAATACCTTGCTCTTCTAC                                |
| <b>3223</b> | TAATACGACTCACTATAGAACTCATGAATGCTTGTAGCC                     |
| <b>3224</b> | AGGTTGAGATATATATAAAAATTTAGCCGCT                             |

|             |  |
|-------------|--|
| <b>3225</b> | TAATACGACTCACTATAGTTGAAAATGATTATCAATACCACATAGAACATCGGGGGCACAAC-<br>GTTTCGTTCTTGTGGATTGGTCATTTTCAAATATTGGGGTTTTATATGGGGGTAAAAGACAAT<br>ATACGTTATAACAACGTTTTATAAAAAGCAGTAAACCCTTACGACAC-<br>TTTAGGTTTACTGCTTTTGT |
| <b>3226</b> | TAATACGACTCACTATAGTTGAAAATGATTATCAATACCACATAGAACATCGGGGGCACAAC-<br>GTTTCGTTCTTGTGGATTGGTCATTTTCAAATATTCCCCTTTTATATGCCCGTAAAAGACAAT<br>ATACGTTATAACAACGTTTTATAAAAAGCAGTAAACCCTTACGACAC-<br>TTTAGGTTTACTGCTTTTGT |
| <b>3227</b> | TAATACGACTCACTATAGAAGGCATATAAA-<br>TATAAAAATGTATCAACCCCCATCATTAAATGGCTGCAAATTTTAAAGAGCAATCAAAAAACA<br>TTTTGACTTGAATGGCCAAAGTTATACTTACTATGATTTAAAAGCTGTAGAAGAG-<br>CAAGGTATTACTAAAGTTT                          |
| <b>3228</b> | TAATACGACTCACTATAGAACTCATGAATGCTTGTAGCCATGAAAGTTCAATAATTGAA-<br>TAATTTATCCCCCAAATTATGAAGATTGAAGACTATCGTTTACTAATAACATTAGACGAAACG<br>AAAACGTTACGTAAAGCGGCTGAAATTTTATATATATCTCAACCT                               |

**Table S4. HG003  $\Delta$ *isrR* vs HG003 transcriptomic analysis in iron starved growth condition**

| Id            | FoldChange | padj     | gene        | Product                              |
|---------------|------------|----------|-------------|--------------------------------------|
| IsrR          | 0,03       | 1,05E-89 | <i>isrR</i> | sRNA                                 |
| SAOUHSC_02400 | 0,329      | 1,20E-04 | <i>mtIF</i> | PTS system mannitol-specific protein |
| SAOUHSC_02825 | 5          | 4,21E-03 | <i>mhqD</i> | hypothetical protein                 |

Padj; p-value adjusted, Yellow; genes overexpressed in  $\Delta$ *isrR*, Blue; genes underexpressed in  $\Delta$ *isrR*. Only the genes having a fold-change < 0.5 or >2 and a p-value <0.005 as well as at least 20 reads in all conditions are represented.

**Table S5. HG003 *citB*<sub>RBP</sub> vs HG003 transcriptomic analysis in iron starved growth condition**

| <b>Id</b>     | <b>FoldChange</b> | <b>padj</b> | <b>gene</b>  | <b>product</b>                       |
|---------------|-------------------|-------------|--------------|--------------------------------------|
| SAOUHSC_01801 | 3,11              | 9,6E-87     | <i>citC</i>  | isocitrate dehydrogenase             |
| SAOUHSC_01347 | 4,253             | 1,5E-86     | <i>citB</i>  | aconitate hydratase                  |
| SAOUHSC_01064 | 0,265             | 2,6E-56     | <i>pycA</i>  | pyruvate carboxylase                 |
| SAOUHSC_01802 | 2,731             | 1,2E-36     | <i>citZ</i>  | citrate synthase                     |
| SAOUHSC_02729 | 2,491             | 4,3E-17     |              | ABC transporter-like protein         |
| SAOUHSC_03000 | 0,363             | 5,4E-13     | <i>cap1A</i> | capsular polysaccharide biosynthesis |
| SAOUHSC_03016 | 0,417             | 2,3E-12     |              | hypothetical protein                 |
| SAOUHSC_00415 | 0,161             | 3,2E-10     |              | transmembrane hypothetical protein   |
| SAOUHSC_02025 | 2,221             | 7,1E-07     |              | phi SLT orf 99-like protein          |
| SAOUHSC_00560 | 0,492             | 1,9E-05     |              | hypothetical protein                 |
| SAOUHSC_02400 | 0,324             | 2,1E-05     | <i>mtIF</i>  | PTS system mannitol-specific protein |
| SAOUHSC_00962 | 0,194             | 3,1E-05     |              | hypothetical protein                 |
| SAOUHSC_01708 | 2,046             | 3,2E-05     | <i>pxpA</i>  | LamB/YcsF family protein             |
| SAOUHSC_01144 | 0,477             | 5,2E-05     | <i>ftsL</i>  | cell division protein                |
| SAOUHSC_02992 | 0,334             | 7,8E-05     |              | hypothetical protein                 |
| SAOUHSC_02641 | 0,43              | 8,2E-05     | <i>hrtB</i>  | permease domain-containing protein   |
| SAOUHSC_02832 | 0,256             | 9,1E-05     |              | hypothetical protein                 |
| SAOUHSC_01324 | 0,475             | 9,9E-05     |              | hypothetical protein                 |
| S414          | 0,292             | 1,2E-04     |              | sRNA                                 |
| SAOUHSC_01315 | 0,266             | 1,8E-04     |              | hypothetical protein                 |
| SAOUHSC_02973 | 0,48              | 1,8E-04     |              | hypothetical protein                 |
| SAOUHSC_01850 | 2,18              | 2,0E-04     | <i>ccpA</i>  | catabolite control protein A         |
| SAOUHSC_01944 | 0,458             | 2,1E-04     |              | hypothetical protein                 |
| SAOUHSC_00825 | 0,31              | 2,4E-04     |              | hypothetical protein                 |
| SAOUHSC_00465 | 0,396             | 2,5E-04     | <i>veg</i>   | hypothetical protein                 |
| SAOUHSC_00295 | 2,551             | 2,9E-04     | <i>nanA</i>  | N-acetylneuraminate lyase            |

|               |       |         |               |                                 |
|---------------|-------|---------|---------------|---------------------------------|
| SAOUHSC_01180 | 0,409 | 3,1E-04 |               | hypothetical protein            |
| SAOUHSC_00556 | 0,452 | 3,1E-04 | <i>proP</i>   | proline/betaine transporter     |
| SAOUHSC_02993 | 0,367 | 5,0E-04 |               | hypothetical protein            |
| SAOUHSC_00923 | 0,376 | 5,3E-04 | <i>opp-3B</i> | hypothetical protein            |
| SAOUHSC_01394 | 0,334 | 7,0E-04 | <i>lysC</i>   | aspartate kinase                |
| SAOUHSC_01853 | 0,471 | 7,0E-04 |               | hypothetical protein            |
| SAOUHSC_01142 | 0,422 | 7,0E-04 | <i>mraZ</i>   | cell division protein           |
| SAOUHSC_02923 | 0,361 | 8,2E-04 | <i>bcaP</i>   | hypothetical protein            |
| SAOUHSC_01103 | 0,383 | 8,2E-04 | <i>sdhC</i>   | succinate dehydrogenase subunit |
| SAOUHSC_00843 | 0,46  | 9,5E-04 | <i>metP</i>   | hypothetical protein            |
| SAOUHSC_01569 | 3,209 | 1,1E-03 |               | hypothetical protein            |
| SAOUHSC_00064 | 0,461 | 1,4E-03 | <i>norG</i>   | hypothetical protein            |
| SAOUHSC_00924 | 0,355 | 1,8E-03 | <i>opp3C</i>  | hypothetical protein            |
| SAOUHSC_01641 | 0,342 | 2,0E-03 | <i>comGB</i>  | hypothetical protein            |
| SAOUHSC_02424 | 0,382 | 2,0E-03 |               | hypothetical protein            |
| SAOUHSC_01331 | 0,154 | 2,6E-03 |               | hypothetical protein            |
| SAOUHSC_00232 | 0,094 | 2,8E-03 | <i>lrgA</i>   | murein hydrolase regulator      |
| SAOUHSC_00347 | 0,447 | 2,9E-03 |               | hypothetical protein            |
| SAOUHSC_00316 | 0,398 | 3,1E-03 | <i>mepB</i>   | hypothetical protein            |
| SAOUHSC_00437 | 0,492 | 4,5E-03 | <i>treP</i>   | hypothetical protein            |
| SAOUHSC_01292 | 0,387 | 4,9E-03 |               | hypothetical protein            |

Padj; p-value adjusted, Pink; genes overexpressed in CitB<sub>RBP</sub>, Blue; genes underexpressed in CitB<sub>RBP</sub>. Only the genes having a fold-change < 0.5 or >2 and a p-value <0.005 as well as at least 20 reads in one condition are presented.

## Figure S1. RNA sequences used for gel retardation

### IsrR:

UUGAAAUGAUUAUCAAUACCACAUAGAACAUCCCCCACAACGUUUCGUUCUUGUUGGAU-  
UGGUCAUUUUCAAAUAUUCUUUUUAUAUGCCCGUAAAAGACAAUAUACGUUAUAACAACGUUUUAU  
AAAAGCAGUAAAACCCUACGACACUUUAGGUUUACUGCUUUUGU

### citB:

AAGGCAUAUAAAUAUAAAAUGUAUCAAGGGGAUCAUAAAUGGCUGCAAAUUUUAAAAGAG-  
CAAUCAAAAAACAUUUGAC

### ccpE:

AACUCAUGAAUGCUUGUAGCCAUGAAAGUCAAUAAUUGAAUAAUUUAUGGGGGGAAAU-  
UAUGAAGAUUGAAGACUAUCGUUUACUAAUAACAUUA

### citBmut:

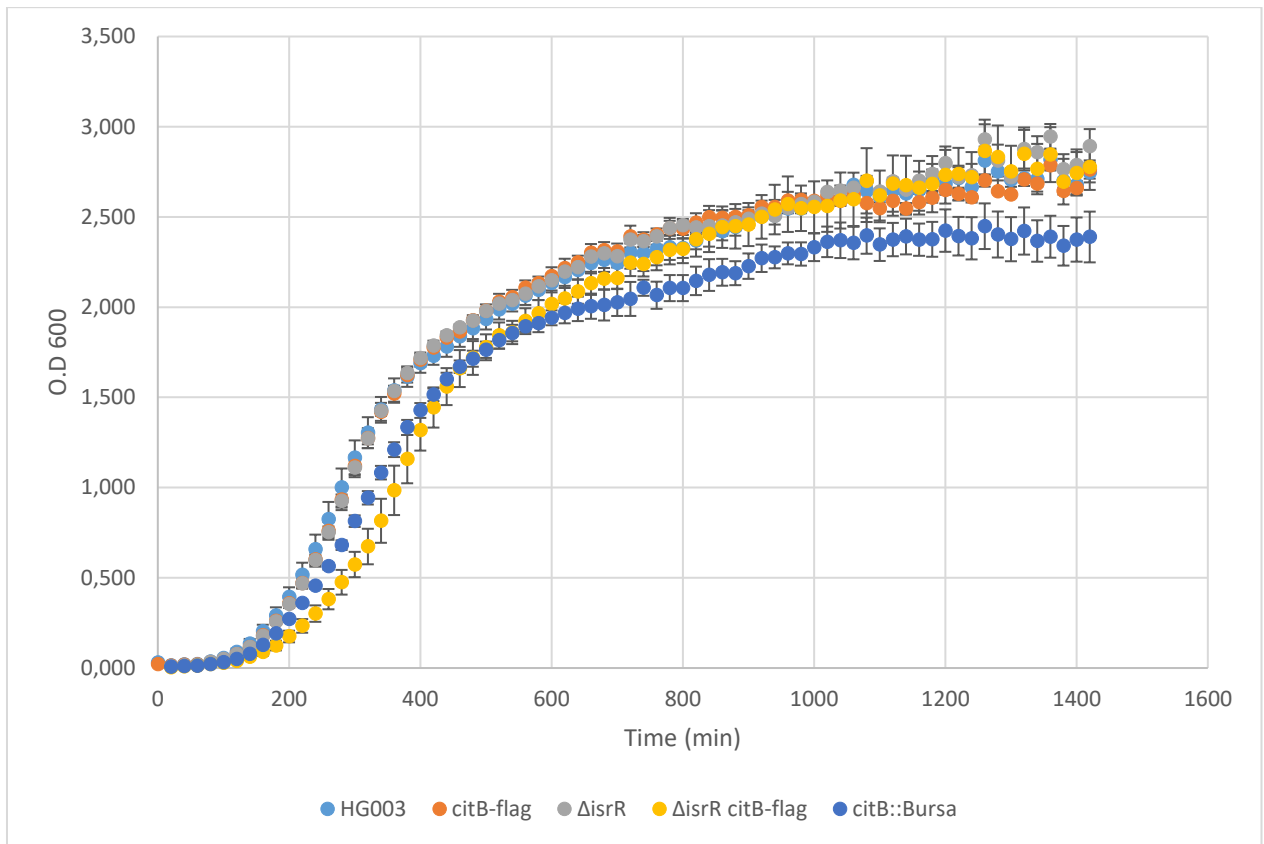
AACCGAUUAAAUAUAAAAUCUAUCAACCCCCAUCAUAAAUCGGUGCAAAUUUUAAAAGAG-  
CAAUCAAAAAACAUUUGAC

### ccpEmut:

AACUCAUGAAUGCUUGUAGCCAUGAAAGUCAAUAAUUGAAUAAUUUAUCCCCCAAU-  
UAUGAAGAUUGAAGACUAUCGUUUACUAAUAACAUUA

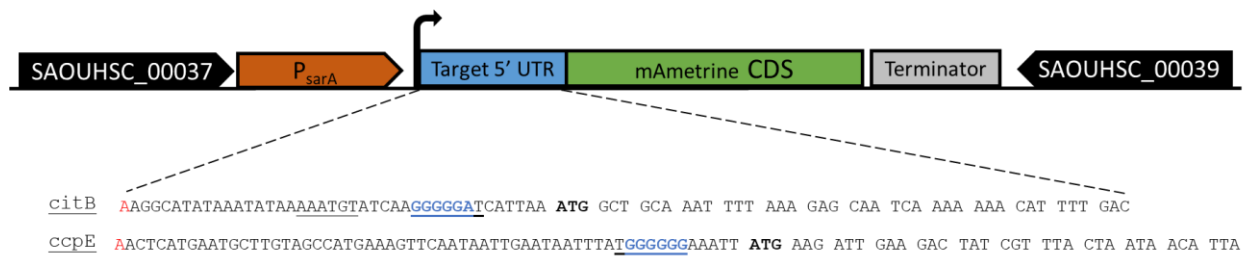
RNA sequences used for gel retardation assays. Red, modified nucleotides.

**Figure S2: Growth in BHI of HG003 and HG003  $\Delta$ isrR with *citB*<sup>+</sup> and *citB*-flag alleles**



Overnight cultures were diluted 100 times and grown in rich medium (BHI) at 37°C under agitation in a microplate (Vol=200  $\mu$ L) for 24 hours. Incubation and measurement of OD600 were obtained using a Clariostar microplate reader. The *citB*::*Bursa* strain serve as a control for a non-functional CitB. The error bars were calculated using the standard deviation of three independent biological replicates (n=3).

**Figure S3. Chromosomal reporter fusions for detection of IsrR activity**



The reporter fusion consists in a region containing the 5' UTR of each target (in blue) containing the predicted interaction region (underlined) fused in frame with the CDS of a fluorescent protein, mAmetrine (in green). This fusion is under the control of a constitutive promoter (P<sub>sarA</sub>, in orange) that allows for a strong expression of the fusion, and a strong promoter (in grey). The reporter fusions were inserted on *S. aureus* chromosome at a neutral locus between genes SAOUHSC\_00037 and SAOUHSC\_00039 using integrative plasmid pRN112 (3).

**Figure S4. IntaRNA pairing predictions**

**A**

|                      |  |                    |
|----------------------|--|--------------------|
| IsrR-<br>$\Delta$ C1 | <pre>           3           46                         5'-AA      AAUAU  AAAUGUAUCA  CAUU      UGCAA..GAC-   GGCAUAUA  AA      AAGGGGAU  AAAUGGC   3'-UGU..AAUGC  CCGUAUAU  UU      UCCCCUUA  UUUACUG   88           58           </pre> | E= -11 kcal/mol    |
|                      |  | HE= -20,9 kcal/mol |
| IsrR-<br>$\Delta$ C2 | <pre>           18           35                         5'-AAG..UAUAA  AUCAA  CAUUA..GAC-3'   AAAUGU  GGGGGAU                                      UUUGCA  CCCCCUA 3'-UGU..CUUGC  ACACC  CAAGA..GUU-5'                                   48           31           </pre>  | E= -12,8 kcal/mol  |
|                      |  | HE= -15,9 kcal/mol |
| IsrR-<br>$\Delta$ C3 | <pre>           18           35                         5'-AAG..UAUAA  AUCAA  CAUUA..GAC-3'   AAAUGU  GGGGGAU                                      UUUGCA  CCCCCUA 3'-UGU..CUUGC  ACACC  CAAGA..GUU-5'                                   48           31           </pre>  | E= -12,7 kcal/mol  |
|                      |  | HE= -15,9 kcal/mol |

**B**

|                      |  |                    |
|----------------------|--|--------------------|
| IsrR-<br>$\Delta$ C1 | <pre>           52           68                         5'-AAC..UAUGG  AUUA  UGAAG..UUA-3'   GGGGAA  UGAAGAU                                      CCCC UU  ACUUUUA 3'-UGU..AUUUU  AUAA  CUGGU..GUU-5'                                   77           61           </pre> | E= -6,5 kcal/mol   |
|                      |  | HE= -13,8 kcal/mol |
| IsrR-<br>$\Delta$ C2 | <pre>           49           55                         5'-AAC..AUUUA  AAUU..UUA-3'                                   UGGGGG                           ACCCCCC 3'-UGU..GCAAC  CUACA..GUU-5'                                   40           34           </pre>   | E= -11,9 kcal/mol  |
|                      |  | HE= -14,7 kcal/mol |
| IsrR-<br>$\Delta$ C3 | <pre>           49           55                         5'-AAC..AUUUA  AAUU..UUA-3'                                   UGGGGG                           ACCCCCC 3'-UGU..GCAAC  CUACA..GUU-5'                                   40           34           </pre>   | E= -11,8 kcal/mol  |
|                      |  | HE= -14,6 kcal/mol |

IntaRNA predictions (5) for pairings between IsrR and *citB* mRNA (A) or *ccpE* mRNA (B). Blue sequences, SD; red sequences, Cs; E, Energy; HE, Hybridization energy.

## Figure S5. Enzymatic and RBP aconitase sites

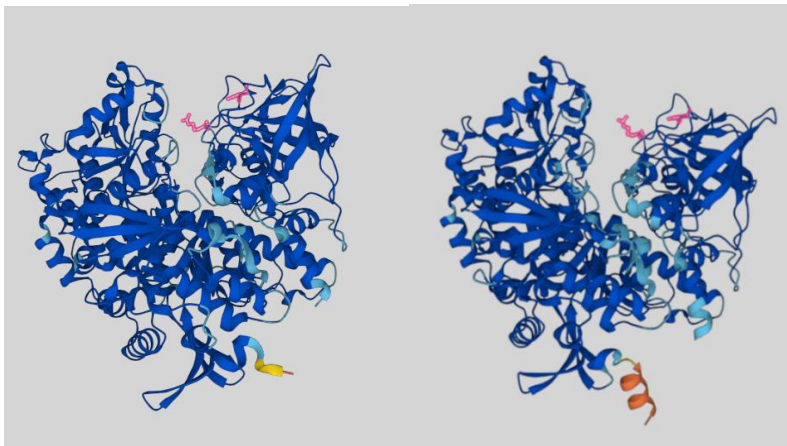
A

```

Homo_sapiens      K-TFIYDNTFEFTLAHGSVVIAAITSCTNTSNPSVMLGAGLLAKKAVDAGLNVMPIKTSL 451
Escherichia_coli PVDYVMNGHQYQLPDGAVVIAAITSCTNTSNPSVLMAGLLAKKAVTLGLKRQPWVKASL 469
Staphylococcus_aureus AEINFKDGSKATMKTGDIATAAITSCTNTSNPYVMLGAGLVAKKAVEKGLKVPEYVKTSL 477
Bacillus_subtilis IKFKLLNGEETVMKTAIAIAAITSCTNTSNPYVLIAGLVAKKAVELGLKVPNYVKTSL 471
      . : . : : * : .*****★***** * : .***:***** **: : :*:**

...
Homo_sapiens      RRGNDAVMARGTFANIRLLNRFINK-QAPQTIHLPSGEILDVFDAAERYQQAGLPLIVLA 750
Escherichia_coli RRGNHEVMVRGTFANIRIRNEMVPGVEGGMTRHLPDSVVSIIYDAAMRYKQEQTFLAVIA 768
Staphylococcus_aureus RRGNHEVMVRGTFANIRIKNQLAPGTEGGFTTYWPTNEVMPIFDAAMKYKEDGTGLVVLA 777
Bacillus_subtilis RRGNHEVMVRGTFANIRIKNQIAPGTEGGFTTYWPTGEVTSIIDACMKYKEDKTGLVVLA 771
      ****. ** *****★: * : . : . * : * . : : :*: . : : : * * :*
  
```

B

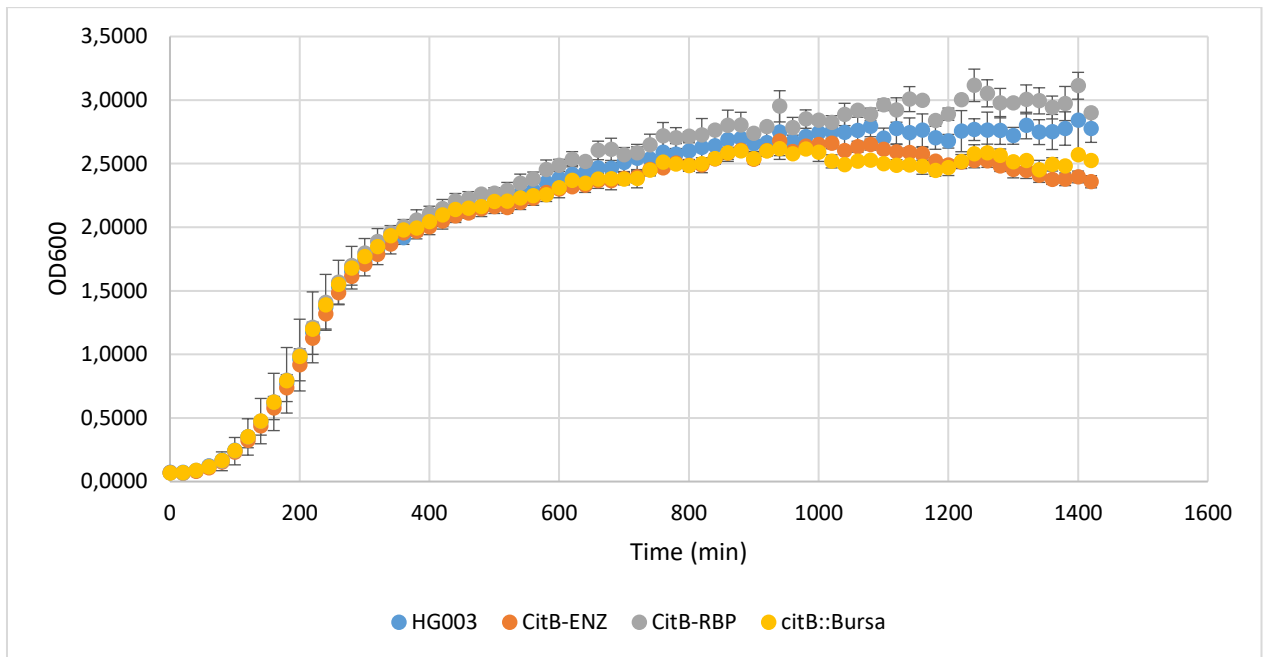


C

|                            |     |     |            |     |            |     |            |     |     |
|----------------------------|-----|-----|------------|-----|------------|-----|------------|-----|-----|
| CitB                       | A   | I   | T          | S   | C          | T   | N          | T   | S   |
| <i>citB</i>                | GCA | ATT | ACA        | TCA | TGT        | ACA | AAT        | ACA | TCT |
| CitB <sub>ENZ</sub>        | A   | I   | T          | S   | <b>S</b>   | T   | N          | T   | S   |
| <i>citB</i> <sub>ENZ</sub> | GCA | ATT | ACA        | TCA | <b>TCA</b> | ACA | AAT        | ACA | TCT |
| CitB                       | N   | I   | R          | I   | K          | N   | Q          | L   | A   |
| <i>citB</i>                | AAT | ATA | CGT        | ATT | AAA        | AAC | GAA        | TTA | GCG |
| CitB <sub>RBP</sub>        | N   | I   | <b>E</b>   | I   | K          | N   | <b>E</b>   | L   | A   |
| <i>citB</i> <sub>RBP</sub> | AAT | ATA | <b>GAA</b> | ATT | AAA        | AAC | <b>GAA</b> | TTA | GCG |

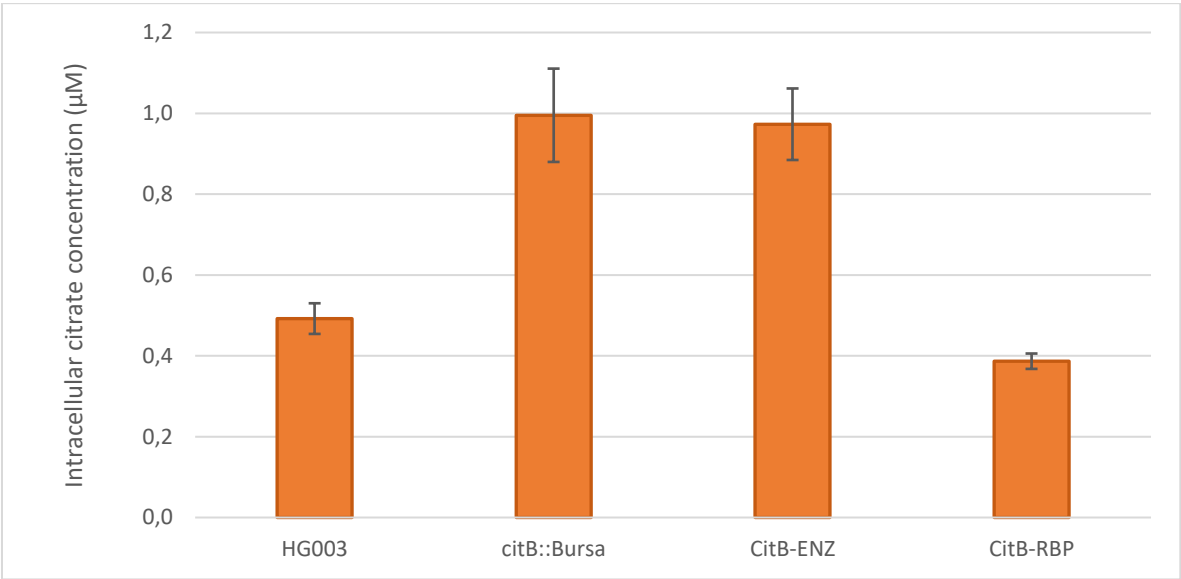
A) Clustal alignment of aconitases sequences from *H. sapiens*, *E. coli*, *S. aureus* and *B. subtilis* (selected regions). Red, amino acids that were changed. B) AlphaFold structures from *S. aureus* (left) and *B. subtilis* aconitases (right). The arginine and glutamine required for the RBP activity are shown in red. C) protein and DNA sequences of CitB/*citB* and mutated CitB/*citB* (selected region). Upper panel CitB<sub>ENZ</sub>/*citB*<sub>ENZ</sub>, lower panel CitB<sub>RBP</sub>/*citB*<sub>RBP</sub>.

**Figure S6. Growth in BHI of HG003 and *citB* mutant derivatives**



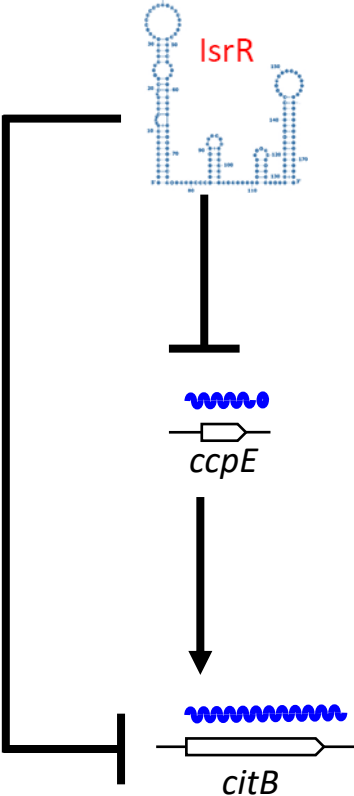
Overnight cultures were diluted 100 times and grown in rich medium (BHI) at 37°C under agitation in a microplate (Vol=200  $\mu$ L) for 24 hours. Incubation and measurement of OD600 were obtained using a Clariostar microplate reader. The *citB::Bursa* strain serve as a control for a non-functional CitB. The error bars were calculated using the standard deviation of three independent biological replicates (n=3).

**Figure S7. Intracellular citrate concentration in HG003 and *citB* mutant derivatives**



Error bars represent the standard deviation of three independent biological replicates (n=3).

Figure S8: IsrR regulation of aconitase as a feedforward loop



## References

1. Herbert, S., Ziebandt, A.K., Ohlsen, K., Schafer, T., Hecker, M., Albrecht, D., Novick, R. and Gotz, F. (2010) Repair of global regulators in *Staphylococcus aureus* 8325 and comparative analysis with other clinical isolates. *Infect Immun*, **78**, 2877-2889.
2. Fey, P.D., Endres, J.L., Yajjala, V.K., Widhelm, T.J., Boissy, R.J., Bose, J.L. and Bayles, K.W. (2013) A genetic resource for rapid and comprehensive phenotype screening of nonessential *Staphylococcus aureus* genes. *mBio*, **4**, e00537-00512.
3. de Jong, N.W., van der Horst, T., van Strijp, J.A. and Nijland, R. (2017) Fluorescent reporters for markerless genomic integration in *Staphylococcus aureus*. *Sci Rep*, **7**, 43889.
4. Coronel-Tellez, R.H., Pospiech, M., Barrault, M., Liu, W., Bordeau, V., Vasnier, C., Felden, B., Sargueil, B. and Bouloc, P. (2022) sRNA-controlled iron sparing response in Staphylococci. *Nucleic Acids Research*, **50**, 8529-8546.
5. Mann, M., Wright, P.R. and Backofen, R. (2017) IntaRNA 2.0: enhanced and customizable prediction of RNA-RNA interactions. *Nucleic Acids Research*, **45**, W435-W439.

**G: *Staphylococcal*sRNA IsrR down-regulates methylthiotransferase MiaB under iron-deficient conditions**

---

***Staphylococcal* sRNA IsrR down-regulates methylthiotransferase MiaB  
under iron-deficient conditions**

Maxime Barrault\*, Elise Leclair\*, and Philippe Bouloc#

Université Paris-Saclay, CEA, CNRS, Institute for Integrative Biology of the Cell (I2BC), 91198 Gif-sur-Yvette, France

N° ORCID:

- Maxime Barrault: [0000-0003-3949-7598](https://orcid.org/0000-0003-3949-7598)
- Elise Leclair: [0009-0000-3706-6554](https://orcid.org/0009-0000-3706-6554)
- Philippe Bouloc: [0000-0003-4601-3387](https://orcid.org/0000-0003-4601-3387)

\*Contributed equally.

#Correspondence: [philippe.bouloc@i2bc.paris-saclay.fr](mailto:philippe.bouloc@i2bc.paris-saclay.fr)

**Running title:** Staphylococcal sRNA IsrR down-regulates *miaB*.

**Keywords:** *Staphylococcus aureus*, IsrR, iron homeostasis, [Fe-S] clusters, small regulatory RNA, translational regulation.

## ABSTRACT

*Staphylococcus aureus* is a major contributor to bacterial-associated mortality, owing to its exceptional adaptability across diverse environments. Iron, vital for most organisms, poses toxicity risks in excess. To manage iron, *S. aureus*, like many pathogens, employs intricate systems. We have recently identified *IsrR* as a key regulatory RNA induced during iron starvation. Its role is to curtail the synthesis of non-essential iron-containing proteins under iron-depleted conditions. In this study, we unveil *IsrR*'s regulatory action on *MiaB*, an enzyme responsible for methylthio group addition to specific sites on transfer RNAs (tRNAs). We use predictive tools and reporter fusion assays to demonstrate *IsrR*'s binding to the Shine-Dalgarno sequence of *miaB* RNA, thereby impeding its translation. The effectiveness of *IsrR* hinges on the integrity of a specific C-rich region. As *MiaB* is non-essential and contains two [4Fe-4S] clusters, *IsrR* induction spares iron by downregulating *miaB*. This likely enhances *S. aureus* fitness and aids in navigating the host's nutritional immune defenses.

## IMPORTANCE

In numerous biotopes, including those found within an infected host, bacteria confront the challenge of iron deficiency. They employ various strategies to adapt to this scarcity of nutrients, one of which involves the regulation of iron-containing proteins through the action of small regulatory RNAs. In our study, we demonstrate how *IsrR*, a small RNA from *S. aureus*, inhibits the translation of *MiaB*, a tRNA-modifying enzyme containing [Fe-S] clusters. Through this illustration, we shed light on a novel substrate for a small RNA sparing iron, thereby unveiling a way by which bacteria conserve their iron resource.

## INTRODUCTION

*Staphylococcus aureus* is the leading cause of bacteria-associated mortality worldwide (1). Its pathogenicity is due to its adaptability across various biotopes and the expression of multiple virulence determinants. Iron is a trace element universally required for growth, but toxic in excess. *S. aureus*, akin to other pathogens, possesses elaborate systems for maintaining its intracellular iron homeostasis to match environmental conditions (2).

We recently identified and characterized *IsrR*, a regulatory RNA of *S. aureus*, contributing to an adaptive response to iron scarcity (3). By restricting non-essential iron-containing protein synthesis, *IsrR* spares iron for indispensable functions. *isrR* expression is repressed by the ferric uptake regulator (Fur) which is active in iron-rich environments. Induced during iron deficiency, *IsrR* targets Shine-Dalgarno motifs on mRNAs coding for iron-containing proteins, notably restraining translation of specific mRNAs (*fdhA*, *narG*, *nasD*, and *gltB2*) linked to nitrate respiration and encoding [Fe-S] cluster-dependent enzymes. Given the limited iron demands, fermentative pathways gain favor under limited iron conditions. *IsrR* is a functional analog from *E. coli* *RyhB* (4) and of other sRNAs found in diverse bacterial species (reviewed in (5, 6)) sharing targets and iron regulation. These similarities highlight a common evolutionary pressure, although *IsrR* is not an ortholog of these sRNAs, hinting at convergent evolution.

Hosts prevent pathogen growth through an arsenal of defense mechanisms, one of which, known as nutritional immunity, is the sequestration of nutrients such as iron (7). We reported that *IsrR* deficiency results in reduced virulence of *S. aureus* in a murine infection model, highlighting the role of *IsrR* in facilitating optimal spread of *S. aureus* in the host environment, probably critical for evasion of nutritional immunity (3).

Here, we demonstrate that *IsrR* downregulates *miaB* encoding a non-essential protein containing [Fe-S] clusters. This new example shows that *IsrR* is a central player in the maintenance of iron homeostasis in *S. aureus*.

## **MATERIALS AND METHODS**

### **Bacterial strains, plasmids and growth conditions**

Bacterial strains, plasmids and primers used for this study are described in Table 1. Plasmids were engineered by Gibson assembly (8) in *Escherichia coli* IM08B (9) as described (Table 1), using the indicated appropriate primers for PCR amplification. Plasmids were verified by DNA sequencing and then transferred into *S. aureus*.

*S. aureus* strains were grown aerobically in Brain Heart Infusion (BHI) broth at 37°C. *E. coli* strains were grown aerobically in Luria-Bertani (LB) broth at 37°C. Antibiotics were added to media as needed: ampicillin 100 µg/ml and chloramphenicol 20 µg/ml for *E. coli*; chloramphenicol 5 µg/ml and kanamycin 60 µg/ml for *S. aureus*. Iron-depleted media was obtained by the addition of DIP (2,2'-dipyridyl) 0.5 mM incubated for 30 min prior to any use.

### **Biocomputing analysis**

Pairing predictions between IsrR and the mRNA targets were made using IntaRNA (10) set with default parameters except for suboptimal interaction overlap set to “can overlap in both”. The sequences used for IsrR and mRNA targets were extracted from the *S. aureus* NCTC8325 strain (NCBI RefSeq NC\_007795.1). For the mRNA targets, the sequences used started at the TSS when known (e.g., EMOTES (11)) or were arbitrarily made to start at nucleotide -60 with respect to the +1 of translation. The sequences contain the 5' UTR and the 17 first codons of the CDS. Statistical analysis were made using a t-test. Error bars represent the 95% confidence interval following a Student's test.

### **Western blot analysis**

The chromosomal *miaB-flag* reporter gene was constructed as described (Table 1). Strains were grown overnight with and without DIP. Protein extracts were prepared as follows: 4 mL of the bacterial culture were harvested by centrifugation at 4°C and 4500 RPM for 5 minutes. The resulting pellet was resuspended in 400 µL of 50 mM Tris-HCl. Cell disruption was achieved using a Fast-Prep homogenizer (MP Biomedicals). After disruption, protein extracts were obtained by centrifugation at 4°C and 15000 RPM for 15 minutes. The protein concentration of each extract was determined using the Bradford protein assay method. Ten µg of each protein extract were loaded onto a NuPAGE 4%-12% Bis-Tris gel. Electrophoresis was carried out at 150V for 45 minutes.

Proteins were transferred from the gel to a PVDF membrane using the iBind system (Invitrogen). Immunolabeling was performed overnight with a rabbit anti-Flag antibody. After incubation with the primary antibody, an anti-rabbit IgG HRP-conjugated antibody (Promega) was used for detection. The iBlot system (Invitrogen) was employed for antibody incubation. Images of the immunolabeled membrane were acquired using a ChemiDoc MP imaging system (Bio-Rad).

### **Fluorescent translational reporter assay**

A *miaB* translational reporter ( $P_{sarA}$ -5'*miaB*-*mAm*) was inserted between genes *SAOUHSC\_00037* and *SAOUHSC\_00039* in HG003 and HG003  $\Delta$ *isrR*::*tag135* using pRN112-5'*miaB* (Table 1), a pRN112 derivative, as described (12). Notably, the mAmetrine reporter gene (*mAm*) was placed in-frame and downstream *miaB* 18<sup>th</sup> codon with the *miaB* 5'UTR placed under the control of the P1 promoter of *sarA* ( $P1_{sarA}$ ). Subsequently, the strains carrying the reporter fusion were transformed with plasmids expressing *isrR*, along with its various derivatives featuring CRR deletions. These plasmids are pRMC2 $\Delta$ R-*IsrR*, pRMC2 $\Delta$ R-*IsrR* $\Delta$ C1, pRMC2 $\Delta$ R-*IsrR* $\Delta$ C2, pRMC2 $\Delta$ R-*IsrR* $\Delta$ C3, pRMC2 $\Delta$ R-*IsrR* $\Delta$ C1C2, pRMC2 $\Delta$ R-*IsrR* $\Delta$ C1C3, pRMC2 $\Delta$ R-*IsrR* $\Delta$ C2C3, and pRMC2 $\Delta$ R-*IsrR* $\Delta$ C1C2C3. For fluorescence measurements, the transformed strains were cultured overnight in BHI medium supplemented with chloramphenicol and DIP. Subsequently, cultures were washed three times with 1x phosphate-buffered saline (PBS). Fluorescence levels were quantified using a microplate reader (CLARIOstar) with excitation at 425 nm and emission at 525 nm. To ensure accuracy, fluorescence measurements were normalized by subtracting the auto-fluorescence of the HG003 strain (lacking the reporter construct), and all cultures were adjusted to an optical density at 600 nm ( $OD_{600}$ ) of 1.

## RESULTS

### MiaB is a putative IsrR-target

We used CopraRNA (13), a software designed for predicting targets of bacterial sRNAs across diverse species, to unveil potential targets of IsrR. Given its conservation throughout the *Staphylococcus* genus, CopraRNA emerged as an efficient tool for IsrR target prediction, resulting in the successful validation of four of its targets as reported (3). Among the predicted targets, was the *miaB* messenger RNA (3, 14). The latter encodes MiaB, a methylthiotransferase catalyzing the addition of a methylthio group ( $ms^2$ ) to isopentenyl adenine ( $i^6A$ ) at position 37 ( $ms^2i^6A-37$ ) of transfer RNA (tRNA) anticodons (15). This modification present in most tRNAs reading codons starting with a U is conserved from bacteria to human (16) contributing to stabilizes the codon–anticodon interaction (17) and affects translational accuracy (18).

To substantiate the proposed interaction between IsrR and *miaB* mRNA, we use the IntaRNA software (10). Our inputs were the complete IsrR sequence and the *miaB* 5' untranslated region (UTR) with 25 codons. IsrR is characterized by three single-stranded C-rich regions, denoted as CRR1, CCR1, and CRR3 (3). These sequences are common features among Firmicutes' regulatory RNAs binding to mRNAs (19). IntaRNA analysis indicated the potential pairing of IsrR with the Shine-Dalgarno sequence of the *miaB* RNA (Figure 1). The pairing involves 55 nucleotides, a significant energy of a predicted RNA-RNA score of -22.33 kcal/mol and the GCCCG of CCR3 being likely the seed motif of the interaction.

### IsrR-dependent reduction of MiaB expression

To explore the potential influence of IsrR on *miaB* expression, a gene fusion was constructed wherein the native *miaB* gene was replaced by a copy harboring the complete *miaB* open reading frames extended with a C-terminal Flag sequence (Figure 2A). The resulting MiaB-Flag fusion protein was detectable through anti-Flag antibodies, thereby serving as a quantifiable surrogate for wild-type gene expression levels. This reporter fusion was integrated into the chromosomes of both HG003 and its corresponding  $\Delta isrR::tag135$  isogenic derivative. Western blot analyses conducted on HG003 cultures cultivated under nutrient-rich conditions unveiled an unaltered MiaB-Flag abundance, irrespective of the presence or absence of *isrR*. This status quo was in line with the known Fur-mediated repression of *isrR* under iron-replete

conditions. However, introducing the iron chelator 2,2'-dipyridyl (DIP) into the growth medium elicits a release from Fur repression, consequently inducing *IsrR* expression (3). Remarkably, under DIP-induced conditions, no MiaB-Flag was detected regardless of the *isrR* background (Figure 2B). This result is interpreted as iron depletion leading to apo-MiaB being unstable. To overcome this issue, a *fur::tet* allele (20) was introduced by phage-mediated transduction in the *miaB-flag* and  $\Delta$ *isrR miaB-flag* strains rendering *isrR* constitutively expressed (3). Expectedly, in this genetic background, MiaB-Flag was barely visible in the *fur* strain as opposed to its *fur*  $\Delta$ *isrR* derivative (Figure 2C).

### **IsrR-mediated post-transcriptional regulation of *miaB* expression**

In the absence of Fur, *isrR* is expressed and *miaB* is downregulated; the observation is explained by the base pairing interaction between *IsrR* and *miaB* RNA, putatively inhibiting *miaB* RNA translation. To examine this hypothesis, a genetic reporter system, based on pRN112 (12), was constructed wherein the 5' untranslated region (5'UTR) of *miaB*, along with an additional 54 nucleotides, was cloned under the transcriptional control of the P1 *sarA* promoter (P1<sub>*sarA*</sub>) (Figure 3A). Furthermore, to monitor the translation from this leader sequence, the mAmetrine gene (*mAm*) was inserted in-frame downstream of this sequence. The resulting fluorescence served as a proxy for *miaB* expression levels independently of its transcriptional regulation. To mitigate concerns associated with multi-copy reporter plasmids, the P1<sub>*sarA*</sub>*miaB\_5'UTRmAm* construct was integrated into the chromosome of both HG003 strain and its *isrR::tag135* derivative. As for the endogenous *miaB*, the 5'UTR*miaB*-*mAm* reporter exhibited significant downregulation under iron-starved conditions in an *IsrR*-dependent manner, while its transcription was driven from P1<sub>*sarA*</sub> (Figure 3B). Our experimental findings conclusively demonstrate that *IsrR* exerts its regulatory influence at the translational level.

### **The C-rich region 3 (CRR3) of *IsrR* plays a pivotal role in the downregulation of *miaB* mRNA.**

Pairing interactions between sRNAs and their targets are initiated by a kissing complex between single-stranded regions, which then propagates within both partners (21). sRNAs can have multiple seed regions, usually C-rich in *S. aureus* (19), specific to given targets as exemplified by RNAIII (review in (22)) or with redundant activities as in RsaE (23). To determine specific regions of *IsrR* responsible for its regulatory activity

against *miaB* mRNA, experiments using the HG003  $\Delta$ *isrR::tag135* strain, harboring the 5'UTR *miaB* fluorescent reporter were conducted. Plasmids expressing various IsrR derivatives, including wild-type IsrR, IsrR lacking CRR1, CRR2, CRR3, or all three CRRs were used. *isrR* was placed under the control of the *tet* promoter ( $P_{tet}$ ) in the absence of the Tet repressor (TetR), although it should be noted that a Fur binding site is present within the transcribed sequence (3). Consequently, we supplemented the growth media with DIP to prevent a Fur repression on *isrR* expression.

The presence of a plasmid expressing IsrR markedly diminished the fluorescence of the reporter fusion when compared to a control plasmid or a plasmid expressing IsrR with no CRR motif. In contrast, the deletion of CRR3 resulted in a significant increase in mAmetrine fluorescence. However, the deletion of CRR1 and CRR2 in isolation had no substantial impact on IsrR's activity against the *miaB* 5'UTR reporter (Figure 3C). This observation suggests that these two motifs may either be dispensable for the regulatory activity or possess redundant functions with respect to the *miaB* 5'UTR.

To discern between these possibilities, we introduced into the  $\Delta$ *isrR::tag135* strain plasmids expressing different *isrR* derivatives with deletions of two CRRs. As expected, strains carrying alleles with the CRR3 deletion (*isrR* $\Delta$ C1C3 and *isrR* $\Delta$ C2C3) failed to complement the  $\Delta$ *isrR* allele. In contrast, *isrR* $\Delta$ C1C2 was still capable of downregulating the fluorescence of the  $P_{sarA}$ *miaB*\_5'UTR*mAm* reporter (Figure 3C). These findings align with the results obtained from IntaRNA analysis, which indicates that the *IsrR/miaB* mRNA pairing energy remains substantial as long as CRR3 and its surrounding region remain intact (Figure 1).

It is worth noting that the requirement for CRRs in IsrR activity appears to be contingent upon its target mRNA (Figure 4). For instance, the absence of CRR3 does not impede the downregulation of *gltB2* and *fdhA* mRNAs (3). Conversely, for the latter mRNAs, the integrity of both CRR1 and CRR2 is indispensable, presenting a contrast to *miaB* mRNA regulation. This observation suggests that the acquisition of multiple CRRs, together with their adjacent regions, confers on regulatory RNAs the ability to control a wider range of target mRNAs. sRNAs likely evolve by acquiring new domains to interact with different targets (*e.g.* *miaB* RNA vs *gltB2* mRNA). At the same time, mRNAs may evolve to adapt to the sRNA motifs that are available (*e.g.* *gltB2* RNA vs *fdhA* mRNA).

## DISCUSSION

The relationship between iron metabolism and the MiaB enzyme has been a subject of scientific interest for several decades. As far back as the 1960s, researchers noted the absence of certain tRNA modifications in *E. coli* cultured in iron-free media, underscoring the connection between iron availability and tRNA modifications (24). Subsequent investigations revealed that the *miaB* gene encodes the tRNA methylthiotransferase responsible for these modifications, and mutations in *miaB* were found to reduce decoding efficiencies under specific conditions (15). Notably, MiaB contains two [4Fe-4S] clusters, and under iron-starved conditions, these clusters become depleted, rendering MiaB inactive (25). Furthermore, as shown here, in iron-starved condition, MiaB-Flag was not detectable suggesting that in the absence of iron cluster, MiaB is degraded.

In *E. coli*, MiaB's influence extends to the regulation of Fur through a distinctive mechanism (26). The *fur* gene is preceded by *uof*, an open reading frame located “upstream of fur”, and the translation of *fur* is tightly coupled to that of *uof*. An intriguing aspect of this regulatory relationship is the presence of a codon UCA, decoded by a MiaB-dependent tRNA<sup>Ser</sup>. Consequently, efficient *uof/fur* translation relies on functional MiaB. When iron-starvation conditions prevail, MiaB becomes inactive, impairing tRNA methylthiolation. This, in turn, leads to reduced *uof/fur* translation, ultimately favoring the expression of iron uptake genes. However, this regulation is not conserved in *S. aureus* since no *uof*-like sequence was observed.

In standard laboratory conditions, Enterobacteria appear to be resilient to the absence of MiaB (27). Despite limited knowledge regarding MiaB in staphylococci, similar trends are observed in other bacterial species, where MiaB is not essential (28). Consequently, inhibiting MiaB synthesis is likely to have minimal or no discernible consequences in various growth conditions. Since MiaB relies on [Fe-S] clusters as cofactors, suppressing its synthesis in iron-starved environments spares iron, allowing it to be redirected toward essential cellular processes.

This iron conservation strategy is exemplified by IsrR in *S. aureus*, which prevents *miaB* translation upon induction in iron-depleted conditions, thus likely contributing to improved bacterial fitness. Surprisingly, in *E. coli*, RyhB does not target *miaB* mRNA presumably because its function is critical to some cellular functions in this organism (29). Notably, inhibition of *miaB* RNA translation by a sRNA associated with the iron-

sparing response is a novel feature that has not been reported in other organisms than *S. aureus* to date.

## **ACKNOWLEDGMENTS**

This work was funded by the *Agence Nationale pour la Recherche* (ANR) ANR grant [ANR-19-CE12-0006-01 (sRNA-RRARE)] and by the *OI Microbes* from the *Université Paris-Saclay*. MB was the recipient of fellowships from the *Ministère de l'enseignement supérieur et de la recherche*. We thank our lab colleagues and Dos Equis for helpful discussions and warm support.

## REFERENCES

1. Collaborators GBDAR. 2023. Global mortality associated with 33 bacterial pathogens in 2019: a systematic analysis for the Global Burden of Disease Study 2019. *Lancet* 400:2221-2248.
2. Sheldon JR, Laakso HA, Heinrichs DE. 2016. Iron acquisition strategies of bacterial pathogens. *Microbiol Spectr* 4.
3. Coronel-Tellez RH, Pospiech M, Barrault M, Liu W, Bordeau V, Vasnier C, Felden B, Sargueil B, Bouloc P. 2022. sRNA-controlled iron sparing response in *Staphylococci*. *Nucleic Acids Research* 50:8529-8546.
4. Masse E, Gottesman S. 2002. A small RNA regulates the expression of genes involved in iron metabolism in *Escherichia coli*. *Proc Natl Acad Sci U S A* 99:4620-5.
5. Chareyre S, Mandin P. 2018. Bacterial iron homeostasis regulation by sRNAs. *Microbiol Spectr* 6.
6. Oglesby-Sherrouse AG, Murphy ER. 2013. Iron-responsive bacterial small RNAs: variations on a theme. *Metallomics* 5:276-86.
7. Murdoch CC, Skaar EP. 2022. Nutritional immunity: the battle for nutrient metals at the host-pathogen interface. *Nat Rev Microbiol* 20:657-670.
8. Gibson DG. 2011. Enzymatic assembly of overlapping DNA fragments. *Methods in Enzymology* 498:349-61.
9. Monk IR, Tree JJ, Howden BP, Stinear TP, Foster TJ. 2015. Complete bypass of restriction systems for major *Staphylococcus aureus* lineages. *MBio* 6:e00308-15.
10. Mann M, Wright PR, Backofen R. 2017. IntaRNA 2.0: enhanced and customizable prediction of RNA-RNA interactions. *Nucleic Acids Research* 45:W435-W439.
11. Prados J, Linder P, Redder P. 2016. TSS-EMOTE, a refined protocol for a more complete and less biased global mapping of transcription start sites in bacterial pathogens. *BMC Genomics* 17:849.
12. de Jong NW, van der Horst T, van Strijp JA, Nijland R. 2017. Fluorescent reporters for markerless genomic integration in *Staphylococcus aureus*. *Sci Rep* 7:43889.
13. Wright PR, Georg J, Mann M, Sorescu DA, Richter AS, Lott S, Kleinkauf R, Hess WR, Backofen R. 2014. CopraRNA and IntaRNA: predicting small RNA

- targets, networks and interaction domains. *Nucleic Acids Research* 42:W119-23.
14. Mader U, Nicolas P, Depke M, Pane-Farre J, Debarbouille M, van der Kooi-Pol MM, Guerin C, Derozier S, Hiron A, Jarmer H, Leduc A, Michalik S, Reilman E, Schaffer M, Schmidt F, Bessieres P, Noirot P, Hecker M, Msadek T, Volker U, van Dijl JM. 2016. *Staphylococcus aureus* transcriptome architecture: from laboratory to infection-mimicking conditions. *PLoS Genet* 12:e1005962.
  15. Esberg B, Leung HC, Tsui HC, Bjork GR, Winkler ME. 1999. Identification of the *miaB* gene, involved in methylthiolation of isopentenylated A37 derivatives in the tRNA of *Salmonella typhimurium* and *Escherichia coli*. *Journal of Bacteriology* 181:7256-65.
  16. Grosjean H, Nicoghosian K, Haumont E, Soll D, Cedergren R. 1985. Nucleotide sequences of two serine tRNAs with a GGA anticodon: the structure-function relationships in the serine family of *E. coli* tRNAs. *Nucleic Acids Research* 13:5697-706.
  17. Lim VI. 1997. Analysis of interactions between the codon-anticodon duplexes within the ribosome: their role in translation. *Journal of Molecular Biology* 266:877-90.
  18. Bouadloun F, Srichaiyo T, Isaksson LA, Bjork GR. 1986. Influence of modification next to the anticodon in tRNA on codon context sensitivity of translational suppression and accuracy. *Journal of Bacteriology* 166:1022-7.
  19. Geissmann T, Chevalier C, Cros MJ, Boisset S, Fechter P, Noirot C, Schrenzel J, Francois P, Vandenesch F, Gaspin C, Romby P. 2009. A search for small noncoding RNAs in *Staphylococcus aureus* reveals a conserved sequence motif for regulation. *Nucleic Acids Res* 37:7239-57.
  20. Horsburgh MJ, Ingham E, Foster SJ. 2001. In *Staphylococcus aureus*, Fur is an interactive regulator with PerR, contributes to virulence, and is necessary for oxidative stress resistance through positive regulation of catalase and iron homeostasis. *J Bacteriol* 183:468-75.
  21. Tomizawa J. 1984. Control of ColE1 plasmid replication: the process of binding of RNA I to the primer transcript. *Cell* 38:861-70.
  22. Felden B, Vandenesch F, Bouloc P, Romby P. 2011. The *Staphylococcus aureus* RNome and its commitment to virulence. *PLoS Pathog* 7:e1002006.
  23. Rochat T, Bohn C, Morvan C, Le Lam TN, Razvi F, Pain A, Toffano-Nioche C,

- Ponien P, Jacq A, Jacquet E, Fey PD, Gautheret D, Bouloc P. 2018. The conserved regulatory RNA RsaE down-regulates the arginine degradation pathway in *Staphylococcus aureus*. *Nucleic Acids Res* 46:8803-8816.
24. Rosenberg AH, Gefter ML. 1969. An iron-dependent modification of several transfer RNA species in *Escherichia coli*. *Journal of Molecular Biology* 46:581-4.
  25. Hernandez HL, Pierrel F, Elleingand E, Garcia-Serres R, Huynh BH, Johnson MK, Fontecave M, Atta M. 2007. MiaB, a bifunctional radical-S-adenosylmethionine enzyme involved in the thiolation and methylation of tRNA, contains two essential [4Fe-4S] clusters. *Biochemistry* 46:5140-7.
  26. Vecerek B, Moll I, Blasi U. 2007. Control of Fur synthesis by the non-coding RNA RyhB and iron-responsive decoding. *EMBO J* 26:965-75.
  27. Esberg B, Bjork GR. 1995. The methylthio group (ms<sup>2</sup>) of N<sup>6</sup>-(4-hydroxyisopentenyl)-2-methylthioadenosine (ms<sup>2</sup>io<sup>6</sup>A) present next to the anticodon contributes to the decoding efficiency of the tRNA. *Journal of Bacteriology* 177:1967-75.
  28. Fey PD, Endres JL, Yajjala VK, Widhelm TJ, Boissy RJ, Bose JL, Bayles KW. 2013. A genetic resource for rapid and comprehensive phenotype screening of nonessential *Staphylococcus aureus* genes. *mBio* 4:e00537-12.
  29. Beauchene NA, Myers KS, Chung D, Park DM, Weisnicht AM, Keles S, Kiley PJ. 2015. Impact of Anaerobiosis on Expression of the Iron-Responsive Fur and RyhB Regulons. *mBio* 6:e01947-15.
  30. Herbert S, Ziebandt AK, Ohlsen K, Schafer T, Hecker M, Albrecht D, Novick R, Gotz F. 2010. Repair of global regulators in *Staphylococcus aureus* 8325 and comparative analysis with other clinical isolates. *Infect Immun* 78:2877-89.

Table 1; Strains, plasmids, and DNA primers used in this study.

| <b>Strains</b>  |   |   |
|-----------------|---|---|
| <i>Name</i>     | <i>Background/genotype</i>  | <i>Reference or construction</i>                  |
| HG003           | as NCTC8325 <i>rsbU</i> and <i>tcaR</i> repaired  | (30)  |
| SAPhB1231       | as HG003 $\Delta$ <i>isrR::tag135</i>   | (3)   |
| SAPhB1542       | As HG003 <i>fur::tet</i>  | (3)   |
| SAPhB2338       | as HG003 P1 <sub>sarA</sub> -5'UTR <i>miaB::mAm</i> (integrated downstream of <i>sqr</i> )  | HG003 + pRN112-5'miaB                             |
| SAPhB2339       | as HG003 P1 <sub>sarA</sub> -5'UTR <i>miaB::mAm</i> (integrated downstream of <i>sqr</i> ) $\Delta$ <i>isrR::tag135</i>                                       | SAPhB1231+ pRN112-5'miaB                          |
| SAPhB2351       | as HG003 P1 <sub>sarA</sub> -5'UTR <i>miaB::mAm</i> (integrated downstream of <i>sqr</i> ) $\Delta$ <i>isrR::tag135</i> pRMC2 $\Delta$ R-IsrR                 | SAPhB2339 + pRMC2 $\Delta$ R-IsrR                 |
| SAPhB2352       | as HG003 P1 <sub>sarA</sub> -5'UTR <i>miaB::mAm</i> (integrated downstream of <i>sqr</i> ) $\Delta$ <i>isrR::tag135</i> pRMC2 $\Delta$ R-IsrR $\Delta$ C1C2C3 | SAPhB2339 + pRMC2 $\Delta$ R-IsrR $\Delta$ C1C2C3 |
| SAPhB2353       | as HG003 P1 <sub>sarA</sub> -5'UTR <i>miaB::mAm</i> (integrated downstream of <i>sqr</i> ) $\Delta$ <i>isrR::tag135</i> pRMC2 $\Delta$ R-IsrR $\Delta$ C1     | SAPhB2339 + pRMC2 $\Delta$ R-IsrR $\Delta$ C1     |
| SAPhB2354       | as HG003 P1 <sub>sarA</sub> -5'UTR <i>miaB::mAm</i> (integrated downstream of <i>sqr</i> ) $\Delta$ <i>isrR::tag135</i> pRMC2 $\Delta$ R-IsrR $\Delta$ C2     | SAPhB2339 + pRMC2 $\Delta$ R-IsrR $\Delta$ C2     |
| SAPhB2355       | as HG003 P1 <sub>sarA</sub> -5'UTR <i>miaB::mAm</i> (integrated downstream of <i>sqr</i> ) $\Delta$ <i>isrR::tag135</i> pRMC2 $\Delta$ R-IsrR $\Delta$ C3     | SAPhB2339 + pRMC2 $\Delta$ R-IsrR $\Delta$ C3     |
| SAPhB2356       | as HG003 P1 <sub>sarA</sub> -5'UTR <i>miaB::mAm</i> (integrated downstream of <i>sqr</i> ) $\Delta$ <i>isrR::tag135</i> pRMC2 $\Delta$ R-IsrR $\Delta$ C1C2   | SAPhB2339 + pRMC2 $\Delta$ R-IsrR $\Delta$ C1C2   |
| SAPhB2357       | as HG003 P1 <sub>sarA</sub> -5'UTR <i>miaB::mAm</i> (integrated downstream of <i>sqr</i> ) $\Delta$ <i>isrR::tag135</i> pRMC2 $\Delta$ R-IsrR $\Delta$ C1C3   | SAPhB2339 + pRMC2 $\Delta$ R-IsrR $\Delta$ C1C3   |
| SAPhB2358       | as HG003 P1 <sub>sarA</sub> -5'UTR <i>miaB::mAm</i> (integrated downstream of <i>sqr</i> ) $\Delta$ <i>isrR::tag135</i> pRMC2 $\Delta$ R-IsrR $\Delta$ C2C3   | SAPhB2339 + pRMC2 $\Delta$ R-IsrR $\Delta$ C2C3   |
| SAPhB2366       | as HG003 <i>miaB-flag</i>   | HG003 + pIMmiaBflag                               |
| SAPhB2367       | as HG003 <i>miaB-flag</i> , $\Delta$ <i>isrR::tag135</i>  | SAPhB1231+ pIMmiaBflag                            |
| SAPhB2374       | as HG003 <i>miaB-flag</i> , <i>fur::tet</i>   | SAPhB2366 + $\phi$ 80 on SAPhB1542                |
| SAPhB2376       | as HG003 <i>miaB-flag</i> , <i>fur::tet</i> , $\Delta$ <i>isrR::tag135</i>  | SAPhB2367+ $\phi$ 80 on SAPhB1542                 |
| <b>Plasmids</b> |   |   |
| <i>Name</i>     | <i>Relevant properties</i>  | <i>Reference or construction*</i>                 |
| pRN112          | pJB28-NWMN29-30 + P1 <sub>sarA</sub> -mAmetrine   | (12)  |
| pRN112-5'miaB   | Chromosomal integration of the P1 <sub>sarA</sub> -5'miaB-mAm gene fusion between   | 2600/2906 on pRN112 +                             |

|                     |   |   |
|---------------------|---|---|
|                     | SAOUHSC_00037 and SAOUHSC_00039   | 3189/3190 on HG003  |
| pIMAY               | Chromosome engineering  | (9)   |
| pIMmiaBflag         | <i>miaB</i> gene replacement with <i>miaB-flag</i>                                      | 1536/1537 on pIMAY +<br>3229/3230 and 3231/3232 on<br>HG003 |
| pRMC2ΔR             | pRMC2 derivative with a tetR deletion.<br>Constitutive expression from P <sub>tet</sub> | (Coronel-Tellez, <i>et al.</i> , 2022)                      |
| pRMC2ΔR-IsrRΔC1     | Constitutive expression of <i>isrRΔC1</i>   | (3)   |
| pRMC2ΔR-IsrRΔC2     | Constitutive expression of <i>isrRΔC2</i>   | (3)   |
| pRMC2ΔR-IsrRΔC3     | Constitutive expression of <i>isrRΔC3</i>   | (3)   |
| pRMC2ΔR-IsrRΔC1C2   | Constitutive expression of <i>isrRΔC1C2</i>   | (3)   |
| pRMC2ΔR-IsrRΔC2C3   | Constitutive expression of <i>isrRΔC2C3</i>   | 2789/2790 on<br>pRMC2ΔR-IsrRΔC2                             |
| pRMC2ΔR-IsrRΔC1C3   | Constitutive expression of <i>isrRΔC1C3</i>   | 2667/2668 on<br>pRMC2ΔR-IsrRΔC1                             |
| pRMC2ΔR-IsrRΔC1C2C3 | Constitutive expression of <i>isrRΔC1C2C3</i>   | 2789/2790 on<br>pRMC2ΔR-IsrRΔC1C2                           |

### Primers

| Name | Sequence   |
|------|--|
| 1536 | GGTACCCAGCTTTTGTTCCTTTAGTGAGG                              |
| 1537 | GAGCTCCAATTCGCCCTATAGTGAGTCG                               |
| 2600 | TTAGTTAATTATACTAATTAATAAATGAGAAGTAAAC                      |
| 2667 | CCCTTTTATATGGTAAAAGACAATATACGTTATAACAACG                   |
| 2668 | ATTGTCTTTTACCATATAAAAAGGGGAATATTTGAAAATGA                  |
| 2789 | GATTGGTCATTTTCAAATATTTTTTATATGGTAAAAGACAATATACGTTATAACAACG |
| 2790 | GTTGTTATAACGTATATTGTCTTTTACCATATAAAAATATTTGAAAATGACCAATCC  |
| 2906 | GTTTCAAAGGTGAAGAATTATTTAC                                  |
| 3189 | TTCTCATTTTTAATTAGTTATAATTAATACTAAAATGATACGGGCAAATAGAAAGGAT |
| 3190 | AATAATTCTTCACCTTTTGAAACATCTCTCTCAGCTAAAACATCTACAG          |
| 3229 | CTAAAGGGAACAAAAGCTGGGTACCATGGTTGTTGAAGTATGGTCTA            |
| 3230 | CTTGTCGTCATCGTCTTTGTAGTCTTGAATCACCATTTCCGGCT               |
| 3231 | GACTACAAAGACGATGACGACAAGTAAATGTATAATAAAGATGACGTGTTGAAC     |
| 3232 | CTCACTATAGGGCGAATTGGAGCTCTGTCAATAGCATGTTTAGAATTAAATTA      |

\* Plasmids were constructed by isothermal assembly with the indicated PCR product(s) (8). Numbers (##) are primer pairs used for PCR amplifications on the indicated substrate. For primer sequences, see Table 1 bottom part.

## FIGURE LEGENDS

### Figure 1: Computer prediction of *IsrR* and mutated *IsrR* pairing with *miaB* mRNA

IntaRNA (10) pairing prediction of *IsrR* and *IsrR* derivatives deleted for CRR1, CRR2 or CRR3 with *miaB* mRNA. Blue sequences, SD; red sequences, CRRs; bold underline characters, GUG start codon; E, energy; HE, hybridization energy.

### Figure 2: *MiaB*-Flag reporter detection

A) Schematic representation of the *MiaB*-Flag reporter fusion. Green, 3' end of *miaB* ORF; pink, *flag* sequence; blue, native stop codon; grey, first nts of *miaB* 3' UTR. B) Western blot experiment with anti-Flag antibodies in present or absence of iron chelators (n=4). Genotypes and growth conditions are indicated. 75 kDa, non-specific signal present in all samples including Flag-less strain. 60 kDa, signals corresponding to *MiaB*-Flag. C) Western blot experiment with anti-Flag antibodies with *fur* and *fur::tet* strains (n=4) as explained in Figure 2B.

### Figure 3: Translational repression of *miaB* reporter fusion by *IsrR*

A) Chromosomal reporter fusion for detection of *IsrR* activity. Red nt; transcription start site, blue bold nts; RBS, black bold nts; start codon, underlined nts; nts in interaction with *IsrR* as predicted by IntaRNA. B) The translational activity of the *miaB-mAm* reporter fusion was quantified by growing strains HG003 and  $\Delta isrR$  HG003 harboring the fusion on BHI and BHI supplemented with DIP. Results (n=3) are normalized to  $OD_{600}=1$ . C) The  $\Delta isrR$  strain harboring the *miaB-mAm* reporter fusion was transformed with plasmids expressing different versions of *IsrR* and cultured in BHI supplemented with DIP. The translational activity of the reporter fusion was quantified by measuring the fluorescence. Results (n=3) are normalized to  $OD_{600}=1$ . \*\*, P-value < 0.01; \*\*\*, P-value < 0.001.

### Figure 4: Contribution of CRRs to downregulate different mRNA targets

Negative arrows starting for either CRR1, 2 or 3 and pointing to mRNA targets indicate CRRs required for *IsrR* activity toward the corresponding targets. Data from in vivo

results with fluorescent reporters in (3) and this work.

Table 1; Strains, plasmids, and DNA primers used in this study.

| <b>Strains</b>  |  |   |
|-----------------|--|---|
| <i>Name</i>     | <i>Background/genotype</i>   | <i>Reference or construction</i>                          |
| HG003           | as NCTC8325 <i>rsbU</i> and <i>tcaR</i> repaired   | (Herbert, <i>et al.</i> , 2010)                           |
| SAPhB1231       | as HG003 $\Delta$ <i>isrR::tag135</i>  | (Coronel-Tellez, <i>et al.</i> , 2022)                    |
| SAPhB1542       | As HG003 <i>fur::tet</i>   | (Coronel-Tellez, <i>et al.</i> , 2022)                    |
| SAPhB2338       | as HG003 P1 <sub>sarA</sub> _5'UTR <i>miaB::mAm</i> (integrated downstream of <i>sqr</i> )   | HG003 + pRN112-5' <i>miaB</i>                             |
| SAPhB2339       | as HG003 P1 <sub>sarA</sub> _5'UTR <i>miaB::mAm</i> (integrated downstream of <i>sqr</i> ) $\Delta$ <i>isrR::tag135</i>  | SAPhB1231+ pRN112-5' <i>miaB</i>                          |
| SAPhB2351       | as HG003 P1 <sub>sarA</sub> _5'UTR <i>miaB::mAm</i> (integrated downstream of <i>sqr</i> ) $\Delta$ <i>isrR::tag135</i><br>pRMC2 $\Delta$ R- <i>IsrR</i>                 | SAPhB2339 + pRMC2 $\Delta$ R- <i>IsrR</i>                 |
| SAPhB2352       | as HG003 P1 <sub>sarA</sub> _5'UTR <i>miaB::mAm</i> (integrated downstream of <i>sqr</i> ) $\Delta$ <i>isrR::tag135</i><br>pRMC2 $\Delta$ R- <i>IsrR</i> $\Delta$ C1C2C3 | SAPhB2339 + pRMC2 $\Delta$ R- <i>IsrR</i> $\Delta$ C1C2C3 |
| SAPhB2353       | as HG003 P1 <sub>sarA</sub> _5'UTR <i>miaB::mAm</i> (integrated downstream of <i>sqr</i> ) $\Delta$ <i>isrR::tag135</i><br>pRMC2 $\Delta$ R- <i>IsrR</i> $\Delta$ C1     | SAPhB2339 + pRMC2 $\Delta$ R- <i>IsrR</i> $\Delta$ C1     |
| SAPhB2354       | as HG003 P1 <sub>sarA</sub> _5'UTR <i>miaB::mAm</i> (integrated downstream of <i>sqr</i> ) $\Delta$ <i>isrR::tag135</i><br>pRMC2 $\Delta$ R- <i>IsrR</i> $\Delta$ C2     | SAPhB2339 + pRMC2 $\Delta$ R- <i>IsrR</i> $\Delta$ C2     |
| SAPhB2355       | as HG003 P1 <sub>sarA</sub> _5'UTR <i>miaB::mAm</i> (integrated downstream of <i>sqr</i> ) $\Delta$ <i>isrR::tag135</i><br>pRMC2 $\Delta$ R- <i>IsrR</i> $\Delta$ C3     | SAPhB2339 + pRMC2 $\Delta$ R- <i>IsrR</i> $\Delta$ C3     |
| SAPhB2356       | as HG003 P1 <sub>sarA</sub> _5'UTR <i>miaB::mAm</i> (integrated downstream of <i>sqr</i> ) $\Delta$ <i>isrR::tag135</i><br>pRMC2 $\Delta$ R- <i>IsrR</i> $\Delta$ C1C2   | SAPhB2339 + pRMC2 $\Delta$ R- <i>IsrR</i> $\Delta$ C1C2   |
| SAPhB2357       | as HG003 P1 <sub>sarA</sub> _5'UTR <i>miaB::mAm</i> (integrated downstream of <i>sqr</i> ) $\Delta$ <i>isrR::tag135</i><br>pRMC2 $\Delta$ R- <i>IsrR</i> $\Delta$ C1C3   | SAPhB2339 + pRMC2 $\Delta$ R- <i>IsrR</i> $\Delta$ C1C3   |
| SAPhB2358       | as HG003 P1 <sub>sarA</sub> _5'UTR <i>miaB::mAm</i> (integrated downstream of <i>sqr</i> ) $\Delta$ <i>isrR::tag135</i><br>pRMC2 $\Delta$ R- <i>IsrR</i> $\Delta$ C2C3   | SAPhB2339 + pRMC2 $\Delta$ R- <i>IsrR</i> $\Delta$ C2C3   |
| SAPhB2366       | as HG003 <i>miaB-flag</i>  | HG003 + pIM <i>miaB</i> flag                              |
| SAPhB2367       | as HG003 <i>miaB-flag</i> , $\Delta$ <i>isrR::tag135</i>   | SAPhB1231+ pIM <i>miaB</i> flag                           |
| SAPhB2374       | as HG003 <i>miaB-flag</i> , <i>fur::tet</i>  | SAPhB2366 + $\phi$ 80 on SAPhB1542                        |
| SAPhB2376       | as HG003 <i>miaB-flag</i> , <i>fur::tet</i> , $\Delta$ <i>isrR::tag135</i>   | SAPhB2367+ $\phi$ 80 on SAPhB1542                         |
| <b>Plasmids</b> |  |   |
| <i>Name</i>     | <i>Relevant properties</i>   | <i>Reference or construction*</i>                         |
| pRN112          | pJB28-NWMN29-30 + P1 <sub>sarA</sub> -mAmetrine  | (de Jong, <i>et al.</i> , 2017)                           |

|                     |   |   |
|---------------------|---|---|
| pRN112-5'miaB       | Chromosomal integration of the P1 <sub>sarA</sub> -5'miaB-mAm gene fusion between SAOUHSC_00037 and SAOUHSC_00039 | 2600/2906 on pRN112 + 3189/3190 on HG003              |
| pIMAY               | Chromosome engineering  | (Monk, <i>et al.</i> , 2015)                          |
| pIMmiaBflag         | <i>miaB</i> gene replacement with <i>miaB-flag</i>  | 1536/1537 on pIMAY + 3229/3230 and 3231/3232 on HG003 |
| pRMC2ΔR             | pRMC2 derivative with a tetR deletion. Constitutive expression from P <sub>tet</sub>                              | (Coronel-Tellez, <i>et al.</i> , 2022)                |
| pRMC2ΔR-IsrRΔC1     | Constitutive expression of <i>isrRΔC1</i>   | (Coronel-Tellez, <i>et al.</i> , 2022)                |
| pRMC2ΔR-IsrRΔC2     | Constitutive expression of <i>isrRΔC2</i>   | (Coronel-Tellez, <i>et al.</i> , 2022)                |
| pRMC2ΔR-IsrRΔC3     | Constitutive expression of <i>isrRΔC3</i>   | (Coronel-Tellez, <i>et al.</i> , 2022)                |
| pRMC2ΔR-IsrRΔC1C2   | Constitutive expression of <i>isrRΔC1C2</i>   | (Coronel-Tellez, <i>et al.</i> , 2022)                |
| pRMC2ΔR-IsrRΔC2C3   | Constitutive expression of <i>isrRΔC2C3</i>   | 2789/2790 on pRMC2ΔR-IsrRΔC2                          |
| pRMC2ΔR-IsrRΔC1C3   | Constitutive expression of <i>isrRΔC1C3</i>   | 2667/2668 on pRMC2ΔR-IsrRΔC1                          |
| pRMC2ΔR-IsrRΔC1C2C3 | Constitutive expression of <i>isrRΔC1C2C3</i>   | 2789/2790 on pRMC2ΔR-IsrRΔC1C2                        |

### Primers

| Name | Sequence   |
|------|--|
| 1536 | GGTACCCAGCTTTTGTTCCTTTAGTGAGG                              |
| 1537 | GAGCTCCAATTCGCCCTATAGTGAGTCG                               |
| 2600 | TTAGTTAATTATAACTAATTA AAAATGAGAAGTAAAC                     |
| 2667 | CCCTTTTATATGGTAAAAGACAATATACGTTATAACAACG                   |
| 2668 | ATTGTCTTTTACCATATAAAAAGGGGAATATTTGAAAATGA                  |
| 2789 | GATTGGTCATTTTCAAATATTTTTTATATGGTAAAAGACAATATACGTTATAACAACG |
| 2790 | GTTGTTATAACGTATATTGTCTTTTACCATATAAAAATATTTGAAAATGACCAATCC  |
| 2906 | GTTTCAAAGGTGAAGAATTATTTAC                                  |
| 3189 | TTCTCATTTTTAATTAGTTATAATTA ACTAAAATGATACGGGCAAATAGAAAGGAT  |
| 3190 | AATAATTCTTCACCTTTTGAAACATCTCTCTCAGCTAAAACATCTACAG          |
| 3229 | ctaaaggggaacaaaagctgggtaccATGGTTGTTGAAGTATGGTCTA           |
| 3230 | CTTGTCGTCATCGTCTTTGTAGTCTTGAATCACCATTTCCGGCT               |
| 3231 | GACTACAAAGACGATGACGACAAGTAAATGTATAATAAAGATGACGTGTTGAAC     |
| 3232 | ctcactatagggcgaattggagctcTGTC AATAGCATGTTTAGAATTAAATTA AA  |

\* Plasmids were constructed by isothermal assembly with the indicated PCR product(s) (Gibson, 2011). Numbers (##) are primer pairs used for PCR amplifications on the indicated substrate. For primer sequences, see Table 1 bottom part.



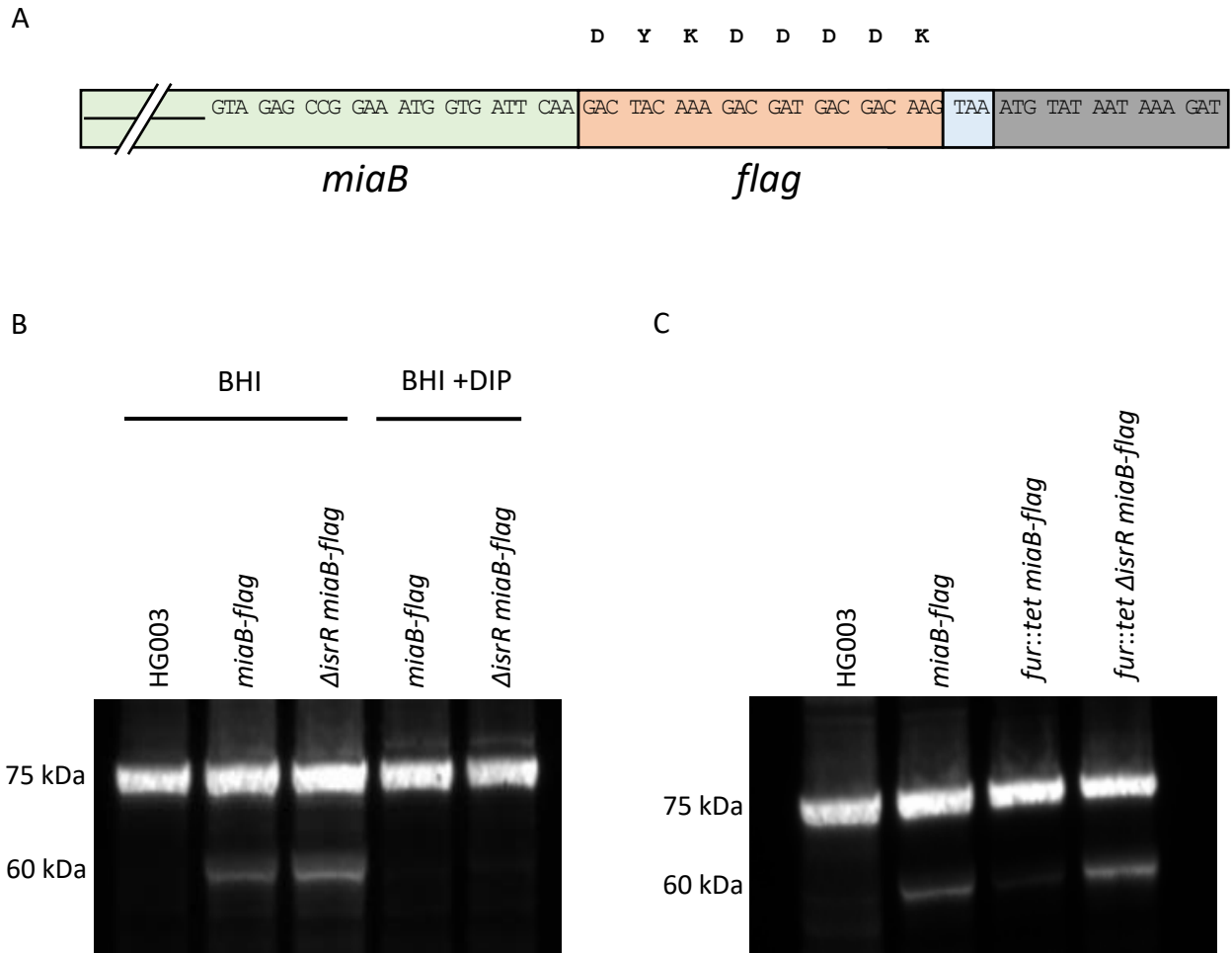


## Figure 2: MiaB-Flag reporter detection

A) Schematic representation of the MiaB-Flag reporter fusion. Green, 3' end of *miaB* ORF; pink, *flag* sequence; blue, native stop codon; grey, first nts of *miaB* 3' UTR. B) Western blot experiment with anti-Flag antibodies in present or absence of iron chelators (n=4). Genotypes and growth conditions are indicated. 75 kDa, non-specific signal present in all samples including Flag-less strain. 60 kDa, signals corresponding to MiaB-Flag. C) Western blot experiment with anti-Flag antibodies with *fur* and *fur::tet* strains (n=4) as explained in Figure 2B.

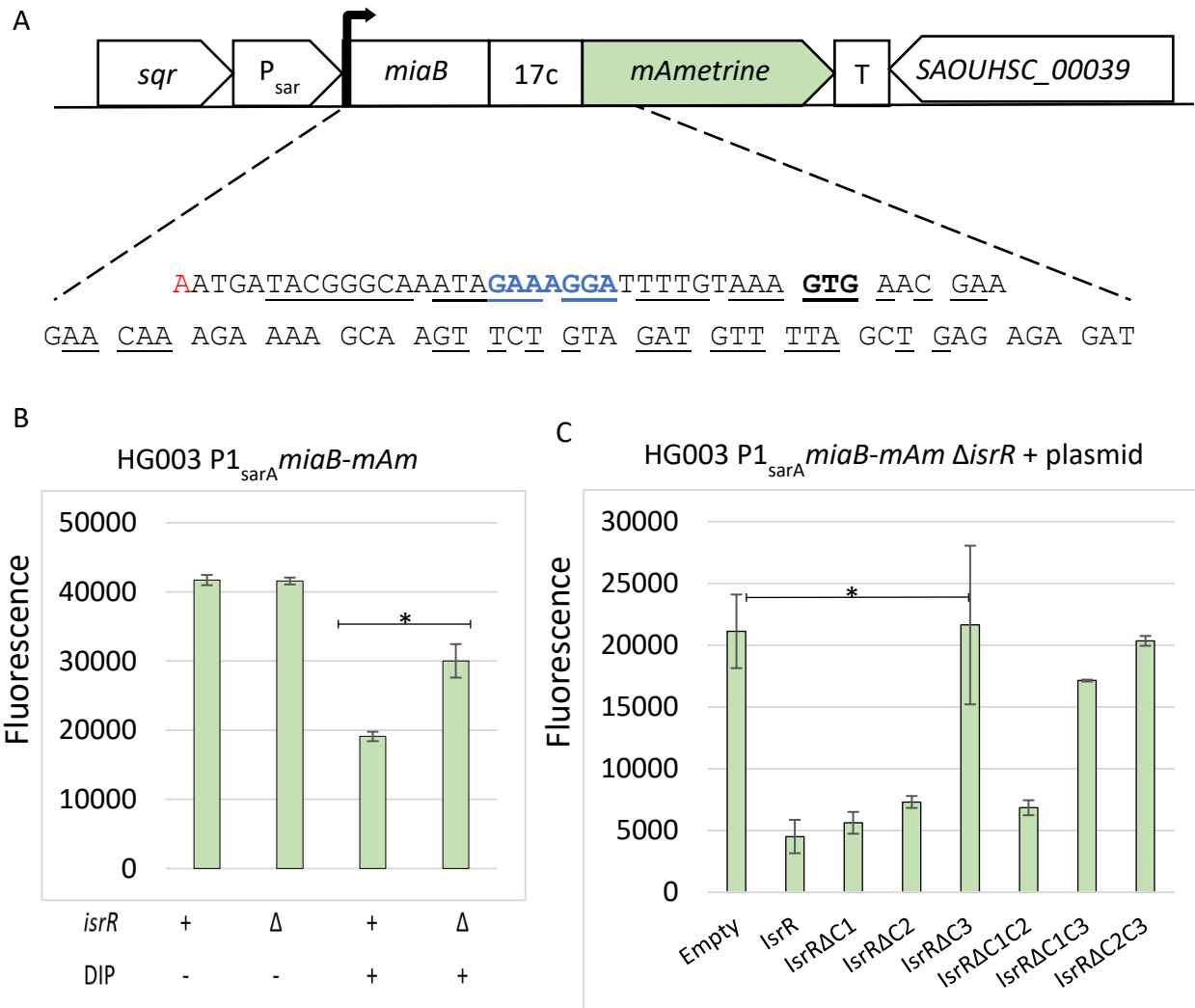


**Figure 3: Translational repression of *miaB* reporter fusion by *IsrR***

A) Chromosomal reporter fusion for detection of *IsrR* activity. Red nt; transcription start site, blue bold nts; RBS, black bold nts; start codon, underlined nts; nts in interaction with *IsrR* as predicted by IntaRNA. B) The translational activity of the *miaB-mAm* reporter fusion was quantified by growing strains HG003 and Δ*isrR* HG003 harboring the fusion on BHI and BHI supplemented with DIP. Results (n=3) are normalized to OD<sub>600</sub>=1. C) The Δ*isrR* strain harboring the *miaB-mAm* reporter fusion was transformed with plasmids expressing different versions of *IsrR* and cultured in BHI supplemented with DIP. The translational activity of the reporter fusion was quantified by measuring the fluorescence. Results (n=3) are normalized to OD<sub>600</sub>=1. \*\*, P-value < 0.01; \*\*\*, P-value < 0.001.



## H: Additional discussion

---

Pathogenic bacteria, such as *S. aureus*, have evolved to adapt to a plethora of environments, which differs in terms of physico-chemical conditions. During infection of a host, bacteria must face multiple stresses. One of them is the nutritional immunity, which consists in the sequestration of essential nutrients, such as iron, to prevent bacterial growth. In response to that, most of the bacterial pathogens have developed systems that allows them to circumvent this process by reprogramming gene expression and changing their metabolism. Most of these modifications are associated with the activity of transcriptional regulators. Thus, during iron starvation, Fur repression is released to activate a set of genes allowing an adaptation this stress condition. Among them are genes encoding iron uptake systems. In addition, In many bacteria, it was shown that Fur controls the expression of sRNA, providing an additional layer of gene regulation (Chareyre and Mandin 2018).

Recently, our lab discovered IsrR, a sRNA of *S. aureus* involved in the adaptive response to iron starvation (Coronel-Tellez et al. 2022). Notably, IsrR represses the translation of nitrate respiration genes. As nitrate respiration is not essential and requires iron, it is assumed that the general function of IsrR is to prevent the expression of non-essential genes leading to iron utilization. Thus, the spare iron can be directed to essential systems.

The use of a sRNA to regulate gene expression upon iron starvation is not specific to *S. aureus*. The first and most documented example of this mechanism is the sRNA RyhB in *E. coli* (Massé and Gottesman 2002). Since then, several sRNAs mediating the response to iron starvation have been discovered in several pathogens, but many differ in terms of their sequences, seed motifs, synteny, and targets, highlighting that this regulation, in many cases, did not emerge from horizontal transfer but is rather the result of an evolutionary convergence responding to an essential need.

We elucidated the secondary structure of IsrR alone or in interaction with *fdhA* and *gltB* mRNAs using Selective 2' Hydroxyl Acylation analyzed by Primers Extension (SHAPE). We used 1-methyl-7-nitroisatoic anhydride (1M7) as a probing agent in order to detect nucleotides located on unpaired regions of the RNA and obtain an image of its secondary structure by bioinformatics after sequencing. The advantage of using SHAPE instead of other probing techniques such as DMS or RNase probing is that the reagent used (1M7) does not have any preference for base cleavage. Our results showed that part of the nucleotides predicted to be on unpaired regions by bioinformatics predictions were showing high reactivities, thus confirming their localization. However, some of the nucleotides predicted to be on single-stranded regions, including CRRs, did not show any reactivity on SHAPE. These results could be explained by the existence of a ternary structure within IsrR itself and during the

interactions with the mRNA targets. Indeed, the bioinformatics predictions which serve as constraints for the mapping of nucleotide reactivities do not take into account the possibilities of a third player in the interaction, which could be for example an RNA chaperon. One way to bypass these limitations is to realize an *in vivo* SHAPE study (SHAPE-MaP), This method, which has already been used in *E. coli* (McGinnis et al. 2015) could be applied to *S. aureus* in order to obtain a global view of the RNA secondary structure and possibly discover putative seed motifs for sRNAs.

To characterize the functioning of IsrR, we looked for a potential RNA chaperone that might be required for its activity. Indeed the RNA chaperon Hfq is a RyhB partner to induce target degradations (Lalaouna et al. 2021). Furthermore, IsrR has stem-loop sequences which are surprisingly highly conserved between distantly related bacteria (Coronel-Tellez et al. 2022) that are a possible protein binding site. Hfq is present in *S. aureus*, however, its activity remains elusive and IsrR activity did not require Hfq on the tested substrates (Bohn, Rigoulay, and Bouloc 2007)(Coronel-Tellez et al. 2022). To find IsrR-interacting proteins, we used the MS2 affinity purification approach (Slobodin and Gerst 2010), with IsrR as bait. No proteins were enriched, leaving the question open (data not shown).

Bioinformatic predictions suggested three IsrR targets related to citrate metabolism, *citM*, *ccpE*, and *citB* mRNAs encoding a citrate transporter, a citrate-responsive regulator, and the aconitase, respectively. Citrate, and the enzymes assuring its metabolization, are part of the TCA cycle, which provides energy and amino acids essential for the functioning of the cell. However, several of the enzymes that compose it contain [Fe-S] clusters, which makes them particularly sensitive to iron starvation and oxidative stress, two conditions that the bacteria has to face during infection. As a result, these enzymes are known targets of several sRNAs expressed in these conditions (Massé, Vanderpool, and Gottesman 2005; Smaldone et al. 2012). Therefore, it seemed reasonable to assume that *citB* would be a target of IsrR. The analysis of the interaction predictions between IsrR, *citB*, and *ccpE* mRNAs revealed a potential post-transcriptional regulation in which IsrR would bind on the RBS and prevent mRNA translation. This mode of action is quite common in *S. aureus*, where sRNAs have C-rich regions (CRRs). Indeed, *S. aureus* has a very low GC content (approximately 33%). Therefore, G-rich regions, which are often RBS, are easily recognized and bound by the CRRs of sRNAs. The result for the interaction with *ccpE* mRNA was indicating an interaction between CRR1 and the RBS. In the case of *citB* mRNA, however, the predictions indicate two alternative pairings with the RBS, involving either CRR1 or CRR2/CRR3. This result is not surprising and has already been observed for other IsrR targets. However, all CRRs are necessary to get the IsrR response on all its targets.

We tested if a transcriptomic approach could be used to uncover IsrR targets. Indeed, in Gram-negative bacteria, most sRNA-mediated post-transcriptional regulation seem associated with a modification of mRNA stability with often a

degradation of target mRNAs by the action of RNases (Saramago et al. 2014). In *E. coli*, the pairing of RyhB on mRNA targets is commonly associated with an inhibition of translation and the recruitment of RNase E degrading both RyhB and its mRNA targets (Massé, Escorcia, and Gottesman 2003) (10.1101/gad.1330405). In *B. subtilis*, the iron-sparing response RNA FsrA prevents translation and provoke degradation of its mRNA targets, but the RNases involved are still unknown. In *S. aureus*, both systems seems to be present. Indeed, RNase III seems to be involved in the sRNA-associated degradation of mRNAs, such as with RNAIII (Boisset et al. 2007; Le Scornet and Redder 2019). However, our results obtained using a rifampicin assay showed that in the case of IsrR, blocking translation was not associated with mRNA degradation on two substrates (Coronel-Tellez et al. 2022). Transcriptomic data comparing WT and  $\Delta isrR$  strains indicate that IsrR do not affect mRNA quantity and therefore stability. This result illustrate the particular mode of action of IsrR. As a result, in the particular case of IsrR, the use of proteomics is particularly adapted for finding targets.

Assessment of CitB and CcpE quantities by western-blot showed a decrease in CitB and CcpE quantities upon iron starvation in the WT strain but not in the  $\Delta isrR$ , thus confirming the role of IsrR in their regulation. The advantage of using this technique is that we are able to see the effects of IsrR at the final level, but the main drawback is that we are potentially affected by other potential regulations, such as for example transcriptional regulators. Previous experiments in *S. aureus* highlighted the fact that CcpE is a transcriptional activator of *citB* sensitive to citrate concentration, like CcpC in *B. subtilis* (Kim, Jourlin-Castelli, et al. 2003). Therefore, inactivation of CcpE by IsrR should indirectly lead to a decrease in *citB* expression, which could explain western-blot results. However, transcriptomic results did not show *citB* as regulated by IsrR. This result raises a question on the effective role of CcpE regulation. Indeed, in addition to CcpE, aconitase is regulated indirectly by CcpA, which prevents CcpC expression in presence of glucose. Therefore, *citB* expression is probably activated by CcpE in late exponential phase when glucose starts to be exhausted. In *B. subtilis*, expression of *citB* is also regulated by CodY, a transcriptional regulator which mediates the transition from exponential to stationary phase (Kim, Kim, et al. 2003). Taken together, these results highlight a complex regulation of the aconitase in which its activation and more globally the activation of genes involved in the TCA cycle is a metabolic switch during the transition from exponential to stationary phase. Since RNA extracts were taken at  $OD_{600} = 1$  (meaning in exponential phase), it is possible that the effects of *ccpE* inactivation on *citB* expression could not have been seen and that the *citB* mRNA levels are corresponding to its basal expression.

We confirmed the direct interaction between IsrR and its mRNA targets using translational reporter fusions. These fusions were under the control of a constitutive promoter to bypass potential regulations that could affect *citB* or *ccpE* expression. Therefore, the observed IsrR-dependent regulations should be only post-transcriptional. Reporter genes are often used to detect gene regulation, however in *S.*

*aureus* most of them are located on plasmids. As a result, reporter fusions are generally more expressed than necessary due to plasmid copy number. To prevent these side effects that could affect results interpretation, the reporter fusions were inserted on the chromosome. The other advantage of using gene fusions inserted on the chromosome is that it could allow for direct visualization of the gene expression *in vivo* in animal models. To date, some plasmids are stabilized and can be kept in *S. aureus* cells infecting animals for up to 6 days (Rodriguez et al. 2017) but by using integrated fusions, the fluorescence could be kept as long as the cells are alive. In our case, we could imagine infecting animal models with an *isrR::mAmetrine* fusion and look where the fusion is expressed, thus indicating organs more prone to exert iron starvation.

Native IsrR expression, by DIP addition in the media, led to a decrease in the fluorescence of the *citB::mAmetrine* and *ccpE::mAmetrine* reporter fusions, thus confirming the results obtained by western blot and indicating that down-regulation of *citB* via IsrR happens directly and indirectly via down-regulation of its activator CcpE. To investigate the role of the CRRs, we used different versions of IsrR in which one or several CRRs were deleted. CRR1 only was important for the interaction with *ccpE* mRNA. For *citB* mRNA, the use of versions of IsrR deleted for two or three CRRs showed that CRR1 and CRR2 were independently active on *citB* mRNA, which is in accordance with the bioinformatics predictions. Interestingly, it is important to note that in the case of IsrR, bioinformatics predictions were so far always in accordance with the experimental results, which comforts us in the use of bioinformatics to predict novel IsrR targets in the future.

Using transcriptomics, we confirmed that *S. aureus* aconitase was autoregulated by its moonlighting activity upon iron starvation. They suggest that apo-aconitase remodels *S. aureus* metabolism by shutting off TCA cycle and promoting the formation of oxaloacetate through the pyruvate carboxylase. The moonlighting activity of aconitase is widely conserved through Eukaryotes and Prokaryotes, which is revealing of its essential role in the response to iron starvation. Our results showed that apo-CitB represses the first three steps of the TCA cycle, by decreasing *citZ*, *citB*, and *citC* mRNA quantity. Finding three adjacent enzymes involved in the TCA cycle and all repressed by apo-CitB is very unlikely to happen randomly and is rather the sign of a necessity of shutting down this metabolic pathway upon iron starvation, probably because of its high consumption of iron through [Fe-S] clusters. We also observed an increase in the *pycA* mRNA quantities when CitB had a functional RNA-binding activity. *pycA* encodes for the pyruvate carboxylase, which catalyzes the formation of oxaloacetate, which is part of the TCA cycle but also numerous metabolic pathways such as neoglucogenesis, urea cycle, fatty acids synthesis etc. By putting together the obtained results, we propose that upon iron starvation, apo-CitB acts as a metabolic switch to redirect metabolism by shutting off TCA cycle and favoring other pathways that are less iron consuming. In the past few years, numerous studies have highlighted the role of moonlighting proteins in metabolism regulation. In particular, while several studies

focused on aconitase, recent results suggest that other metabolic enzymes could also possess an RNA-binding activity (Gerovac et al. 2020). Therefore, this work is only a first step in the understanding of the roles of RBPs in the responses to environmental stresses.

We showed that the RNA-binding activity of apo-CitB on its own mRNA was independent of the IsrR regulation. Indeed, in *E. coli*, the apo-aconitase protects its own mRNA from RyhB-induced degradation by binding on the cleavage site (Benjamin and Massé 2014). However, we never observed any modification of the target mRNA stability caused by IsrR, and we observed no change in any mRNA quantities during the transcriptomics study, which indicates that IsrR solely represses the translation of its targets and that therefore, the autoregulation of CitB is independent of that. This result is another argument highlighting the differences between IsrR and RyhB

We used two reporter systems that failed to detect *citM* expression. The results align with *S. aureus* transcriptomic data in 44 grow conditions as well as our transcriptomic study showing that *citM* is poorly expressed (Mäder et al. 2016). *citM* encodes a putative citrate transporter from the CitHMS family, and indeed, *B. subtilis* CitM (sharing 31% sequence similarity of *S. aureus* CitM) imports citrate and isocitrate complexed with divalent metal ions into the cell (Krom et al. 2000). *B. subtilis*, CitM is required for growth when using citrate as the sole carbon source, and *citM* expression is triggered by the presence of 5 mM trisodium citrate or DL-isocitrate in growth media (Warner and Lolkema 2002). Despite using a growth media supplemented with trisodium citrate, we could not detect the expression of a CitM reporter fusion protein (data not shown), possibly because the proper conditions for *citM* expression were not tested. In *B. subtilis*, *citM* expression is subject to carbon catabolite repression, and therefore *citM* is strongly repressed in presence of glucose (Warner and Lolkema 2002), which could explain the absence of *citM* expression without using a specific media containing citrate as the sole carbon source (Warner and Lolkema 2002). The predicted pairing between IsrR and *citM* mRNA is on a G-rich region located before the RBS of the gene, which is unusual since all the targets confirmed up to this date had a pairing located on the RBS. In *E. coli*, RyhB is known to promote the expression of *shiA*, a gene encoding a shikimate permease which is a siderophore precursor (Prévost et al. 2007). By homology, since *citM* encodes for a citrate transporter and that citrate is a precursor of the two *S. aureus* siderophores (staphyloferrin A and B), we hypothesized that *citM* could be positively regulated by IsrR in order to stimulate siderophore production. Finding the right conditions for *citM* expression will be a necessary step to elucidate its potential regulation by IsrR and its role in siderophore production.

Additional work concluded that IsrR was preventing the translation of a new target not related to citrate metabolism: *miaB* mRNA. *miaB* encodes for a methylthiotransferase containing a [Fe-S] cluster responsible for the addition of a methylthiol group on tRNAs that reads codons starting with a U to improves the

decoding efficiency. In *E. coli*, MiaB is rapidly inactivated upon iron starvation by the loss of its [Fe-S] cluster, causing a stalling of ribosomes on the *uof-fur* mRNA, thus preventing Fur production. This phenomenon allows for a longer repression of RyhB and thus a better survival of the bacteria during iron starvation. In *S. aureus*, *fur* is in operon with *nudF* and *xerD*, but so far, no experiment has shown that these two genes could exert a role on Fur production, and there is no *uof*-like gene. Therefore, we propose that the repression of *miaB* by IsrR is only due to the fact that this enzyme possesses a [Fe-S] cluster.

These studies enlarge the panel of genes regulated by IsrR. However, they also bring new evidences for the hypothesis of an evolutionary convergence of sRNAs responding to iron starvation in bacteria. Indeed, while the regulation of aconitase by IsrR is not uncommon, as it is also found in other species (RyhB in *E. coli*, FsrA in *B. subtilis*), we also uncovered that its mode of action consists in a repression of translation but is not associated with modification of mRNA stability. However, there are still probably several targets of IsrR which remains to be identified in order to understand the extent of its regulatory network.

Furthermore, we assessed for the first time the role of apo-aconitase in the response to iron starvation in *S. aureus*. We provide transcriptomic data which suggest that apo-aconitase serve as another layer in the adaptation of the cell in response to iron starvation. The experimental confirmation of this transcriptomic data should provide exciting insights on the modification of *S. aureus* metabolism upon infection.

# I: References

---

- Abo, Tatsuhiko, Koji Ueda, Takafumi Sunohara, Kazuko Ogawa, and Hiroji Aiba. 2002. "SsrA-Mediated Protein Tagging in the Presence of Miscoding Drugs and Its Physiological Role in *Escherichia Coli*: Trans-Translation and Antibiotics." *Genes to Cells* 7 (7): 629–38. <https://doi.org/10.1046/j.1365-2443.2002.00549.x>.
- Ahmad-Mansour, Nour, Paul Loubet, Cassandra Pouget, Catherine Dunyach-Remy, Albert Sotto, Jean-Philippe Lavigne, and Virginie Molle. 2021. "Staphylococcus Aureus Toxins: An Update on Their Pathogenic Properties and Potential Treatments." *Toxins* 13 (10): 677. <https://doi.org/10.3390/toxins13100677>.
- Alen, C., and A. L. Sonenshein. 1999. "Bacillus Subtilis Aconitase Is an RNA-Binding Protein." *Proceedings of the National Academy of Sciences* 96 (18): 10412–17. <https://doi.org/10.1073/pnas.96.18.10412>.
- Allouche, Delphine, Gergana Kostova, Marion Hamon, Christophe H. Marchand, Mathias Caron, Sihem Belhocine, Ninon Christol, Violette Charteau, Ciarán Condon, and Sylvain Durand. 2023. "New RoxS sRNA Targets Identified in Bacillus Subtilis by Pulsed SILAC." Edited by Olga Soutourina. *Microbiology Spectrum*, June, e00471-23. <https://doi.org/10.1128/spectrum.00471-23>.
- Altuvia, Shoshy, Dalit Weinstein-Fischer, Aixia Zhang, Lisa Postow, and Gisela Storz. 1997. "A Small, Stable RNA Induced by Oxidative Stress: Role as a Pleiotropic Regulator and Antimutator." *Cell* 90 (1): 43–53. [https://doi.org/10.1016/S0092-8674\(00\)80312-8](https://doi.org/10.1016/S0092-8674(00)80312-8).
- Amor, Matthieu, Mickaël Tharaud, Alexandre Gélabert, and Arash Komeili. 2020. "Single-cell Determination of Iron Content in Magnetotactic Bacteria: Implications for the Iron Biogeochemical Cycle." *Environmental Microbiology* 22 (3): 823–31. <https://doi.org/10.1111/1462-2920.14708>.
- Andrews, Simon C., Andrea K. Robinson, and Francisco Rodríguez-Quiñones. 2003. "Bacterial Iron Homeostasis." *FEMS Microbiology Reviews* 27 (2–3): 215–37. [https://doi.org/10.1016/S0168-6445\(03\)00055-X](https://doi.org/10.1016/S0168-6445(03)00055-X).
- Archibald, Frederick. 1983. "*Lactobacillus Plantarum*, an Organism Not Requiring Iron." *FEMS Microbiology Letters* 19 (1): 29–32. <https://doi.org/10.1111/j.1574-6968.1983.tb00504.x>.
- Ariza-Mateos, Ascensión, Ashok Nuthanakanti, and Alexander Serganov. 2021. "Riboswitch Mechanisms: New Tricks for an Old Dog." *Biochemistry (Moscow)* 86 (8): 962–75. <https://doi.org/10.1134/S0006297921080071>.
- Arthur, David C., Ross A. Edwards, Susan Tsutakawa, John A. Tainer, Laura S. Frost, and J. N. Mark Glover. 2011. "Mapping Interactions between the RNA Chaperone FinO and Its RNA Targets." *Nucleic Acids Research* 39 (10): 4450–63. <https://doi.org/10.1093/nar/gkr025>.
- Austin, Crystal M., Ge Wang, and Robert J. Maier. 2015. "Aconitase Functions as a Pleiotropic Posttranscriptional Regulator in Helicobacter Pylori." Edited by I. B. Zhulin. *Journal of Bacteriology* 197 (19): 3076–86. <https://doi.org/10.1128/JB.00529-15>.
- Baek, Seung-Hun, Alice H. Li, and Christopher M. Sassetti. 2011. "Metabolic Regulation of Mycobacterial Growth and Antibiotic Sensitivity." Edited by Matthew K. Waldor. *PLoS Biology* 9 (5): e1001065. <https://doi.org/10.1371/journal.pbio.1001065>.

- Baker, Heather M., and Edward N. Baker. 2004. "Lactoferrin and Iron: Structural and Dynamic Aspects of Binding and Release." *BioMetals* 17 (3): 209–16. <https://doi.org/10.1023/B:BIOM.0000027694.40260.70>.
- Balaban, Naomi, and Avraham Rasooly. 2000. "Staphylococcal Enterotoxins." *International Journal of Food Microbiology* 61 (1): 1–10. [https://doi.org/10.1016/S0168-1605\(00\)00377-9](https://doi.org/10.1016/S0168-1605(00)00377-9).
- Banerjee, Sharmistha, Ashok Kumar Nandyala, Podili Raviprasad, Niyaz Ahmed, and Seyed E. Hasnain. 2007. "Iron-Dependent RNA-Binding Activity of *Mycobacterium Tuberculosis* Aconitase." *Journal of Bacteriology* 189 (11): 4046–52. <https://doi.org/10.1128/JB.00026-07>.
- Baothman, Othman A. S., Matthew D. Rolfe, and Jeffrey Green. 2013. "Characterization of Salmonella Enterica Serovar Typhimurium Aconitase A." *Microbiology* 159 (Pt\_6): 1209–16. <https://doi.org/10.1099/mic.0.067934-0>.
- Beasley, Federico C., Cristina L. Marolda, Johnson Cheung, Suzana Buac, and David E. Heinrichs. 2011. "Staphylococcus Aureus Transporters Hts, Sir, and Sst Capture Iron Liberated from Human Transferrin by Staphyloferrin A, Staphyloferrin B, and Catecholamine Stress Hormones, Respectively, and Contribute to Virulence." Edited by S. M. Payne. *Infection and Immunity* 79 (6): 2345–55. <https://doi.org/10.1128/IAI.00117-11>.
- Benito, Yvonne, Fabrice A. Kolb, Pascale Romby, Gerard Lina, Jerome Etienne, and François Vandenesch. 2000. "Probing the Structure of RNAIII, the Staphylococcus Aureus Agr Regulatory RNA, and Identification of the RNA Domain Involved in Repression of Protein A Expression." *RNA* 6 (5): 668–79. <https://doi.org/10.1017/S1355838200992550>.
- Benjamin, Julie-Anna M., and Eric Massé. 2014. "The Iron-Sensing Aconitase B Binds Its Own mRNA to Prevent sRNA-Induced mRNA Cleavage." *Nucleic Acids Research* 42 (15): 10023–36. <https://doi.org/10.1093/nar/gku649>.
- Bennett, Brittany D., Evan D. Brutinel, and Jeffrey A. Gralnick. 2015. "A Ferrous Iron Exporter Mediates Iron Resistance in *Shewanella Oneidensis* MR-1." Edited by F. E. Löffler. *Applied and Environmental Microbiology* 81 (22): 7938–44. <https://doi.org/10.1128/AEM.02835-15>.
- Bergé, Matthieu, Julian Pezzatti, Víctor González-Ruiz, Laurence Degeorges, Geneviève Mottet-Osman, Serge Rudaz, and Patrick H Viollier. 2020. "Bacterial Cell Cycle Control by Citrate Synthase Independent of Enzymatic Activity." *eLife* 9 (March): e52272. <https://doi.org/10.7554/eLife.52272>.
- Bhubhanil, Sakkarin, Jareeya Chamsing, Panida Sittipo, Paweena Chaoprasid, Rojana Sukchawalit, and Skorn Mongkolsuk. 2014. "Roles of *Agrobacterium Tumefaciens* Membrane-Bound Ferritin (MbfA) in Iron Transport and Resistance to Iron under Acidic Conditions." *Microbiology* 160 (5): 863–71. <https://doi.org/10.1099/mic.0.076802-0>.
- Biswas, Lalitha, Raja Biswas, Christiane Nerz, Knut Ohlsen, Martin Schlag, Tina Schäfer, Tobias Lamkemeyer, et al. 2009. "Role of the Twin-Arginine Translocation Pathway in *Staphylococcus*." *Journal of Bacteriology* 191 (19): 5921–29. <https://doi.org/10.1128/JB.00642-09>.
- Blancato, Víctor S., Guillermo D. Repizo, Cristian A. Suárez, and Christian Magni. 2008. "Transcriptional Regulation of the Citrate Gene Cluster of *Enterococcus Faecalis* Involves the GntR Family Transcriptional Activator CitO." *Journal of Bacteriology* 190 (22): 7419–30. <https://doi.org/10.1128/JB.01704-07>.

- Bogdan, Alexander R., Masaki Miyazawa, Kazunori Hashimoto, and Yoshiaki Tsuji. 2016. "Regulators of Iron Homeostasis: New Players in Metabolism, Cell Death, and Disease." *Trends in Biochemical Sciences* 41 (3): 274–86. <https://doi.org/10.1016/j.tibs.2015.11.012>.
- Bohn, Binet, and Bouloc. 2002. "Screening for Stabilization of Proteins with a Trans-Translation Signature in Escherichia Coli Selects for Inactivation of the ClpXP Protease." *Molecular Genetics and Genomics* 266 (5): 827–31. <https://doi.org/10.1007/s00438-001-0601-1>.
- Bohn, Chantal, Candice Rigoulay, and Philippe Bouloc. 2007. "No Detectable Effect of RNA-Binding Protein Hfq Absence in Staphylococcus Aureus." *BMC Microbiology* 7 (1): 10. <https://doi.org/10.1186/1471-2180-7-10>.
- Bohn, Chantal, Candice Rigoulay, Svetlana Chabelskaya, Cynthia M. Sharma, Antonin Marchais, Patricia Skorski, Elise Borezée-Durant, et al. 2010. "Experimental Discovery of Small RNAs in Staphylococcus Aureus Reveals a Riboregulator of Central Metabolism." *Nucleic Acids Research* 38 (19): 6620–36. <https://doi.org/10.1093/nar/gkq462>.
- Boisset, Sandrine, Thomas Geissmann, Eric Huntzinger, Pierre Fechter, Nadia Bendridi, Maria Possedko, Clément Chevalier, et al. 2007. "Staphylococcus Aureus RNAIII Coordinately Represses the Synthesis of Virulence Factors and the Transcription Regulator Rot by an Antisense Mechanism." *Genes & Development* 21 (11): 1353–66. <https://doi.org/10.1101/gad.423507>.
- Boles, Blaise R., and Alexander R. Horswill. 2011. "Staphylococcal Biofilm Disassembly." *Trends in Microbiology* 19 (9): 449–55. <https://doi.org/10.1016/j.tim.2011.06.004>.
- Boncella, Amy E., Emily T. Sabo, Robert M. Santore, Jens Carter, Jaclyn Whalen, Jesse D. Hudspeth, and Christine N. Morrison. 2022. "The Expanding Utility of Iron-Sulfur Clusters: Their Functional Roles in Biology, Synthetic Small Molecules, Maquettes and Artificial Proteins, Biomimetic Materials, and Therapeutic Strategies." *Coordination Chemistry Reviews* 453 (February): 214229. <https://doi.org/10.1016/j.ccr.2021.214229>.
- Bortolus, Marco, Paola Costantini, Davide Doni, and Donatella Carbonera. 2018. "Overview of the Maturation Machinery of the H-Cluster of [FeFe]-Hydrogenases with a Focus on HydF." *International Journal of Molecular Sciences* 19 (10): 3118. <https://doi.org/10.3390/ijms19103118>.
- Bott, M. 1997. "Anaerobic Citrate Metabolism and Its Regulation in Enterobacteria." *Archives of Microbiology* 167 (2–3): 78–88. <https://doi.org/10.1007/s002030050419>.
- Bott, Michael, and Peter Dimroth. 1994. "Klebsiella Pneumoniae Genes for Citrate Lyase and Citrate Lyase Ligase: Localization, Sequencing, and Expression." *Molecular Microbiology* 14 (2): 347–56. <https://doi.org/10.1111/j.1365-2958.1994.tb01295.x>.
- Bott, Michael, Margareta Meyer, and Peter Dimroth. 1995. "Regulation of Anaerobic Citrate Metabolism in Klebsiella Pneumoniae." *Molecular Microbiology* 18 (3): 533–46. [https://doi.org/10.1111/j.1365-2958.1995.mmi\\_18030533.x](https://doi.org/10.1111/j.1365-2958.1995.mmi_18030533.x).
- Boudry, P., C. Gracia, M. Monot, J. Caillet, L. Saujet, E. Hajnsdorf, B. Dupuy, I. Martin-Verstraete, and O. Soutourina. 2014. "Pleiotropic Role of the RNA Chaperone Protein Hfq in the Human Pathogen Clostridium Difficile." *Journal of Bacteriology* 196 (18): 3234–48. <https://doi.org/10.1128/JB.01923-14>.
- Bradley, Justin M., Dimitry A. Svistunenko, Michael T. Wilson, Andrew M. Hemmings, Geoffrey R. Moore, and Nick E. Le Brun. 2020. "Bacterial Iron Detoxification at the Molecular Level." *Journal of Biological Chemistry* 295 (51): 17602–23. <https://doi.org/10.1074/jbc.REV120.007746>.

- Brantl, Sabine. 2002. "Antisense-RNA Regulation and RNA Interference." *Biochimica et Biophysica Acta (BBA) - Gene Structure and Expression* 1575 (1–3): 15–25. [https://doi.org/10.1016/S0167-4781\(02\)00280-4](https://doi.org/10.1016/S0167-4781(02)00280-4).
- Brantl, Sabine, and Peter Müller. 2021. "Cis- and Trans-Encoded Small Regulatory RNAs in *Bacillus Subtilis*." *Microorganisms* 9 (9): 1865. <https://doi.org/10.3390/microorganisms9091865>.
- Brenz, Yannick, Denise Ohnezeit, Hanne C. Winther-Larsen, and Monica Hagedorn. 2017. "Nramp1 and NrampB Contribute to Resistance against *Francisella* in *Dictyostelium*." *Frontiers in Cellular and Infection Microbiology* 7 (June): 282. <https://doi.org/10.3389/fcimb.2017.00282>.
- Brot, N, and J Goodwin. 1968. "Regulation of 2,3-Dihydroxybenzoylserine Synthetase by Iron." *Journal of Biological Chemistry* 243 (3): 510–13. [https://doi.org/10.1016/S0021-9258\(18\)93633-1](https://doi.org/10.1016/S0021-9258(18)93633-1).
- Brozyna, Jeremy R., Jessica R. Sheldon, and David E. Heinrichs. 2014. "Growth Promotion of the Opportunistic Human Pathogen, *Staphylococcus Lugdunensis*, by Heme, Hemoglobin, and Coculture with *Staphylococcus Aureus*." *MicrobiologyOpen* 3 (2): 182–95. <https://doi.org/10.1002/mbo3.162>.
- Caballero, Carlos J, Pilar Menendez-Gil, Arancha Catalan-Moreno, Marta Vergara-Irigaray, Begoña García, Víctor Segura, Naiara Irurzun, et al. 2018. "The Regulon of the RNA Chaperone CspA and Its Auto-Regulation in *Staphylococcus Aureus*." *Nucleic Acids Research* 46 (3): 1345–61. <https://doi.org/10.1093/nar/gkx1284>.
- Carpenter, Chandra, and Shelley M. Payne. 2014. "Regulation of Iron Transport Systems in Enterobacteriaceae in Response to Oxygen and Iron Availability." *Journal of Inorganic Biochemistry* 133 (April): 110–17. <https://doi.org/10.1016/j.jinorgbio.2014.01.007>.
- Castro, Laura, Verónica Tórtora, Santiago Mansilla, and Rafael Radi. 2019. "Aconitases: Non-Redox Iron–Sulfur Proteins Sensitive to Reactive Species." *Accounts of Chemical Research* 52 (9): 2609–19. <https://doi.org/10.1021/acs.accounts.9b00150>.
- Chambers, Ian G., Mathilda M. Willoughby, Iqbal Hamza, and Amit R. Reddi. 2021. "One Ring to Bring Them All and in the Darkness Bind Them: The Trafficking of Heme without Deliverers." *Biochimica et Biophysica Acta (BBA) - Molecular Cell Research* 1868 (1): 118881. <https://doi.org/10.1016/j.bbamcr.2020.118881>.
- Chareyre, Sylvia, and Pierre Mandin. 2018. "Bacterial Iron Homeostasis Regulation by sRNAs." *Microbiology Spectrum* 6 (2). <https://doi.org/10.1128/microbiolspec.RWR-0010-2017>.
- Cheung, Gordon Y. C., Justin S. Bae, and Michael Otto. 2021. "Pathogenicity and Virulence of *Staphylococcus Aureus*." *Virulence* 12 (1): 547–69. <https://doi.org/10.1080/21505594.2021.1878688>.
- Cheung, Gordon Y.C., Hwang-Soo Joo, Som S. Chatterjee, and Michael Otto. 2014. "Phenol-Soluble Modulins – Critical Determinants of Staphylococcal Virulence." *FEMS Microbiology Reviews* 38 (4): 698–719. <https://doi.org/10.1111/1574-6976.12057>.
- Choby, Jacob E., and Eric P. Skaar. 2016. "Heme Synthesis and Acquisition in Bacterial Pathogens." *Journal of Molecular Biology* 428 (17): 3408–28. <https://doi.org/10.1016/j.jmb.2016.03.018>.
- Clarke, Simon R., and Simon J. Foster. 2006. "Surface Adhesins of *Staphylococcus Aureus*." In *Advances in Microbial Physiology*, 51:187–224. Elsevier. [https://doi.org/10.1016/S0065-2911\(06\)51004-5](https://doi.org/10.1016/S0065-2911(06)51004-5).

- Clauditz, Alexandra, Alexandra Resch, Karsten-Peter Wieland, Andreas Peschel, and Friedrich Götz. 2006. "Staphyloxanthin Plays a Role in the Fitness of *Staphylococcus Aureus* and Its Ability To Cope with Oxidative Stress." *Infection and Immunity* 74 (8): 4950–53. <https://doi.org/10.1128/IAI.00204-06>.
- Collier, Justine, Emmanuelle Binet, and Philippe Bouloc. 2002. "Competition between SsrA Tagging and Translational Termination at Weak Stop Codons in Escherichia Coli: SsrA Tagging and Translational Termination." *Molecular Microbiology* 45 (3): 745–54. <https://doi.org/10.1046/j.1365-2958.2002.03045.x>.
- Collier, Justine, Chantal Bohn, and Philippe Bouloc. 2004. "SsrA Tagging of Escherichia Coli SecM at Its Translation Arrest Sequence." *Journal of Biological Chemistry* 279 (52): 54193–201. <https://doi.org/10.1074/jbc.M314012200>.
- Conroy, Brigid S., Jason C. Grigg, Maxim Kolesnikov, L. Daniela Morales, and Michael E. P. Murphy. 2019. "Staphylococcus Aureus Heme and Siderophore-Iron Acquisition Pathways." *BioMetals* 32 (3): 409–24. <https://doi.org/10.1007/s10534-019-00188-2>.
- Contreras, Heidi, Nicholas Chim, Alfredo Credali, and Celia W Goulding. 2014. "Heme Uptake in Bacterial Pathogens." *Current Opinion in Chemical Biology* 19 (April): 34–41. <https://doi.org/10.1016/j.cbpa.2013.12.014>.
- Cornelis, Pierre, Qing Wei, Simon C. Andrews, and Tiffany Vinckx. 2011. "Iron Homeostasis and Management of Oxidative Stress Response in Bacteria." *Metallomics* 3 (6): 540. <https://doi.org/10.1039/c1mt00022e>.
- Coronel-Tellez, Rodrigo H, Mateusz Pospiech, Maxime Barrault, Wenfeng Liu, Valérie Bordeau, Christelle Vasnier, Brice Felden, Bruno Sargueil, and Philippe Bouloc. 2022. "sRNA-Controlled Iron Sparing Response in Staphylococci." *Nucleic Acids Research* 50 (15): 8529–46. <https://doi.org/10.1093/nar/gkac648>.
- Cunningham, Louise, Megan J. Gruer, and John R. Guest. 1997. "Transcriptional Regulation of the Aconitase Genes (acnA and acnB) of Escherichia Coli." *Microbiology* 143 (12): 3795–3805. <https://doi.org/10.1099/00221287-143-12-3795>.
- Dai, Shang, Ye Jin, Tao Li, Yulan Weng, Xiaolin Xu, Genlin Zhang, Jiulong Li, Renjiang Pang, Bing Tian, and Yuejin Hua. 2018. "DR1440 Is a Potential Iron Efflux Protein Involved in Maintenance of Iron Homeostasis and Resistance of Deinococcus Radiodurans to Oxidative Stress." Edited by Roy Martin Roop. *PLOS ONE* 13 (8): e0202287. <https://doi.org/10.1371/journal.pone.0202287>.
- Deng, Zhongliang, Xiangrong Meng, Shanchun Su, Zizhong Liu, Xiaolan Ji, Yiquan Zhang, Xiangna Zhao, Xiaoyi Wang, Ruifu Yang, and Yanping Han. 2012. "Two sRNA RyhB Homologs from Yersinia Pestis Biovar Microtus Expressed in Vivo Have Differential Hfq-Dependent Stability." *Research in Microbiology* 163 (6–7): 413–18. <https://doi.org/10.1016/j.resmic.2012.05.006>.
- Desnoyers, Guillaume, Audrey Morissette, Karine Prévost, and Eric Massé. 2009. "Small RNA-Induced Differential Degradation of the Polycistronic mRNA iscRSUA." *The EMBO Journal* 28 (11): 1551–61. <https://doi.org/10.1038/emboj.2009.116>.
- Dimroth, Peter, and Christoph Von Ballmoos. 2007. "ATP Synthesis by Decarboxylation Phosphorylation." In *Bioenergetics*, edited by Günter Schäfer and Harvey S. Penefsky, 45:153–84. Results and Problems in Cell Differentiation. Berlin, Heidelberg: Springer Berlin Heidelberg. [https://doi.org/10.1007/400\\_2007\\_045](https://doi.org/10.1007/400_2007_045).

- Ding, Huangen, Elena Hidalgo, and Bruce Dimple. 1996. "The Redox State of the [2Fe-2S] Clusters in SoxR Protein Regulates Its Activity as a Transcription Factor." *Journal of Biological Chemistry* 271 (52): 33173–75. <https://doi.org/10.1074/jbc.271.52.33173>.
- Ding, Yue, Xing Liu, Feifei Chen, Hongxia Di, Bin Xu, Lu Zhou, Xin Deng, Min Wu, Cai-Guang Yang, and Lefu Lan. 2014a. "Metabolic Sensor Governing Bacterial Virulence in *Staphylococcus Aureus*." *Proceedings of the National Academy of Sciences* 111 (46). <https://doi.org/10.1073/pnas.1411077111>.
- . 2014b. "Metabolic Sensor Governing Bacterial Virulence in *Staphylococcus Aureus*." *Proceedings of the National Academy of Sciences* 111 (46): E4981–90. <https://doi.org/10.1073/pnas.1411077111>.
- Divyakolu, Sireesha, Rosy Chikkala, Kamaraju Suguna Ratnakar, and Venkataraman Sritharan. 2019. "Hemolysins of *Staphylococcus Aureus*—An Update on Their Biology, Role in Pathogenesis and as Targets for Anti-Virulence Therapy." *Advances in Infectious Diseases* 09 (02): 80–104. <https://doi.org/10.4236/aid.2019.92007>.
- Djapgne, Louise, and Amanda G. Oglesby. 2021. "Impacts of Small RNAs and Their Chaperones on Bacterial Pathogenicity." *Frontiers in Cellular and Infection Microbiology* 11 (July): 604511. <https://doi.org/10.3389/fcimb.2021.604511>.
- D'Onofrio, Anthony, Jason M. Crawford, Eric J. Stewart, Kathrin Witt, Ekaterina Gavrish, Slava Epstein, Jon Clardy, and Kim Lewis. 2010. "Siderophores from Neighboring Organisms Promote the Growth of Uncultured Bacteria." *Chemistry & Biology* 17 (3): 254–64. <https://doi.org/10.1016/j.chembiol.2010.02.010>.
- Drider, Djamel, Sadjia Bekal, and Hervé Prévost. 2004. "Genetic Organization and Expression of Citrate Permease in Lactic Acid Bacteria." *Genetics and Molecular Research*.
- Durand, Sylvain, Frédérique Braun, Efthimia Lioliou, Cédric Romilly, Anne-Catherine Helfer, Laurianne Kuhn, Noé Quittot, Pierre Nicolas, Pascale Romby, and Ciarán Condon. 2015. "A Nitric Oxide Regulated Small RNA Controls Expression of Genes Involved in Redox Homeostasis in *Bacillus Subtilis*." Edited by Danielle A. Garsin. *PLOS Genetics* 11 (2): e1004957. <https://doi.org/10.1371/journal.pgen.1004957>.
- Dutta, Tanmay, and Shubhangi Srivastava. 2018. "Small RNA-Mediated Regulation in Bacteria: A Growing Palette of Diverse Mechanisms." *Gene* 656 (May): 60–72. <https://doi.org/10.1016/j.gene.2018.02.068>.
- Ellermeier, Jeremy R., and James M. Slauch. 2008. "Fur Regulates Expression of the *Salmonella* Pathogenicity Island 1 Type III Secretion System through HilD." *Journal of Bacteriology* 190 (2): 476–86. <https://doi.org/10.1128/JB.00926-07>.
- Esberard, Marick, Marc Hallier, Wenfeng Liu, Claire Morvan, Lionello Bossi, Nara Figueroa-Bossi, Brice Felden, and Philippe Bouloc. 2022. "6S RNA-Dependent Susceptibility to RNA Polymerase Inhibitors." *Antimicrobial Agents and Chemotherapy* 66 (5): e02435-21. <https://doi.org/10.1128/aac.02435-21>.
- Esquilin-Lebron, Karla, Sarah Dubrac, Frédéric Barras, and Jeffrey M. Boyd. 2021. "Bacterial Approaches for Assembling Iron-Sulfur Proteins." Edited by Jacob Yount. *mBio* 12 (6): e02425-21. <https://doi.org/10.1128/mBio.02425-21>.
- Falugi, Fabiana, Hwan Keun Kim, Dominique M. Missiakas, and Olaf Schneewind. 2013. "Role of Protein A in the Evasion of Host Adaptive Immune Responses by *Staphylococcus Aureus*." Edited by Michael S. Gilmore. *mBio* 4 (5): e00575-13. <https://doi.org/10.1128/mBio.00575-13>.

- Fedtke, I., A. Kamps, B. Krismer, and F. Götz. 2002. "The Nitrate Reductase and Nitrite Reductase Operons and the *narT* Gene of *Staphylococcus Carnosus* Are Positively Controlled by the Novel Two-Component System NreBC." *Journal of Bacteriology* 184 (23): 6624–34. <https://doi.org/10.1128/JB.184.23.6624-6634.2002>.
- Fillat, María F. 2014. "The FUR (Ferric Uptake Regulator) Superfamily: Diversity and Versatility of Key Transcriptional Regulators." *Archives of Biochemistry and Biophysics* 546 (March): 41–52. <https://doi.org/10.1016/j.abb.2014.01.029>.
- Fontenot, Chelsey R., and Huang Ding. 2023. "Ferric Uptake Regulator (Fur) Binds a [2Fe-2S] Cluster to Regulate Intracellular Iron Homeostasis in Escherichia Coli." *Journal of Biological Chemistry* 299 (6): 104748. <https://doi.org/10.1016/j.jbc.2023.104748>.
- Fontenot, Chelsey R., Homyra Tasnim, Kathryn A. Valdes, Codrina V. Popescu, and Huang Ding. 2020. "Ferric Uptake Regulator (Fur) Reversibly Binds a [2Fe-2S] Cluster to Sense Intracellular Iron Homeostasis in Escherichia Coli." *Journal of Biological Chemistry* 295 (46): 15454–63. <https://doi.org/10.1074/jbc.RA120.014814>.
- Frawley, Elaine R., Marie-Laure V. Crouch, Lacey K. Bingham-Ramos, Hannah F. Robbins, Wenliang Wang, Gerard D. Wright, and Ferric C. Fang. 2013. "Iron and Citrate Export by a Major Facilitator Superfamily Pump Regulates Metabolism and Stress Resistance in *Salmonella Typhimurium*." *Proceedings of the National Academy of Sciences* 110 (29): 12054–59. <https://doi.org/10.1073/pnas.1218274110>.
- Frey, Perry A., and George H. Reed. 2012. "The Ubiquity of Iron." *ACS Chemical Biology* 7 (9): 1477–81. <https://doi.org/10.1021/cb300323q>.
- Futerman, Anthony H., and Yusuf A Hannun. 2004. "The Complex Life of Simple Sphingolipids." *EMBO Reports* 5 (8): 777–82. <https://doi.org/10.1038/sj.embor.7400208>.
- G. Chaulk, Steven, Michelle N. Smith–Frieday, David C. Arthur, Doreen E. Culham, Ross A. Edwards, Patrick Soo, Laura S. Frost, Robert A. B. Keates, J. N. Mark Glover, and Janet M. Wood. 2011. "ProQ Is an RNA Chaperone That Controls ProP Levels in *Escherichia Coli*." *Biochemistry* 50 (15): 3095–3106. <https://doi.org/10.1021/bi101683a>.
- Gaballa, Ahmed, Haike Antelmann, Claudio Aguilar, Sukhjit K. Khakh, Kyung-Bok Song, Gregory T. Smaldone, and John D. Helmann. 2008. "The *Bacillus Subtilis* Iron-Sparing Response Is Mediated by a Fur-Regulated Small RNA and Three Small, Basic Proteins." *Proceedings of the National Academy of Sciences* 105 (33): 11927–32. <https://doi.org/10.1073/pnas.0711752105>.
- Gabashvili, Anna N., Nelly S. Chmelyuk, Maria V. Efremova, Julia A. Malinovskaya, Alevtina S. Semkina, and Maxim A. Abakumov. 2020. "Encapsulins—Bacterial Protein Nanocompartments: Structure, Properties, and Application." *Biomolecules* 10 (6): 966. <https://doi.org/10.3390/biom10060966>.
- Galaris, Dimitrios, Alexandra Barbouti, and Kostas Pantopoulos. 2019. "Iron Homeostasis and Oxidative Stress: An Intimate Relationship." *Biochimica et Biophysica Acta (BBA) - Molecular Cell Research* 1866 (12): 118535. <https://doi.org/10.1016/j.bbamcr.2019.118535>.
- Ganz, Tomas. 2013. "Systemic Iron Homeostasis." *Physiol Rev* 93.
- Garcia, Victor Blancato, and Guillermo Repizo. 2008. *Molecular Aspects of Lactic Acid Bacteria for Traditional and New Applications*.
- Garcia, Pierre Simon, Francesca D'Angelo, Sandrine Ollagnier De Choudens, Macha Dussouchaud, Emmanuelle Bouveret, Simonetta Gribaldo, and Frédéric Barras. 2022. "An Early

- Origin of Iron–Sulfur Cluster Biosynthesis Machineries before Earth Oxygenation." *Nature Ecology & Evolution* 6 (10): 1564–72. <https://doi.org/10.1038/s41559-022-01857-1>.
- Gaudu, Namdoo Moon, and Bernard Weiss. 1997. "Regulation of the soxRS Oxidative Stress Regulon." *Journal of Biological Chemistry* 272 (8): 5082–86. <https://doi.org/10.1074/jbc.272.8.5082>.
- Gaudu, Philippe, and Bernard Weiss. 1996. "SoxR, a [2Fe-2S] Transcription Factor, Is Active Only in Its Oxidized Form." *Proceedings of the National Academy of Sciences* 93 (19): 10094–98. <https://doi.org/10.1073/pnas.93.19.10094>.
- Gaupp, Rosmarie, Nagender Ledala, and Greg A. Somerville. 2012. "Staphylococcal Response to Oxidative Stress." *Frontiers in Cellular and Infection Microbiology* 2. <https://doi.org/10.3389/fcimb.2012.00033>.
- Geissmann, Thomas, Clément Chevalier, Marie-Josée Cros, Sandrine Boisset, Pierre Fechter, Céline Noirot, Jacques Schrenzel, et al. 2009. "A Search for Small Noncoding RNAs in *Staphylococcus Aureus* Reveals a Conserved Sequence Motif for Regulation." *Nucleic Acids Research* 37 (21): 7239–57. <https://doi.org/10.1093/nar/gkp668>.
- Georg, Jens, and Wolfgang R. Hess. 2018. "Widespread Antisense Transcription in Prokaryotes." Edited by Gisela Storz and Kai Papenfort. *Microbiology Spectrum* 6 (4): 6.4.12. <https://doi.org/10.1128/microbiolspec.RWR-0029-2018>.
- Gerovac, Milan, Youssef El Mouali, Jochen Kuper, Caroline Kisker, Lars Barquist, and Jörg Vogel. 2020. "Global Discovery of Bacterial RNA-Binding Proteins by RNase-Sensitive Gradient Profiles Reports a New FinO Domain Protein."
- Gerrick, Elias R., Thibault Barbier, Michael R. Chase, Raylin Xu, Josie François, Vincent H. Lin, Matthew J. Szucs, et al. 2018. "Small RNA Profiling in *Mycobacterium Tuberculosis* Identifies MrsI as Necessary for an Anticipatory Iron Sparing Response." *Proceedings of the National Academy of Sciences* 115 (25): 6464–69. <https://doi.org/10.1073/pnas.1718003115>.
- Giessen, Tobias W. 2022. "Encapsulins." *Annual Review of Biochemistry* 91 (1): 353–80. <https://doi.org/10.1146/annurev-biochem-040320-102858>.
- Gkouvatsos, Konstantinos, George Papanikolaou, and Kostas Pantopoulos. 2012. "Regulation of Iron Transport and the Role of Transferrin." *Biochimica et Biophysica Acta (BBA) - General Subjects* 1820 (3): 188–202. <https://doi.org/10.1016/j.bbagen.2011.10.013>.
- Goetz, David H, Margaret A Holmes, Niels Borregaard, Martin E Bluhm, Kenneth N Raymond, and Roland K Strong. 2002. "The Neutrophil Lipocalin NGAL Is a Bacteriostatic Agent That Interferes with Siderophore-Mediated Iron Acquisition." *Molecular Cell* 10 (5): 1033–43. [https://doi.org/10.1016/S1097-2765\(02\)00708-6](https://doi.org/10.1016/S1097-2765(02)00708-6).
- Goforth, Jeremy B., Sheila A. Anderson, Christopher P. Nizzi, and Richard S. Eisenstein. 2010. "Multiple Determinants within Iron-Responsive Elements Dictate Iron Regulatory Protein Binding and Regulatory Hierarchy." *RNA* 16 (1): 154–69. <https://doi.org/10.1261/rna.1857210>.
- Gogol, Emily B., Virgil A. Rhodius, Kai Papenfort, Jörg Vogel, and Carol A. Gross. 2011. "Small RNAs Endow a Transcriptional Activator with Essential Repressor Functions for Single-Tier Control of a Global Stress Regulon." *Proceedings of the National Academy of Sciences* 108 (31): 12875–80. <https://doi.org/10.1073/pnas.1109379108>.

- Gouaux, Eric, Michael Hobaugh, and Langzhou Song. 2008. " $\alpha$ -Hemolysin,  $\gamma$ -Hemolysin, and Leukocidin from *Staphylococcus Aureus*: Distant in Sequence but Similar in Structure." *Protein Science* 6 (12): 2631–35. <https://doi.org/10.1002/pro.5560061216>.
- Grass, Gregor, Markus Otto, Beate Fricke, Christopher J. Haney, Christopher Rensing, Dietrich H. Nies, and Doreen Munkelt. 2005. "FieF (YiiP) from *Escherichia Coli* Mediates Decreased Cellular Accumulation of Iron and Relieves Iron Stress." *Archives of Microbiology* 183 (1): 9–18. <https://doi.org/10.1007/s00203-004-0739-4>.
- Gruer, M. J., and J. R. Guest. 1994. "Two Genetically-Distinct and Differentially-Regulated Aconitases (AcnA and AcnB) in *Escherichia Coli*." *Microbiology* 140 (10): 2531–41. <https://doi.org/10.1099/00221287-140-10-2531>.
- Gruss, Alexandra, Elise Borezée-Durant, and Delphine Lechardeur. 2012. "Environmental Heme Utilization by Heme-Auxotrophic Bacteria." In *Advances in Microbial Physiology*, 61:69–124. Elsevier. <https://doi.org/10.1016/B978-0-12-394423-8.00003-2>.
- Gu, Mianzhi, and James A. Imlay. 2013. "Superoxide Poisons Mononuclear Iron Enzymes by Causing Mismetallation: Superoxide Poisons Mononuclear Iron Enzymes." *Molecular Microbiology* 89 (1): 123–34. <https://doi.org/10.1111/mmi.12263>.
- Guan, Guohua, Azul Pinochet-Barros, Ahmed Gaballa, Sarju J. Patel, José M. Argüello, and John D. Helmann. 2015. "PfeT, a P<sub>1B4</sub>-Type ATPase, Effluxes Ferrous Iron and Protects *Bacillus Subtilis* against Iron Intoxication: *Bacillus Subtilis* PfeT Effluxes Ferrous Iron." *Molecular Microbiology* 98 (4): 787–803. <https://doi.org/10.1111/mmi.13158>.
- Haikarainen, Teemu, and Anastassios C. Papageorgiou. 2010. "Dps-like Proteins: Structural and Functional Insights into a Versatile Protein Family." *Cellular and Molecular Life Sciences* 67 (3): 341–51. <https://doi.org/10.1007/s00018-009-0168-2>.
- Hall, H K, and J W Foster. 1996. "The Role of Fur in the Acid Tolerance Response of *Salmonella Typhimurium* Is Physiologically and Genetically Separable from Its Role in Iron Acquisition." *Journal of Bacteriology* 178 (19): 5683–91. <https://doi.org/10.1128/jb.178.19.5683-5691.1996>.
- Hämmerle, Hermann, Fabian Amman, Branislav Večerek, Jörg Stülke, Ivo Hofacker, and Udo Bläsi. 2014. "Impact of Hfq on the *Bacillus Subtilis* Transcriptome." Edited by Lennart Randau. *PLoS ONE* 9 (6): e98661. <https://doi.org/10.1371/journal.pone.0098661>.
- Hannauer, Mélissa, Andrew J. Arifin, and David E. Heinrichs. 2015. "Involvement of Reductases IruO and NtrA in Iron Acquisition by *S Taphylococcus Aureus*. IruO and NtrA Involvement in Iron Acquisition." *Molecular Microbiology* 96 (6): 1192–1210. <https://doi.org/10.1111/mmi.13000>.
- Hantke, Klaus. 1981. "Regulation of Ferric Iron Transport in *Escherichia Coli* K12: Isolation of a Constitutive Mutant." *Molecular and General Genetics MGG* 182 (2): 288–92. <https://doi.org/10.1007/BF00269672>.
- . 1987. "Ferrous Iron Transport Mutants in *Escherichia Coli* K12." *FEMS Microbiology Letters* 44 (1): 53–57. <https://doi.org/10.1111/j.1574-6968.1987.tb02241.x>.
- Harford, S, and P D J Weitzman. 1975. "Evidence of Isosteric and Allosteric Nucleotide Inhibition of Citrate Synthase from Multiple-Inhibition Studies." *Biochemical Journal* 151 (2): 455–58. <https://doi.org/10.1042/bj1510455>.
- Hartmann, Torsten, Bo Zhang, Grégory Baronian, Bettina Schulthess, Dagmar Homerova, Stephanie Grubmüller, Erika Kutzner, et al. 2013. "Catabolite Control Protein E (CcpE) Is

- a LysR-Type Transcriptional Regulator of Tricarboxylic Acid Cycle Activity in *Staphylococcus Aureus*." *Journal of Biological Chemistry* 288 (50): 36116–28. <https://doi.org/10.1074/jbc.M113.516302>.
- Hentze, Matthias W., Martina U. Muckenthaler, Bruno Galy, and Clara Camaschella. 2010. "Two to Tango: Regulation of Mammalian Iron Metabolism." *Cell* 142 (1): 24–38. <https://doi.org/10.1016/j.cell.2010.06.028>.
- Herman, C, T Ogura, T Tomoyasu, S Hiraga, Y Akiyama, K Ito, R Thomas, R D'Ari, and P Bouloc. 1993. "Cell Growth and Lambda Phage Development Controlled by the Same Essential *Escherichia Coli* Gene, *ftsH/hflB*." *Proceedings of the National Academy of Sciences* 90 (22): 10861–65. <https://doi.org/10.1073/pnas.90.22.10861>.
- Herman, C., D. Thevenet, P. Bouloc, G. C. Walker, and R. D'Ari. 1998. "Degradation of Carboxy-Terminal-Tagged Cytoplasmic Proteins by the *Escherichia Coli* Protease *HflB* (*FtsH*)." *Genes & Development* 12 (9): 1348–55. <https://doi.org/10.1101/gad.12.9.1348>.
- Herman, C, D Thévenet, R D'Ari, and P Bouloc. 1995. "Degradation of Sigma 32, the Heat Shock Regulator in *Escherichia Coli*, Is Governed by *HflB*." *Proceedings of the National Academy of Sciences* 92 (8): 3516–20. <https://doi.org/10.1073/pnas.92.8.3516>.
- Hindley, J. 1967. "Fractionation of <sup>32</sup>P-Labelled Ribonucleic Acids on Polyacrylamide Gels and Their Characterization by Fingerprinting." *Journal of Molecular Biology* 30 (1): 125–36. [https://doi.org/10.1016/0022-2836\(67\)90248-3](https://doi.org/10.1016/0022-2836(67)90248-3).
- Hood, M. Indriati, and Eric P. Skaar. 2012. "Nutritional Immunity: Transition Metals at the Pathogen–Host Interface." *Nature Reviews Microbiology* 10 (8): 525–37. <https://doi.org/10.1038/nrmicro2836>.
- Horn, Jessica, Maximilian Klepsch, Michelle Manger, Christiane Wolz, Thomas Rudel, and Martin Fraunholz. 2018. "Long Noncoding RNA SSR42 Controls *Staphylococcus Aureus* Alpha-Toxin Transcription in Response to Environmental Stimuli." Edited by Thomas J. Silhavy. *Journal of Bacteriology* 200 (22). <https://doi.org/10.1128/JB.00252-18>.
- Hotta, Kinya, Chu-Young Kim, David T. Fox, and Andrew T. Koppisch. 2010. "Siderophore-Mediated Iron Acquisition in *Bacillus Anthracis* and Related Strains." *Microbiology* 156 (7): 1918–25. <https://doi.org/10.1099/mic.0.039404-0>.
- Hristova, Daniela, Chia-Hung Wu, Wei Jiang, Carsten Krebs, and JoAnne Stubbe. 2008. "Importance of the Maintenance Pathway in the Regulation of the Activity of *Escherichia Coli* Ribonucleotide Reductase." *Biochemistry* 47 (13): 3989–99. <https://doi.org/10.1021/bi702408k>.
- Hu, Jialing, Kaixi Jin, Zheng-Guo He, and Hua Zhang. 2020. "Citrate Lyase *CitE* in *Mycobacterium Tuberculosis* Contributes to Mycobacterial Survival under Hypoxic Conditions." Edited by Olivier Neyrolles. *PLOS ONE* 15 (4): e0230786. <https://doi.org/10.1371/journal.pone.0230786>.
- Huta, Brian, Joshua J. Lensboeur, Adam J. Lowe, Jon Zubieta, and Robert P. Doyle. 2012. "Metal-Citrate Complex Uptake and *CitMHS* Transporters: From Coordination Chemistry to Possible Vaccine Development." *Inorganica Chimica Acta* 393 (December): 125–34. <https://doi.org/10.1016/j.ica.2012.06.025>.
- Ikuta, Kevin S, Lucien R Swetschinski, Gisela Robles Aguilar, Fablina Sharara, Tomislav Mestrovic, Authia P Gray, Nicole Davis Weaver, et al. 2022. "Global Mortality Associated with 33 Bacterial Pathogens in 2019: A Systematic Analysis for the Global Burden of Disease Study 2019." *The Lancet* 400 (10369): 2221–48. [https://doi.org/10.1016/S0140-6736\(22\)02185-7](https://doi.org/10.1016/S0140-6736(22)02185-7).

- Jaebson, Marty R, Valerie L Cash, Mary C Weiss, Nancy F Laird, William E Newton, and Dennis R Dean. 1989. "Biochemical and Genetic Analysis of the nitIJSVWZM Cluster from *Azotobacter Vinelandii*."
- Johnson, Deborah C., Dennis R. Dean, Archer D. Smith, and Michael K. Johnson. 2005. "Structure, Function and Formation of Biological Iron-Sulfur Clusters." *Annual Review of Biochemistry* 74 (1): 247–81. <https://doi.org/10.1146/annurev.biochem.74.082803.133518>.
- Jones, Alexander J., Keerthi P. Venkataramanan, and Terry Papoutsakis. 2016. "Overexpression of Two Stress-Responsive, Small, Non-Coding RNAs, 6S and tmRNA, Imparts Butanol Tolerance in *Clostridium Acetobutylicum*." Edited by Michael Sauer. *FEMS Microbiology Letters* 363 (8): fnw063. <https://doi.org/10.1093/femsle/fnw063>.
- Jourlin-Castelli, Cécile, Nagraj Mani, Michiko M Nakano, and Abraham L Sonenshein. 2000. "CcpC, a Novel Regulator of the LysR Family Required for Glucose Repression of the citB Gene in *Bacillus Subtilis*." *Journal of Molecular Biology* 295 (4): 865–78. <https://doi.org/10.1006/jmbi.1999.3420>.
- Jr Benz, Edward J. 2015. "Iron-Loading Anaemia." In *eLS*, edited by John Wiley & Sons, Ltd, 1st ed., 1–10. Wiley. <https://doi.org/10.1002/9780470015902.a0002272.pub2>.
- Jung, Yean-Sung, and Young-Man Kwon. 2008. "Small RNA ArrF Regulates the Expression of sodB and feSII Genes in *Azotobacter Vinelandii*." *Current Microbiology* 57 (6): 593–97. <https://doi.org/10.1007/s00284-008-9248-z>.
- Kassebaum, Nicholas J., Rashmi Jasrasaria, Mohsen Naghavi, Sarah K. Wulf, Nicole Johns, Rafael Lozano, Mathilda Regan, et al. 2014. "A Systematic Analysis of Global Anemia Burden from 1990 to 2010." *Blood* 123 (5): 615–24. <https://doi.org/10.1182/blood-2013-06-508325>.
- Kastner, Christopher N., Karin Schneider, Peter Dimroth, and Klaas M. Pos. 2002. "[No Title Found]." *Archives of Microbiology* 177 (6): 500–506. <https://doi.org/10.1007/s00203-002-0420-8>.
- Katsuya-Gaviria, Kai, Giulia Paris, Tom Dendooven, and Katarzyna J. Bandyra. 2022. "Bacterial RNA Chaperones and Chaperone-like Riboregulators: Behind the Scenes of RNA-Mediated Regulation of Cellular Metabolism." *RNA Biology* 19 (1): 419–36. <https://doi.org/10.1080/15476286.2022.2048565>.
- Kawamoto, Hiroshi, Yukari Koide, Teppei Morita, and Hiroji Aiba. 2006. "Base-Pairing Requirement for RNA Silencing by a Bacterial Small RNA and Acceleration of Duplex Formation by Hfq." *Molecular Microbiology* 61 (4): 1013–22. <https://doi.org/10.1111/j.1365-2958.2006.05288.x>.
- Keiler, Kenneth C., Patrick R. H. Waller, and Robert T. Sauer. 1996. "Role of a Peptide Tagging System in Degradation of Proteins Synthesized from Damaged Messenger RNA." *Science* 271 (5251): 990–93. <https://doi.org/10.1126/science.271.5251.990>.
- Kim, Cécile Jourlin-Castelli, Sam-In Kim, and Abraham L. Sonenshein. 2002. "Regulation of the *Bacillus Subtilis* ccpC Gene by CcpA and CcpC: Complex Regulation of *B. Subtilis* ccpC." *Molecular Microbiology* 43 (2): 399–410. <https://doi.org/10.1046/j.1365-2958.2002.02751.x>.
- Kim, Sam-In Kim, Manoja Ratnayake-Lecamwasam, Kiyoshi Tachikawa, Abraham L Sonenshein, and Mark Strauch. 2003. "Complex Regulation of the *Bacillus Subtilis* Aconitase Gene." *Journal of Bacteriology* 185.

- Kim, Agnes Roux, and Abraham L. Sonenshein. 2002. "Direct and Indirect Roles of CcpA in Regulation of *Bacillus Subtilis* Krebs Cycle Genes." *Molecular Microbiology* 45 (1): 179–90. <https://doi.org/10.1046/j.1365-2958.2002.03003.x>.
- Kim, Sam-In, Cécile Jourlin-Castelli, Stephen R. Wellington, and Abraham L. Sonenshein. 2003. "Mechanism of Repression by *Bacillus Subtilis* CcpC, a LysR Family Regulator." *Journal of Molecular Biology* 334 (4): 609–24. <https://doi.org/10.1016/j.jmb.2003.09.078>.
- Kolaj-Robin, Olga, David Russell, Kevin A. Hayes, J. Tony Pembroke, and Tewfik Soulimane. 2015. "Cation Diffusion Facilitator Family: Structure and Function." *FEBS Letters* 589 (12): 1283–95. <https://doi.org/10.1016/j.febslet.2015.04.007>.
- Kourtis, Athena P., Kelly Hatfield, James Baggs, Yi Mu, Isaac See, Erin Epton, Joelle Nadle, et al. 2019. "Vital Signs: Epidemiology and Recent Trends in Methicillin-Resistant and in Methicillin-Susceptible *Staphylococcus Aureus* Bloodstream Infections — United States." *MMWR. Morbidity and Mortality Weekly Report* 68 (9): 214–19. <https://doi.org/10.15585/mmwr.mm6809e1>.
- Kramer, Jos, Özhan Özkaya, and Rolf Kümmerli. 2020. "Bacterial Siderophores in Community and Host Interactions." *Nature Reviews Microbiology* 18 (3): 152–63. <https://doi.org/10.1038/s41579-019-0284-4>.
- Krismer, Bernhard, Christopher Weidenmaier, Alexander Zipperer, and Andreas Peschel. 2017. "The Commensal Lifestyle of *Staphylococcus Aureus* and Its Interactions with the Nasal Microbiota." *Nature Reviews Microbiology* 15 (11): 675–87. <https://doi.org/10.1038/nrmicro.2017.104>.
- Krom, Bastiaan P., Jessica B. Warner, Wil N. Konings, and Juke S. Lolkema. 2000. "Complementary Metal Ion Specificity of the Metal-Citrate Transporters CitM and CitH of *Bacillus Subtilis*." *Journal of Bacteriology* 182 (22): 6374–81. <https://doi.org/10.1128/JB.182.22.6374-6381.2000>.
- Kühlbrandt, Werner. 2004. "Biology, Structure and Mechanism of P-Type ATPases." *Nature Reviews Molecular Cell Biology* 5 (4): 282–95. <https://doi.org/10.1038/nrm1354>.
- Kumar, Manjusha Lekshmi, Ammini Parvathi, Manisha Ojha, Nicholas Wenzel, and Manuel F. Varela. 2020. "Functional and Structural Roles of the Major Facilitator Superfamily Bacterial Multidrug Efflux Pumps." *Microorganisms* 8 (2): 266. <https://doi.org/10.3390/microorganisms8020266>.
- Kumar, Esha Sharma, Alexandra Marley, Mark A Samaan, and Matthew James Brookes. 2022. "Iron Deficiency Anaemia: Pathophysiology, Assessment, Practical Management." *BMJ Open Gastroenterology* 9 (1): e000759. <https://doi.org/10.1136/bmjgast-2021-000759>.
- Laakso, Holly A., Cristina L. Marolda, Tyler B. Pinter, Martin J. Stillman, and David E. Heinrichs. 2016. "A Heme-Responsive Regulator Controls Synthesis of Staphyloferrin B in *Staphylococcus Aureus*." *Journal of Biological Chemistry* 291 (1): 29–40. <https://doi.org/10.1074/jbc.M115.696625>.
- Lalaouna, David, Karine Prévost, Seongjin Park, Thierry Chénard, Marie-Pier Bouchard, Marie-Pier Caron, Carin K. Vanderpool, Jingyi Fei, and Eric Massé. 2021. "Binding of the RNA Chaperone Hfq on Target mRNAs Promotes the Small RNA RyhB-Induced Degradation in *Escherichia Coli*." *Non-Coding RNA* 7 (4): 64. <https://doi.org/10.3390/ncrna7040064>.
- Lambertz, Camilla, Nils Leidel, Kajsa G.V. Havelius, Jens Noth, Petko Chernev, Martin Winkler, Thomas Happe, and Michael Haumann. 2011. "O<sub>2</sub> Reactions at the Six-Iron Active Site (H-Cluster) in [FeFe]-Hydrogenase." *Journal of Biological Chemistry* 286 (47): 40614–23. <https://doi.org/10.1074/jbc.M111.283648>.

- Lau, Cheryl K. Y., Karla D. Krewulak, and Hans J. Vogel. 2016. "Bacterial Ferrous Iron Transport: The Feo System." Edited by Wilbert Bitter. *FEMS Microbiology Reviews* 40 (2): 273–98. <https://doi.org/10.1093/femsre/fuv049>.
- Le Lam, Thao Nguyen, Claire Morvan, Wenfeng Liu, Chantal Bohn, Yan Jaszczyszyn, and Philippe Bouloc. 2017. "Finding sRNA-Associated Phenotypes by Competition Assays: An Example with *Staphylococcus Aureus*." *Methods* 117 (March): 21–27. <https://doi.org/10.1016/j.ymeth.2016.11.018>.
- Le Scornet, Alexandre, and Peter Redder. 2019. "Post-Transcriptional Control of Virulence Gene Expression in *Staphylococcus Aureus*." *Biochimica et Biophysica Acta (BBA) - Gene Regulatory Mechanisms* 1862 (7): 734–41. <https://doi.org/10.1016/j.bbagr.2018.04.004>.
- Lee, Chi Chung, Michael A. Blank, Aaron W. Fay, Janice M. Yoshizawa, Yilin Hu, Keith O. Hodgson, Britt Hedman, and Markus W. Ribbe. 2009. "Stepwise Formation of P-Cluster in Nitrogenase MoFe Protein." *Proceedings of the National Academy of Sciences* 106 (44): 18474–78. <https://doi.org/10.1073/pnas.0909149106>.
- Liu, Wenfeng, Pierre Boudry, Chantal Bohn, and Philippe Bouloc. 2020. "Staphylococcus Aureus Pigmentation Is Not Controlled by Hfq." *BMC Research Notes* 13 (1): 63. <https://doi.org/10.1186/s13104-020-4934-4>.
- Lokken, Kristen L, Renée M Tsohis, and Andreas J Bäumlér. 2014. "Hypoferremia of Infection: A Double-Edged Sword?" *Nature Medicine* 20 (4): 335–37. <https://doi.org/10.1038/nm.3526>.
- Lopez, Anthony, Patrice Cacoub, Iain C Macdougall, and Laurent Peyrin-Biroulet. 2016. "Iron Deficiency Anaemia." *The Lancet* 387 (10021): 907–16. [https://doi.org/10.1016/S0140-6736\(15\)60865-0](https://doi.org/10.1016/S0140-6736(15)60865-0).
- Los, Ferdinand C. O., Tara M. Randis, Raffi V. Aroian, and Adam J. Ratner. 2013. "Role of Pore-Forming Toxins in Bacterial Infectious Diseases." *Microbiology and Molecular Biology Reviews* 77 (2): 173–207. <https://doi.org/10.1128/MMBR.00052-12>.
- Mäder, Ulrike, Pierre Nicolas, Maren Depke, Jan Pané-Farré, Michel Debarbouille, Magdalena M. van der Kooi-Pol, Cyprien Guérin, et al. 2016. "Staphylococcus Aureus Transcriptome Architecture: From Laboratory to Infection-Mimicking Conditions." Edited by Daniel B. Kearns. *PLOS Genetics* 12 (4): e1005962. <https://doi.org/10.1371/journal.pgen.1005962>.
- Mah, Thien-Fah C, and George A O'Toole. 2001. "Mechanisms of Biofilm Resistance to Antimicrobial Agents." *Trends in Microbiology* 9 (1): 34–39. [https://doi.org/10.1016/S0966-842X\(00\)01913-2](https://doi.org/10.1016/S0966-842X(00)01913-2).
- Mandin, Pierre, Sylvia Chareyre, and Frédéric Barras. 2016. "A Regulatory Circuit Composed of a Transcription Factor, IscR, and a Regulatory RNA, RyhB, Controls Fe-S Cluster Delivery." Edited by Howard A. Shuman. *mBio* 7 (5): e00966-16. <https://doi.org/10.1128/mBio.00966-16>.
- Martin, Mauricio G., Christian Magni, Diego De Mendoza, and Paloma López. 2005. "CitI, a Transcription Factor Involved in Regulation of Citrate Metabolism in Lactic Acid Bacteria." *Journal of Bacteriology* 187 (15): 5146–55. <https://doi.org/10.1128/JB.187.15.5146-5155.2005>.
- Masse, E., and S. Gottesman. 2002. "A Small RNA Regulates the Expression of Genes Involved in Iron Metabolism in *Escherichia Coli*." *Proceedings of the National Academy of Sciences* 99 (7): 4620–25. <https://doi.org/10.1073/pnas.032066599>.

- Massé, Eric, Freddy E. Escorcia, and Susan Gottesman. 2003. "Coupled Degradation of a Small Regulatory RNA and Its mRNA Targets in *Escherichia Coli*." *Genes & Development* 17 (19): 2374–83. <https://doi.org/10.1101/gad.1127103>.
- Massé, Eric, and Susan Gottesman. 2002. "A Small RNA Regulates the Expression of Genes Involved in Iron Metabolism in *Escherichia Coli*." *Proceedings of the National Academy of Sciences* 99 (7): 4620–25. <https://doi.org/10.1073/pnas.032066599>.
- Massé, Eric, Carin K. Vanderpool, and Susan Gottesman. 2005. "Effect of RyhB Small RNA on Global Iron Use in *Escherichia Coli*." *Journal of Bacteriology* 187 (20): 6962–71. <https://doi.org/10.1128/JB.187.20.6962-6971.2005>.
- McCarter, L, and M Silverman. 1989. "Iron Regulation of Swarmer Cell Differentiation of *Vibrio Parahaemolyticus*." *Journal of Bacteriology* 171 (2): 731–36. <https://doi.org/10.1128/jb.171.2.731-736.1989>.
- McCormick, John K., Jeremy M. Yarwood, and Patrick M. Schlievert. 2001. "Toxic Shock Syndrome and Bacterial Superantigens: An Update." *Annual Review of Microbiology* 55 (1): 77–104. <https://doi.org/10.1146/annurev.micro.55.1.77>.
- McGinnis, Jennifer L., Qi Liu, Christopher A. Lavender, Aishwarya Devaraj, Sean P. McClory, Kurt Fredrick, and Kevin M. Weeks. 2015. "In-Cell SHAPE Reveals That Free 30S Ribosome Subunits Are in the Inactive State." *Proceedings of the National Academy of Sciences* 112 (8): 2425–30. <https://doi.org/10.1073/pnas.1411514112>.
- McHugh, Colleen A, Juan Fontana, Daniel Nemecek, Naiqian Cheng, Anastasia A Aksyuk, J Bernard Heymann, Dennis C Winkler, et al. 2014. "A Virus Capsid-like Nanocompartment That Stores Iron and Protects Bacteria from Oxidative Stress." *The EMBO Journal* 33 (17): 1896–1911. <https://doi.org/10.15252/emboj.201488566>.
- Melamed, Sahar, Philip P. Adams, Aixia Zhang, Hongen Zhang, and Gisela Storz. 2020. "RNA-RNA Interactomes of ProQ and Hfq Reveal Overlapping and Competing Roles." *Molecular Cell* 77 (2): 411–425.e7. <https://doi.org/10.1016/j.molcel.2019.10.022>.
- Mellin, J.R., Sulip Goswani, Susan Grogan, Brian Tjaden, and Caroline A. Genco. 2007. "A Novel Fur- and Iron-Regulated Small RNA, NrrF, Is Required for Indirect Fur-Mediated Regulation of the *sdhA* and *sdhC* Genes in *Neisseria Meningitidis*." *Journal of Bacteriology* 189 (May): 3686–94. <https://doi.org/10.1128/JB.01890-06>.
- Mestrovic, Tomislav, Gisela Robles Aguilar, Lucien R Swetschinski, Kevin S Ikuta, Authia P Gray, Nicole Davis Weaver, Chieh Han, et al. 2022. "The Burden of Bacterial Antimicrobial Resistance in the WHO European Region in 2019: A Cross-Country Systematic Analysis." *The Lancet Public Health* 7 (11): e897–913. [https://doi.org/10.1016/S2468-2667\(22\)00225-0](https://doi.org/10.1016/S2468-2667(22)00225-0).
- Meyer, Margareta, Peter Dimroth, and Michael Bott. 2001. "Catabolite Repression of the Citrate Fermentation Genes in *Klebsiella Pneumoniae*: Evidence for Involvement of the Cyclic AMP Receptor Protein." *Journal of Bacteriology* 183 (18): 5248–56. <https://doi.org/10.1128/JB.183.18.5248-5256.2001>.
- Michta, Ewelina, Klaus Schad, Kai Blin, Regina Ort-Winklbauer, Marc Röttig, Oliver Kohlbacher, Wolfgang Wohlleben, Eva Schinko, and Yvonne Mast. 2012. "The Bifunctional Role of Aconitase in *Streptomyces Viridochromogenes* Tü494: Aconitase in *Streptomyces Viridochromogenes* Tü494." *Environmental Microbiology* 14 (12): 3203–19. <https://doi.org/10.1111/1462-2920.12006>.

- Miethke, Marcus, and Mohamed A. Marahiel. 2007. "Siderophore-Based Iron Acquisition and Pathogen Control." *Microbiology and Molecular Biology Reviews* 71 (3): 413–51. <https://doi.org/10.1128/MMBR.00012-07>.
- Miethke, Marcus, Carmine G. Monteferrante, Mohamed A. Marahiel, and Jan Maarten Van Dijk. 2013. "The Bacillus Subtilis EfeUOB Transporter Is Essential for High-Affinity Acquisition of Ferrous and Ferric Iron." *Biochimica et Biophysica Acta (BBA) - Molecular Cell Research* 1833 (10): 2267–78. <https://doi.org/10.1016/j.bbamcr.2013.05.027>.
- Mittal, Meghna, Kieran B. Pechter, Silvia Picossi, Hyun-Jin Kim, Kathryn O. Kerstein, and Abraham L. Sonenshein. 2013. "Dual Role of CcpC Protein in Regulation of Aconitase Gene Expression in Listeria Monocytogenes and Bacillus Subtilis." *Microbiology* 159 (Pt\_1): 68–76. <https://doi.org/10.1099/mic.0.063388-0>.
- Monk, Ian R., Jai J. Tree, Benjamin P. Howden, Timothy P. Stinear, and Timothy J. Foster. 2015. "Complete Bypass of Restriction Systems for Major Staphylococcus Aureus Lineages." Edited by Steven J. Projan. *mBio* 6 (3): e00308-15. <https://doi.org/10.1128/mBio.00308-15>.
- Montgomery, Christopher P., Susan Boyle-Vavra, Patricia V. Adem, Jean C. Lee, Aliya N. Husain, Julia Clasen, and Robert S. Daum. 2008. "Comparison of Virulence in Community-Associated Methicillin-Resistant *Staphylococcus Aureus* Pulsotypes USA300 and USA400 in a Rat Model of Pneumonia." *The Journal of Infectious Diseases* 198 (4): 561–70. <https://doi.org/10.1086/590157>.
- Moore, and Robert T. Sauer. 2007. "The tmRNA System for Translational Surveillance and Ribosome Rescue." *Annual Review of Biochemistry* 76 (1): 101–24. <https://doi.org/10.1146/annurev.biochem.75.103004.142733>.
- Mortenson, L.E., R.C. Valentine, and J.E. Carnahan. 1962. "An Electron Transport Factor from Clostridium Pasteurianum." *Biochemical and Biophysical Research Communications* 7 (6): 448–52. [https://doi.org/10.1016/0006-291X\(62\)90333-9](https://doi.org/10.1016/0006-291X(62)90333-9).
- Müller, Peter, Matthias Gimpel, Theresa Wildenhain, and Sabine Brantl. 2019. "A New Role for CsrA: Promotion of Complex Formation between an sRNA and Its mRNA Target in *Bacillus Subtilis*." *RNA Biology* 16 (7): 972–87. <https://doi.org/10.1080/15476286.2019.1605811>.
- Murdoch, Caitlin C., and Eric P. Skaar. 2022. "Nutritional Immunity: The Battle for Nutrient Metals at the Host–Pathogen Interface." *Nature Reviews Microbiology* 20 (11): 657–70. <https://doi.org/10.1038/s41579-022-00745-6>.
- Nemeth, Elizabeta, Erika V. Valore, Mary Territo, Gary Schiller, Alan Lichtenstein, and Tomas Ganz. 2003. "Hepcidin, a Putative Mediator of Anemia of Inflammation, Is a Type II Acute-Phase Protein." *Blood* 101 (7): 2461–63. <https://doi.org/10.1182/blood-2002-10-3235>.
- Novick, and Edward Geisinger. 2008. "Quorum Sensing in Staphylococci." *Annual Review of Genetics* 42 (1): 541–64. <https://doi.org/10.1146/annurev.genet.42.110807.091640>.
- Novick, R.P., H.F. Ross, S.J. Projan, J. Kornblum, B. Kreiswirth, and S. Moghazeh. 1993. "Synthesis of Staphylococcal Virulence Factors Is Controlled by a Regulatory RNA Molecule." *The EMBO Journal* 12 (10): 3967–75. <https://doi.org/10.1002/j.1460-2075.1993.tb06074.x>.
- Oglesby, Amanda G., John M. Farrow, Joon-Hee Lee, Andrew P. Tomaras, E.P. Greenberg, Everett C. Pesci, and Michael L. Vasil. 2008. "The Influence of Iron on Pseudomonas Aeruginosa Physiology." *Journal of Biological Chemistry* 283 (23): 15558–67. <https://doi.org/10.1074/jbc.M707840200>.

- Otto, Michael. 2018. "Staphylococcal Biofilms." Edited by Vincent A. Fischetti, Richard P. Novick, Joseph J. Ferretti, Daniel A. Portnoy, and Julian I. Rood. *Microbiology Spectrum* 6 (4): 6.4.27. <https://doi.org/10.1128/microbiolspec.GPP3-0023-2018>.
- Outten, F. Wayne, Ouliana Djaman, and Gisela Storz. 2004. "A Suf Operon Requirement for Fe-S Cluster Assembly during Iron Starvation in Escherichia Coli: Suf Operon Role during Iron Starvation." *Molecular Microbiology* 52 (3): 861–72. <https://doi.org/10.1111/j.1365-2958.2004.04025.x>.
- Pantel, I, P.-E Lindgren, H Neubauer, and F. Gotz. 1998. "Identification and Characterization of the Staphylococcus Carnosus Nitrate Reductase Operon."
- Pechter, Kieran B., Frederik M. Meyer, Alisa W. Serio, Jörg Stülke, and Abraham L. Sonenshein. 2013a. "Two Roles for Aconitase in the Regulation of Tricarboxylic Acid Branch Gene Expression in Bacillus Subtilis." *Journal of Bacteriology* 195 (7): 1525–37. <https://doi.org/10.1128/JB.01690-12>.
- . 2013b. "Two Roles for Aconitase in the Regulation of Tricarboxylic Acid Branch Gene Expression in Bacillus Subtilis." *Journal of Bacteriology* 195 (7): 1525–37. <https://doi.org/10.1128/JB.01690-12>.
- Pi, Hualiang, and John D. Helmann. 2017. "Ferrous Iron Efflux Systems in Bacteria." *Metallomics* 9 (7): 840–51. <https://doi.org/10.1039/C7MT00112F>.
- Pi, Hualiang, Sarju J. Patel, José M. Argüello, and John D. Helmann. 2016. "The *Listeria Monocytogenes* Fur-Regulated Virulence Protein FrvA Is an Fe(II) Efflux P<sub>184</sub>-Type ATPase: *Listeria Monocytogenes* FrvA Mediates Ferrous Iron Efflux." *Molecular Microbiology* 100 (6): 1066–79. <https://doi.org/10.1111/mmi.13368>.
- Pinchuk, Irina V., Ellen J. Beswick, and Victor E. Reyes. 2010. "Staphylococcal Enterotoxins." *Toxins* 2 (8): 2177–97. <https://doi.org/10.3390/toxins2082177>.
- Pomposiello, Pablo J., Marjon H. J. Bennik, and Bruce Demple. 2001. "Genome-Wide Transcriptional Profiling of the *Escherichia Coli* Responses to Superoxide Stress and Sodium Salicylate." *Journal of Bacteriology* 183 (13): 3890–3902. <https://doi.org/10.1128/JB.183.13.3890-3902.2001>.
- Porcheron, Gaëlle, Rima Habib, Sébastien Houle, Mélissa Caza, François Lépine, France Daigle, Eric Massé, and Charles M. Dozois. 2014. "The Small RNA RyhB Contributes to Siderophore Production and Virulence of Uropathogenic Escherichia Coli." Edited by S. M. Payne. *Infection and Immunity* 82 (12): 5056–68. <https://doi.org/10.1128/IAI.02287-14>.
- Pos, Klaas Martinus, Peter Dimroth, and Michael Bott. 1998. "The *Escherichia Coli* Citrate Carrier CitT: A Member of a Novel Eubacterial Transporter Family Related to the 2-Oxoglutarate/Malate Translocator from Spinach Chloroplasts." *Journal of Bacteriology* 180 (16): 4160–65. <https://doi.org/10.1128/JB.180.16.4160-4165.1998>.
- Posey, James E., and Frank C. Gherardini. 2000. "Lack of a Role for Iron in the Lyme Disease Pathogen." *Science* 288 (5471): 1651–53. <https://doi.org/10.1126/science.288.5471.1651>.
- Pourciau, Christine, Ying-Jung Lai, Mark Gorelik, Paul Babitzke, and Tony Romeo. 2020. "Diverse Mechanisms and Circuitry for Global Regulation by the RNA-Binding Protein CsrA." *Frontiers in Microbiology* 11 (October): 601352. <https://doi.org/10.3389/fmicb.2020.601352>.
- Prévost, Karine, Guillaume Desnoyers, Jean-François Jacques, François Lavoie, and Eric Massé. 2011. "Small RNA-Induced mRNA Degradation Achieved through Both Translation

- Block and Activated Cleavage." *Genes & Development* 25 (4): 385–96. <https://doi.org/10.1101/gad.2001711>.
- Prévost, Karine, Hubert Salvail, Guillaume Desnoyers, Jean-François Jacques, Émilie Phaneuf, and Eric Massé. 2007. "The Small RNA RyhB Activates the Translation of shiA mRNA Encoding a Permease of Shikimate, a Compound Involved in Siderophore Synthesis: RyhB Activates shiA Translation." *Molecular Microbiology* 64 (5): 1260–73. <https://doi.org/10.1111/j.1365-2958.2007.05733.x>.
- Price, Erin E., and Jeffrey M. Boyd. 2020. "Genetic Regulation of Metal Ion Homeostasis in *Staphylococcus Aureus*." *Trends in Microbiology* 28 (10): 821–31. <https://doi.org/10.1016/j.tim.2020.04.004>.
- Reedy, Charles J., and Brian R. Gibney. 2004. "Heme Protein Assemblies." *Chemical Reviews* 104 (2): 617–50. <https://doi.org/10.1021/cr0206115>.
- Reif, Celine, Charlotte Löser, and Sabine Brantl. 2018. "Bacillus Subtilis Type I Antitoxin SR6 Promotes Degradation of Toxin yonT mRNA and Is Required to Prevent Toxic yoyJ Overexpression." *Toxins* 10 (2): 74. <https://doi.org/10.3390/toxins10020074>.
- Rizvanovic, Alisa, Charlotte Michaux, Margherita Panza, Zeynep Iloglu, Sophie Helaine, E. Gerhart H. Wagner, and Erik Holmqvist. 2022. "The RNA-Binding Protein ProQ Promotes Antibiotic Persistence in Salmonella." Edited by Gisela Storz. *mBio* 13 (6): e02891-22. <https://doi.org/10.1128/mbio.02891-22>.
- Rochat, Tatiana, Chantal Bohn, Claire Morvan, Thao Nguyen Le Lam, Fareha Razvi, Adrien Pain, Claire Toffano-Nioche, et al. 2018a. "The Conserved Regulatory RNA RsaE Down-Regulates the Arginine Degradation Pathway in *Staphylococcus Aureus*." *Nucleic Acids Research* 46 (17): 8803–16. <https://doi.org/10.1093/nar/gky584>.
- . 2018b. "The Conserved Regulatory RNA RsaE Down-Regulates the Arginine Degradation Pathway in *Staphylococcus Aureus*." *Nucleic Acids Research* 46 (17): 8803–16. <https://doi.org/10.1093/nar/gky584>.
- Rochat, Tatiana, Philippe Bouloc, Qi Yang, Lionello Bossi, and Nara Figueroa-Bossi. 2012. "Lack of Interchangeability of Hfq-like Proteins." *Biochimie* 94 (7): 1554–59. <https://doi.org/10.1016/j.biochi.2012.01.016>.
- Rochat, Tatiana, Olivier Delumeau, Nara Figueroa-Bossi, Philippe Noirot, Lionello Bossi, Etienne Dervyn, and Philippe Bouloc. 2015. "Tracking the Elusive Function of *Bacillus Subtilis* Hfq." Edited by Lennart Randau. *PLoS ONE* 10 (4): e0124977. <https://doi.org/10.1371/journal.pone.0124977>.
- Roche, Béatrice, Laurent Aussel, Benjamin Ezraty, Pierre Mandin, Béatrice Py, and Frédéric Barbas. 2013. "Reprint of: Iron/Sulfur Proteins Biogenesis in Prokaryotes: Formation, Regulation and Diversity." *Biochimica et Biophysica Acta (BBA) - Bioenergetics* 1827 (8–9): 923–37. <https://doi.org/10.1016/j.bbabi.2013.05.001>.
- Rodriguez, Michelle D., Zubin Paul, Charles E. Wood, Kelly C. Rice, and Eric W. Triplett. 2017. "Construction of Stable Fluorescent Reporter Plasmids for Use in *Staphylococcus Aureus*." *Frontiers in Microbiology* 8 (December): 2491. <https://doi.org/10.3389/fmicb.2017.02491>.
- Romilly, Cédric, Claire Lays, Arnaud Tomasini, Isabelle Caldelari, Yvonne Benito, Philippe Hammann, Thomas Geissmann, Sandrine Boisset, Pascale Romby, and François Vandenesch. 2014. "A Non-Coding RNA Promotes Bacterial Persistence and Decreases Virulence by Regulating a Regulator in *Staphylococcus Aureus*." Edited by Michael S. Gilmore. *PLoS Pathogens* 10 (3): e1003979. <https://doi.org/10.1371/journal.ppat.1003979>.

- Rosenkrantz, M S, D W Dingman, and A L Sonenshein. 1985. "Bacillus Subtilis citB Gene Is Regulated Synergistically by Glucose and Glutamine." *Journal of Bacteriology* 164 (1): 155–64. <https://doi.org/10.1128/jb.164.1.155-164.1985>.
- Salusso, Agostina, and Daniel Raimunda. 2017. "Defining the Roles of the Cation Diffusion Facilitators in Fe<sup>2+</sup>/Zn<sup>2+</sup> Homeostasis and Establishment of Their Participation in Virulence in Pseudomonas Aeruginosa." *Frontiers in Cellular and Infection Microbiology* 7 (March). <https://doi.org/10.3389/fcimb.2017.00084>.
- Saramago, Margarida, Cátia Bárria, Ricardo F Dos Santos, Inês J Silva, Vânia Pobre, Susana Domingues, José M Andrade, Sandra C Viegas, and Cecília M Arraiano. 2014. "The Role of RNases in the Regulation of Small RNAs." *Current Opinion in Microbiology* 18 (April): 105–15. <https://doi.org/10.1016/j.mib.2014.02.009>.
- Sebulsky, M. Tom, Craig D. Speziali, Brian H. Shilton, David R. Edgell, and David E. Heinrichs. 2004. "FhuD1, a Ferric Hydroxamate-Binding Lipoprotein in Staphylococcus Aureus." *Journal of Biological Chemistry* 279 (51): 53152–59. <https://doi.org/10.1074/jbc.M409793200>.
- Seixas, André F., Ana P. Quendera, João P. Sousa, Alda F. Q. Silva, Cecília M. Arraiano, and José M. Andrade. 2022. "Bacterial Response to Oxidative Stress and RNA Oxidation." *Frontiers in Genetics* 12 (January): 821535. <https://doi.org/10.3389/fgene.2021.821535>.
- Serio, Alisa W., Kieran B. Pechter, and Abraham L. Sonenshein. 2006. "Bacillus Subtilis Aconitase Is Required for Efficient Late-Sporulation Gene Expression." *Journal of Bacteriology* 188 (17): 6396–6405. <https://doi.org/10.1128/JB.00249-06>.
- Sheldon, Jessica R., and David E. Heinrichs. 2015. "Recent Developments in Understanding the Iron Acquisition Strategies of Gram Positive Pathogens." Edited by Chris Whitfield. *FEMS Microbiology Reviews* 39 (4): 592–630. <https://doi.org/10.1093/femsre/fuv009>.
- Sheldon, Jessica R., Holly A. Laakso, and David E. Heinrichs. 2016. "Iron Acquisition Strategies of Bacterial Pathogens." Edited by Indira T. Kudva and Nancy A. Cornick. *Microbiology Spectrum* 4 (2): 4.2.05. <https://doi.org/10.1128/microbiolspec.VMBF-0010-2015>.
- Sheldon, Jessica R., Cristina L. Marolda, and David E. Heinrichs. 2014. "TCA Cycle Activity in *S. Taphylococcus Aureus* Is Essential for Iron-Regulated Synthesis of Staphyloferrin A, but Not Staphyloferrin B: The Benefit of a Second Citrate Synthase: *S. Aureus* Requires TCA Cycle for SA Synthesis." *Molecular Microbiology* 92 (4): 824–39. <https://doi.org/10.1111/mmi.12593>.
- Shimamoto, Tadashi, Hiroshi Izawa, Hirohiko Daimon, Naotaka Ishiguro, Morikazu Shinagawa, Yumiko Sakano, Masaaki Tsuda, and Tomofusa Tsuchiya. 1991. "Cloning and Nucleotide Sequence of the Gene (citA) Encoding a Citrate Carrier from Salmonella Typhimurium1." *The Journal of Biochemistry* 110 (1): 22–28. <https://doi.org/10.1093/oxfordjournals.jbchem.a123537>.
- Shin, Ji-Hyun, and Chester W. Price. 2007. "The SsrA-SmpB Ribosome Rescue System Is Important for Growth of *Bacillus Subtilis* at Low and High Temperatures." *Journal of Bacteriology* 189 (10): 3729–37. <https://doi.org/10.1128/JB.00062-07>.
- Shin, Yerin Jin, Jinsub Park, Daye Mun, Soo Rin Kim, Shelley M. Payne, Kyoung Heon Kim, and Younghoon Kim. 2021. "Characterization of an Antibacterial Agent Targeting Ferrous Iron Transport Protein FeoB against *Staphylococcus Aureus* and Gram-Positive Bacteria." *ACS Chemical Biology* 16 (1): 136–49. <https://doi.org/10.1021/acscchembio.0c00842>.

- Siddique, A., and K. V. Kowdley. 2012. "Review Article: The Iron Overload Syndromes." *Alimentary Pharmacology & Therapeutics* 35 (8): 876–93. <https://doi.org/10.1111/j.1365-2036.2012.05051.x>.
- Silva, Inês Jesus, Susana Barahona, Alex Eyraud, David Lalaouna, Nara Figueroa-Bossi, Eric Massé, and Cecília Maria Arraiano. 2019. "SraL sRNA Interaction Regulates the Terminator by Preventing Premature Transcription Termination of *Rho* mRNA." *Proceedings of the National Academy of Sciences* 116 (8): 3042–51. <https://doi.org/10.1073/pnas.1811589116>.
- Simons, Robert W., and Nancy Kleckner. 1983. "Translational Control of IS10 Transposition." *Cell* 34 (2): 683–91. [https://doi.org/10.1016/0092-8674\(83\)90401-4](https://doi.org/10.1016/0092-8674(83)90401-4).
- Skaar, Munir Humayun, Taeok Bae, Kristin L. DeBord, and Olaf Schneewind. 2004. "Iron-Source Preference of *Staphylococcus Aureus* Infections." *Science* 305 (5690): 1626–28. <https://doi.org/10.1126/science.1099930>.
- Skaar, and Olaf Schneewind. 2004. "Iron-Regulated Surface Determinants (Isd) of *Staphylococcus Aureus*: Stealing Iron from Heme." *Microbes and Infection* 6 (4): 390–97. <https://doi.org/10.1016/j.micinf.2003.12.008>.
- Slobodin, Boris, and Jeffrey E. Gerst. 2010. "A Novel mRNA Affinity Purification Technique for the Identification of Interacting Proteins and Transcripts in Ribonucleoprotein Complexes." *RNA* 16 (11): 2277–90. <https://doi.org/10.1261/rna.2091710>.
- Smaldone, G. T., O. Revelles, A. Gaballa, U. Sauer, H. Antelmann, and J. D. Helmann. 2012. "A Global Investigation of the *Bacillus Subtilis* Iron-Sparing Response Identifies Major Changes in Metabolism." *Journal of Bacteriology* 194 (10): 2594–2605. <https://doi.org/10.1128/JB.05990-11>.
- Smirnov, Alexandre, Konrad U. Förstner, Erik Holmqvist, Andreas Otto, Regina Günster, Dörte Becher, Richard Reinhardt, and Jörg Vogel. 2016. "Grad-Seq Guides the Discovery of ProQ as a Major Small RNA-Binding Protein." *Proceedings of the National Academy of Sciences* 113 (41): 11591–96. <https://doi.org/10.1073/pnas.1609981113>.
- Sobczak, Iwona, and Juke S. Lolkema. 2005. "The 2-Hydroxycarboxylate Transporter Family: Physiology, Structure, and Mechanism." *Microbiology and Molecular Biology Reviews* 69 (4): 665–95. <https://doi.org/10.1128/MMBR.69.4.665-695.2005>.
- Sobrero, Patricio Martín, and Claudio Valverde. 2020. "Comparative Genomics and Evolutionary Analysis of RNA-Binding Proteins of the CsrA Family in the Genus *Pseudomonas*." *Frontiers in Molecular Biosciences* 7 (July): 127. <https://doi.org/10.3389/fmolb.2020.00127>.
- Sonenshein, Abraham L. 2007. "Control of Key Metabolic Intersections in *Bacillus Subtilis*." *Nature Reviews Microbiology* 5 (12): 917–27. <https://doi.org/10.1038/nrmicro1772>.
- Soutourina, Olga. 2017. "RNA-Based Control Mechanisms of *Clostridium Difficile*." *Current Opinion in Microbiology* 36 (April): 62–68. <https://doi.org/10.1016/j.mib.2017.01.004>.
- Steere, Ashley N., Shaina L. Byrne, N. Dennis Chasteen, and Anne B. Mason. 2012. "Kinetics of Iron Release from Transferrin Bound to the Transferrin Receptor at Endosomal pH." *Biochimica et Biophysica Acta (BBA) - General Subjects* 1820 (3): 326–33. <https://doi.org/10.1016/j.bbagen.2011.06.003>.
- Steingard, Caroline H., and John D. Helmann. 2023. "Meddling with Metal Sensors: Fur-Family Proteins as Signaling Hubs." Edited by Tina M. Henkin. *Journal of Bacteriology* 205 (4): e00022–23. <https://doi.org/10.1128/jb.00022-23>.

- Stougaard, P, S Molin, and K Nordström. 1981. "RNAs Involved in Copy-Number Control and Incompatibility of Plasmid R1." *Proceedings of the National Academy of Sciences* 78 (10): 6008–12. <https://doi.org/10.1073/pnas.78.10.6008>.
- Sun, Fei, Qianjiang Ji, Marcus B. Jones, Xin Deng, Haihua Liang, Bryan Frank, Joshua Telser, Scott N. Peterson, Taeok Bae, and Chuan He. 2012. "AirSR, a [2Fe-2S] Cluster-Containing Two-Component System, Mediates Global Oxygen Sensing and Redox Signaling in *Staphylococcus Aureus*." *Journal of the American Chemical Society* 134 (1): 305–14. <https://doi.org/10.1021/ja2071835>.
- Svetlanov, Anton, Neha Puri, Patricio Mena, Antonius Koller, and A. Wali Karzai. 2012. "Francisella Tularensis tmRNA System Mutants Are Vulnerable to Stress, Avirulent in Mice, and Provide Effective Immune Protection: The SmpB-tmRNA System and F. Tularensis Virulence." *Molecular Microbiology* 85 (1): 122–41. <https://doi.org/10.1111/j.1365-2958.2012.08093.x>.
- Takahashi, Yasuhiro, and Umechiyo Tokumoto. 2002. "A Third Bacterial System for the Assembly of Iron-Sulfur Clusters with Homologs in Archaea and Plastids." *Journal of Biological Chemistry* 277 (32): 28380–83. <https://doi.org/10.1074/jbc.C200365200>.
- Tang, Yue, and John R. Guest. 1999. "Direct Evidence for mRNA Binding and Post-Transcriptional Regulation by *Escherichia Coli* Aconitases." *Microbiology* 145 (11): 3069–79. <https://doi.org/10.1099/00221287-145-11-3069>.
- Tang, Yue, John R. Guest, Peter J. Artymiuk, Robert C. Read, and Jeffrey Green. 2004. "Post-Transcriptional Regulation of Bacterial Motility by Aconitase Proteins: Bacterial Motility and Aconitase Proteins." *Molecular Microbiology* 51 (6): 1817–26. <https://doi.org/10.1111/j.1365-2958.2003.03954.x>.
- Tiwari, Kiran B., Jacob Birlingmair, Brian J. Wilkinson, and Radheshyam K. Jayaswal. 2015. "Role of the Twin-Arginine Translocase (Tat) System in Iron Uptake in *Listeria Monocytogenes*." *Microbiology* 161 (2): 264–71. <https://doi.org/10.1099/mic.0.083642-0>.
- Tjaden, B., S. S. Goodwin, J. A. Opdyke, M. Guillier, D. X. Fu, S. Gottesman, and G. Storz. 2006. "Target Prediction for Small, Noncoding RNAs in Bacteria." *Nucleic Acids Research* 34 (9): 2791–2802. <https://doi.org/10.1093/nar/gkl356>.
- Tong, Yong, and Maolin Guo. 2009. "Bacterial Heme-Transport Proteins and Their Heme-Coordination Modes." *Archives of Biochemistry and Biophysics* 481 (1): 1–15. <https://doi.org/10.1016/j.abb.2008.10.013>.
- Torres, Victor J., Gleb Pishchany, Munir Humayun, Olaf Schneewind, and Eric P. Skaar. 2006. "*Staphylococcus Aureus* IsdB Is a Hemoglobin Receptor Required for Heme Iron Utilization." *Journal of Bacteriology* 188 (24): 8421–29. <https://doi.org/10.1128/JB.01335-06>.
- Troxell, Bryan, and Hosni M. Hassan. 2013. "Transcriptional Regulation by Ferric Uptake Regulator (Fur) in Pathogenic Bacteria." *Frontiers in Cellular and Infection Microbiology* 3. <https://doi.org/10.3389/fcimb.2013.00059>.
- Turlin, Evelyne, Michel Débarbouillé, Katarzyna Augustyniak, Anne-Marie Gilles, and Cécile Wandersman. 2013. "Staphylococcus Aureus FepA and FepB Proteins Drive Heme Iron Utilization in *Escherichia Coli*." Edited by Alain Charbit. *PLoS ONE* 8 (2): e56529. <https://doi.org/10.1371/journal.pone.0056529>.

- Turner, Andrew G., Karrera Y. Djoko, Cheryl-lynn Y. Ong, Timothy C. Barnett, Mark J. Walker, and Alastair G. McEwan. 2019. "Group A *Streptococcus* Co-Ordinates Manganese Import and Iron Efflux in Response to Hydrogen Peroxide Stress." *Biochemical Journal* 476 (3): 595–611. <https://doi.org/10.1042/BCJ20180902>.
- Uden, Gottfried, and Jan Schirawski. 1997. "The Oxygen-Responsive Transcriptional Regulator FNR of *Escherichia Coli*: The Search for Signals and Reactions." *Molecular Microbiology* 25 (02): 205–10. <https://doi.org/10.1046/j.1365-2958.1997.4731841.x>.
- Updegrave, Taylor B, Aixia Zhang, and Gisela Storz. 2016. "Hfq: The Flexible RNA Matchmaker." *Current Opinion in Microbiology* 30 (April): 133–38. <https://doi.org/10.1016/j.mib.2016.02.003>.
- Van Der Rest, M E, D Molenaar, and W N Konings. 1992. "Mechanism of Na(+)-Dependent Citrate Transport in *Klebsiella Pneumoniae*." *Journal of Bacteriology* 174 (15): 4893–98. <https://doi.org/10.1128/jb.174.15.4893-4898.1992>.
- Van Dijk, Madeleine C., Robin M. De Kruijff, and Peter-Leon Hagedoorn. 2022. "The Role of Iron in *Staphylococcus Aureus* Infection and Human Disease: A Metal Tug of War at the Host—Microbe Interface." *Frontiers in Cell and Developmental Biology* 10 (March): 857237. <https://doi.org/10.3389/fcell.2022.857237>.
- Van Hal, Sebastian J., Slade O. Jensen, Vikram L. Vaska, Björn A. Espedido, David L. Paterson, and Iain B. Gosbell. 2012. "Predictors of Mortality in *Staphylococcus Aureus* Bacteremia." *Clinical Microbiology Reviews* 25 (2): 362–86. <https://doi.org/10.1128/CMR.05022-11>.
- Vasil, Michael L. 2007. "How We Learnt about Iron Acquisition in *Pseudomonas Aeruginosa*: A Series of Very Fortunate Events." *BioMetals* 20 (3–4): 587–601. <https://doi.org/10.1007/s10534-006-9067-2>.
- Verdon, Julien, Nicolas Girardin, Christian Lacombe, Jean-Marc Berjeaud, and Yann Héchard. 2009. "δ-Hemolysin, an Update on a Membrane-Interacting Peptide." *Peptides* 30 (4): 817–23. <https://doi.org/10.1016/j.peptides.2008.12.017>.
- Verstraete, Meghan M, L Daniela Morales, Marek J Kobylarz, Slade A Loutet, Holly A Laakso, Tyler B Pinter, X Martin J Stillman, and X David E Heinrichs. 2019. "The Heme-Sensitive Regulator SbnI Has a Bifunctional Role in *Staphyloferrin B* Production by *Staphylococcus Aureus*." *Journal of Biological Chemistry*. <https://doi.org/10.1074/jbc.RA119.007757>.
- Vogel, Jörg, and Ben F. Luisi. 2011. "Hfq and Its Constellation of RNA." *Nature Reviews Microbiology* 9 (8): 578–89. <https://doi.org/10.1038/nrmicro2615>.
- Wadler, Caryn S., and Carin K. Vanderpool. 2007. "A Dual Function for a Bacterial Small RNA: SgrS Performs Base Pairing-Dependent Regulation and Encodes a Functional Polypeptide." *Proceedings of the National Academy of Sciences* 104 (51): 20454–59. <https://doi.org/10.1073/pnas.0708102104>.
- Wagner, E. Gerhart H., and Pascale Romby. 2015. "Small RNAs in Bacteria and Archaea." In *Advances in Genetics*, 90:133–208. Elsevier. <https://doi.org/10.1016/bs.adgen.2015.05.001>.
- Walden, William E., Anna I. Selezneva, Jérôme Dupuy, Anne Volbeda, Juan C. Fontecilla-Camps, Elizabeth C. Theil, and Karl Volz. 2006. "Structure of Dual Function Iron Regulatory Protein 1 Complexed with Ferritin IRE-RNA." *Science* 314 (5807): 1903–8. <https://doi.org/10.1126/science.1133116>.
- Wallace, Daniel F. 2016. "The Regulation of Iron Absorption and Homeostasis."

- Wandersman, Cécile, and Philippe Delepelaire. 2012. "Haemophore Functions Revisited: Haemophore Functions Revisited." *Molecular Microbiology* 85 (4): 618–31. <https://doi.org/10.1111/j.1365-2958.2012.08136.x>.
- Wang, Chen-Hao, and Serena DeBeer. 2021. "Structure, Reactivity, and Spectroscopy of Nitrogenase-Related Synthetic and Biological Clusters." *Chemical Society Reviews* 50 (15): 8743–61. <https://doi.org/10.1039/D1CS00381J>.
- Wang, Ya, Yanli Teng, Juan Geng, Jinzhao Long, Haiyan Yang, Guangcai Duan, and Shuaiyin Chen. 2023. "Involvement of RNA Chaperone Hfq in the Regulation of Antibiotic Resistance and Virulence in *Shigella Sonnei*." *Research in Microbiology* 174 (5): 104047. <https://doi.org/10.1016/j.resmic.2023.104047>.
- Warner, Jessica B, and Juke S Lolkema. 2002. "Growth of *Bacillus Subtilis* on Citrate and Isocitrate Is Supported by the Mg<sup>2+</sup>-Citrate Transporter CitM." *Microbiology* 148: 3405–12.
- Wassarman, Karen M. 2018. "6S RNA, a Global Regulator of Transcription." Edited by Gisela Storz and Kai Papenfort. *Microbiology Spectrum* 6 (3): 6.3.06. <https://doi.org/10.1128/microbiolspec.RWR-0019-2018>.
- Wassarman, Karen M., Francis Repoila, Carsten Rosenow, Gisela Storz, and Susan Gottesman. 2001. "Identification of Novel Small RNAs Using Comparative Genomics and Microarrays." *Genes & Development* 15 (13): 1637–51. <https://doi.org/10.1101/gad.901001>.
- Waters, Lauren S., and Gisela Storz. 2009. "Regulatory RNAs in Bacteria." *Cell* 136 (4): 615–28. <https://doi.org/10.1016/j.cell.2009.01.043>.
- Weinberg, Eugene D. 1975. "Nutritional Immunity: Host's Attempt to Withhold Iron From Microbial Invaders." *JAMA* 231 (1): 39. <https://doi.org/10.1001/jama.1975.03240130021018>.
- Westermann, Alexander J., Elisa Venturini, Mikael E. Sellin, Konrad U. Förstner, Wolf-Dietrich Hardt, and Jörg Vogel. 2019. "The Major RNA-Binding Protein ProQ Impacts Virulence Gene Expression in *Salmonella Enterica* Serovar Typhimurium." Edited by Julian Parkhill. *mBio* 10 (1): e02504-18. <https://doi.org/10.1128/mBio.02504-18>.
- Wiegand, G, and S J Remington. 1986. "Citrate Synthase: Structure, Control, and Mechanism."
- Wilderman, Paula J., Nathaniel A. Sowa, David J. FitzGerald, Peter C. FitzGerald, Susan Gottesman, Urs A. Ochsner, and Michael L. Vasil. 2004. "Identification of Tandem Duplicate Regulatory Small RNAs in *Pseudomonas Aeruginosa* Involved in Iron Homeostasis." *Proceedings of the National Academy of Sciences* 101 (26): 9792–97. <https://doi.org/10.1073/pnas.0403423101>.
- Wright, John A., and Sean P. Nair. 2012. "The Lipoprotein Components of the Isd and Hts Transport Systems Are Dispensable for Acquisition of Heme by *Staphylococcus Aureus*." *FEMS Microbiology Letters* 329 (2): 177–85. <https://doi.org/10.1111/j.1574-6968.2012.02519.x>.
- Yamamoto, Hiroki, Masayoshi Murata, and Junichi Sekiguchi. 2000. "The CitST Two-Component System Regulates the Expression of the Mg-Citrate Transporter in *Bacillus Subtilis*." *Molecular Microbiology* 37 (4): 898–912. <https://doi.org/10.1046/j.1365-2958.2000.02055.x>.
- Yan, Nieng. 2015. "Structural Biology of the Major Facilitator Superfamily Transporters." *Annual Review of Biophysics* 44 (1): 257–83. <https://doi.org/10.1146/annurev-biophys-060414-033901>.

- Yeo, Won-Sik, Joon-Hee Lee, Kyung-Chang Lee, and Jung-Hye Roe. 2006. "IscR Acts as an Activator in Response to Oxidative Stress for the *Suf* Operon Encoding Fe-S Assembly Proteins: Positive Regulation of the *Suf* Operon by IscR." *Molecular Microbiology* 61 (1): 206–18. <https://doi.org/10.1111/j.1365-2958.2006.05220.x>.
- Zanetti, G., and V. Pandini. 2013. "Ferredoxin." In *Encyclopedia of Biological Chemistry*, 296–98. Elsevier. <https://doi.org/10.1016/B978-0-12-378630-2.00176-6>.
- Zheng, Chengkun, Mengdie Jia, Miaomiao Gao, Tianyu Lu, Lingzhi Li, and Pingping Zhou. 2019. "PmtA Functions as a Ferrous Iron and Cobalt Efflux Pump in *Streptococcus Suis*." *Emerging Microbes & Infections* 8 (1): 1254–64. <https://doi.org/10.1080/22221751.2019.1660233>.
- Zheng, Limin, Valerie L. Cash, Dennis H. Flint, and Dennis R. Dean. 1998. "Assembly of Iron-Sulfur Clusters." *Journal of Biological Chemistry* 273 (21): 13264–72. <https://doi.org/10.1074/jbc.273.21.13264>.

# J: Résumé substantiel en français

---

## Introduction:

Le fer est un des éléments chimiques les plus abondants présents sur Terre, en effet il représente près de 6,3% de sa masse totale. C'est un métal de transition qui existe sous différents niveaux d'oxydation, mais la très grande majorité du fer trouvé dans l'environnement se trouve sous la forme de fer ferreux ( $\text{Fe}^{2+}$ ) ou de fer ferrique ( $\text{Fe}^{3+}$ ). Le fer ferreux, soluble, est retrouvé principalement dans les environnements anaérobies tandis que le fer ferrique, insoluble, est retrouvé principalement en présence d'oxygène. Cette capacité du fer à passer de l'état ferreux à l'état ferrique en fait un cofacteur particulièrement intéressant en biologie. Ainsi, le fer est retrouvé dans plusieurs protéines impliquées dans de nombreuses voies métaboliques (Réparation de l'ADN, modification de l'ARN, respiration, cycle de Krebs etc.) sous forme de noyaux Fer-Soufre. Par conséquent, le fer est un élément essentiel pour quasiment tous les microorganismes (à quelques exceptions près, telles que *Borrelia burgdorferi*, *Treponema pallidum* par exemple).

Puisque le fer est un élément essentiel pour la croissance microbienne, une des premières actions mise en place par l'hôte lors d'une infection consiste à séquestrer le fer (via des protéines telles que les transferrines ou les lactoferrines) afin de le rendre indisponible pour les microorganismes, c'est le phénomène d'immunité nutritionnelle. En réponse à cela, les microorganismes ont développé plusieurs mécanismes de captation du fer. Le principal étant la synthèse de siderophores, des molécules sécrétées dans le milieu qui vont aller capter le fer pour qu'il soit ensuite réincorporé et utilisé par les bactéries.

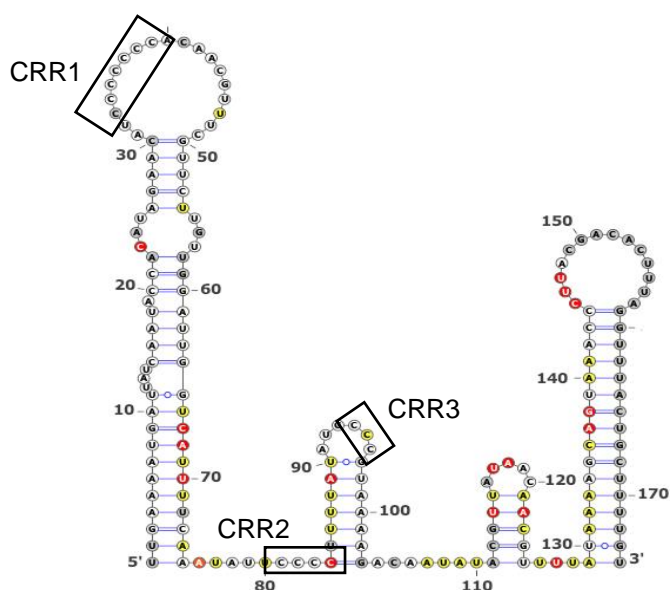
L'organisme modèle sur lequel les travaux présentés ici ont été réalisés est la bactérie *Staphylococcus aureus*. Il s'agit d'une bactérie Gram-positive commensale mais également pathogène opportuniste en faveur d'une immunodépression. Les infections par *S. aureus* représentent un enjeu majeur de santé publique de par l'apparition ces dernières années de nombreuses souches multirésistantes aux antibiotiques. La pathogénicité de *S. aureus* est principalement due à sa capacité d'adaptation lui permettant de croître dans de nombreux environnements, y compris dans des milieux carencés en fer grâce à la présence de plusieurs mécanismes d'acquisition de ce dernier.

Néanmoins, même si l'acquisition du fer est un processus nécessaire pour la croissance de *S. aureus*, la concentration en fer intracellulaire doit être extrêmement régulée. En effet, si une concentration trop faible en fer ne permet pas la croissance,

une concentration trop élevée est quant à elle toxique pour la bactérie car elle mène à la production d'espèces réactives de l'oxygène via la réaction de Fenton. Par conséquent, la concentration en fer intracellulaire résulte d'un équilibre entre son acquisition et son utilisation dans la cellule.

Chez la plupart des bactéries, les gènes permettant l'acquisition du fer sont sous le contrôle du régulateur transcriptionnel Fur (Ferric Uptake Regulator). En présence de fer dans le milieu, Fur s'apparie sur des séquences spécifiques (Fur box) se trouvant en 5' de certains gènes. La formation de ce complexe empêche l'appariement de l'ARN polymérase et par conséquent réprime la transcription de ces gènes. En absence en fer, Fur devient inactif et ne peut plus s'apparier sur les Fur box, ce qui active donc la transcription des gènes impliqués dans l'acquisition du fer.

Au sein de notre laboratoire, nous nous intéressons à un autre type de régulateur qui sont les ARNs régulateurs. Récemment, nous avons identifié un ARN régulateur impliqué dans la réponse à la carence en fer et la virulence de *S. aureus* que nous avons nommé IsrR (pour Iron-Sparing Response Regulator) (Coronel-Tellez et al. 2022). IsrR est largement conservé au sein du genre *Staphylococcus* et son expression est régulée par Fur. IsrR possède trois régions riches en C (CRRs) (**figure 1**) qui lui permettent d'interagir avec le RBS de ses ARNs messagers cibles, ce qui donne lieu à une répression de leur traduction. En étudiant la liste des 23 cibles les plus probables d'IsrR, on retrouve sept ARNs messagers codant pour des protéines contenant des noyaux fer-Soufre, ce qui suggère donc qu'en conditions de carence en fer, IsrR réprimerait la production de certaines protéines contenant des noyaux Fer-Soufre, probablement dans le but de conserver le peu de fer présent pour des fonctions essentielles uniquement.



### Structure secondaire d'IsrR

La structure secondaire d'IsrR a été obtenue par SHAPE. La couleur des bases reflète leur réactivité. Gris : Non déterminé ; Blanc : faible ; jaune : modérée ; rouge : haute. Les CRRs sont encadrées en noir.

## Contenu de la thèse

Le concept d'utilisation d'ARNs régulateurs comme mécanismes pour surmonter la carence en fer est bien décrit chez les bactéries (Chareyre and Mandin 2018). L'idée est que lorsque la bactérie est confrontée à une carence en fer, les ARN régulateurs répriment les gènes non essentiels codant pour des protéines qui contiennent du fer (par exemple sous forme de noyaux Fer-soufre) afin de conserver le fer restant pour le redistribuer vers des processus essentiels, tels que la respiration ou la synthèse de l'ADN. Ce phénomène a été très étudié chez *E. coli*, avec la description de RyhB. Cependant, jusqu'à récemment, l'adaptation de *S. aureus* à des conditions de croissance sans fer n'était associée à aucun ARN régulateur (Price and Boyd 2020). Grâce à une méthode développée au sein de notre laboratoire afin d'identifier les phénotypes associés aux ARNs régulateurs (Le Lam et al. 2017), IsrR, un ARN régulateur requis pour la croissance dans des milieux carencés en fer, a été découvert. Cet homologue fonctionnel, mais non orthologue de RyhB chez *S. aureus* est exprimé uniquement en conditions de carence en fer et est également impliqué dans la virulence.

Au cours de ma première année de thèse, j'ai eu l'occasion de participer à la caractérisation d'IsrR. En particulier, j'ai contribué à l'obtention de la structure secondaire d'IsrR seul et en interaction avec les ARNm *fdhA* et *gltB* par SHAPE. J'ai également contribué à des expériences *in vitro* confirmant les interactions d'IsrR avec

ses ARNs messagers cibles par retard de gel. Ces résultats figurent dans une publication que j'ai cosignée ((Coronel-Tellez et al. 2022), chapitre E).

Il a été démontré qu'IsrR réprime de nombreuses enzymes impliquées dans la respiration du nitrate, mais les données de bio-informatique suggèrent qu'IsrR a de nombreuses autres cibles et qu'il est certainement associé à la régulation de plusieurs autres voies métaboliques. J'ai poursuivi la caractérisation d'IsrR en identifiant de nouvelles cibles. J'ai notamment découvert qu'IsrR régula le métabolisme du citrate en réprimant simultanément l'aconitase et son activateur transcriptionnel (chapitre F). Nous avons également confirmé que l'aconitase de *S. aureus* possédait une activité RNA binding en conditions de carence en fer et nous avons mis au jour plusieurs gènes régulés par cette dernière, complexifiant ainsi l'étendue du réseau de régulation de la réponse à la carence en fer chez *S. aureus*.

MiaB est une protéine contenant deux noyaux Fer-Soufre. C'est une enzyme de modification des ARNt qui permet d'augmenter la fidélité de la traduction. Avec Elise Leclair, une étudiante en Master que j'ai co-encadrée, nous avons montré que l'expression de *miaB* est réprimée par IsrR (chapitre G). Ce travail met en évidence le rôle d'IsrR dans la répression des protéines à noyaux fer-Soufre et souligne également le rôle essentiel de ses CRRs pour son activité.

# Régulation de l'expression de l'aconitase en conditions de carence en fer chez *S. aureus*: Contrôle par un ARN régulateur et activité moonlight

## Le métabolisme du citrate est régulé par IsrR en conditions de carence en fer :

Le logiciel CopraRNA a révélé plusieurs cibles putatives d'IsrR, dont trois liées au métabolisme du citrate : l'ARNm *citB* (codant pour l'aconitase), l'ARNm *citM* (codant pour un transporteur de citrate putatif) et *ccpE* (codant pour un activateur transcriptionnel de *citB*). Ces cibles, conservées dans diverses espèces du genre *Staphylococcus*, soulignent le rôle potentiel du citrate dans l'adaptation de *S. aureus* aux milieux carencés en fer. Le logiciel IntaRNA prédit un appariement d'IsrR avec les régions 5' non traduites de ces ARNm, ce qui indique une potentielle régulation négative de l'expression de *citB* et *ccpE*. Des expériences de gel retard ont confirmé l'appariement d'IsrR aux ARNm *citB* et *ccpE*. Un mutant d'IsrR dans lesquels les CRRs impliquées dans l'interaction ont été mutées ne provoque pas de retard sur gel, ce qui suggère que l'interaction entre IsrR et les ARNm impliqués dans le métabolisme du citrate impliquent les CRRs.

## IsrR réprime la production d'aconitase et de CcpE :

Afin de comprendre le rôle d'IsrR sur l'expression de *citB* et *ccpE*, nous avons créé des fusions de gènes en ajoutant une étiquette FLAG en C-ter des séquences codantes des protéines CitB et CcpE dans une souche sauvage et une souche  $\Delta isrR$ . La production des protéines peut ainsi être visualisée par western-blot en utilisant des anticorps anti-FLAG. En présence d'un milieu riche, les niveaux d'expression des protéines CitB-FLAG et CcpE-FLAG sont similaires entre la souche sauvage et la souche  $\Delta isrR$ . En revanche, lors d'une croissance dans un milieu carencé en fer (par l'ajout de 2,2'-dipyridyl (DIP), un chélateur du fer) qui conduit à l'induction d'IsrR, une diminution significative des quantités de CitB-FLAG et CcpE-FLAG ont été observées dans la souche sauvage mais pas dans la souche  $\Delta isrR$ . Ainsi, l'expression d'IsrR est associée à une diminution de la production de CitB et de CcpE.

## **IsrR n'agit pas sur les quantités d'ARNm**

Afin d'étudier le mode d'action d'IsrR et d'identifier de potentielles nouvelles cibles, une analyse transcriptomique a été réalisée en comparant une souche sauvage et une souche  $\Delta isrR$  en conditions de carence en fer. De manière surprenante, seul le gène *isrR* semble significativement moins exprimé chez la souche  $\Delta isrR$  (ce qui est attendu puisque le gène y est délété). Deux autres gènes, *mtlF* et *mhqD*, ont montré une expression différentielle significative, mais l'analyse bioinformatique n'a pas confirmé d'appariement direct entre IsrR et ces ARNm. Ces résultats, qui sous-entendent que IsrR a seulement un effet sur la traduction des ARNs messenger et non sur leur stabilité, contrastent avec le mode d'action des ARNs régulateurs des bactéries Gram-négatives, où l'action d'un ARN régulateur entraîne généralement une diminution de la stabilité des ARNs messagers. Ces résultats remettent en question les dogmes actuels sur la régulation médiée par les ARNs régulateurs, par l'observation de mécanismes de régulation uniques chez les bactéries Gram-positives, en particulier dans le cas d'IsrR.

## **IsrR cible les régions 5' UTR de *citB* et *ccpE***

Les données de bioinformatique suggèrent que la régulation de *citB* et *ccpE* par IsrR se déroule au niveau post-transcriptionnel, par une diminution de la traduction due à l'appariement d'IsrR sur la région 5' UTR des ARNs messagers. Afin de confirmer cela, les régions 5'UTR de *ccpE* et *citB* ont été fusionnées à la protéine fluorescente mAmetrine et placées sous le contrôle du promoteur constitutif  $P_{sar1}$  avant d'être insérées au chromosome d'une souche sauvage ou  $\Delta isrR$  de *S. aureus*. En présence d'un milieu riche, des niveaux de fluorescence similaires ont été observés entre les souches sauvage et  $\Delta isrR$ . Cependant, en présence d'un milieu carencé en fer, la fluorescence des deux fusions rapportrices a significativement diminué dans la souche sauvage mais pas dans la souche  $\Delta isrR$ . Ces résultats soutiennent fortement l'hypothèse d'une régulation post-transcriptionnelle de *ccpE* et *citB* par IsrR, mettant en évidence une interaction directe entre IsrR et les régions 5' UTR de *citB* et *ccpE*.

## **Les CRRs d'IsrR sont requises pour la régulation traductionnelle des ARNm de *citB* et *ccpE***

Afin d'identifier les régions d'IsrR essentielles pour son activité contre les ARNm de *ccpE* et *citB*, nous avons transformé les souches  $\Delta isrR$  contenant les fusions rapportrices avec des plasmides contenant différentes versions d'IsrR sauvage ou mutées pour une ou plusieurs CRRs. Pour la fusion *citB*-mAmetrine, la présence d'IsrR sauvage a significativement réduit la fluorescence, et la délétion de CRR1 ou CRR2 n'a pas eu d'impact significatif, ce qui suggère leur interchangeabilité potentielle. En

revanche, la délétion de CRR3 seul ou en combinaison avec d'autres CRRs réduit modérément l'activité d'IsrR, et la suppression de CRR1 et CRR2 entraîne une forte fluorescence de la mAmetrine. Ces résultats impliquent que la répression de la traduction de l'ARNm *citB* par IsrR implique la CRR1 ou la CRR2. Pour la fusion *ccpE*-mAmetrine, la délétion de la CRR1 de IsrR le rend inactif, tandis que la délétion de CRR2 ou CRR3 n'a pas d'effet, ce qui est cohérent avec les prédictions bioinformatiques indiquant un appariement avec CCR1.

### **L'aconitase de *S.aureus* est autorégulée par son activité moonlight**

L'aconitase, responsable de la conversion du citrate en isocitrate, peut acquérir une activité de liaison à l'ARN (RBP) en conditions de carence en fer et est capable de réguler l'expression de certains gènes. Pour étudier le rôle de l'activité RBP de l'aconitase de *S. aureus* et son rôle en tant que régulateur en conditions de carence en fer, nous avons généré des mutants de l'aconitase déficients soit pour son activité enzymatique (CitB<sub>ENZ</sub>) soit pour son activité RBP (CitB<sub>RBP</sub>). Nous avons ensuite réalisé une analyse transcriptomique entre une souche sauvage et une souche CitB<sub>RBP</sub> en conditions de carence en fer afin d'identifier d'éventuels gènes dont l'expression serait modifiée par l'apo-aconitase. L'analyse transcriptomique a révélé une augmentation significative des ARNm *citB* et *citZ-citC* chez CitB<sub>RBP</sub> par rapport à la souche sauvage, ce qui indique que l'apo-aconitase sauvage réprime ces ARNm en conditions de carence en fer. Les résultats ont également mis en évidence une diminution de l'ARNm *pycA* chez CitB<sub>RBP</sub> par rapport à la souche sauvage, suggérant donc que l'apo-aconitase stabilise l'ARNm *pycA* pendant la carence en fer. Par conséquent, lors d'une carence en fer, l'apo-aconitase ferme le cycle de Krebs tout en promouvant la formation d'oxaloacetate par *pycA*.

### **La régulation de *citB* par IsrR est indépendante de l'activité moonlight de l'aconitase**

Chez *E. coli*, RyhB, un homologue fonctionnel de IsrR, cible également l'aconitase encodée sur le gène *acnB* afin de réprimer sa traduction et déstabiliser l'ARNm. Cependant, l'apo-aconitase, exprimée dans les mêmes conditions que RyhB, est capable de s'apparier sur son propre ARNm et d'empêcher sa dégradation induite par RyhB. Afin de vérifier si l'activité RBP de l'aconitase de *S. aureus* jouait un rôle dans la régulation de *citB* par IsrR, nous avons introduit la mutation CitB<sub>RBP</sub> dans les souches sauvage et  $\Delta$ *isrR* contenant la fusion *citB::flag*. Des expériences de Western blot avec anti-Flag ont démontré que IsrR régule de façon similaire *citB::flag* et *citB<sub>RBP</sub>::flag*, suggérant que la régulation de *citB* par IsrR est indépendante de l'activité RBP de CitB. Cependant, en conditions de carence en fer, la protéine CitB<sub>RBP</sub>-FLAG s'accumule plus

que la protéine CitB-FLAG, ce qui est cohérent avec l'hypothèse selon laquelle l'incapacité de de la protéine apo-CitB<sub>RBP</sub> à réprimer son propre transcrit entraîne l'accumulation de sa protéine. Ces résultats suggèrent un effet additif d'IsrR et de l'apo-CitB contre l'ARNm *citB*.

## **L'ARN régulateur IsrR réprime la méthylthiotransférase MiaB en conditions de carence en fer chez *S. aureus***

### **MiaB est une cible putative de IsrR**

En utilisant CopraRNA, un logiciel conçu pour prédire les cibles des ARNs régulateurs bactériens, nous avons pu obtenir une liste de cibles potentielles d'IsrR, un ARN régulateur impliqué dans la réponse à la carence en fer et conservé dans le genre *Staphylococcus*. Parmi les cibles prédites se trouvait l'ARN messager *miaB*, qui code pour une méthylthiotransférase contenant deux noyaux Fer-Soufre et qui modifie certains ARNs de transfert afin d'augmenter la fidélité de la traduction.

Par la suite, le logiciel IntaRNA a été utilisé pour prédire bioinformatiquement l'interaction entre IsrR et l'ARNm *miaB*. En entrant la séquence complète d'IsrR et la région 5' non traduite de *miaB*, l'analyse a révélé un appariement potentiel impliquant 55 nucléotides et une énergie de -22,33 kcal/mol, ce qui est significatif. L'analyse des prédictions d'IntaRNA montre que IsrR s'apparierait sur la séquence de Shine-Dalgarno de MiaB via la région CRR3, ce qui devrait avoir pour effet de réprimer sa traduction.

### **La réduction de MiaB est dépendante d'IsrR**

Pour étudier l'impact potentiel d'IsrR sur l'expression de *miaB*, une fusion de gènes a été créée en ajoutant au chromosome une étiquette Flag en C-ter de la séquence codante du gène *miaB*. La protéine MiaB-Flag a ainsi pu servir d'indicateur des niveaux d'expression du gène *miaB* dans les souches HG003 sauvage et  $\Delta$ *isrR*. En milieu riche, la quantité de protéine MiaB-FLAG est la même indépendamment de la présence ou de l'absence d'isrR, ce qui est cohérent puisque IsrR est réprimé par Fur en présence de fer dans le milieu. Cependant, l'ajout d'un chélateur du fer dans le milieu de culture, le 2,2'-dipyridyl (DIP), inactivant Fur et induisant l'expression d'IsrR, a entraîné l'absence de détection de MiaB-Flag, ce qui suggère que la protéine apo-MiaB (qui ne possède plus de noyaux Fer-Soufre) est instable en conditions de carence

en fer. Pour résoudre ce problème, la mutation *fur::tet* a été introduite dans les souches sauvage et  $\Delta$ *isrR* contenant la fusion *miaB-flag* afin d'exprimer IsrR de manière constitutive sans pour autant entraîner la perte des noyaux Fer-Soufre de MiaB. Dans ce contexte génétique, MiaB-Flag était à peine visible dans la souche *fur::tet* mais présente en grande quantité dans la souche *fur::tet*  $\Delta$ *isrR*, ce qui confirme le rôle d'IsrR dans la diminution de la quantité de MiaB-Flag.

### **La régulation de l'expression de *miaB* par IsrR se déroule au niveau post-transcriptionnel**

En l'absence de Fur, IsrR est exprimé et *miaB* est réprimé. Cette observation s'explique par un appariement entre IsrR et l'ARN messager de *miaB* au niveau de son RBS, qui inhiberait donc sa traduction. Pour examiner cette hypothèse, un système de rapporteur génétique, basé sur pRN112, a été construit dans lequel la région 5' non traduite (5'UTR) de *miaB*, ainsi que les 54 premiers nucléotides de la séquence codante, ont été clonés sous le contrôle transcriptionnel du promoteur constitutif P1 *sarA* (P1<sub>sarA</sub>). De plus, afin de pouvoir visualiser la traduction de cette séquence, le gène codant pour la protéine fluorescente mAmetrine (*mAm*) a été inséré en aval de cette dernière. La fluorescence a ainsi pu servir d'indicateur de l'expression de *miaB* indépendamment de sa régulation transcriptionnelle. Pour éviter les problèmes éventuels associés à l'utilisation de plasmides, la construction P1<sub>sarA</sub>*miaB*\_5'UTR*mAm* a été intégrée au chromosome de la souche HG003 et de son dérivé *isrR::tag135*. La fluorescence de la fusion rapportrice a significativement diminué dans des conditions de carence en fer d'une manière dépendante de IsrR, alors que sa transcription était pilotée par P1<sub>sarA</sub>. Nos résultats expérimentaux démontrent donc de manière concluante que IsrR exerce sa régulation au niveau de la traduction.

### **La région riche en C numéro 3 (CRR3) d'IsrR joue un rôle crucial dans la régulation de *miaB***

L'initiation d'un appariement entre un ARN régulateur et sa cible implique la formation d'un complexe entre deux régions simple-brin. En général, chez *S. aureus*, les ARNs régulateurs possèdent des régions riches en C qui sont nécessaires pour l'interaction avec leurs cibles. En utilisant la souche  $\Delta$ *isrR* possédant le système rapporteur fluorescent décrit auparavant et en la complétant avec des dérivés d'IsrR dans lesquels une ou plusieurs CRR ont été supprimées, nous avons cherché à savoir la ou les CRRs importantes pour l'interaction avec l'ARNm *miaB*. Alors que la présence d'IsrR sauvage diminue significativement la fluorescence, la délétion de la CRR3 n'entraîne aucune diminution, ce qui suggère une perte de l'activité d'IsrR envers la fusion. Il est intéressant de noter que CRR1 et CRR2 semblent dispensables ou redondants pour la régulation de *miaB*. D'autres analyses avec des délétions doubles de CRRs confirment ces observations. La dépendance à l'égard d'une ou plusieurs CRRs

varie en fonction de l'ARNm cible, comme démontré précédemment (Coronel-Tellez et al. 2022). Cela suggère que l'acquisition de plusieurs CRRs confère à IsrR une polyvalence lui permettant de contrôler une gamme plus large d'ARNm cibles.

## Conclusion

IsrR est un ARN régulateur contrôlant différents aspects du métabolisme de *S. aureus* afin de favoriser son adaptation et donc sa survie dans des conditions de carence en fer, classiquement retrouvées lors d'une infection suite aux mécanismes d'immunité nutritionnelle mis en place par l'hôte. IsrR agit sur ses ARNs messagers cibles selon un mode d'action très particulier. En effet, il exerce une répression traductionnelle qui n'est pas associée à une dégradation des ARNs messagers, contrairement à son homologue chez *E. coli*/RyhB. L'activité d'IsrR est intrinsèquement liée à ses trois régions riches en C (CRR). Nous avons pu montrer que chaque CRR était importante et que chacune avait un set de cibles définies.

Des travaux réalisés précédemment au sein du laboratoire ont montré que IsrR permettait d'inhiber la voie de dégradation du nitrate, une voie métabolique très énergivore en terme de Fer, en conditions d'anaérobiose. Les travaux présentés dans le cadre de cette thèse montrent que IsrR réprime également l'aconitase ainsi que son activateur transcriptionnel CcpE d'une manière simultanée (feedforward loop) afin d'assurer un blocage du cycle de Krebs. IsrR réprime également la production de la méthylthiotransférase MiaB, une enzyme contenant deux noyaux Fe-S. IsrR semble donc être un régulateur central du métabolisme de *S. aureus* en conditions de carence en fer, ayant pour but d'économiser le fer présent dans le milieu et de le redistribuer uniquement vers des fonctions essentielles pour la bactérie.

Cependant, les travaux présentés ici ont également montré que l'aconitase de *S. aureus* possède également un rôle clé dans la réponse à la carence en fer. En effet, nous avons montré qu'en conditions de carence en fer, l'aconitase de *S. aureus* était une protéine *moonlight* et devenait une protéine se liant à l'ARN (apo-aconitase) qui est capable elle aussi d'effectuer une régulation métabolique. En effet, nous avons montré qu'en conditions de carence en fer, l'apo-aconitase réprimait l'expression de plusieurs gènes impliqués dans le cycle de Krebs tout en favorisant l'expression de la pyruvate carboxylase. Ces résultats ouvrent un nouvel axe de recherche sur la réponse à la carence en fer de *S. aureus*, mais également sur le rôle des protéines *moonlight* dans l'adaptation bactérienne.

## Schéma récapitulatif :

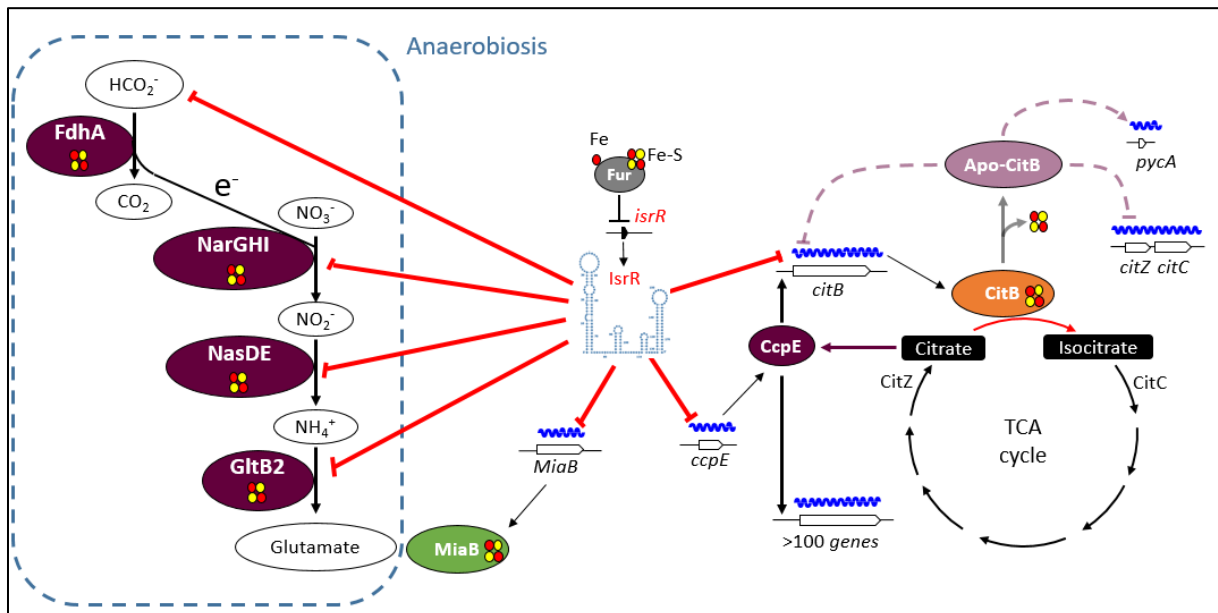


Figure 33: La régulation du métabolisme de *S. aureus* en conditions de carence en fer

IsrR, qui est régulé par Fur, réprime plusieurs gènes codant pour des protéines contenant des noyaux Fer-Soufre. Il réprime notamment plusieurs gènes impliqués dans le métabolisme du nitrate en conditions d'anaérobiose (Coronel-Tellez et al. 2022), mais également la méthylthiostransférase MiaB, l'aconitase CitB et son activateur transcriptionnel CcpE, qui en plus d'activer la production d'aconitase régule aussi l'expression d'une centaine d'autres gènes. En parallèle de l'action d'IsrR, la carence en fer cause également la perte du noyau Fer-Soufre de CitB, qui passe alors d'une activité enzymatique à une activité de liaison à l'ARN (apo-CitB). La protéine Apo-CitB va alors réguler négativement plusieurs gènes impliqués dans le cycle de Krebs, à savoir son propre ARNm ainsi que l'opéron *citZ-citC* (contenant les gènes codant pour la citrate synthase et l'isocitrate déshydrogénase). En parallèle, Apo-CitB va également stabiliser l'ARNm du gène *pycA*, codant pour la pyruvate carboxylase.